5-2015

Induction of caspase-dependent death by proteasome targeted therapy in glioblastoma

Christa A. Manton

INDUCTION OF CASPASE-DEPENDENT DEATH BY PROTEASOME

TARGETED THERAPY IN GLIOBLASTOMA

by

Christa Ann Manton, B.S.

APPROVED:

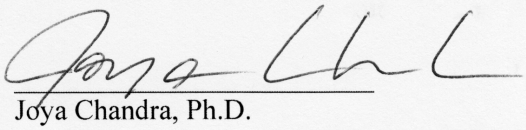

Joya Chandra, Ph.D.

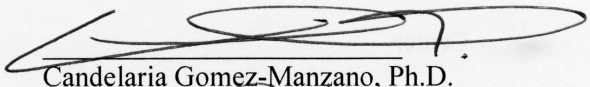

Candelaria Gomez-Manzano, Ph.D.

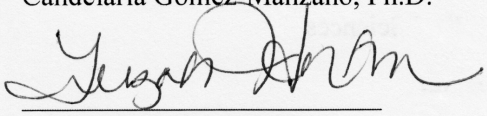

Terzah Horton, M.D., Ph.D.

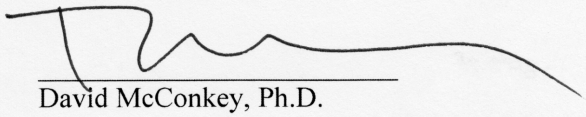

David McConkey, Ph.D.

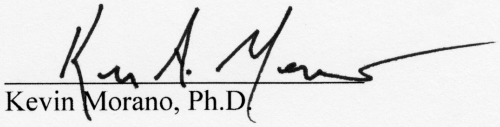

Kevin Morano, Ph.D.

APPROVED:

Dean, The University of Texas
Graduate School of Biomedical Sciences at Houston

INDUCTION OF CASPASE-DEPENDENT DEATH BY PROTEASOME TARGETED THERAPY IN GLIOBLASTOMA

A

DISSERTATION

Presented to the Faculty of

The University of Texas

Health Science Center at Houston

and

The University of Texas

MD Anderson Cancer Center

Graduate School of Biomedical Sciences

in Partial Fulfillment

of the Requirements

for the Degree of

DOCTOR OF PHILOSOPHY

by

Christa Ann Manton, B.S.

Houston, TX

May 2015

DEDICATION

To my parents, for always believing that I will accomplish what I set my mind to and for being my biggest encouragers along the way. Mom, thank you for the serious stuff-keeping me grounded and reminding me of the reasons why I keep pushing forward-and the not-so-serious stuff-like driving all the way to Texas to continue a much-anticipated movie watching tradition. Dad, thank you for always making me laugh, for your sense of humor, and for continually watching out for me. I am grateful to you both for the Christian faith that you instilled in me that gives me guidance and peace, and for always reminding me that I have a safe place to come home to when I need to recharge and rest for awhile. I also dedicate this to my sister, who knows me well and still chooses to love, support, and claim me anyway.

ACKNOWLEDGEMENTS

First, I would like to express my deep gratitude to my mentor, Dr. Joya Chandra. Her unflagging support, encouragement, and guidance have been the driving force behind my development as a scientist during these past years. She has helped me through countless experimental designs, troubleshooting sessions, proposals, abstracts, presentations, and papers. When everything has seemed too overwhelming, she has bought me cupcakes and made me write a list of all my experiments that have succeeded to refocus me on the fact that even at its toughest, the pleasures of science outweigh the struggles.

I would also like to thank the members of the Chandra lab-past and present-who have helped me as a graduate student: Melissa Singh, Claudia Miller, Nilsa Rivera-Del Valle, Blake Johnson, Mary Irwin, Hayley Donnella, and Phillip Knouse, Leslie Grasse, and Selena Hernandez. Thank you Claudia for entrusting me with your precious proteasome knowledge. I am grateful to Melissa for helping me find my way, both in the lab and out. Thank you to Blake Johnson for your help with animal experiments, as well as for your strangely confident, unflagging reassurance that everything is going to work out, both professionally and personally.

I am also grateful for the support and guidance of the members of my committee: Dr. McConkey, Dr. Gomez-Manzano, Dr. Morano, and Dr. Horton. Your insight has helped shape my project as well as the way that I think about science.

Thank you to Dr. Lisa Bouchier-Hayes at Baylor College of Medicine, as well as the members of her lab, for their feedback regarding caspase experiments and their generosity of time and resources that made my caspase 2 experiments possible. I would like to thank Dr. Lance Barton at Austin College for reagents for the PA28γ experiments. I would also like to

acknowledge the assistance I have received from Verlene Henry and Lindsey Holmes for the intracranial GBM model, as well as from Nancy Otto at the Smithville histology facility for immunohistochemistry and Dr. Preeti Purwaha, Dr. Philip Lorenzi, and Dr. David Hawke in the MD Anderson Proteomics Core for their help with the amino acid studies.

Finally, I would like to thank the friends who have made Houston feel like home. Thank you to the Reuther, Singh, Tucker, Corso, and Hillenburg families for inviting me into your homes and pretending like you had an extra daughter for holidays and gatherings. I will be forever grateful to Amy Hillenburg for being an amazing sounding board, and for her incredible gift for knowing when to spontaneously show up at my house with cheesecake or Mexican food. Thank you Jacquelyn Reuther for being my friend who "gets it" and for always reassuring me that I am not, in fact, losing my mind. And thank you to my Mosaic family at Houston's First Baptist Church, particularly my small group ladies, for sharing the highs and the lows for the past several years and for allowing me to be a part of your beautiful community of caring and supportive people.

ABSTRACT

INDUCTION OF CASPASE-DEPENDENT DEATH BY PROTEASOME TARGETED THERAPY IN GLIOBLASTOMA

Christa Ann Manton, B.S.

Advisory Professor: Joya Chandra, Ph.D.

New therapeutic options are needed for glioblastoma, a deadly disease with a median survival of only 14 months with current treatment. The proteasome inhibitor bortezomib (BTZ) shows efficacy in cancers like myeloma, but its clinical utility in other cancer types has been more limited. Newer proteasome inhibitors such as marizomib (MRZ) have unique inhibitory and death inducing properties that have not been well examined in GBM. Additionally, targeting other components of the ubiquitin-proteasome system is possible, but has not been explored in GBM. Questions also still remain about the ability of BTZ and MRZ to be delivered to brain tumors in a relevant orthotopic system. The goal of this study was to determine the kinetics and mechanism of death induced by proteasome inhibitors in GBM and to compare the ability of BTZ and MRZ to cause proteasome inhibition in orthotopic brain tumors in order to establish a framework for the use of these drugs in the clinic by identifying potential biomarkers of efficacy and enabling design of a combination treatment strategy for potentiation of cell death in GBM. Using strategies that inhibited multiple proteasome components, I determined that inhibition of the standard proteasome by BTZ and MRZ was sufficient for optimal targeting of the ubiquitin-proteasome system in GBM. I then determined that both BTZ and MRZ induced caspase-dependent death in GBM cells that was dependent upon activation of caspase 9. Using an orthotopic xenograft model of GBM, I found that both BTZ and MRZ increased levels of the proteasome substrates p21

and p27 in intracranial tumors, with MRZ exerting slightly stronger effects, indicating that these drugs do affect brain tumors. Examination of cleaved caspase 3 and lamin A as markers of apoptosis in brain tumors from mice showed increased cell death after treatment with BTZ or MRZ and the histone deacetylase inhibitor vorinostat. Together, this data clarifies the optimal strategy for proteasome targeting in GBM, clarifies the hierarchy of caspase induction by proteasome inhibitors, and provides evidence that proteasome inhibitors can reach brain tumors where they exert functional effects and increase death in combination with vorinostat.

TABLE OF CONTENTS

Title page ii

Dedication iii

Acknowledgements iv

Abstract vi

Table of Contents viii

List of Figures xii

List of Tables xvii

Chapter 1: Introduction: background research plan, and relevance 1

Glioblastoma 2

The proteasome 5

Proteasome inhibitors 8

Induction of apoptosis and autophagy by proteasome inhibitors in cancer 11

Apoptosis: activation of caspases 11

Increases in reactive oxygen species 14

Stimulation of autophagy 15

Clinical challenges to treatment of GBM with proteasome inhibitors 16

The blood brain barrier 16

Adverse effects 18

Drug resistance 19

Need for combination treatment strategies 21

Research plan 24

Importance to the area of cancer research 25

Chapter 2: Kinetics of proteasome inhibition by BTZ and MRZ, and targeting of alternative proteasome components, in GBM 27

Specific Aim 1: Examine the kinetics of proteasome inhibition by the inhibitors BTZ and MRZ, as well as by methods targeting alternative proteasome components 28

BTZ causes longer-lasting inhibition of the proteasome than MRZ in GBM cells .. 29

Immunoproteasoeme expression, correlation with survival, and specific targeting in GBM..... 40

Targeting PA28γ in GBM 46

Summary and Conclusions..... 48

Chapter 3: Induction of caspase 9-dependent death by BTZ and MRZ and attenuation of death by thiol reducing agents in GBM..... 50

Specific Aim 2: Determine the mechanism of death induction by BTZ and MRZ in GBM 51

Caspase-dependence of death induction by proteasome inhibitors in GBM..... 52

Early cleavage of caspase 2 by proteasome inhibitors may impede death..... 55

Caspase 9 functions upstream of caspase 8 to induce death after proteasome inhibitors in GBM 61

Role of the mitochondria in proteasome inhibitor-induced death..... 67

Caspase 9 activation and death are blocked by reducing agents..... 74

BTZ and MRZ do not deplete cellular amino acid levels..... 82

Summary and Conclusions 86

Chapter 4: BTZ and MRZ modulation of proteasome substrates in orthotopic brain tumors, and *in vitro* and *in vivo* synergy between proteasome inhibitors and HDACi in GBM 88

Specific Aim 3: Evaluate the ability of BTZ and MRZ to inhibit proteasomes and induce death in combination with HDACi in an orthotopic GBM model 89

BTZ and MRZ cause accumulation of proteasome substrates in orthotopic brain tumors 90

Chemical inhibitors of IAPs potentiate proteasome inhibitor-induced death, but siRNA against IAPs does not 94

HDACi potentiate the apoptotic mechanism of BTZ and MRZ *in vitro* 98

Vorinostat interact with the proteasome pathway by reducing PSMB5 mRNA 101

Vorinostat augments caspase cleavage in combination with proteasome inhibitors *in vitro* and *in vivo* 108

Summary and Conclusions 113

Chapter 5: Discussion and Future Directions 115

Chapter 2 Discussion 116

Targeting standard proteasome subunits with BTZ and MRZ 116

Targeting the immunoproteasome in GBM 120

Targeting of regulatory cap elements: PA28γ 121

Chapter 2 Future Directions: The future of proteasome targeting in GBM 122

Chapter 3 Discussion 126

Death induction by proteasome inhibitors in GBM 126

Activation of caspase 2 by proteasome inhibitors in GBM 127

Induction of death by caspase 9 after proteasome inhibition in GBM 129
Bcl-XL protection from proteasome inhibitor-induced death, but not caspase 9 cleavage 133
The protective effect of thiol reducing agents against proteasome inhibitor-induced death in GBM 134
Chapter 3 Future Directions: Looking at indicators of sensitivity to caspase 9-dependent apoptosis following proteasome inhibition in GBM 135
Chapter 4 Discussion 136
Accumulation of proteasome substrates in orthotopic brain tumors after BTZ and MRZ treatment 136
Proteasome inhibition combination therapy: targeting IAPs 137
Proteasome inhibition combination therapy: targeting HDACi 138
Chapter 4 Future Directions: Confirming effects of proteasome inhibitors on survival of orthotopic GBM models 140
Concluding Remarks 141
Chapter 6: Materials & Methods 144
Chapter 7: References 158
Vita 194

LIST OF FIGURES

Figure 1.1: Poor survival of GBM patients with or without temozolomide treatment 3

Figure 1.2: Standard and alternative proteasome components 6

Figure 1.3: Reversible and irreversible analogs of MRZ 10

Figure 1.4: Structure and inhibitory function of BTZ and MRZ 10

Figure 1.5: Activation of initiator caspases 12

Figure 1.6: Structure of the blood brain barrier. 17

Figure 2.1: Inhibition of chymotrypsin-like proteasome activity by MRZ and BTZ in GBM cells. 30

Figure 2.2: Inhibition of caspase-like and trypsin-like proteasome activity by MRZ and BTZ in GBM cells 30

Figure 2.3: Accumulation of ubiquitin tagged proteins and p27 after proteasome inhibition 32

Figure 2.4: Levels of proteasome subunit β5 after treatment with proteasome inhibitors 32

Figure 2.5: Drug efflux through P-glycoprotein does not affect proteasome inhibitor efficacy 34

Figure 2.6: MRZ and BTZ cause equivalent levels of proteasome inhibition in cell lysates 35

Figure 2.7: MRZ causes stronger proteasome inhibition and more DNA fragmentation than BTZ after short pulse treatments 37

Figure 2.8: Effects of reversible and irreversible MRZ analogs. 39

Figure 2.9: Immunoproteasome expression in GBM cells and patient samples 41

Figure 2.10: Decreased expression of the immunoproteasome subunit LMP7 correlates with increased survival in GBM patients 41
Figure 2.11: The immunoproteasome inhibitor ONX-0914 induces death in GBM cells with continuous exposure to high dose 42
Figure 2.12: ONX-0914 specifically inhibits LMP7 at certain low doses 44
Figure 2.13: ONX-0914 does not synergize with standard proteasome inhibitors 45
Figure 2.14: Reducing PA28γ does not alter sensitivity to proteasome inhibitors 47
Figure 3.1: Reduction in cell viability after proteasome inhibitor treatment in GBM cell lines 53
Figure 3.2: Induction of DNA fragmentation by proteasome inhibitors 54
Figure 3.3: Reduction in colony growth by proteasome inhibitors 54
Figure 3.4: Activation of caspases by protesaome inhibitors 56
Figure 3.5: Pan-caspase inhibition prevents DNA fragmentation caused by proteasome inhibitors 57
Figure 3.6: Activation of caspase 2 by proteasome inhibitors 59
Figure 3.7: Knockdown of caspase 2 with siRNA does not effect sensitivity to proteasome inhibitors 60
Figure 3.8: Increased caspase activation and death in shCASP2 cells in response to proteasome inhibitors. 62
Figure 3.9: Silencing caspase 2 does not prevent proteasome inhibitor-induced death 63
Figure 3.10: Caspase 2 +/+ MEFs and caspase 2 -/- MEFs are similarly sensitive to proteasome inhibitors 63

Figure 3.11: Specific inhibition of either caspase 8 or 9 reduces DNA fragmentation caused by proteasome inhibitors 65
Figure 3.12: Chemical inhibition of caspase 9 prevents cleavage of caspase 8 66
Figure 3.13: Knockdown of caspase 9 diminishes cleavage of caspase 8, while knockdown of caspase 8 increases cleavage of caspase 9 68
Figure 3.14: After 24 h of treatment, MRZ-induced death is partially blocked in cells expressing shCASP8 or shCASP9; BTZ-induced death is partially blocked only in shCASP 9 cells..... 69
Figure 3.15: Stable knockdown of caspase 8 slightly increases death, while knockdown of caspase 9 slightly decreases death after 48 h 69
Figure 3.16: Proteasome inhibitors induce release of cytochrome C into the cytoplasm 71
Figure 3.17: Proteasome inhibitors cause decreases in mitochondrial membrane potential..... 71
Figure 3.18: Overexpression of Bcl-XL protects against proteasome inhibitor-induced death 72
Figure 3.19: Overexpression of Bcl-XL does not prevent proteasome inhibitor-induced mitochondrial permeability 73
Figure 3.20: Proteasome inhibitors do not greatly increase ROS in LN18 cells 75
Figure 3.21: NAC prevents caspase 2 activation by proteasome inhibitors 76
Figure 3.22: Inhibition of proteasome inhibitor-induced apoptosis in cells pre-treated with reducing agents 78
Figure 3.23: NAC and DTT, but not GSHee, attenuate proteasome inhibitor-

induced death 79

Figure 3.24: Depletion of glutathione levels does not prevent NAC protection against proteasome inhibitors 81

Figure 3.25: NAC and DTT do not suppress the ability of proteasome inhibitors to reduce CT-L proteasome activity 81

Figure 3.26: Cysteine and asparagine supplementation and proteasome inhibitor induced death 83

Figure 3.27: Amino acid and metabolite levels after treatment with proteasome inhibitors 85

Figure 4.1: Accumulation of p27 in brain tumors of mice treated with MRZ 92

Figure 4.2: Accumulation of p21 in brain tumors of mice treated with proteasome inhibitors 93

Figure 4.3: Initiator caspase cleavage after treatment with equipotent BTZ and MRZ 95

Figure 4.4: Effect of proteasome inhibitor treatment on XIAP levels 96

Figure 4.5: Death induction by combinations of proteasome inhibitors and IAP inhibitors 97

Figure 4.6: Death induction by proteasome inhibitors after knockdown of IAPs 99

Figure 4.7: Increased death with proteasome inhibitors and vorinostat 100

Figure 4.8: Increased death with proteasome inhibitors and panobinostat 100

Figure 4.9: Death induction by proteasome inhibitors and entinostat 103

Figure 4.10: Vorinostat, but not proteasome inhibitors, alters histone acetylation 104

Figure 4.11: Vorinostat suppresses transcription of the proteasome subunit PSMB5 104

Figure 4.12: Vorinostat and panobinostat suppress CT-L proteasome activity,

alone and in combination with proteasome inhibitors 106

Figure 4.13: Vorinostat enhances proteasome suppression in combination with low doses of MRZ and BTZ 107

Figure 4.14: Synergistic induction of caspase 9 cleavage by combinations of vorinostat and proteasome inhibitors 109

Figure 4.15: Treatment schedule for mice with orthotopic brain tumors treated with proteasome inhibitors and vorinostat 109

Figure 4.16: Cleaved caspase 3 in brain tumors of mice treated with vorinostat plus proteasome inhibitors 111

Figure 4.17: Lamin A cleavage in brain tumors of mice treated with vorinostat plus proteasome inhibitors 112

Figure 5.1: Targeting the ubiquitin-proteasome pathway 124

Figure 5.2: Activation of death pathways following proteasome inhibition in GBM 130

LIST OF TABLES

Table 1.1: Clinical trials with proteasome inhibitors and HDACi…….23

Table 4.1: Combination index (CI) values for synergy of proteasome inhibitors plus HDACi. 102

Chapter 1

Introduction: background, research plan, and relevance

1. Glioblastoma

Glioblastoma multiforme (GBM) includes brain tumors that arise *de novo*, as well as astrocytomas that progress from lower grades to grade IV disease. GBM is the most common type of malignant brain tumor, with an incidence of 3 cases per 100,000 person-years; studies have also found a trend toward increased GBM incidence, though the reasons for this are unclear [1, 2].

Before 2005, GBM was treated by surgical resection and radiation. Due to the aggressive nature of this disease, the median survival of patients who received this treatment was only 12 months [3]. The standard of care guidelines were expanded after promising clinical trial results showed increased survival in GBM patients treated with radiation plus temozolomide, an alkylating agent that causes DNA damage-induced cancer cell death [4]. Even with this improvement in treatment, however, the median survival of patients only increased incrementally to 14.2 months (Fig. 1.1) [3, 4]. The continued poor prognosis of GBM patients highlights the need for novel therapeutic strategies to enhance survival.

One of the largest efforts to understand GBM biology has been The Cancer Genome Atlas Network, which first reported the full sequencing of 206 GBM samples in 2008 [5], and expanded their analysis to include more than 500 GBM tumors in 2013 [6]. This extensive sequence information allowed classification of GBM into 4 main molecular subtypes: the proneural subtype, which is characterized by aberrations in platelet-derived growth factor receptor alpha (*PDGFRA*), isocitrate dehydrogenase 1 (*IDH1*), and tumor protein p53 (*TP53*); the classical subtype, which is characterized by aberrant epidermal growth factor receptor (*EGFR*) expression; the mesenchymal subtype, with defects in neurofibromin 1 (*NF1*) expression; and the neural subtype, which is associated with gene

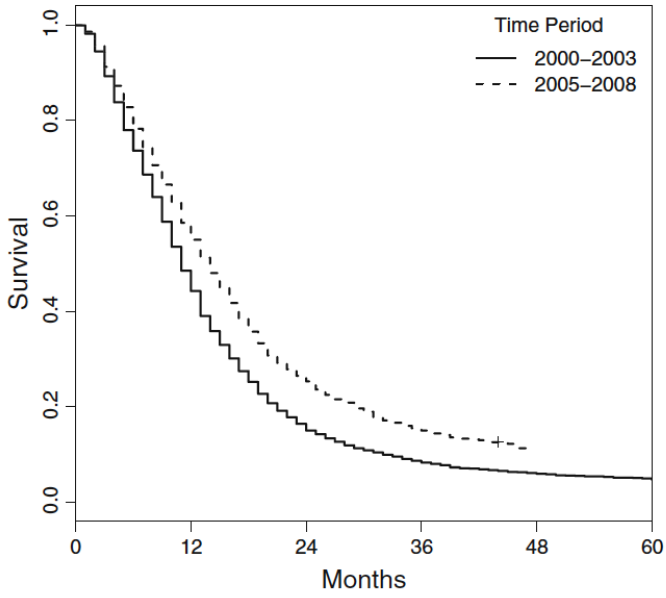

Figure 1.1: Poor survival of GBM patients with or without temozolomide treatment. Kaplan-Meier survival plot for GBM patients treated between 2000-2003 (pre-temozolomide era, median survival = 12 months) versus 2005-2008 (post-temozolomide era, median survival = 14.2 months). Reprinted with permission from Springer from Johnson DR, O'Neill BP (2011) Glioblastoma survival in the United States before and during the temozolomide era. J Neurooncol 107:359–364 (License #3503270379443, Ref. [3]).

signatures closer to more differentiated cells such as astrocytes and neurons [7]. Another effort to pull together a large amount of data from sequencing of brain tumors is the Repository of Molecular Brain Neoplasia Data (REMBRANDT), which includes data for gene expression and clinical endpoints for over 800 samples from different kinds of brain tumors [8].

Though these efforts have greatly contributed to our knowledge base about GBM, more recent studies have indicated that these large scale sequencing efforts can greatly underestimate the remarkable heterogeneity that occurs within individual GBM tumors. Single cell studies identified subpopulations of cells within individual tumors that had a single clonal origin, but had acquired expression of receptor tyrosine kinases from multiple tumor subtypes, particularly of *EGFR*, *MET,* and *PDGFRA* [9, 10]. Expression of these receptors was often mutually exclusive in the different subpopulations within the tumor. Additionally, another study performed single cell RNA sequencing in multiple cells for 5 different primary GBM samples and found remarkable heterogeneity within single tumors [11]. Notably, they identified cells that represented different subtypes (mesenchymal, classical, proneural, and neural) within the same tumor.

This heterogeneity has important implications for therapeutic strategies, as it indicates that targeting just one or even two of these abnormalities may not be effective. This is highlighted by a phase I and II study that combined the *EGFR* inhibitor erlotinib with temozolomide and radiation in newly diagnosed GBM patients [12]. Not only was there no survival benefit in patients that received erlotinib, but specific analysis of the subset of patients with *EGFR* amplifications showed that there was no significant survival advantage in this subpopulation.

The current body of knowledge emphasizes the complexity of GBM and highlights a need for therapeutic strategies that can target broad mechanisms at work in cancer cells that may have a variety of genetic mutations. One potential approach to this problem is targeting the ubiquitin-proteasome system for GBM therapy.

2. The proteasome

The ubiquitin-proteasome system is responsible for the bulk of protein degradation in cells (Fig. 1.2) [13]. The proteasome is in a key position to regulate many cellular pathways, as it degrades misfolded and oxidatively damaged proteins [14], as well as key substrates involved in processes such as cell cycle regulation [15] and cell death [16].

In this process, proteins are first marked for degradation by the addition of ubiquitin chains in a series of steps that requires an E1 ubiquitin activating enzyme [17], an E2 ubiquitin-conjugating protein [18], and finally an E3 ubiquitin-protein ligase that recognizes the specific protein to be degraded and transfers the ubiquitin to it [19, 20]. Polyubiquitin chains form through attachment of the C-terminal glycine of one ubiquitin residue to a lysine of the previous ubiquitin. [21]. Ubiquitin chains can form using several different linkages, with chains attached at lysine 11 or 48 being most commonly associated with recognition and degradation by the proteasome [22].

The proteasome was originally identified through purification experiments that identified a high molecular weight protease complex that degraded proteins in an ATP-dependent manner [23, 24]. Subsequent experiments revealed that the proteasome consists of 20S core particles paired with either one or two 19S regulatory particles that together form the 26S proteasome [25, 26].

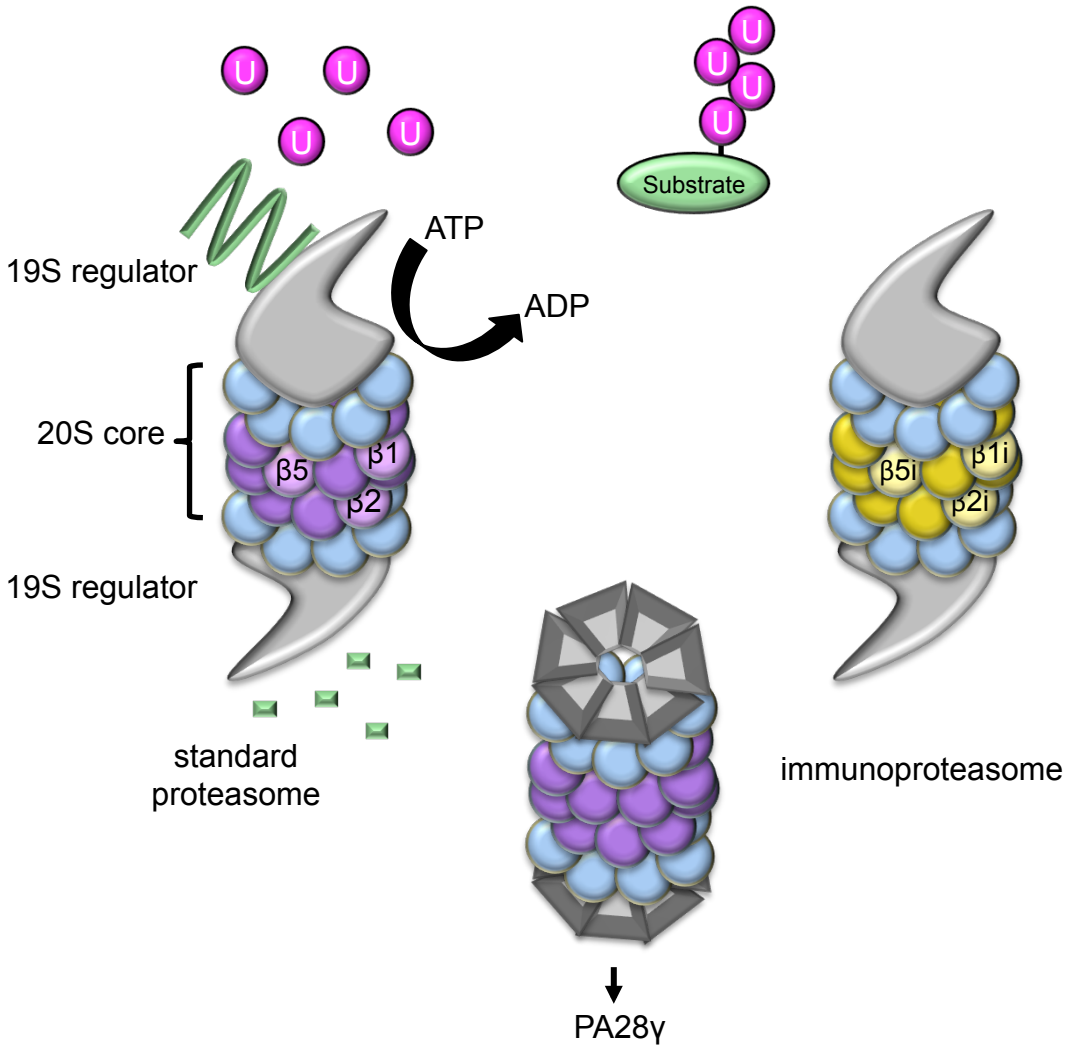

Figure 1.2: Standard and alternative proteasome components. The standard proteasome consists of 1 or 2 19S regulatory caps paired with a 20S catalytic core consisting of 2 outer "alpha" and 2 inner "beta" heptameric rings. The beta subunits include the catalytic subunits, β1, β2, and β5. These subunits can be substituted with β1i, β2i, and β5i to form the immunoproteasome. Alternative cap subunits, such as caps composed of PA28γ, can also be paired with catalytic cores. Proteins are degraded after addition of a ubiquitin chain, which is recognized by the cap subunits. Then, in an ATP-dependent process, proteins are deubiquitinated, unwound, and fed into the 20S core where they are broken down into small peptide chains.

The 19S proteasome regulatory cap is a multisubunit complex that recognizes ubiquitinated proteins, deubiquitinates them, and unwinds them in an ATP-dependent manner [27, 28]. Proteins are then fed into the barrel-shaped 20S core particle. The core particle consists of 4 heptameric rings: 2 outer "alpha" rings and 2 inner "beta" rings. The beta rings contain the catalytic activities of the proteasome: the β1 subunit contains the caspase-like activity, the β2 subunit contains the trypsin-like activity, and the β5 subunit contains the chymotrypsin-like activity [29, 30]. These activities allow the proteasome to cleave substrates after acidic, basic, and hydrophobic residues, respectively. Each β subunit contains a nucleophilic N-terminal threonine residue that reacts with protein substrates [31].

Though the 19S caps and 20S core make up the "standard" proteasome, several alternative proteasome components have also been described. In addition to 19S regulators, proteasome core particles can also associate with PA28 regulators (also known as 11S regulators), which change the core to a more open conformation and facilitate increased production of antigens for presentation on class I major histocompatibility complexes [32, 33]. There are three PA28 subunits: PA28α and β, which are inducible by interferon-γ and form heteroheptameric complexes, and PA28γ, which is not induced by interferon-γ and forms a homoheptamer [32, 34]. Studies of the tissue distribution of various subunits have found that the brain contains very low levels of PA28α and β, but very high levels of PA28γ [35]. PA28γ has been shown to be able to facilitate degradation of cell cycle inhibitory proteins, most notably including p21, in a ubiquitin-independent manner, indicating that it has effects on key cellular functions [36].

The proteasome also has alternative catalytic subunits that are inducible by interferon-γ and that make up what is known as the immunoproteasome, named because it

increases production of antigens suitable for presentation on class I major histocompatibility complex molecules [37, 38]. The immunoproteasome is characterized by incorporation of LMP-7 (β5i), LMP-2 (β1i), and MECL-1 (β2i) into the 20S core particle and increased cleavage after hydrophobic amino acids due to the specificity of both β1i and β5i for this cleavage site [39]. Though immunoproteasome subunits are usually not expressed in normal brain [35], immunohistochemical analysis revealed increased levels of immunoproteasome subunits, particularly β1i and β5i, in a subset of GBM patient specimens [40].

3. Proteasome inhibitors

Inhibitors of the proteasome were originally developed as biological tools for studying protein degradation and its role in muscle wasting [41]. There are 5 main classes of proteasome inhibitors. Reversible inhibitors are classified as either peptide aldehydes (e.g. MG132) or peptide boronates (e.g. bortezomib [BTZ]). Irreversible inhibitors can be divided into β-lactones (e.g. marizomib [MRZ]), peptide vinyl sulfones, or peptide epoxyketones (e.g. carfilzomib) [31]. Subsequent experiments revealed the potential of proteasome inhibition for cancer therapy.

The most well-established, clinically utilized proteasome inhibitor is the dipeptide boronic acid BTZ. Determination of the crystal structure of BTZ in complex with yeast 20S proteasomes revealed that the boronic acid moiety of BTZ interacts with amino acids surrounding the 20S proteasome active site threonine, forming a tetrahedral boronate adduct. BTZ also forms a hydrogen bridge between a hydroxyl group from the boronate group and the proteasome active site threonine itself [42]. Studies of the binding mechanism have revealed that BTZ inhibits the proteasome in a manner that is slowly reversible. Crystal structure experiments as well as a study that utilized a probe for the active sites of the

proteasome revealed that, while BTZ has the strongest affinity for binding and inhibiting β5, it can also inhibit β1 and β1i [42, 43].

Studies of BTZ have identified its anticancer potential in a variety of tumors including colorectal cancer [44], pancreatic cancer [45, 46], and lung cancer [47]. BTZ has been particularly successful in myeloma, as it induces death in multiple myeloma cells at doses that are non-toxic to normal peripheral blood mononuclear cells, establishing it as a potential therapeutic agent for this disease [48]. Subsequent clinical trials demonstrated therapeutic activity of BTZ [49]. In the phase III Assessment of Proteasome Inhibition for Extending Remissions (APEX) trial, BTZ increased median survival from 23.7 months in patients receiving dexamethasone to 29.8 months [50]. Additionally, BTZ treatment was associated with a 43% overall response rate and 9% complete response rate in the APEX trial. Promising clinical trial results led to FDA approval of BTZ for relapsed or refractory multiple myeloma [51, 52], and later for mantle cell lymphoma [53].

The success of BTZ fueled development of other inhibitors in this class, including MRZ (formerly NPI-0052) [54, 55]. MRZ is a nonpeptide proteasome inhibitor that was isolated from the marine actinomycete *Salinispora tropica* and structurally resembles the natural proteasome inhibitor omuralide [56-58]. MRZ contains a β-lactone ring with a chloride leaving group that is important for the irreversible inhibitory nature of MRZ; the leaving group allows formation of a cyclic ether with the active site threonine in the proteasome [59]. To study the importance of the chloride leaving group, MRZ analogs with a leaving group ("LG" analogs) or without a leaving group ("non-LG" analogs) were developed (Fig. 1.3). LG analogs caused sustained proteasome inhibition (>24 h), while non-LG analogs only inhibited the proteasome for short periods (≤12 h) [60]. A study in leukemia

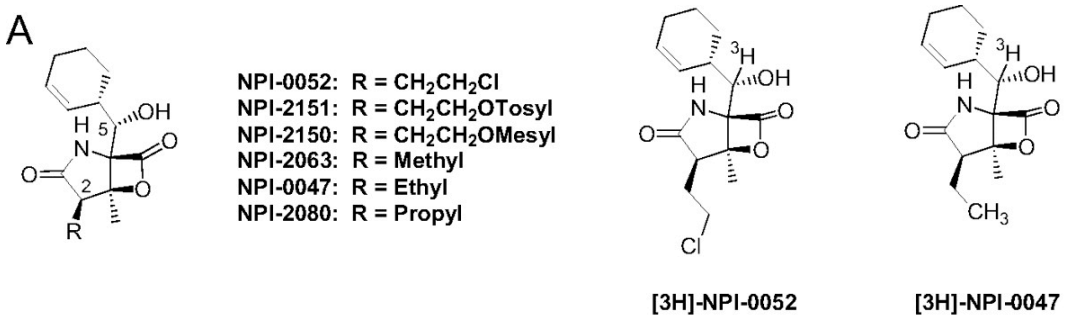

Figure 1.3: Reversible and irreversible analogs of MRZ. Examples of R-group substitutions used to create irreversible NPI analogs with leaving groups (NPI-0052 [MRZ], NPI-2151, and NPI-2150) and reversible NPI analogs without leaving groups (NPI-2063, NPI-0047, and NPI-2080). Reprinted with permission from the American Society for Pharmacology and Experimental Therapeutics from Obaidat A, Weiss J, Wahlgren B, Manam RR, Macherla VR, Mcarthur K, Chao T-H, Palladino MA, Lloyd GK, Potts BC, Enna SJ, Neuteboom STC, Hagenbuch B (2011) Proteasome regulator marizomib (NPI-0052) exhibits prolonged inhibition, attenuated efflux, and greater cytotoxicity than its reversible analogs. J Pharmacol Exp Ther 1–35 (Ref. [161]).

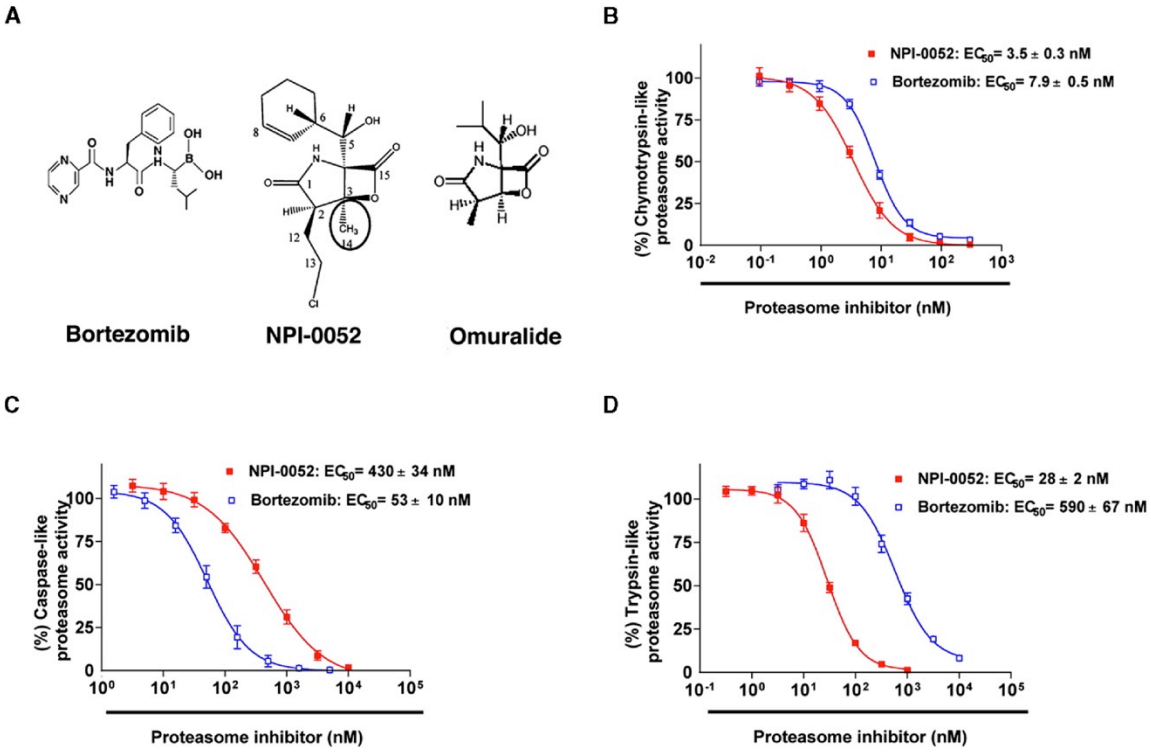

Figure 1.4: Structure and inhibitory function of BTZ and MRZ. A) Structure of the proteasome inhibitors BTZ and MRZ (NPI-0052), which is structurally similar to omuralide. The methylated C3 position of MRZ, which is one of the features that distinguish it from omuralide, is circled. B-D) Determination of the inhibitory activity of MRZ and BTZ on the chymotrypsin-like (B), caspase-like (C), and trypsin-like (D) activities of proteasomes isolated from human erythrocytes. Reprinted with permission from Elsevier Limited from Chauhan D, Catley L, Li G, Podar K, Hideshima T, Velankar M, Mitsiades C, Mitsiades N, Yasui H, Letai A, Ovaa H, Berkers C, Nicholson B, Chao T-H, Neuteboom STC, Richardson P, Palladino MA, Anderson KC (2005) A novel orally active proteasome inhibitor induces apoptosis in multiple myeloma cells with mechanisms distinct from Bortezomib. Cancer Cell 8:407–419 (License #3503271470606, Ref. [62]).

cells revealed increased cell death after treatment with the LG versus non-LG analogs [61]. In addition to causing more sustained proteasome inhibition compared to BTZ, MRZ also inhibits the β5 and β2 proteasome subunits at lower doses than BTZ (Fig. 1.4) [62]. Differences in the mode of proteasome binding (irreversible for MRZ versus reversible for BTZ) and target specificity (β5 and β2 for MRZ versus β5 and β1 for BTZ) have led to some key differences in how these drugs induce death in cancer cells.

While BTZ and MRZ both target the "standard" 20S proteasome, specific inhibitors of the immunoproteasome have also been developed. IPSI-001, a specific inhibitor of β1i, induced death in myeloma cells and overcame resistance to BTZ [63]. ONX-0914 (also called PR-957) is another immunoproteasome-specific inhibitor. It specifically targets LMP7 (β5i), and most current studies have focused on ability to attenuate immune-related diseases such as arthritis and colitis [64, 65]. Future work targeting alternative proteasome components in cancer is warranted.

4. Induction of apoptosis and autophagy by proteasome inhibitors in cancer

4.1 Apoptosis: activation of caspases

Proteasome inhibitors have been shown to induce caspase-dependent apoptosis in a variety of cancer types, including leukemia and myeloma [66-68]. Apoptosis is carried out by a family of cysteine proteases known as caspases. Caspases 2, 8, and 9 are initiator caspases; these proteases exist as inactive pro-caspases that are activated in response to signals that induce their recruitment to activation platforms and proteolytic processing of these caspases to their active forms (Figure 1.5) [69]. Activation of initiator caspases is a multi-step process that includes caspase dimerization, cleavage of the pro-domain, and cleavage to separate the

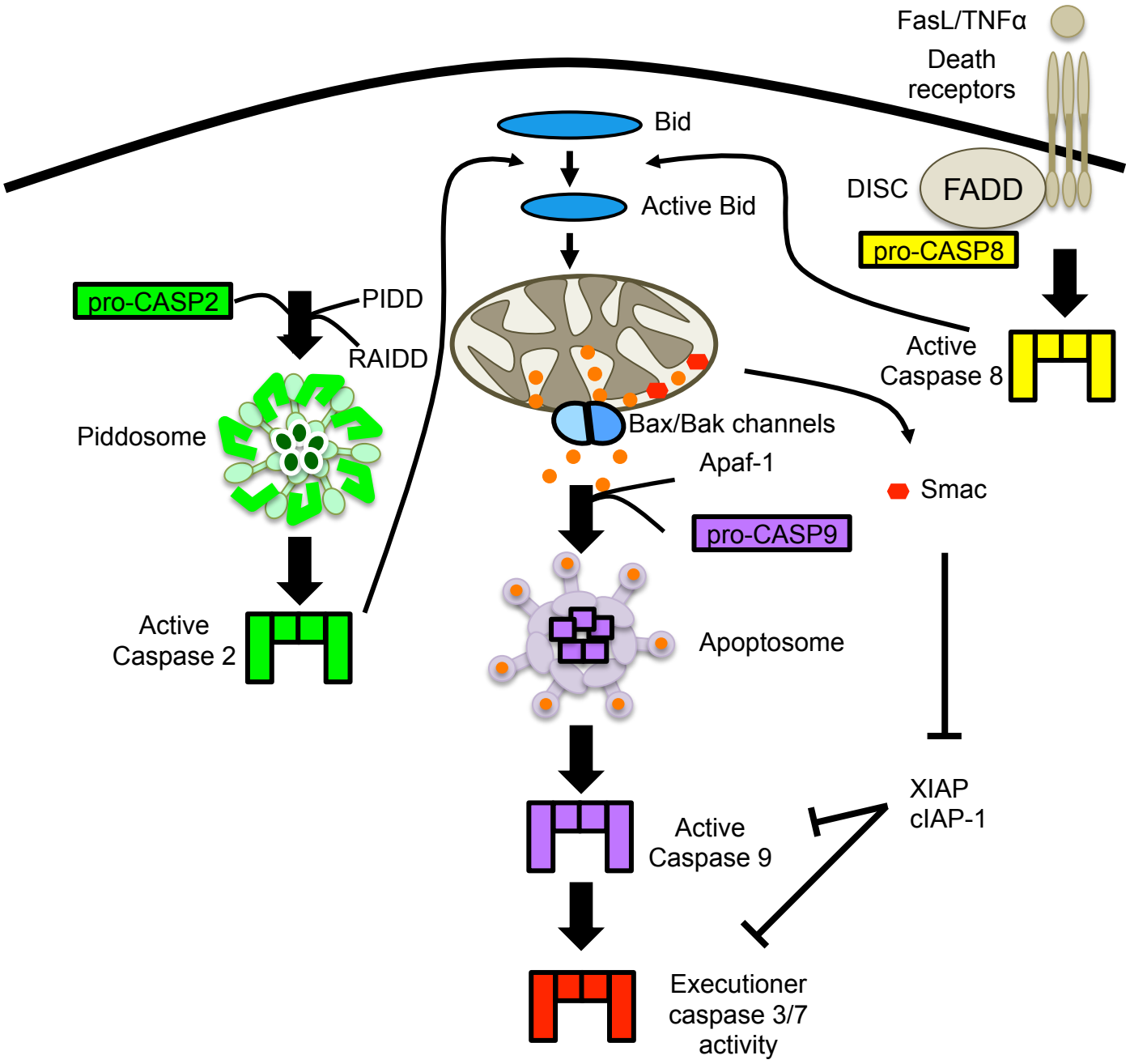

Figure 1.5: Activation of initiator caspases. Caspase 2 is activated by recruitment to the PIDDosome, caspase 8 is activated by death receptor signaling and recruitment to the death-inducing signaling complex (DISC), and caspase 9 is activated after release of cytochrome C from the mitochondria comes together with Apaf-1 to form the apoptosome. Active initiator caspases activate executioner caspases. Activation of apoptosis is antagonized by inhibitor of apoptosis proteins, including XIAP and cIAP-1, which bind and inhibit active caspases. This inhibition of apoptosis is released as Smac, an inhibitor of IAPs, is released from the mitochondria

small and large subunits; active caspases consist of dimers with the large subunits on the outside and the small subunits on the inside [70]. Each initiator caspase is activated in response to unique cellular signals and initiates a cascade of events that leads to activation of the effector caspases 3 and 7.

Caspase 8, which is part of the extrinsic apoptosis pathway, is activated in response to binding of ligands such as Fas ligand or tumor necrosis factor-related apoptosis-inducing ligand (TRAIL) to death receptors. Active death receptors then recruit caspase 8 to the death-inducing signaling complex for activation [69].

Caspase 9, which is part of the intrinsic apoptosis pathway, is activated downstream of cytochrome C release from the mitochondria. The pro-apoptotic Bcl-2 family members Bax and Bak form pores that facilitate release of cytochrome C from the mitochondria [71]. Cytochrome C then forms a complex known as the apoptosome with Apaf-1 and pro-caspase 9, facilitating activation of caspase 9 [72].

A third, less well-studied mode of caspase activation involves the initiator caspase 2. Upon cellular stress, caspase 2 is recruited to and activated in a complex known as the PIDDosome that consists of p53-induced protein with a death domain (PIDD) and RIP-associated ICH-1/CED-3-homologous protein with a death domain (RAIDD) [73]. It is then thought to induce apoptosis by causing mitochondrial permeability and downstream activation of caspase 9 in a manner that is dependent on cleavage of BID, a pro-apoptotic Bcl-2 family member [74-76]. Caspase 2 has also been reported to act as a tumor suppressor, as cells deficient in caspase 2 showed increased proliferation and defective cell cycle checkpoint regulation in response to DNA damage [77].

Specific apoptotic studies in other cancer models have found that BTZ and MRZ rely

on different caspases; MRZ induced caspase 8-dependent apoptosis in leukemia and myeloma, while BTZ was more equally dependent on caspases 8 and 9 [62, 68]. Further evidence that these inhibitors act by different mechanisms was provided by a study that showed that MRZ can induce death in BTZ-resistant myeloma cells [62].

Studies have found that BTZ can induce death in GBM cells as measured by MTT assay [78]. BTZ also induces cell cycle arrest and cleavage of poly ADP ribose polymerase in GBM cells, suggesting that death may occur due to caspase activation and apoptosis but without clarifying the role of specific caspases [79]. Preliminary evidence also suggests that MRZ can induce death in glioma cells, but a more specific examination of the death mechanism is lacking [80]. The dependence of proteasome inhibitors on activation of specific initiator caspases has not yet been reported in GBM.

4.2 Increases in reactive oxygen species (ROS)

One stimulus for proteasome inhibitor-induced death is increased ROS levels after proteasome inhibition. ROS, which are derived from oxygen molecules, include superoxides (O_2^-), hydroxyl radicals (OH^-) and hydrogen peroxide (H_2O_2). High levels of ROS are capable of causing damage to many cellular components including DNA, proteins, and lipids. Proteasome inhibitors have been shown to increase ROS in numerous types of cancer, including multiple myeloma, mantle cell lymphoma, colon cancer, and lung cancer [47, 81-84]. Inhibition of mitochondrial electron transport chain components prevented BTZ-induced ROS increases, suggesting that ROS is likely produced by mitochondrial dysfunction, which is also upstream of caspase 9 activation [47].

The importance of ROS was solidified by the fact that proteasome inhibitor-induced

death in mantle cell lymphoma was blocked by treatment with the antioxidants glutathione ethyl ester (GSHee) and *N*-acetyl cysteine, which acts as an antioxidant by increasing levels of the antioxidant glutathione [82]. MRZ was also shown to cause ROS-dependent cell death in leukemia [68]. Some studies have presented conflicting findings. One study showed that lung cancer cells did not have increased ROS after BTZ treatment, and also were not protected from BTZ-induced death by NAC [85], while a conflicting study reported that induction of ROS and mitochondrial dysfunction were important events in BTZ-mediated apoptosis in lung cancer cells [47]. These results suggest that effects on ROS and the protective effect of antioxidants may be cell-specific, possibly due to factors such as differences in basal antioxidant capacity in different cell types.

4.3 Stimulation of autophagy

Another pathway of cellular protein breakdown is autophagy, a process in which proteins and organelles are first engulfed by autophagosomes, followed by degradation in lysosomes. The role of autophagy in cancer and therapeutics is complex: autophagy can aid survival by clearing cells of damaged proteins and aggregates, but may also promote death when stimulated at high levels [86]. Proteasome inhibitors have been found to induce autophagy in a variety of cell types including prostate cancer [87] and melanoma [88]. Induction of autophagy is generally thought to be a protective mechanism in cancer cells treated with proteasome inhibitors, and dual inhibition of the proteasome and autophagy has been shown to increase cell death [87, 89]. Increased death after dual inhibition of the proteasome and autophagy appears to be specific to transformed cells, possibly indicating an increased reliance of cancer cells on these cellular processes [90]. Though it is possible that autophagy may also be responsible for cell death in some cases [91], careful studies are

necessary to delineate whether this process is acting as a pro-death or pro-survival mechanism.

5. Clinical challenges to treatment of GBM with proteasome inhibitors

5.1 The Blood Brain Barrier (BBB)

The BBB is formed by association among the endothelial cells that form capillaries in the brain, pericytes, and astrocyte endfeet (Fig. 1.6) [92]. Together, these cells form a barrier that serves many functions, including restriction of the substances that are able to exit the capillaries in the brain. The BBB is therefore thought to prevent some therapeutic agents from being effectively delivered to lesions in the brain. Though there is evidence that brain tumors disrupt the BBB [93], enhancing delivery of various therapeutics, it is still important to ensure that drugs are able to effectively reach brain tumors.

The BBB may partially explain why, despite results indicating that BTZ causes death in GBM cells *in vitro*, results *in vivo* have been mixed. One study in an orthotopic xenograft model of GBM investigated BTZ in combination with neural stem cells (NSCs) expressing TRAIL [94]. NSCs have been shown to migrate to intracranial tumors, and expression of TRAIL allows them to trigger death receptors on cancer cells. This study found that BTZ increased 100-day survival by 20% in mice also receiving NSC-TRAIL. However, strong *in vitro* data showing the efficacy of the combination of BTZ and the histone deacetylase inhibitor (HDACi) vorinostat [95, 96] did not translate in a clinical trial; a phase II study of BTZ and the HDACi vorinostat in relapsed GBM patients was closed at the interim analysis due to failure to prevent disease progression [97]. This clinical trial did not include molecular markers of efficacy, such as analysis of proteasome substrates or histone acetylation, to

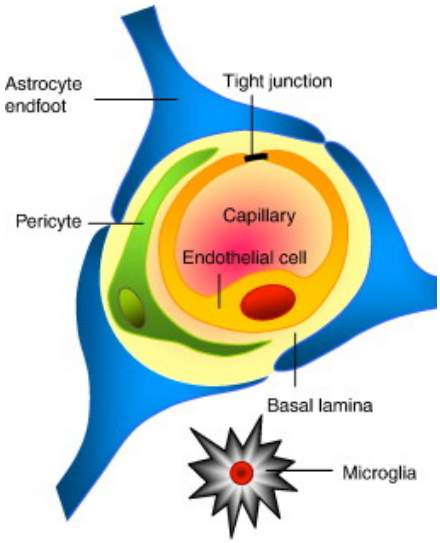

Figure 1.6: Structure of the blood brain barrier. The blood brain barrier is formed from the endothelial cells that form capillaries in the brain, along with pericytes and astrocyte endfeet. Microglia are the immunocompetent cells in the brain. Reprinted with permission from Elsevier Limited from Abbott NJ, Patabendige AAK, Dolman DEM, Yusof SR, Begley DJ (2010) Structure and function of the blood-brain barrier. Neurobiol Dis 37:13–25 (License #3503280146440, Ref. [92]).

indicate whether the drugs were successfully affecting their targets in the brain tumors at the doses and treatment schedules used.

Additionally, subcutaneous models are frequently used for *in vivo* GBM studies, and these experiments do not answer questions about delivery of agents to orthotopic tumor sites [80, 98]. BTZ did increase the efficacy of NSC-TRAIL therapy in orthotopic brain tumors, but specific markers of proteasome inhibition were not reported in this study, so there was no direct measurement of proteasome inhibition [94]. For MRZ, a previous report examined proteasome activity in mice 10 min to 24 h following intravenous injection of 0.15 mg/kg MRZ and reported that MRZ did not decrease proteasome activity in the brain; however, this study was performed in mice without brain tumors, and therefore with intact BBB [54, 99]. Therefore, the current body of evidence concerning the extent of proteasome inhibition achieved by BTZ and MRZ in relevant orthotopic brain tumor models is incomplete.

5.2 Adverse Effects

Between 33% and 66% of myeloma patients treated with BTZ experience peripheral neuropathy [100]. Though the incidence of peripheral neuropathy tends to be lower in patients with solid tumors treated with BTZ [101], it is still an important consideration for patients. Treatment with antioxidants such as Vitamin E, NAC, and glutathione have produced promising results for decreasing peripheral neuropathy [102, 103]. However, supplementation with antioxidants must be implemented with caution. Studies have shown that Vitamin C can directly inactivate BTZ, reducing its efficacy [85]. Additionally, given previous reports that ROS production is important for the mechanism of death following proteasome inhibition, it is important to make sure that any antioxidant used clinically reduces adverse effects while not diminishing the efficacy of proteasome inhibition. Notably,

a phase I trial in myeloma indicated that MRZ was not associated with peripheral neuropathy [104].

5.3 Drug Resistance

Though BTZ does achieve responses in the clinic, some patients do not respond, and many patients treated with BTZ eventually do relapse [50]. Several mechanisms of BTZ resistance have been described. In some cases, cells induce changes to the proteasome itself; this may include up-regulation of proteasome subunits, alterations in the composition of the proteasome subunit pool, or mutations that limit binding of BTZ [105, 106]. For these cases, resistance may be overcome by new-generation proteasome inhibitors such as MRZ, which targets the proteasome at lower concentrations and induces death by mechanisms different from BTZ, or immunoproteasome inhibitors, which target alternative catalytic subunits [62-64, 107, 108].

In other cases, resistance occurs due to differences in the cellular environment that attenuate the toxic functions of proteasome inhibition. For example, cells with a higher basal antioxidant capacity, such as elevated expression of the antioxidant transcription factor Nrf2, have been found to be more resistant to proteasome inhibitors [109, 110]. Also, activation of autophagy, an alternative cellular degradation pathway, was found to protect cells from proteasome inhibitors in prostate cancer [111]. Together, these studies indicate that cells may have ways of escaping the toxic effects of proteasome inhibitors by modulating the cellular environment and inducing alternative pathways for protein disposal.

Another route of resistance involves direct inhibition of apoptosis pathways. Overexpression of anti-apoptotic regulators of mitochondrial integrity such as Bcl-2 and Bcl-XL is seen in some types of cancer, including GBM, which could make these cells resistant

to therapies that target the intrinsic pathway of apoptosis [112]. Targeting Bcl-2 and Bcl-XL induces apoptosis in GBM cell lines, suggesting these proteins are important mediators of apoptosis in GBM [113].

Another class of proteins involved in death regulation is the inhibitor of apoptosis protein (IAP) family, which includes several proteins that directly bind and inhibit caspases. This family includes X-linked IAP (XIAP), cIAP-1, and cIAP-2, which inhibit caspases 3, 7, and 9, as well as other members such as survivin, which inhibits caspases 3 and 7 [114]. IAPs bind to caspases through baculovirus inhibitory repeat (BIR) domains, and several family members possess ubiquitin ligase activity which can be used to target caspases for degradation [115]. Upregulation of IAP expression has been documented in several cancer types, including lung cancer, prostate cancer, and leukemia, and several studies have found links between IAP expression and poor patient outcomes [116-118]. Members of the IAP family have been found to be upregulated in GBM, with XIAP, cIAP-1, cIAP-2, and survivin being expressed at high levels on CD133+ putative GBM stem cells [112, 119, 120]. In cells, second mitochondria-derived activator of caspases (Smac) is an inhibitor of IAPs. Smac is normally sequestered in the mitochondria, but is released along with cytochrome C upon activation of apoptosis. Smac then binds to the BIR domains of IAPs, preventing interactions between IAPs and caspases, and also antagonizing the ubiquitin ligase activity of IAPs [121, 122]. Therapeutic agents have been developed that mimic the activity of Smac. Birinapant and LCL-161 bind to the BIR domains of XIAP, cIAP-1 and cIAP-2 [123, 124]. Smac mimetics have been shown to sensitize GBM cells to multiple therapeutics including PDGFR inhibition [125], TRAIL [126], and radiation [127]. This suggests that IAPs may play a part

in making GBM cells resistant to apoptosis, and targeting them may be a strategy for overcoming resistance to apoptosis-inducing agents such as proteasome inhibitors.

5.4 Need for Combination Treatment Strategies

To maximize therapeutic efficacy and limit toxicity, many drugs used in the clinic are administered as part of rationally designed combination strategies. MRZ and BTZ are both good candidates for combination therapy strategies. An improved understanding of how BTZ and MRZ induce GBM cell death will aid in the design of rational combination strategies that potentiate the efficacy of these agents in the clinic.

One combination strategy that has been investigated in other cancer types is that of proteasome inhibitors with HDACi. In cells, DNA is packaged around a core octamer of histones. Modifications, such as acetylation, ubiquitin, and methylation, to the tail sections of these histone proteins affects how tightly the DNA is packaged, and therefore impacts gene expression. Acetylation of histone tails is regulated by two types of enzymes: histone acetyltransferases (HATs) that add acetyl groups to histone tails, and histone deacetylases (HDACs) that remove acetyl groups. By removing acetyl groups, HDACs lead to a more closed, transcriptionally repressed DNA conformation [128]. Expression of HDACs has been shown to be altered in several types of cancer, including GBM [129, 130].

The first clinically relevant HDACi was the hydroxamic acid vorinostat (also called SAHA) [131]. There are four classes of HDACs, and vorinostat inhibits classes I and II. Vorinostat leads to accumulation of acetylated histones, and alters expression of 2–10% of genes in transformed cells [132].

Vorinostat induces death in a variety of cancer types, and it is FDA-approval for cutaneous T-cell lymphoma [133-135]. Several other HDACi have been developed. Some

HDACi have more narrow inhibitory profiles, such as the benzamide derivative entinostat, a specific inhibitor of class I HDACs [136]. Alternatively, other HDACi have more broad inhibitory capacity; the hydroxamic acid panobinostat inhibits HDACs 1, 2, 3, 4, 6, 7, 8, and 9 at lower concentrations than vorinostat [137]. Panobinostat is currently in several clinical trials, including a phase I/II trial in combination with the angiogenesis inhibitor bevacizumab for malignant glioma [138].

Past studies have indicated the efficacy of the combination of HDACi with proteasome inhibitors. In leukemia, MRZ induced synergistic cell death that was dependent on ROS and caspase 8 activation in combination with the HDACi entinostat and valproic acid [68]. Miller *et al.* also reported that the HDACi vorinostat and entinostat decreased mRNA levels of all three proteasome catalytic subunits, and MRZ, but not BTZ, increased acetylation of histone H3 on its own in leukemia [139]. These results suggest that there is overlap between the mechanisms of HDACi and proteasome inhibitors that may contribute to their synergistic effects in combination. Combinations of these classes of agents are currently in clinical trials for multiple cancer types (Table 1.1).

A study in GBM cells found that BTZ and vorinostat synergistically induced death that was dependent on ROS and mitochondrial dysfunction [96]. Therefore, the combination of proteasome inhibitors and HDACi may be a potent combination in GBM. Though there was a clinical trial of BTZ and vorinostat in relapsed GBM patients that did not prevent progression [97], this study did not report molecular markers of drug delivery and efficacy. Therefore, future studies with combinations of HDACi and proteasome inhibitors in GBM should focus on molecular markers of drug efficacy and comparisons of efficacy between

Proteasome Inhibitor	HDACi	Additional agents	Trial Phase	Disease
bortezomib	panobinostat		I/II & III	multiple myeloma
			II	T-cell lymphoma
			I	mantle cell lymphoma
bortezomib	vorinostat		III	multiple myeloma
		AMG 655	I	lymphoma
			II	non-Hodgkin lymphoma
		sorafenib	I/II	acute myeloid leukemia
			II	soft tissue sarcoma
			II	mantle cell lymphoma and diffuse large cell lymphoma
			I	pediatric central nervous system tumors and lymphoma
			II	non-small cell lung cancer
			II	glioblastoma
marizomib	vorinostat		I	non-small cell lung cancer, pancreatic cancer, melanoma, lymphoma, and multiple myeloma

Table 1.1: Clinical trials with proteasome inhibitors and HDACi. A selection of the clinical trials that include the proteasome inhibitors BTZ or MRZ with the HDACi vorinostat or panobinostat currently registered at *ClinicalTrials.gov.*

clinically established drugs such as BTZ and vorinostat and newer-generation inhibitors such as MRZ and panobinostat.

6. Research Plan

Past *in vitro* and clinical experience with BTZ has highlighted important needs in 3 avenues of research: 1) evaluation of next-generation proteasome inhibitors like MRZ and immunoproteasome inhibitors, which may have differences in delivery to brain tumors, inhibitory action, and mechanism of death induction that could make them more effective clinically; 2) determination of cellular events that are necessary for proteasome inhibitor efficacy that can help anticipate drug resistance and serve as biomarkers of drug function; and 3) *in vivo* evaluation of the ability of proteasome inhibitors to reach brain tumors and exert function effects as part of combination therapy regimens in relevant orthotopic models. Based on these questions, my central hypothesis was that determination of the mechanism of death induced by proteasome inhibitors and comparison of the ability of BTZ and MRZ to cause proteasome inhibition in orthotopic brain tumors would establish a framework for the use of these drugs in the clinic by identifying potential biomarkers of efficacy and enabling design of a combination treatment strategy for potentiation of cell death in GBM.

To address this hypothesis, I first performed a time course and dose-response analysis of the kinetics of proteasome inhibition and death induction following treatment of GBM cell lines with BTZ and MRZ, alone or in combination with specific inhibitors of the immunoproteasome or the alternative cap subunit PA28γ. After determining that targeting the proteasome with BTZ and MRZ effectively induced death in GBM, I characterized the mechanism of caspase activation in these cells.

Careful time course analysis of initiator caspases 2, 8, and 9 was performed, as well as monitoring of caspase 3/7 activity. Treatment with a pan-caspase inhibitor, as well as specific chemical inhibitors and shRNA blockade of caspases 2, 8, and 9, were used to establish the role of specific caspase pathways in GBM cells after proteasome inhibition. The role of ROS in proteasome inhibitor-mediated death was also examined using the reducing agents DTT and NAC, as well as direct introduction of the antioxidant GSH. The ability of these agents to block caspase activation and death was determined.

These experiments revealed an important role for caspase 9 in proteasome inhibitor-induced death in GBM cells. Therefore, I determined whether combinations of BTZ and MRZ with the HDACi potentiated caspase 9 activation and death. After thorough examination of the synergistic potential of proteasome inhibitors plus HDACi in GBM cell lines, I used an orthotopic xenograft model of GBM to establish the ability of proteasome inhibitors to cause proteasome substrate accumulation in brain tumors, and also to induce molecular markers of apoptosis when administered in combination with vorinostat.

Together, these data explore important questions about the most effective strategy for targeting the proteasome in GBM, the mechanism of death induction by proteasome inhibitors, and the *in vivo* potential of BTZ and MRZ in a therapeutic combination that potentiates their mechanism of death induction.

7. Importance to the Area of Cancer Research

BTZ has been shown to effectively target the proteasome and induce death in cancers such as myeloma and mantle cell lymphoma [52, 53]. However, there are still many unanswered questions about the potential of ubiquitin-proteasome system targeting in GBM. This study provides an examination of a few of these key questions. First, examination of the

efficacy of targeting particular proteasome components, including the standard catalytic subunits with BTZ and MRZ, as well as immunoproteasome subunits and PA28γ, utilized current innovations in the field of proteasome inhibitors to determine which subunits should be targeted for the most effective therapeutic strategy for GBM. Secondly, this study elucidated the mechanism of caspase activation in GBM cells after proteasome inhibition by BTZ and MRZ, and found it to be dependent upon caspase 9. This information is useful for establishing biomarkers of drug efficacy as well as anticipating mechanisms of resistance. Finally, this study provides *in vivo* evaluation of the ability of BTZ and MRZ to inhibit the proteasome in orthotopic brain tumors, and examines the potential of the clinically relevant combination of proteasome inhibitors and HDACi both *in vitro* and *in vivo*. Together, this study provides an evaluation of several aspects of proteasome inhibitor function that will help establish their clinical potential and strategies for their therapeutic use.

Chapter 2

Kinetics of proteasome inhibition by BTZ and MRZ, and targeting of alternative proteasome components, in GBM.

Specific Aim 1: Examine the kinetics of proteasome inhibition by the inhibitors BTZ and MRZ, as well as by methods targeting alternative proteasome components.

In this chapter, I examined the kinetics of proteasome inhibition following treatment of GBM cells with the proteasome inhibitors BTZ and MRZ, and also explored strategies for targeting other proteasome components. The ability of therapeutic agents to cause sustained proteasome inhibition has been linked to their ability to induce cell death [61]. Additionally, BTZ and MRZ target proteasome catalytic subunits with different affinities and can induce death by different mechanisms in multiple myeloma [62], suggesting that targeting of different proteasome components may enhance cell death. Therefore, I hypothesized that the irreversible nature of MRZ would result in more sustained proteasome inhibition compared to the reversible agent BTZ, and that targeting multiple proteasome components would have the largest impact on cell death in GBM.

Proteasome activity was examined in time course experiments after treatment of whole cells or cell lysates with the standard proteasome inhibitors BTZ and MRZ, either continuously or after brief drug pulse exposure. I also examined the role of drug efflux on proteasome inhibitor efficacy by using verapamil to block drug efflux, and used analogs of MRZ to explore the importance of irreversible versus reversible proteasome inhibition.

Based on the previous observation that immunoproteasome subunits were upregulated in immunohistochemistry analysis of GBM tumors specimens [40], the role of the immunoproteasome in GBM was explored. The REMBRANDT database was mined for information about immunoproteasome subunit expression and correlations with disease outcomes. A specific inhibitor of the immunoproteasome, ONX-0914, was used to examine

the importance of the immunoproteasome to GBM cell survival, and the possibility that combined targeting of standard and immunoproteasomes could be beneficial in GBM.

Lastly, PA28γ, which forms an alternative regulatory cap, was considered as a potential proteasome target for GBM therapy based on the fact that PA28γ is enriched in the brain [35]. Together, the data in this chapter characterizes the kinetics of standard proteasome inhibition by BTZ and MRZ and explores targeting of alternative proteasome subunits in order to establish the most effective strategy for targeting the proteasome in GBM.

BTZ causes longer-lasting inhibition of the proteasome than MRZ in GBM cells.

To examine the kinetics of proteasome inhibition following treatment with BTZ and MRZ, a panel of GBM cell lines was treated with these agents for periods of time ranging from 2 h to 48 h. Chymotrypsin-like (CT-L) activity, which is the activity of the β5 subunit that is targeted by both BTZ and MRZ, was measured by incubating treated cells with the fluorogenic substrate suc-LLVY-amc. In LN18 cells, both BTZ and MRZ caused strong initial inhibition of the proteasome at 2 h. MRZ-treated cells began to recover proteasome activity 16 h after treatment, while BTZ caused more sustained inhibition (Fig. 2.1A). A similar trend was observed in 2 other GBM cell lines, U251 and U87, with strong initial inhibition (2 h) after treatment with both BTZ and MRZ, but with proteasome recovery occurring between 16 and 24 h in cells treated with MRZ (Fig. 2.1B).

The other 2 catalytic activities of the proteasome were also examined using the fluorogenic substrates z-LLE-amc for caspase-like proteasome activity (Fig. 2.2A) and boc-LRR-amc for trypsin-like activity (Fig. 2.2B). Both BTZ and MRZ caused decreases in caspase-like activity. Similar to the CT-L activity, caspase-like activity recovered slightly

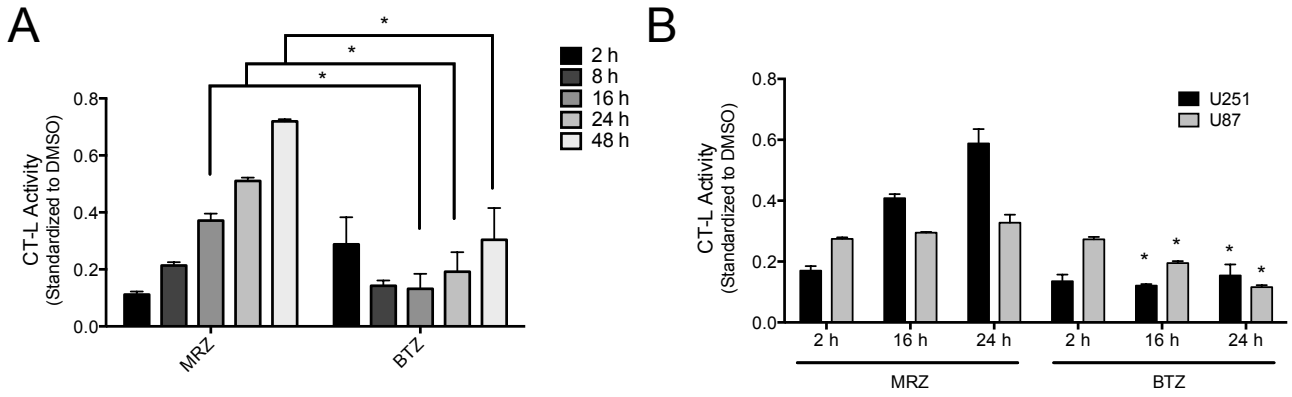

Figure 2.1: Inhibition of chymotrypsin-like proteasome activity by MRZ and BTZ in GBM cells. A) Chymotrypsin-like (CT-L) proteasome activity in LN18 cells treated with 75 nM MRZ or BTZ for increasing periods of time measured using the fluorogenic substrate suc-LLVY-amc (*p < 0.05). B) CT-L proteasome activity in U87 and U251 cells treated with 75 nM MRZ or BTZ for 2, 16, or 24 h (*p < 0.05 compared to MRZ).

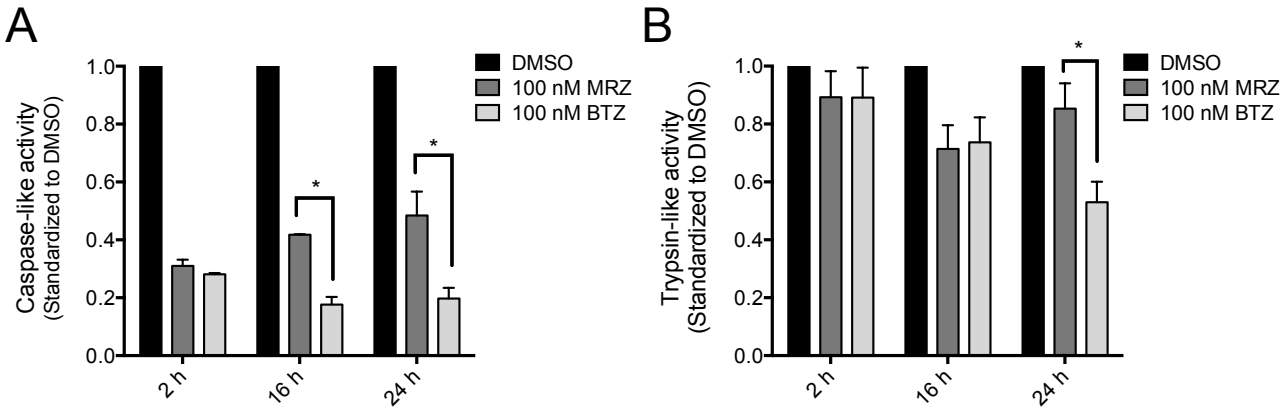

Figure 2.2: Inhibition of caspase-like and trypsin-like proteasome activity by MRZ and BTZ in GBM cells. A) Caspase-like proteasome activity in LN18 cells treated with 100 nM proteasome inhibitors measured using the fluorogenic substrate z-LLE-amc (*p < 0.05). B) Trypsin-like proteasome activity in LN18 cells treated with 100 nM proteasome inhibitors measured using the fluorogenic substrate boc-LRR-amc (*p < 0.05).

16 h after MRZ, but not BTZ, treatment. Both drugs had only slight effects on trypsin-like activity, with BTZ inducing a greater decrease in activity at 24 h.

To confirm that the changes in proteasome activity that I observed were translating into functional effects in cells, I examined levels of ubiquitin and the proteasome substrate p27, both of which should accumulate after proteasome inhibition. LN18 cells were treated for 4 h and 16 h with doses of BTZ and MRZ that were found to cause DNA fragmentation in 50% of cells (290 nM MRZ and 15 nM BTZ; see Chapter 3, Fig. 3.2). Lysates were then probed for ubiquitin and p27 (Fig. 2.3). Ubiquitin accumulation occurred at both 4 h and 16 h, and accumulation of p27 was observed at 16 h. This confirms that the proteasome inhibitors decreased proteasome activity and caused accumulation of proteasome substrates.

The time courses of proteasome inhibition indicated that proteasome activity recovered in cells treated with MRZ, while BTZ led to more sustained decreases in activity. This was unexpected given the fact that MRZ is an irreversible inhibitor, while BTZ is slowly reversible, which should mean that MRZ causes more sustained inhibition of the proteasome. To see whether the increased proteasome activity in MRZ-treated cells was associated with compensatory upregulation of proteasome subunit expression, protein levels of the catalytic subunit β5 (PSMB5) were examined by Western blot (Fig. 2.4). Levels of β5 were unchanged from 1 h to 24 h following treatment with either BTZ or MRZ. To further examine this phenomenon, I evaluated whether drug efflux or differences in the ability of the inhibitors to bind proteasomes could explain the recovery of activity in MRZ-treated cells.

To examine efflux, I used verapamil, an inhibitor of the P-glycoprotein efflux pump that has been shown to reverse efflux-mediated chemotherapy resistance [140]. LN18 cells were pre-treated for 30 min with verapamil, followed by 48 h treatment with MRZ, BTZ, or

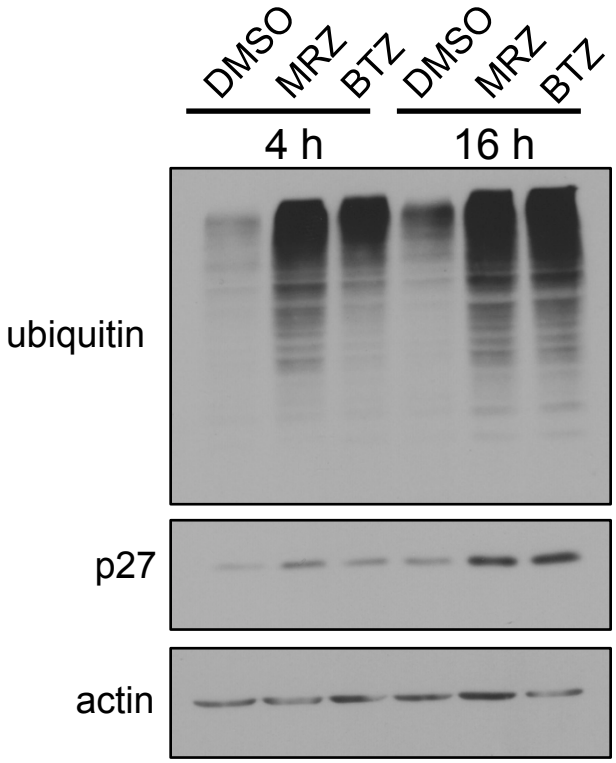

Figure 2.3: Accumulation of ubiquitin tagged proteins and p27 after proteasome inhibition. Lysates from LN18 cells treated 4 or 16 h with 290 nM MRZ or 15 nM BTZ were probed for ubiquitin and p27.

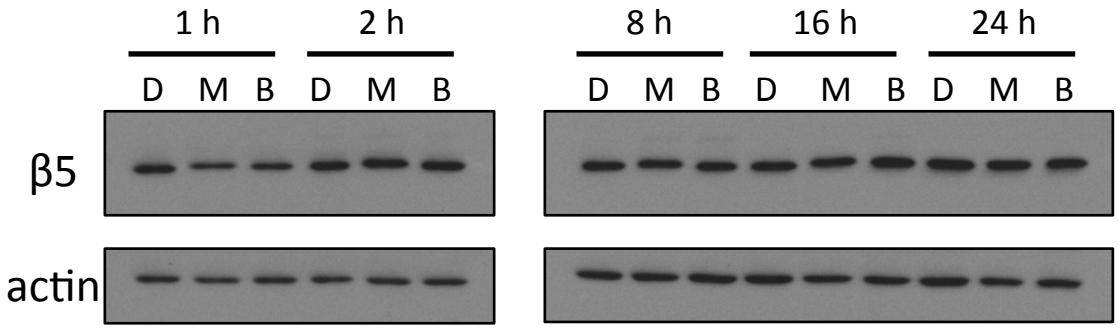

Figure 2.4: Levels of proteasome subunit β5 after treatment with proteasome inhibitors. Lysates from LN18 cells treated for various times with DMSO (D), 100 nM MRZ (M) or 100 nM BTZ (B) were probed for protein expression of the proteasome subunit β5.

the known P-glycoprotein substrate bis-chloroethylnitrosourea (BCNU). After treatment, DNA fragmentation was analyzed by flow cytometric analysis of cells stained with propidium iodide; the subdiploid population was gated for the analysis. By this method, I found that verapamil did increase the amount of DNA damage caused by BCNU, indicating that verapamil blocked BCNU efflux. However, verapamil pre-treatment did not significantly enhance DNA fragmentation in cells treated with either MRZ or BTZ (Fig. 2.5). This indicates that efflux in this manner is not a major mechanism that attenuates the effect of these drugs.

Next, I examined the proteasome binding ability of these drugs in cellular lysates. LN18 cells were lysed by freezing and thawing on dry ice in 20S proteasome lysis buffer (described for proteasome activity assay in the Methods section), which is a gentle lysis that keeps proteasome core particles intact. Lysates were then incubated for 1, 4, or 24 h with BTZ and MRZ. In the lysates, both BTZ and MRZ caused sustained proteasome inhibition with nearly identical kinetics (Fig. 2.6). Notably, there was no recovery of proteasome activity in MRZ-treated cell lysates.

Together, this data indicates that both BTZ and MRZ have equal capacity for proteasome inhibition in cell lysates, and that efflux through P-glycoprotein does not significantly attenuate either drug. Therefore, it is possible that MRZ is modified or metabolized in the whole cell environment in a way that prevents it from having a sustained effect on proteasomes. This could involve modifications that inactivate MRZ or drug breakdown.

To further examine the kinetics of proteasome inhibition by BTZ and MRZ, I also examined inhibition of proteasome activity and induction of death caused by brief exposure

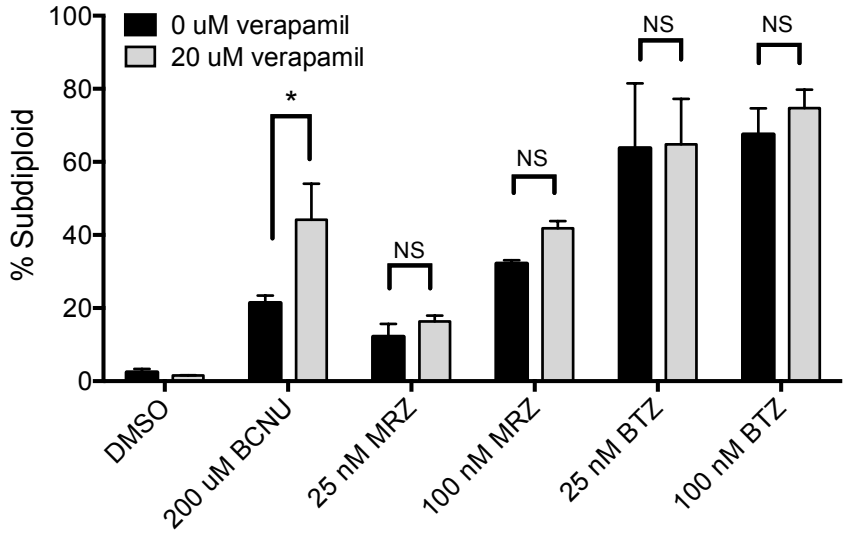

Figure 2.5: Drug efflux through P-glycoprotein does not affect proteasome inhibitor efficacy. LN18 cells were pre-treated for 30 min with verapamil, followed by treatment with proteasome inhibitors or the known P-glycoprotein substrate BCNU for 48 h. Cells were stained with propidium iodide, and DNA fragmentation was assessed.

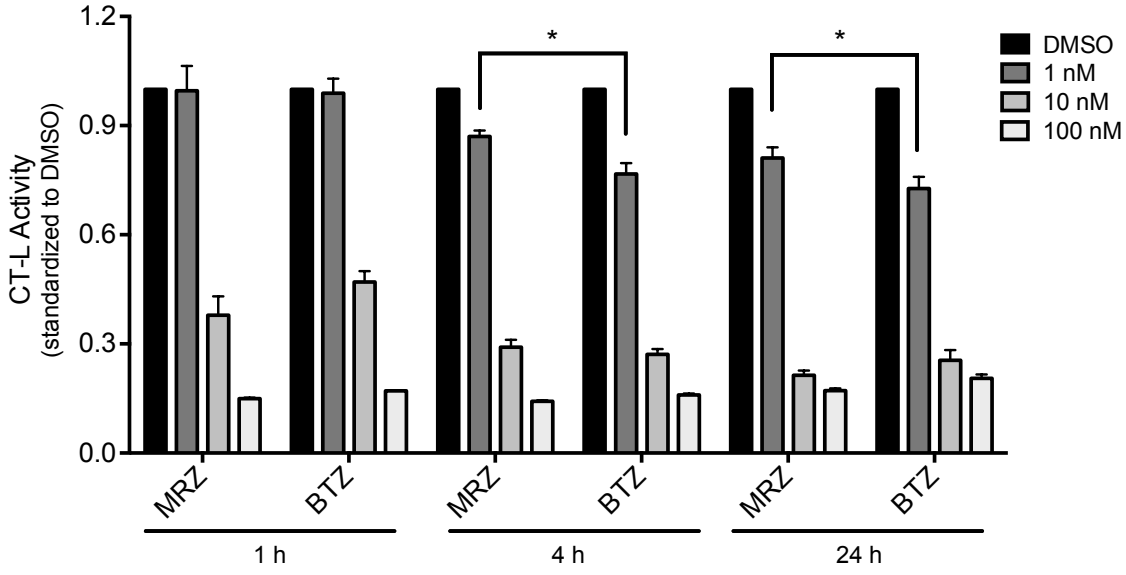

Figure 2.6: MRZ and BTZ cause equivalent levels of proteasome inhibition in cell lysates. LN18 cells lysed in 20S proteasome lysis buffer were plated in a 96-well plate. They were then treated with varying concentrations of proteasome inhibitors, and CT-L activity was assessed at 1, 4, and 24 h. The only significant differences are indicated on the graph (*$p < 0.05$); all other comparisons between MRZ and BTZ were not significant ($p > 0.05$).

of cells to proteasome inhibitors. It is likely that pulse treatment of cells, followed by drug washout, more closely resembles the way the drugs work *in vivo* than a continuous treatment model. The ability of a short exposure time to cause sustained effects could be important for *in vivo* efficacy. LN18 cells were treated for various lengths of time with proteasome inhibitors: 2, 4, 6, 8, 16, or 24 h (Fig. 2.7A). The treatment time indicated in Fig. 2.7A represents the time of drug exposure. After that time, the media with the drug was aspirated, wells were washed 2X with PBS, and fresh media was added to each well for the remaining time until 24 h total. For example, the "2 h" cells were treated with proteasome inhibitors for 2 h, then the drug was washed out and replaced with fresh media for an additional 22 h before harvesting and assessment of proteasome activity. Using this method, I found that all exposure times (2–24 h) caused similar levels of proteasome inhibition for MRZ, indicating a potent effect even after short pulse treatment. However, longer BTZ treatment times led to progressively greater degrees of proteasome inhibition. Treatment with BTZ for around 8 h was required to achieve the levels of inhibition seen with MRZ after 2 h. This indicates that MRZ is a more effective agent for short exposure times.

The effects on proteasome inhibition were mirrored in the results for cell death after washout treatment. For analysis of death, cells were treated for indicated times, then fresh media was added until cells reached a total incubation time of 48 h. MRZ caused similar levels of DNA fragmentation in cells treated for 2 to 24 h, while BTZ caused increasing amounts of DNA fragmentation with longer exposure times (Fig. 2.7B). Notably, BTZ is capable of causing slightly greater levels of DNA fragmentation overall, but requires longer exposure times than MRZ to cause significant death. Therefore, while BTZ is the more

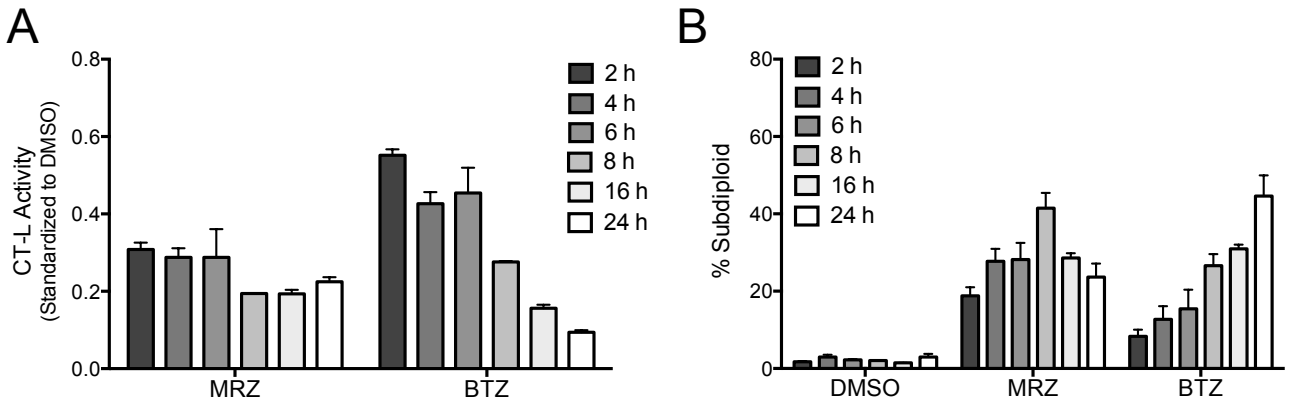

Figure 2.7: MRZ causes stronger proteasome inhibition and more DNA fragmentation than BTZ after short pulse treatments. A) LN18 cells treated with 100 nM proteasome inhibitors for 2–24 h. After indicated time of treatment, drug was removed and fresh media was added to wells. CT-L activity was assessed after a total time of 24 h (treatment + post-washout) for all samples. B) LN18 cells were treated with 100 nM proteasome inhibitors for indicated times, following which drug was removed and fresh media was added to wells. After a total time of 48 h, DNA fragmentation was assessed by propidium iodide staining.

potent inhibitor under continuous conditions, MRZ may be more effective in a washout system that more closely mirrors clinical conditions.

The long-lasting proteasome inhibition caused by MRZ in other model systems has generally been attributed to its properties as an irreversible inhibitor, which is due to the presence of a chloride leaving group. To further study the mechanism of MRZ, several analogs of MRZ were developed that either have leaving groups (LG analogs) or do not have leaving groups (non-LG analogs) [60]. Studies have found that the LG analogs do in fact cause longer lasting proteasome inhibition and greater cell death in leukemia [61]. Since GBM cells continuously treated with MRZ recover proteasome activity, I used the LG and non-LG analogs to see if the irreversible nature of MRZ was still distinguishable from non-LG analogs. Preliminary experiments with MRZ analogs indicated that the LG analogs, including MRZ, did cause stronger proteasome inhibition that was more sustained (at 24 h) compared to the group of non-LG analogs in LN18 cells (Fig. 2.8A). While the LG analogs had some recovery of proteasome activity at 24 h, it was less pronounced than the recovery observed with non-LG analogs. LN18 cells were also examined for viability by trypan blue exclusion after 48 h of treatment. In this case, the LG-analogs caused decreases in viability, while the non-LG analogs did not (Fig. 2.8B). This data demonstrates that there are clear differences between the irreversible (LG) and reversible (non-LG) analogs of MRZ in GBM cells. Interestingly, BTZ acted more similarly to the irreversible analogs than the reversible analogs both in terms of sustained proteasome inhibition and induction of death (Fig. 2.8A-B).

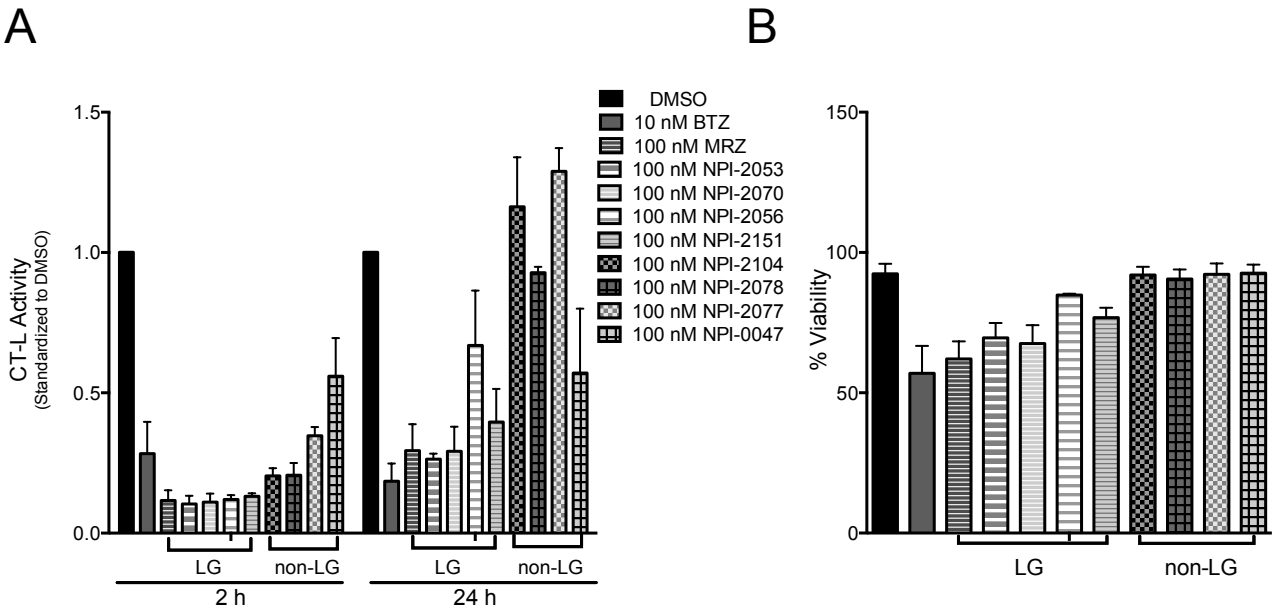

Figure 2.8: Effects of reversible and irreversible MRZ analogs. A) CT-L activity in LN18 cells treated for 2 or 24 h with 10 nM BTZ or 100 nM MRZ and its analogs. B) Viability measured by trypan blue exclusion in LN18 cells treated for 48 h with 10 nM BTZ or 100 nM MRZ and its analogs. (LG = leaving group).

Immunoproteasome expression, correlation with survival, and specific targeting in GBM.

Though immunoproteasome subunits are not highly expressed in normal brain, a past report indicated upregulation of these proteins in a subset of GBM patient specimens by IHC [40]. The immunoproteasome has a distinct profile of protein cleavage characterized by increased cleavage after hydrophobic residues [39] and has also been shown to be important for degradation of oxidatively damaged proteins [141]. Therefore, the immunoproteasome could be an interesting new target in GBM cells.

I first examined expression of the immunoproteasome subunit LMP7 (β5i) in a panel of GBM cells as well as a normal human astrocyte line that was immortalized using the human papilloma virus genes E6/E7 and telomerase reverse transcriptase. I observed variable levels of LMP7 protein expression in the GBM panel (Fig. 2.9A). I also mined data from the REMBRANDT database and found that levels of immunoproteasome subunit gene expression was increased in the set of 228 GBM specimens compared to 28 non-tumor controls, particularly for β1i and β5i (Fig. 2.9B). Expression of β5i also correlated with glioma patient outcomes (Fig. 2.10). Patients with up-regulation of β5i had significantly shorter survival times compared to patients with down-regulation. Together, this information establishes the immunoproteasome as a potential therapeutic target in GBM.

To explore the role of the immunoproteasome in GBM, I obtained the specific immunoproteasome inhibitor ONX-0914 (formerly PR-957). I first treated GBM cells with pulse treatment of ONX-0914, followed by drug washout and examination of DNA fragmentation after a total of 48 h. I found that GBM cells were fairly resistant to ONX-0914, with less than 30% DNA fragmentation seen after the longest pulse treatment (24 h) in both

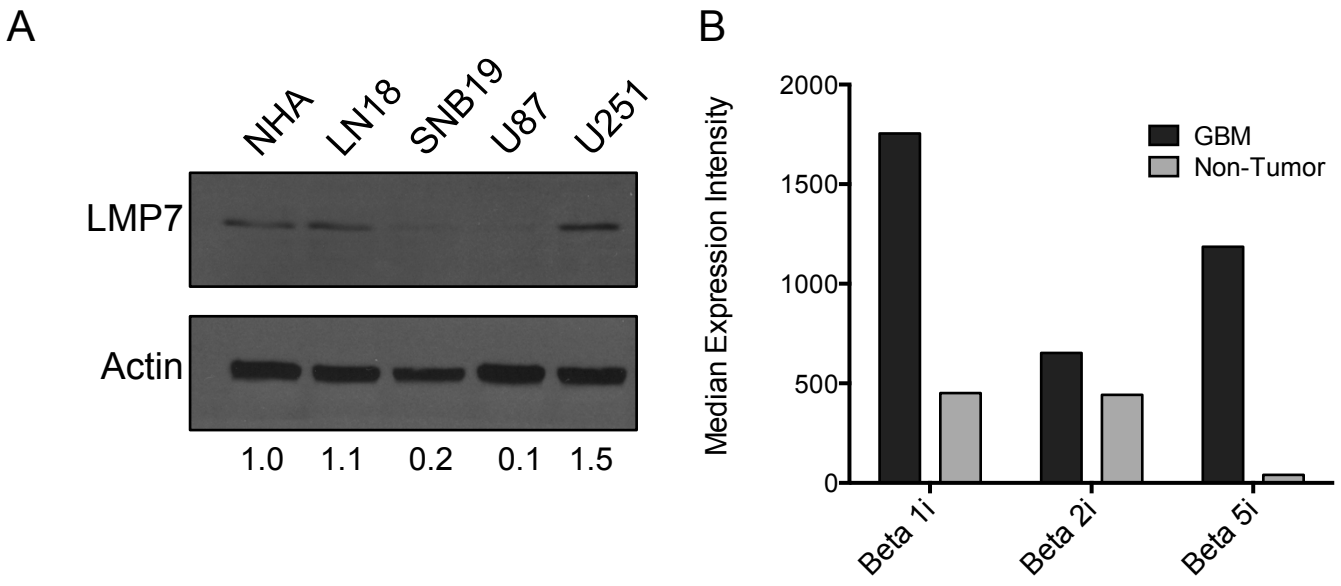

Figure 2.9: Immunoproteasome expression in GBM cells and patient samples. A) The i-proteasome subunit LMP7 is expressed at varying levels in a panel of GBM cell lines and normal human astrocytes. B) Gene expression data from REMBRANDT in 228 GBM and 28 non-tumor specimens reveals increased expression of i-proteasome subunits in GBM samples versus non-tumor controls.

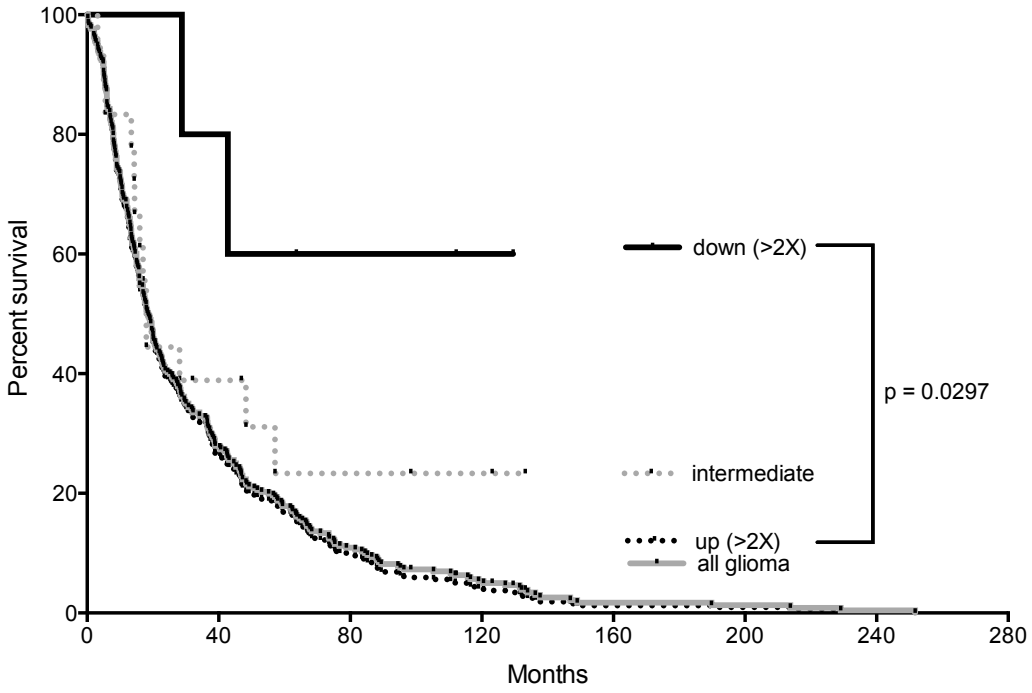

Figure 2.10: Decreased expression of the immunoproteasome subunit LMP7 correlates with increased survival in GBM patients. Survival analysis of glioma patients stratified based on their expression level of LMP7. LMP7 was up-regulated (>2X) in 320 specimens, down-regulated (<2X) in 5 specimens, and intermediately expressed in 18 patients. There was a significant difference in survival between patients with up-regulated versus down-regulated LMP7 ($p = 0.0297$).

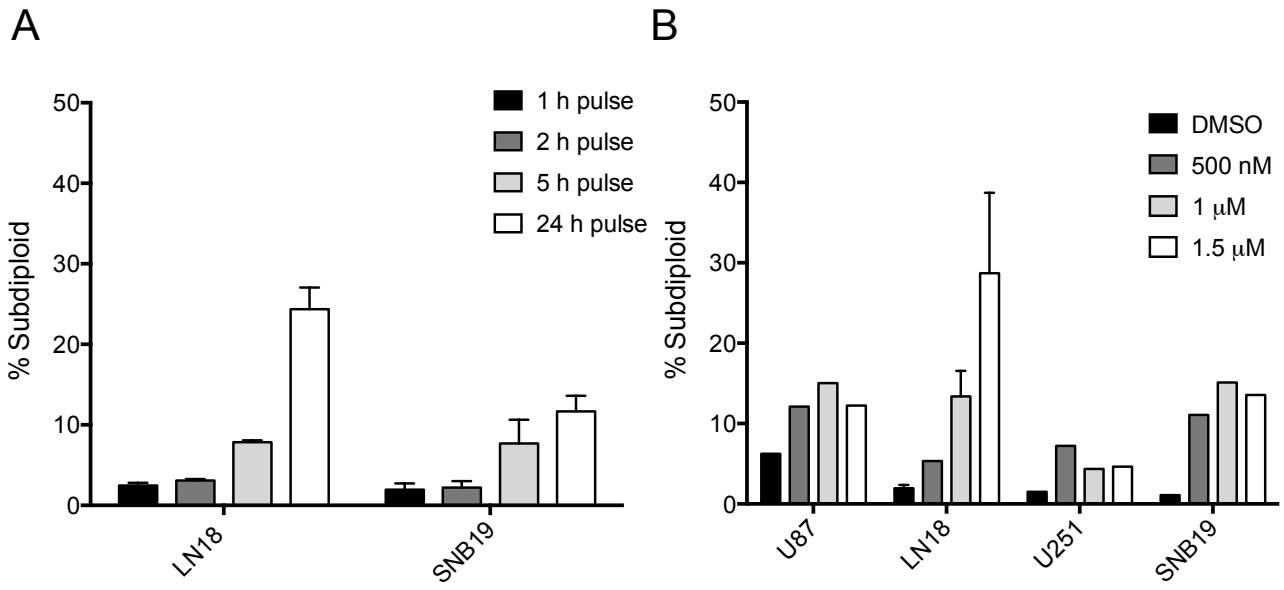

Figure 2.11: The immunoproteasome inhibitor ONX-0914 induces death in GBM cells with continuous exposure to high dose. A) GBM cell lines pulse-treated with 1.5 μM ONX-0914. Following pulse time, drug was removed and fresh media was added. DNA fragmentation was assessed after a total incubation time of 48 h. B) A panel of GBM lines treated with increasing doses of ONX-0914 continuously for 48 h.

LN18 and SNB19 cells (Fig. 2.11A). To further test the potential of ONX-0914, I examined DNA fragmentation after continuous treatment with increasing doses of the drug (500 nM–1.5 μM) in U87, LN18, U251, and SNB19 GBM cells. Even with continuous treatment, high doses of ONX-0914 caused only minor increases in DNA fragmentation. Notably, the expression level of β5i did not correlate with sensitivity, as U251 cells had the highest expression level (Fig. 2.9A), but were not sensitive to ONX-0914.

To ensure that I was achieving complete and selective inhibition of β5i, I performed experiments in collaboration with Onyx Pharmaceuticals. They have developed an enzyme-linked immunosorbent assay (ELISA)-based method for determining specific inhibition of each proteasome and immunoproteasome subunit in cell lysates [142]. Using this method, I was able to assess specific proteasome inhibition of β5 versus β5i. A low, 250 nM dose of ONX-0914 caused nearly complete inhibition of LMP7 after 1 h and 24 h of treatment in LN18 cells, while causing minimal inhibition of β5 (Fig. 2.12). The 1.5 μM dose of ONX-0914 also had significant effects on β5, especially after 24 h of treatment. This indicates that the 250 nM dose of ONX-0914 is sufficient to cause complete inhibition of β5i, while the 1.5 μM dose is less specific. Since the higher dose of ONX-0914 was required to induce DNA fragmentation (Fig. 2.11B), this suggests that specific inhibition of the immunoproteasome itself is insufficient to cause DNA fragmentation in GBM cells.

This is perhaps unsurprising, as the proteasome pool in cells likely contains both standard and immunoproteasomes, and targeting them both in combination may be a more effective strategy. Therefore, I tested combinations of the standard proteasome inhibitors BTZ and MRZ in combination with ONX-0914 at doses that were selective for the immunoproteasome. Combining these agents did not cause strong increases in DNA

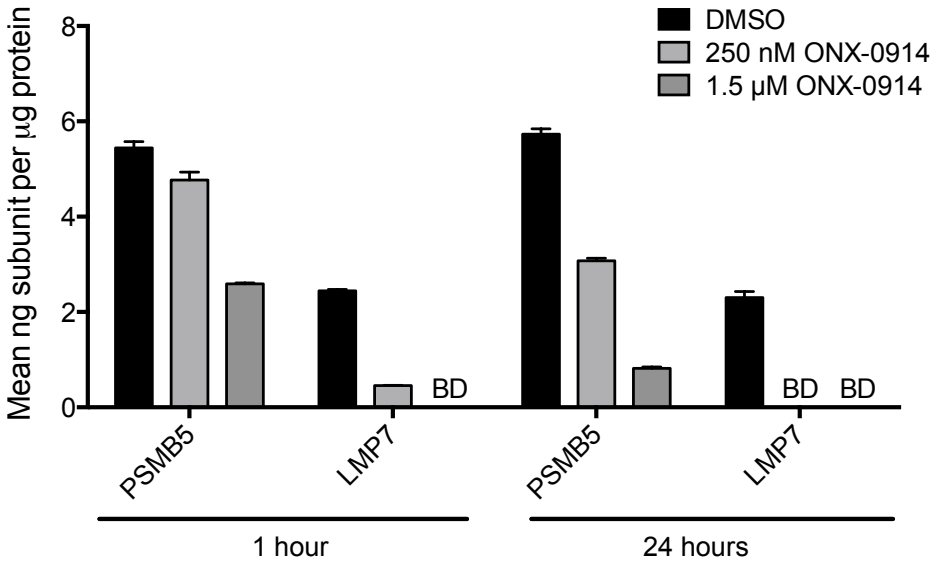

Figure 2.12: ONX-0914 specifically inhibits LMP7 at certain low doses. Inhibition of PSMB5 and LMP7 in LN18 cells treated for 1 or 24 h with ONX-0914 measured using the ELISA-based ProCISE assay.

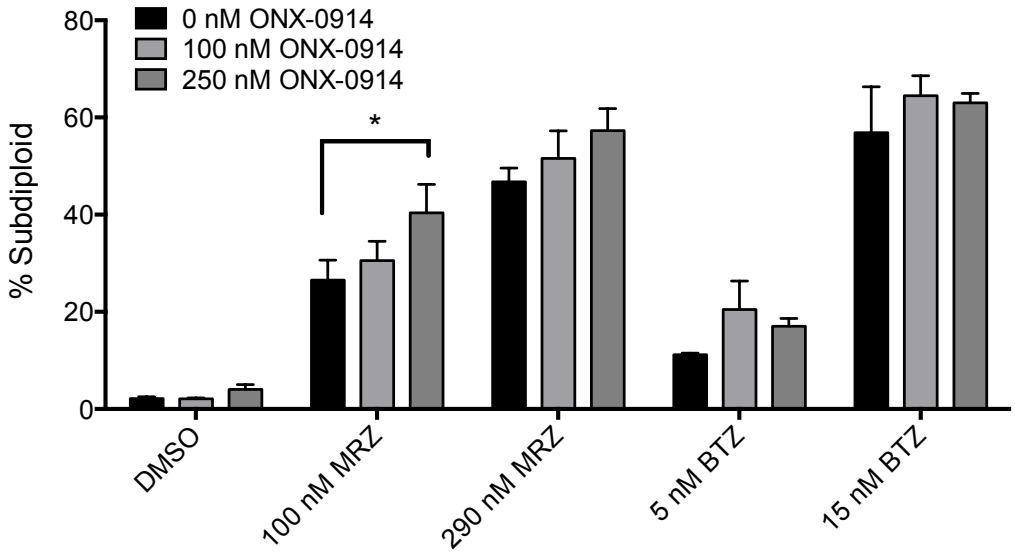

Figure 2.13: ONX-0914 does not synergize with standard proteasome inhibitors. LN18 cells treated 48 h with combinations of standard proteasome inhibitors (MRZ and BTZ) and the i-proteasome inhibitor ONX-0914. DNA fragmentation was assessed by propidium iodide staining. All comparisons between proteasome inhibitor alone and the combinations were not significant ($p > 0.05$), except for the combination of 100 nM MRZ and 250 nM ONX-0914 (*$p = 0.05$).

fragmentation (Fig. 2.13), indicating that this combination did not lead to strong potentiation of cell death in GBM lines.

Targeting PA28γ in GBM.

Studies have also found that the proteasome regulatory subunit PA28γ is highly expressed in the brain [35]. To examine whether PA28γ affected sensitivity to proteasome inhibitors, I compared the sensitivity of wild-type mouse embryonic fibroblasts (MEFs) to PA28$\gamma^{-/-}$ MEFs. After 48 h of treatment with BTZ and MRZ, I examined DNA fragmentation and found that PA28$\gamma^{-/-}$ MEFs showed similar sensitivity as wild-type MEFs to both BTZ and MRZ (Fig. 2.14A).

To determine whether PA28γ played a unique role in GBM, I first examined PA28γ expression in a panel of GBM cell lines and found that it was expressed, though at varying levels (Fig. 2.14B). To test whether PA28γ impacted the sensitivity of GBM cells to proteasome inhibition, I first knocked down PA28γ in LN18 cells using transient transfection of siRNA (Fig. 2.14C). After establishing knockdown, I treated these cells with proteasome inhibitors. Knockdown of PA28γ did not significantly alter the sensitivity of LN18 cells to BTZ or MRZ (Fig. 2.14D). Therefore, it appears that inhibition of the proteasome catalytic activities with BTZ or MRZ is not greatly potentiated when combined with knockdown of PA28γ.

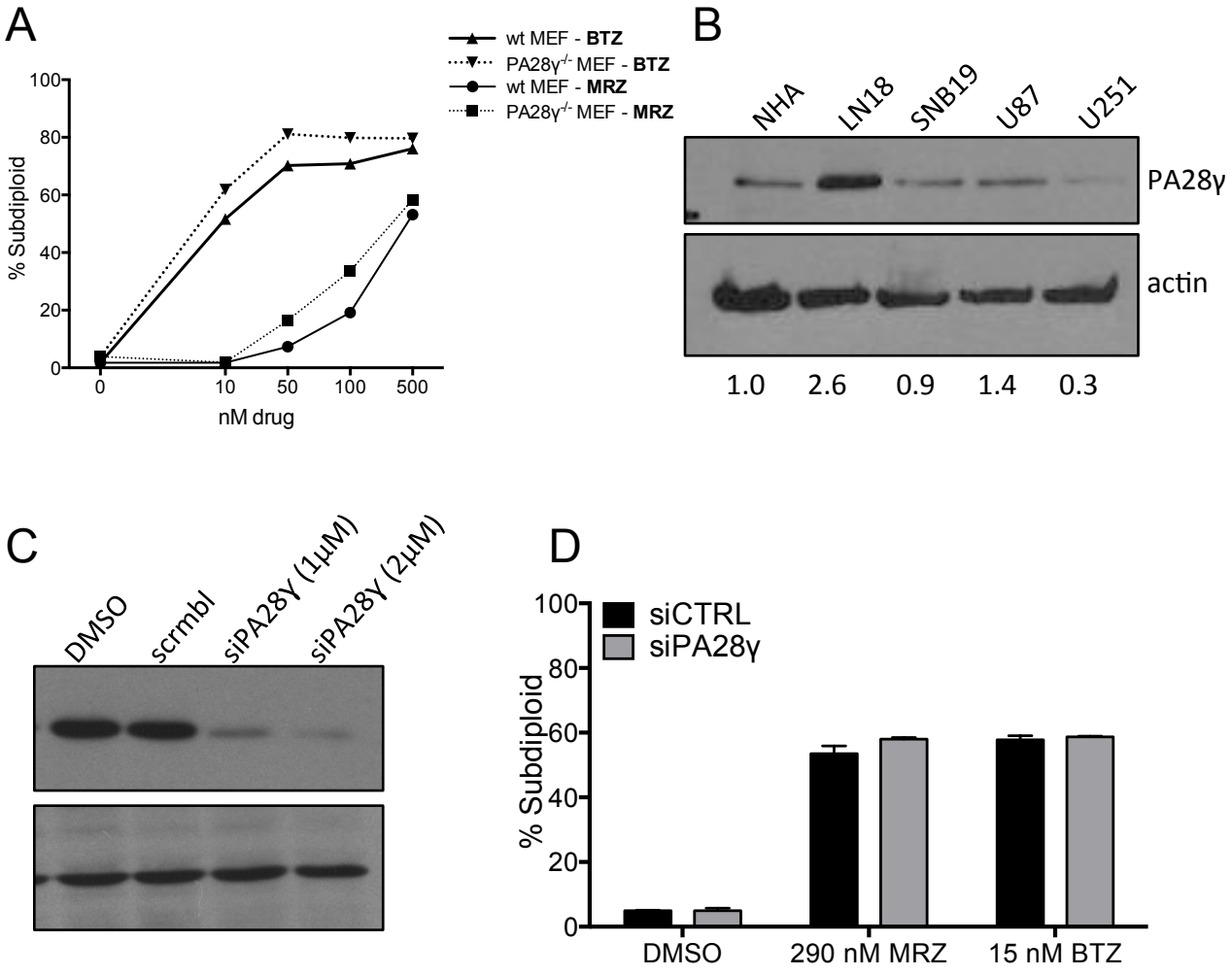

Figure 2.14: Reducing PA28γ does not alter sensitivity to proteasome inhibitors. A) DNA fragmentation in wt MEFs and PA28γ$^{-/-}$ MEFs after proteasome inhibitor treatment. B) Expression of PA28γ in a panel of GBM cell lines. C) Confirmation of knockdown of PA28γ in LN18 cells using siRNA. D) LN18 cells transfected with 2 μg siPA28γ treated with proteasome inhibitors for 48 h, followed by measurement of DNA fragmentation.

Summary

In this chapter, I performed a detailed analysis of the kinetics of proteasome inhibition by the standard proteasome inhibitors BTZ and MRZ, and also examined the potential of targeting various components of the proteasome pool to augment death induction by proteasome inhibitors.

Though both BTZ and MRZ caused strong initial proteasome inhibition, BTZ caused more sustained proteasome inhibition, as cells treated with MRZ started to recover activity by 8 to 16 h. This was unexpected, given the irreversible nature of MRZ. Therefore, I performed a more thorough analysis of the reasons for this dynamic. MRZ potency was unaffected by an inhibitor of P-glycoprotein drug efflux, and MRZ was able to bind and inhibit proteasomes in cell lysates in a manner similar to BTZ. Preliminary experiments with irreversible and reversible analogs of MRZ indicated there was a clear difference between the classes, with irreversibility being important for more sustained proteasome inhibition and effects on viability. Interestingly, BTZ behaved more similarly to the group of irreversible inhibitors in the LN18 GBM cells.

Washout experiments demonstrated that MRZ was able to cause greater proteasome inhibition and DNA fragmentation after short exposures, while BTZ required longer exposure times. This may be an important factor that makes MRZ a more potent clinical inhibitor. Therefore, my hypothesis that MRZ would cause more sustained proteasome inhibition due to its irreversible nature was only true for pulse treatments; with continuous treatment, BTZ was able to more fully block proteasome activity.

In addition to targeting standard subunits, the efficacy of targeting the immunoproteasome was also examined. The immunoproteasome-specific inhibitor ONX-0914 did not strongly induce DNA fragmentation as a single agent. Also, at doses that were specific for immunoproteasome inhibition, ONX-0914 did not potentiate death induction by the standard inhibitors BTZ and MRZ.

The importance of PA28γ in GBM was also examined, and I determined that combined knockdown of PA28γ and treatment with BTZ and MRZ did not lead to strong potentiation of cell death.

Together, the work in this chapter demonstrated that BTZ and MRZ cause strong inhibition of proteasome activity, though with different kinetics. While BTZ is stronger after continuous treatment, MRZ may have greater effects after shorter exposures. Additional targeting of various proteasome components with ONX-0914 or PA28γ siRNA did not significantly augment the effects of BTZ and MRZ, indicating that these drugs alone are the most promising method for targeting the proteasome in GBM.

Chapter 3

Induction of caspase 9-dependent death by BTZ and MRZ and attenuation of death by thiol reducing agents in GBM.

Specific Aim 2: Determine the mechanism of death induction by BTZ and MRZ in GBM.

Having determined the kinetics of proteasome inhibition by BTZ and MRZ in Chapter 2, this chapter focuses on the mechanism of death induced by these inhibitors in GBM cells. Previous studies have indicated that proteasome inhibitors induce caspase-dependent death in other types of cancer [66-68]. I hypothesized that BTZ and MRZ would induce caspases in GBM, and that understanding the hierarchy of caspase activation would help in selection of biomarkers of drug efficacy and prediction of therapeutic resistance. After examining multiple indicators of death induced by proteasome inhibitors, I examined the dependence of this death on caspases. Using chemical inhibitors of caspases as well as siRNA and shRNA knockdown methods, I probed the role of individual initiator caspases: caspases 2, 8, and 9.

I also examined the role of ROS, which has been previously reported as a mechanism of death induction by proteasome inhibitors, on mitochondrial events and cell death. To do this, I used the reducing agents NAC and DTT, as well as direct treatment of cells with the antioxidant GSH ethyl ester (GSHee).

This data provides insight into the mechanism of death induced by proteasome inhibitors in GBM, which is key for providing biomarkers of drug efficacy and for helping anticipate potential mechanisms of resistance. Also, the examination of the role of ROS in proteasome inhibitor-induced death in GBM lends further insight into the mechanism of death and has interesting implications for combined use of proteasome inhibitors with antioxidants for prevention of side effects such as BTZ-induced peripheral neuropathy.

Caspase-dependence of death induction by proteasome inhibitors in GBM.

To examine the ability of proteasome inhibitors to induce death in GBM cells, LN18, SNB19, and U251 GBM cells were treated with increasing doses of BTZ or MRZ for 48 h, followed by analysis of trypan blue exclusion to measure viability. Both BTZ and MRZ decreased viability (Fig. 3.1A). The drug concentrations that caused a 50% decrease in viability, which were determined from the dose-response curves, were in the nanomolar range for both BTZ and MRZ (Fig. 3.1B). BTZ caused death at lower doses than MRZ, as indicated by the significant differences between the IC50 values in all 3 lines. This was consistent with the fact that BTZ produced longer-lasting proteasome inhibition compared to MRZ (Fig. 2.1A-B).

Both MRZ and BTZ also increased DNA fragmentation as measured by staining with propidium iodide followed by flow cytometry analysis of the subdiploid population. BTZ once again caused 50% DNA fragmentation at a lower dose than MRZ (IC50: BTZ = 15 nM, MRZ = 290 nM; Fig. 3.2). To examine the effect of proteasome inhibition, LN18 cells were grown in soft agarose for 5 days, followed by treatment with proteasome inhibitors for 3 days. After the treatment period, colonies were analyzed by multiplying the colony number by the colony volume to reach a value for "biomass." Consistent with results from trypan blue staining and DNA fragmentation analysis, BTZ also caused greater inhibition of colony growth than MRZ (Fig. 3.3).

Previous reports in other models have suggested an important role for caspases in proteasome inhibitor-induced death [62, 68]. To assess whether this is also the case in GBM, I examined caspase cleavage, which is an early step that leads to activation, of the initiator caspases 2, 8, and 9 in LN18 cells treated with MRZ or BTZ for 4, 8, 12, or 16 h.

A

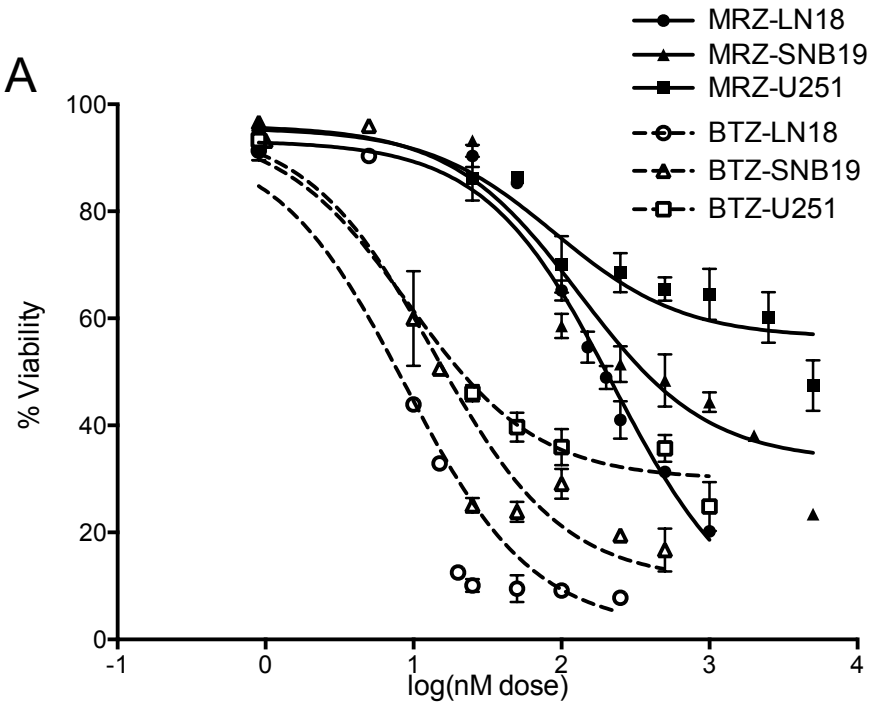

B

Cell line	**MRZ** IC50 (nM)	**BTZ** IC50 (nM)	p-value
LN18	221.4	8.8	<0.05
SNB19	131.4	13.86	<0.05
U251	89.7	9.2	<0.01

Figure 3.1: Reduction in cell viability after proteasome inhibitor treatment in GBM cell lines. A) LN18, SNB19, and U251 GBM cells treated for 48 h with proteasome inhibitors. Viability was determined by trypan blue exclusion. B) IC50 values calculated from (A) and p-values showing significant differences between MRZ and BTZ for each cell line.

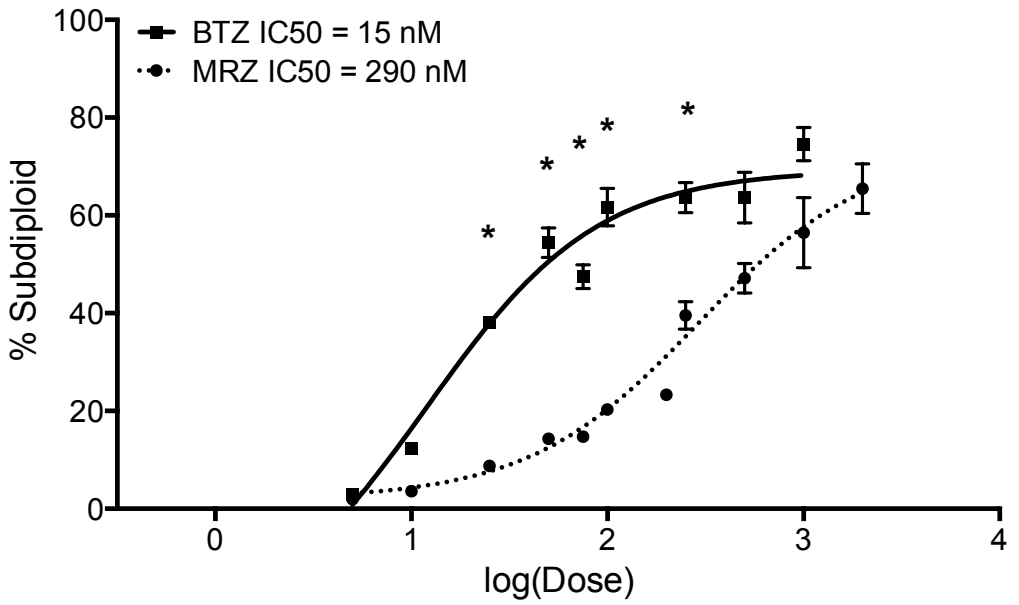

Figure 3.2: Induction of DNA fragmentation by proteasome inhibitors. LN18 cells were treated 48 h with proteasome inhibitors, followed by staining with propidium iodide for analysis of DNA fragmentation (*$p < 0.05$).

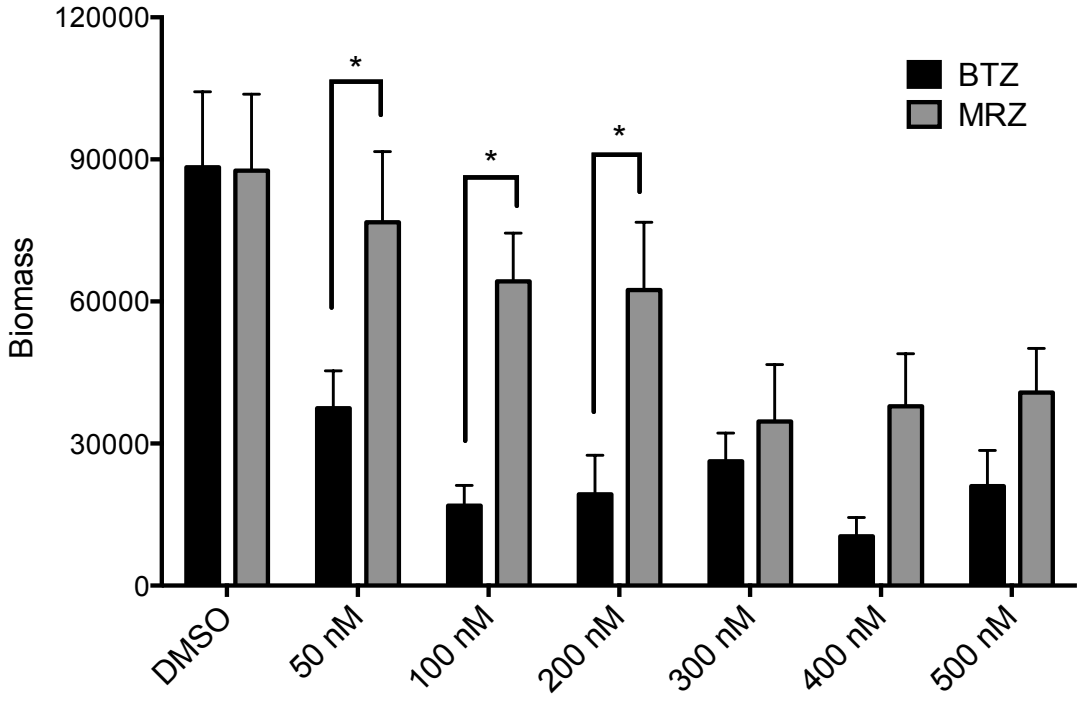

Figure 3.3: Reduction in colony growth by proteasome inhibitors. LN18 cells were grown in soft agarose for 5 days, followed by 3 days of treatment with proteasome inhibitors. Biomass was calculated as the number of colonies multiplied by colony volume (*$p < 0.05$).

Intermediate cleavage bands, which indicate the initial processing of caspases that often leads to activation, were visible for all 3 initiator caspases after treatment with BTZ and MRZ (Fig. 3.4A). Notably, caspase 2 was cleaved early (4 h), particularly with MRZ treatment, whereas caspases 8 and 9 were cleaved later (8–12 h). Activity of the executioner caspases 3/7 was also measured using a fluorogenic substrate for these caspases, DEVD-amc. Caspase 3/7 activity was detected 16–24 h following treatment with BTZ and MRZ (Fig. 3.4B).

To assess whether caspases were necessary for cell death, DNA fragmentation was assessed in LN18 cells pre-treated with the pan-caspase inhibitor z-VAD-fmk. This inhibitor blocked nearly all of the DNA fragmentation induced by BTZ and MRZ, indicating that caspases play a crucial role in death induction by proteasome inhibitors in GBM cells (Fig. 3.5).

Early cleavage of caspase 2 by proteasome inhibitors may impede death.

Since caspase 2 was cleaved early after proteasome inhibition (4 h after MRZ treatment), I further examined the role of caspase 2 in proteasome inhibitor-induced death. To confirm whether the caspase 2 cleavage I observed represented caspase 2 activation following proteasome inhibition, I employed a more direct method for assessing caspase 2 activation. I used a system in which LN18 cells were transfected with a mitochondrial marker (dsRed mito) as well as plasmids encoding 2 halves of the Venus bimolecular fluorescence (BiFC) protein fused to caspase 2 CARD domains. Caspase 2 recruitment to activation platforms is required for its activation, and this brings the CARD domains attached to Venus BiFC into induced proximity and joins together the halves of the Venus BiFC protein; therefore, activation of caspase 2 causes Venus BiFC fluorescence. This is a novel

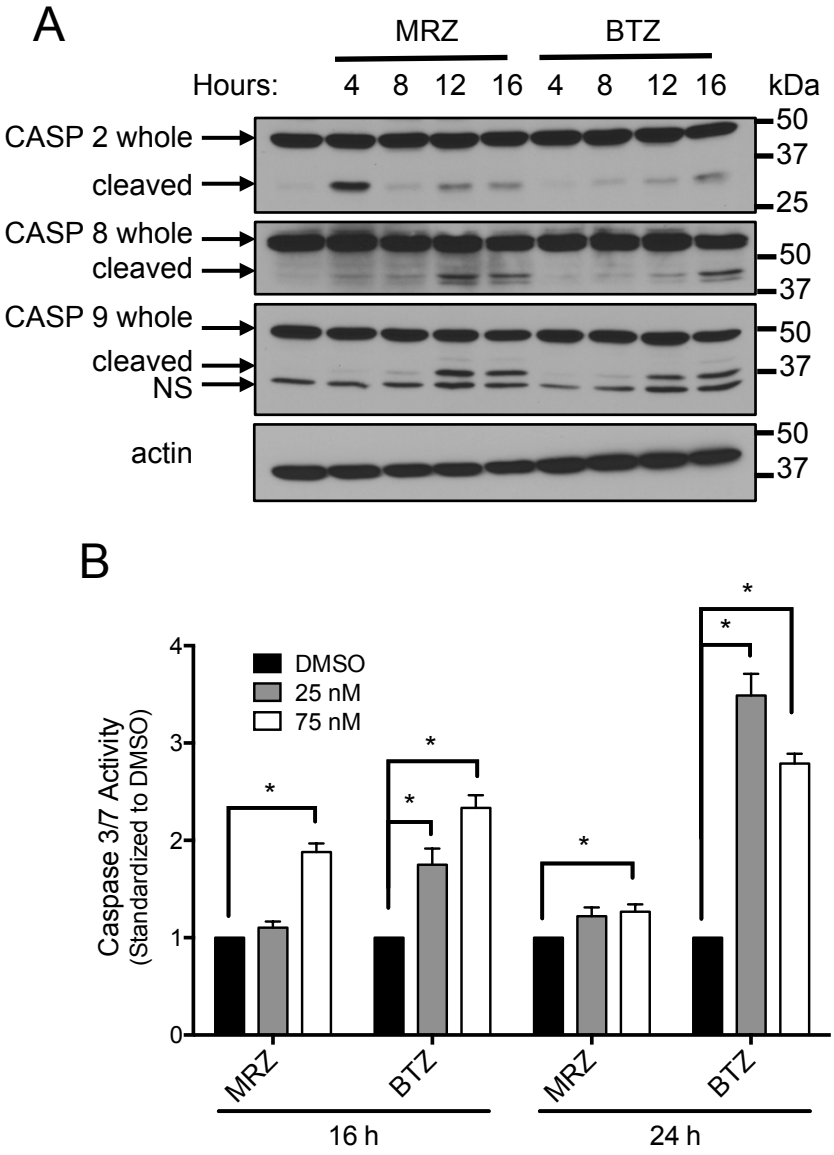

Figure 3.4: Activation of caspases by protesaome inhibitors. A) Western blot showing cleavage of initiator caspases 2, 8, and 9 after treatment of LN18 cells with 100 nM MRZ and BTZ. B) Caspase 3/7 activity measured using the fluorogenic substrate DEVD-amc 16 and 24 h following treatment of LN18 cells with MRZ and BTZ.

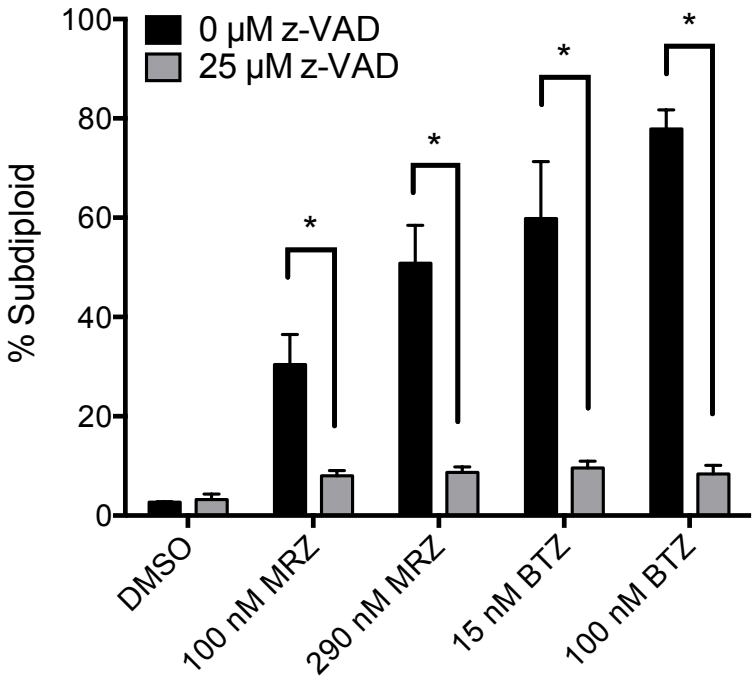

Figure 3.5: Pan-caspase inhibition prevents DNA fragmentation caused by proteasome inhibitors. LN18 cells were pre-treated 30 min with the pan-caspase inhibitor z-VAD-fmk, followed by 48 h treatment with proteasome inhibitors. DNA fragmentation was analyzed by propidium iodide staining.

technique that allows for live imaging of a definitive step in caspase activation, giving a clear readout of caspase 2 activation signaling. Using this fluorescence microscopy-based system, a video was recorded of LN18 cells treated with MRZ, BTZ, or another proteasome inhibitor, carfilzomib (CFZ). The video is composed of images taken of individual cells every 5 minutes for 8 h. Representative images in Figure 3.6A show the appearance of caspase 2 BiFC fluorescence (green) against the background of the mitochondrial fluorescence (red). The average Venus fluorescence intensity was quantified for multiple cells over the course of 8 h (Fig. 3.6B). This analysis revealed that both MRZ and BTZ induced caspase 2 BiFC, indicating that both inhibitors induced caspase 2 activation. MRZ induced caspase 2 activation slightly earlier than BTZ, and CFZ only caused very low levels of caspase 2 activation.

To examine the importance of caspase 2 in proteasome inhibitor-induced death, 2 separate siRNA sequences were used to transiently reduce caspase 2 in LN18 cells (Fig. 3.7A). After transfection with siCASP2, cells were then treated with proteasome inhibitors. Knockdown of caspase 2 did not significantly alter DNA fragmentation induced by either BTZ or MRZ (Fig. 3.7B). Similarly, siCASP2 did not significantly impact the reduction in viability caused by BTZ and MRZ (Fig. 3.7D).

In previous studies, active caspase 2 induced mitochondrial membrane permeability and activation of caspase 9 [74, 75]. However, knockdown of caspase 2 did not reduce cleavage of caspase 9 by Western blot in LN18 cells treated for 16 h with BTZ or MRZ (Fig. 3.7C). Together, this data indicates that transient knockdown of caspase 2 does not impact cleavage of downstream caspase 9 or eventual cell death.

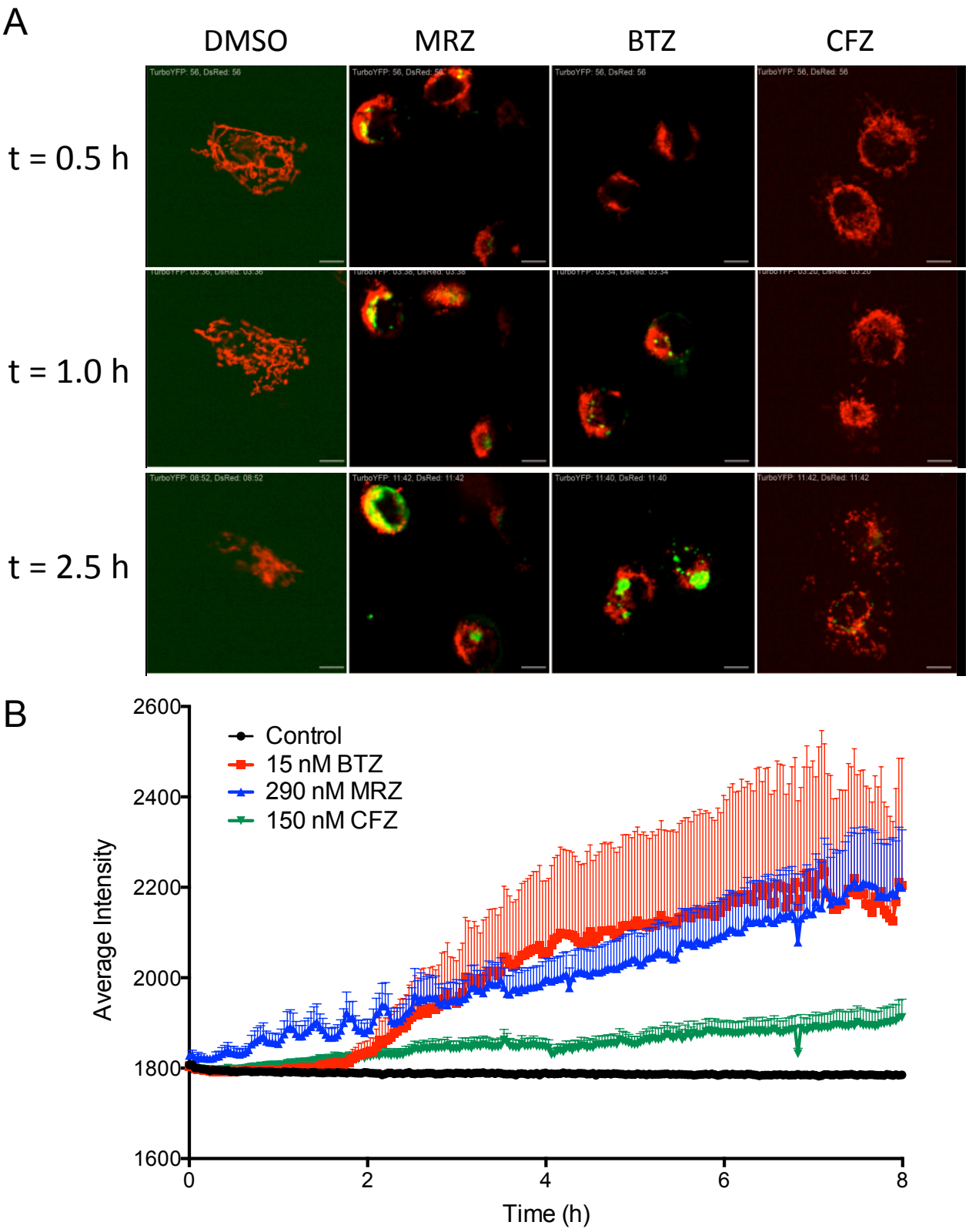

Figure 3.6: Activation of caspase 2 by proteasome inhibitors. A) Still images from live imaging of LN18 cells treated with 290 nM MRZ, 15 nM BTZ, or 250 nM carfilzomib (CFZ). Caspase 2 induced proximity was imaged using the VENUS BiFC-caspase 2-CARD system. Red fluorescence is dsRed mitochondria, YFP is VENUS BiFC-caspase 2. B) Quantification of average intensity of VENUS BiFC from (A) for LN18 cells treated with DMSO (N = 8 cells), BTZ (N = 14 cells), MRZ (N = 13 cells), or CFZ (N=17 cells).

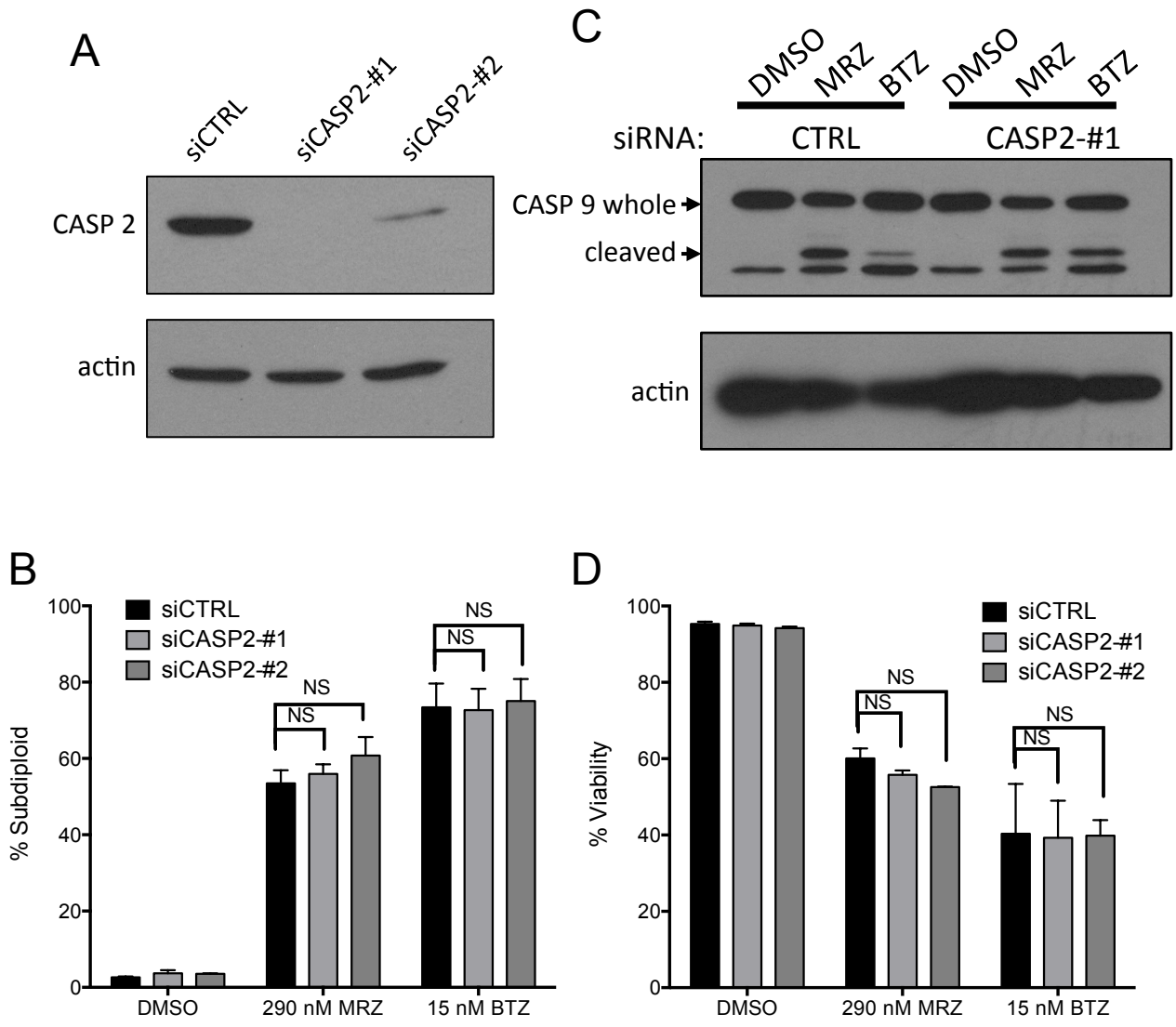

Figure 3.7: Knockdown of caspase 2 with siRNA does not effect sensitivity to proteasome inhibitors. A) Western blot for caspase 2 after lipofection of LN18 cells with siRNA for caspase 2. B&D) After transfection with siCASP2, LN18 cells were treated for 48 h with proteasome inhibitors. Cells were analyzed for DNA fragmentation by propidium iodide staining (B) or viability by trypan blue exlusion (D) (NS = not significant). C) LN18 cells transfected with siCASP2 were treated 16 h with 290 nM MRZ or 15 nM BTZ, and caspase 9 cleavage was assessed by Western blot.

It is possible that the transient nature of the siRNA knockdown was insufficient to fully block caspase 2 activity. Therefore, I generated LN18 cells stably expressing caspase 2 shRNA (Fig. 3.8A). Similarly to the siCASP2, I found that shCASP2 did not block cleavage of other caspases following treatment with BTZ or MRZ. In fact, there was increased cleavage of caspase 9 (Fig. 3.8B) and increased caspase 3/7 activity (Fig. 3.8C) in shCASP2 cells treated with proteasome inhibitors. To see if these increases in caspase activation resulted in changes in death, I measured DNA fragmentation in shCTRL and shCASP2 cells treated for either 24 h (Fig. 3.9A) or 48 h (Fig. 3.9B) with proteasome inhibitors. At both timepoints, there were indications that shCASP2 cells were slightly more sensitive to proteasome inhibitors than shCTRL cells.

To confirm this, the proteasome inhibitor sensitivity of wild-type MEFs and caspase 2 deficient MEFs was examined (Fig. 3.10). There was slightly less DNA fragmentation in caspase 2 deficient MEFs treated with select doses (50 nM MRZ and 100 nM BTZ) of the proteasome inhibitors, but overall, caspase 2 deficiency did not have a large impact on sensitivity to proteasome inhibitors. These results indicate that caspase 2 is not essential for death induction following proteasome inhibition in GBM cells.

Caspase 9 functions upstream of caspase 8 to induce death after proteasome inhibition.

We next examined the initiator caspases 8 and 9, which were both activated 8–12 h following treatment with either BTZ or MRZ (Fig. 3.4A). Previous reports have found differences in the caspase-dependence of death induced by BTZ and MRZ, with MRZ being more dependent on caspase 8 in leukemia, and BTZ being more equally dependent on caspases 8 and 9 in myeloma [68, 143]. Therefore, I set out to examine the specific caspase dependence of these agents in GBM.

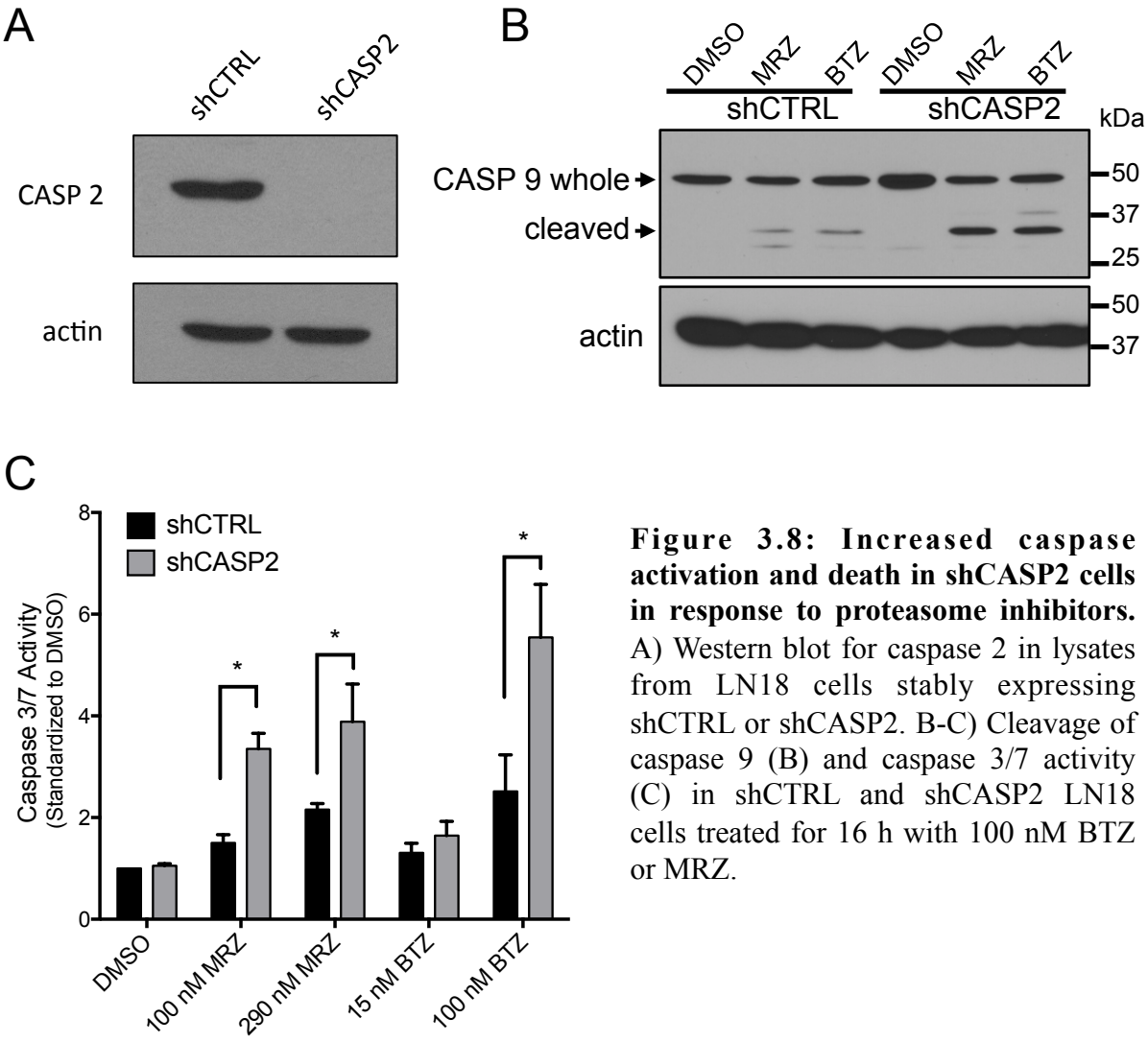

Figure 3.8: Increased caspase activation and death in shCASP2 cells in response to proteasome inhibitors. A) Western blot for caspase 2 in lysates from LN18 cells stably expressing shCTRL or shCASP2. B-C) Cleavage of caspase 9 (B) and caspase 3/7 activity (C) in shCTRL and shCASP2 LN18 cells treated for 16 h with 100 nM BTZ or MRZ.

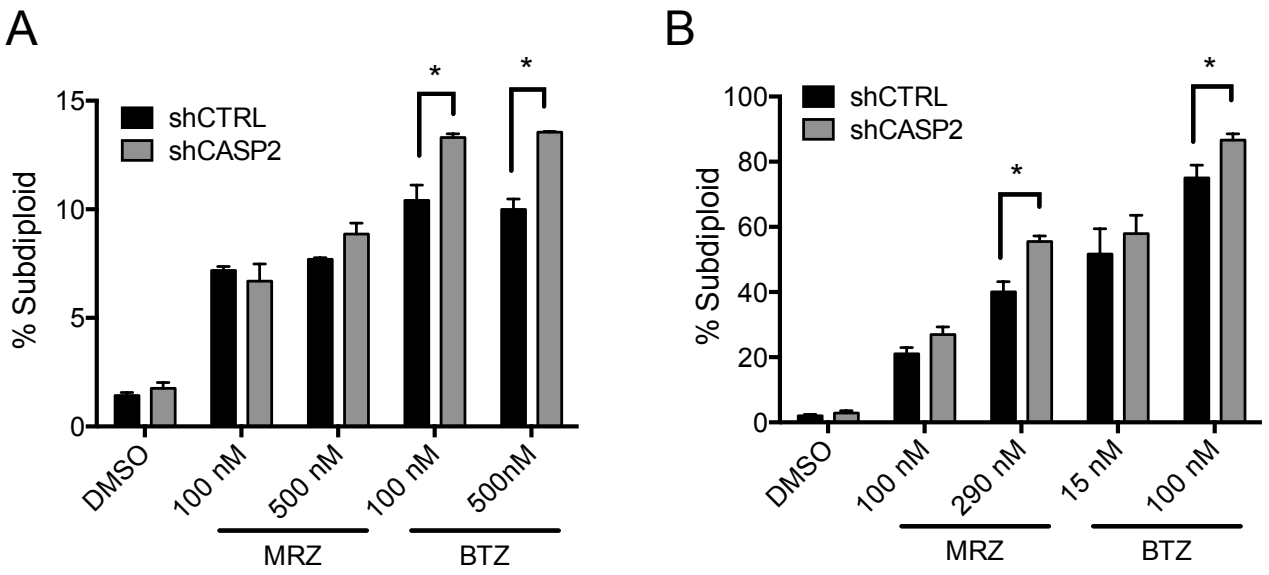

Figure 3.9: Silencing caspase 2 does not prevent proteasome inhibitor-induced death. LN18 cells stably expressing shCTRL or shCASP2 were treated for 24 h (A) or 48 h (B) with MRZ and BTZ, followed by propidium iodide staining for analysis of DNA fragmentation (*$p < 0.05$).

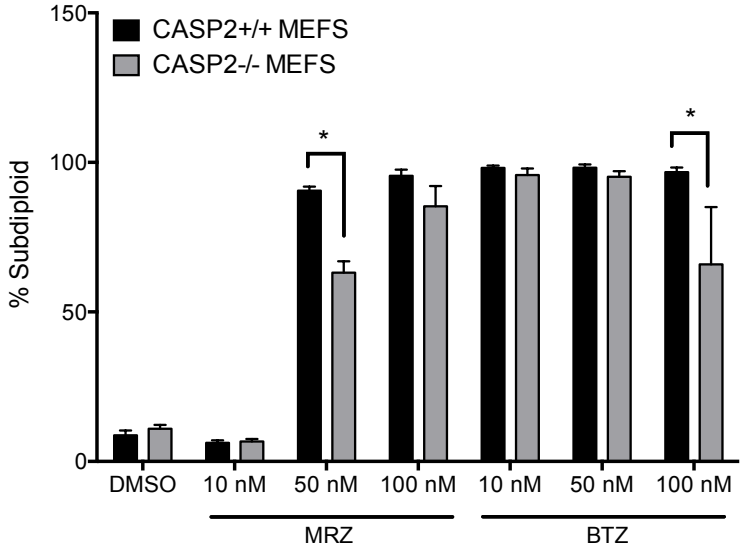

Figure 3.10: Caspase 2 +/+ MEFs and caspase 2 -/- MEFs are similarly sensitive to proteasome inhibitors. Caspase 2 +/+ and -/- MEFs were treated for 48 h with proteasome inhibitors (MRZ and BTZ), followed by propidium iodide staining for analysis of DNA fragmentation (*$p < 0.05$).

LN18 cells pre-treated with specific inhibitors of either caspase 8 (z-IETD-fmk) or caspase 9 (z-LEHD-fmk) were significantly protected from both BTZ- and MRZ-induced DNA fragmentation (Fig. 3.11). To identify whether caspase 8 or 9 was the initiator of the caspase cascade, I examined whether chemical inhibition of either caspase 8 or 9 blocked activation of the other caspase following proteasome inhibition. Notably, these inhibitors block active caspases by acting as specific substrates; therefore, these inhibitors do not prevent initial cleavage and activation of the targeted caspase, but they do bind and inhibit the active caspase to prevent activation of downstream caspases. Using Western blotting to examine cleavage of caspases 8 and 9, I found that inhibition of caspase 8 did not prevent cleavage of caspase 9. However, inhibition of caspase 9 did prevent cleavage of caspase 8 (Fig. 3.12A). Densitometry was used to determine how the specific inhibitors impacted the ratios of cleaved to whole caspases. This analysis confirmed that treatment with the caspase 9 inhibitor did reduce the amount of cleaved caspase 8 (Fig. 3.12B), while treatment with the caspase 8 inhibitor did not reduce caspase 9 cleavage (Fig. 3.12C). Therefore, using chemical inhibitors, I determined that caspase 9 was the initiating caspase upstream of caspase 8 cleavage in LN18 cells.

Caspases have overlapping cleavage site specificities, so chemical inhibitors are not specific for any one caspase family member [144]. Therefore, I confirmed the chemical inhibitor results in cells stably expressing shRNA for caspase 8 or 9. Western blot analysis was used to examine cleavage of caspases 8 and 9 in shCASP8 and shCASP9 cells treated for 16 h with BTZ and MRZ (Fig. 3.13A). Cleavage of caspase 8 was blocked in the shCASP9 cells, which was visible on the Western blot and was confirmed by densitometry analysis that showed a reduction in cleaved caspase 8 in shCASP9 cells (Fig. 3.13B).

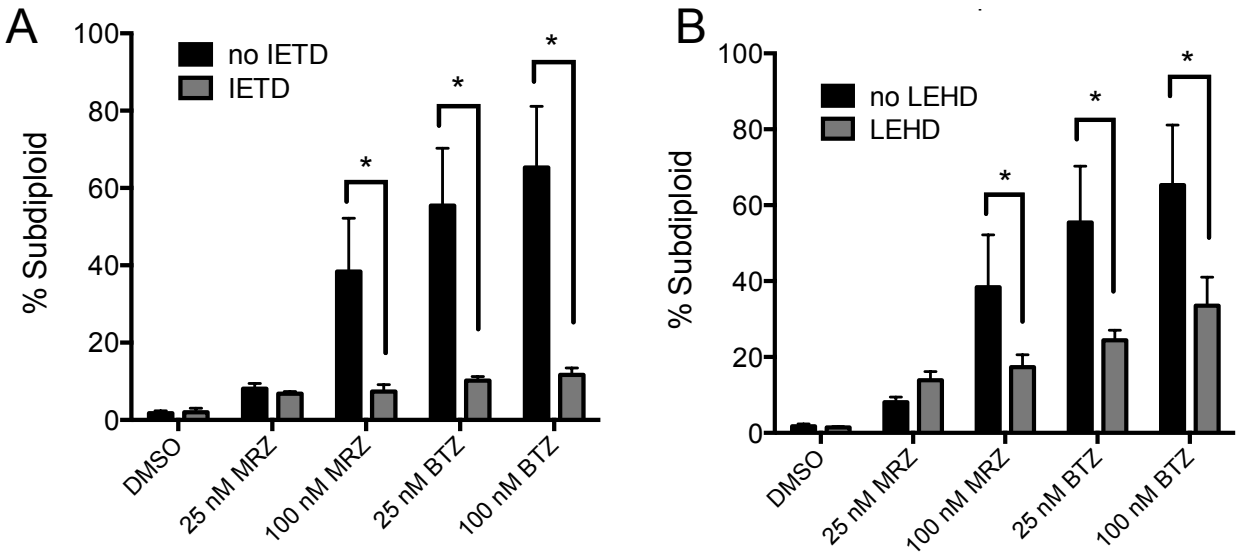

Figure 3.11: Specific inhibition of either caspase 8 or 9 reduces DNA fragmentation caused by proteasome inhibitors. A-B) LN18 cells pre-treated 30 min with 25 μM caspase 8 inhibitor (A, z-IETD-fmk) or caspase 9 inhibitor (B, z-LEHD-fmk) followed by 48 h treatment with proteasome inhibitors. DNA fragmentation was assessed by propidium iodide staining (*$p < 0.05$).

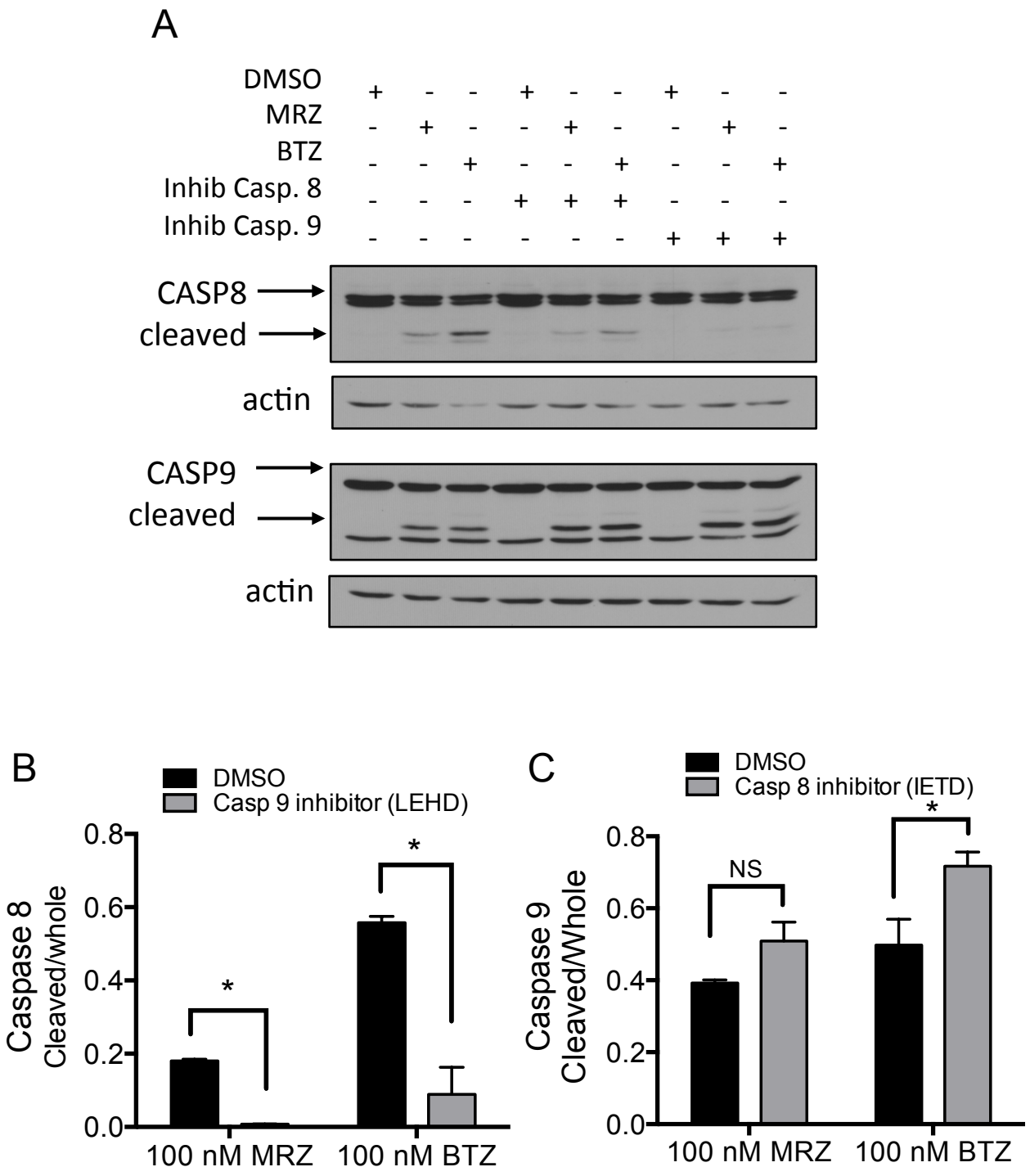

Figure 3.12: Chemical inhibition of caspase 9 prevents cleavage of caspase 8. A) LN18 cells pre-treated for 30 min with 25 μM caspase 8 inhibitor (A, z-IETD-fmk) or caspase 9 inhibitor (B, z-LEHD-fmk) followed by 16 h treatment with proteasome inhibitors. Lysates were probed for caspase 8 and 9. B-C) Densitometry for Western blots from (A) showing the ratio of cleaved to whole caspase 8 in cells pre-treated with caspase 9 inhibitor (B) and the ratio of cleaved to whole caspase 9 in cells pre-treated with caspase 8 inhibitor (C) (*$p < 0.05$, NS = not significant).

Alternatively, caspase 9 cleavage was actually increased in shCASP8 cells treated with BTZ and MRZ; this increase was confirmed by densitometry analysis (Fig. 3.13C). Together, data from both chemical inhibitors and shRNA indicates that caspase 9 cleavage is necessary for caspase 8 cleavage by proteasome inhibitors, placing caspase 9 at the top of the apoptotic cascade induced by both BTZ and MRZ in GBM cells.

I also assessed DNA fragmentation in shCASP8 and shCASP9 cells 24 h after proteasome inhibitor treatment and found that shCASP8 cells showed decreased sensitivity to MRZ, but not BTZ (Fig. 3.14A). Notably, the shCASP9 cells were more resistant to both MRZ and BTZ, indicating that caspase 9 is important for initial death induction by both BTZ and MRZ (Fig. 3.14B). When I examined DNA fragmentation after 48 h of treatment, effects on death were blunted; BTZ treatment caused slightly increased DNA fragmentation in shCASP8 cells and slightly decreased DNA fragmentation in shCASP9 cells compared to shCTRL cells (Fig. 3.15A-B). This may indicate that late compensatory mechanisms obscured the effects of the initiator caspases, but the data at 24 h confirms that caspase 9 is important for death induced by both BTZ and MRZ.

Role of the mitochondria in proteasome inhibitor-induced death.

Caspase 9 is activated downstream of mitochondrial membrane permeabilization, which releases cytochrome C and enables formation of the apoptosome [72]. Since caspase 9 was found to be the initiator of caspase-dependent apoptosis, I next looked at mitochondrial events after proteasome inhibition. LN18 cells were treated with proteasome inhibitors for 8 h, followed by brief, gentle lysis of outer membranes and pelleting of mitochondria to obtain cytoplasmic fractions. Cytochrome C was then examined by Western blot in these cells. Treatment with staurosporine (STS), an ATP-competitive protein kinase inhibitor known to

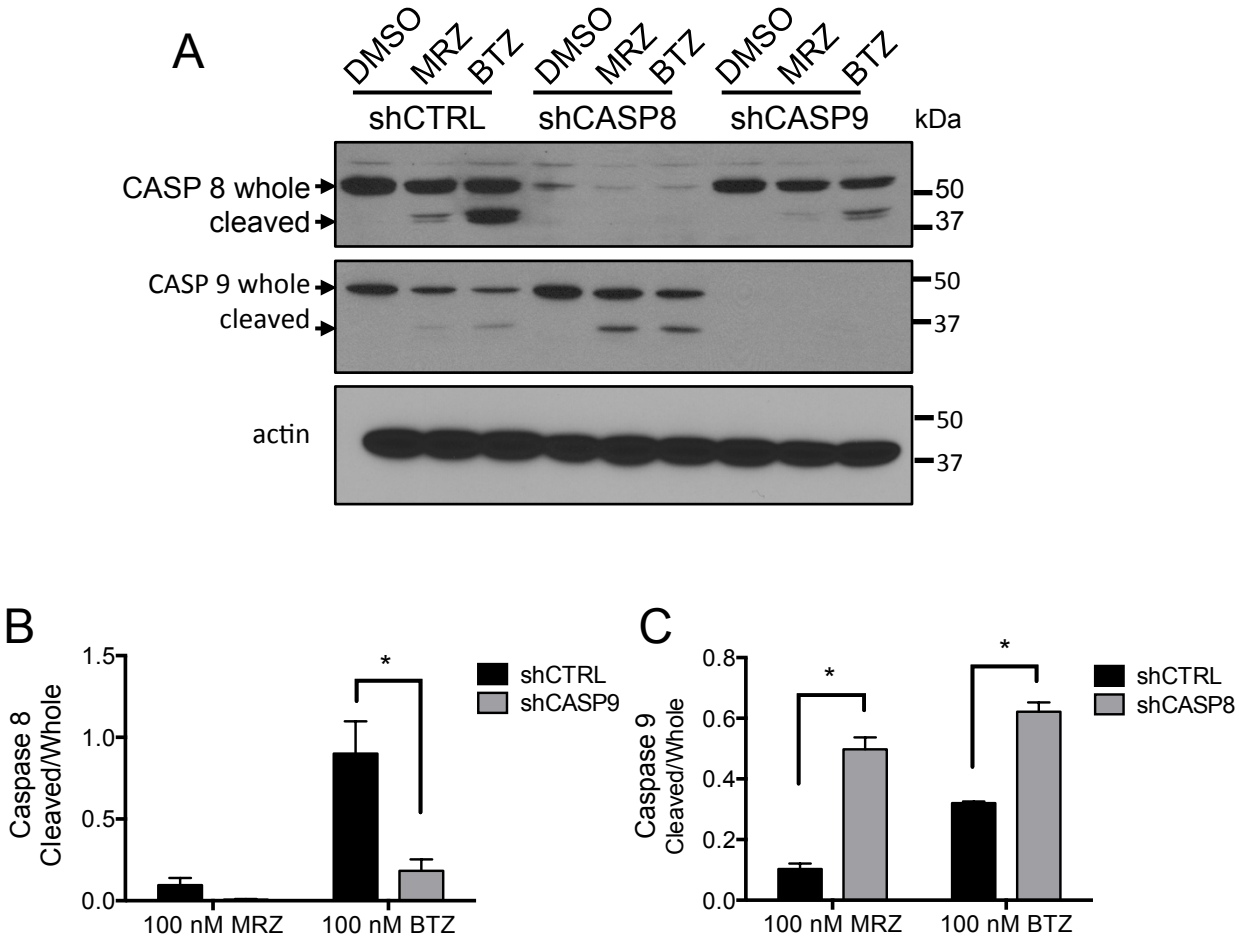

Figure 3.13: Knockdown of caspase 9 diminishes cleavage of caspase 8, while knockdown of caspase 8 increases cleavage of caspase 9. A) LN18 cells stably expressing shCTRL, shCASP8, or shCASP9 were treated for 16 h with 100 nM proteasome inhibitors. Lysates were probed for caspases 8 and 9. B-C) Densitometry showing the ratio of cleaved to whole caspase 8 in shCASP9 cells (B) and the ratio of cleaved to whole caspase 9 in shCASP8 cells (C).

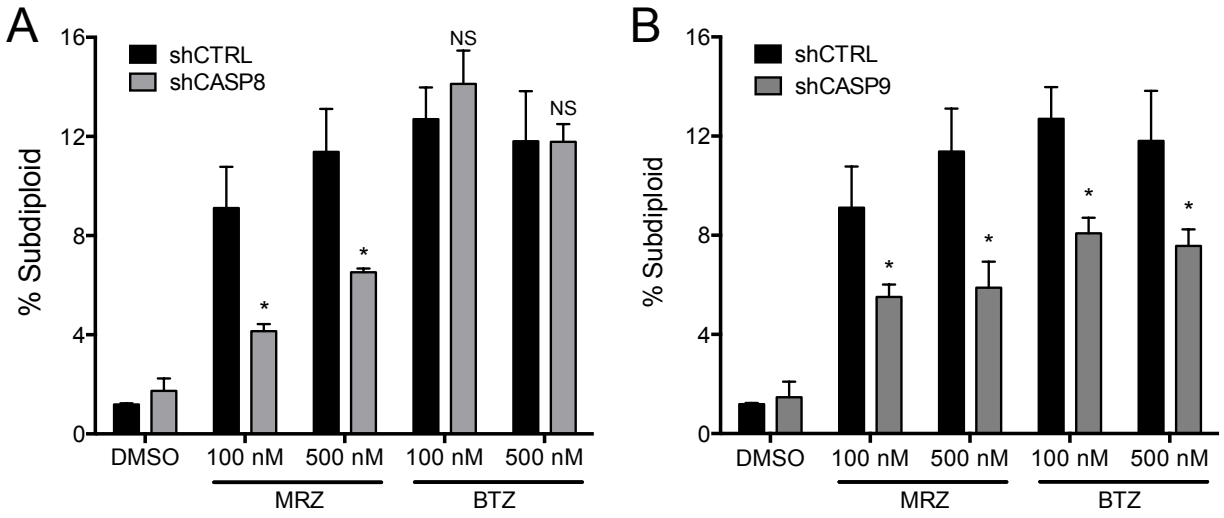

Figure 3.14: After 24 h of treatment, MRZ-induced death is partially blocked in cells expressing shCASP8 or shCASP9; BTZ-induced death is partially blocked only in shCASP 9 cells. A-B) LN18 cells stably expressing shCTRL, shCASP8 (A), or shCASP9 (B) were treated for 24 h with proteasome inhibitors. Cells were stained with propidium iodide for analysis of DNA fragmentation (*$p < 0.05$, NS = not significant).

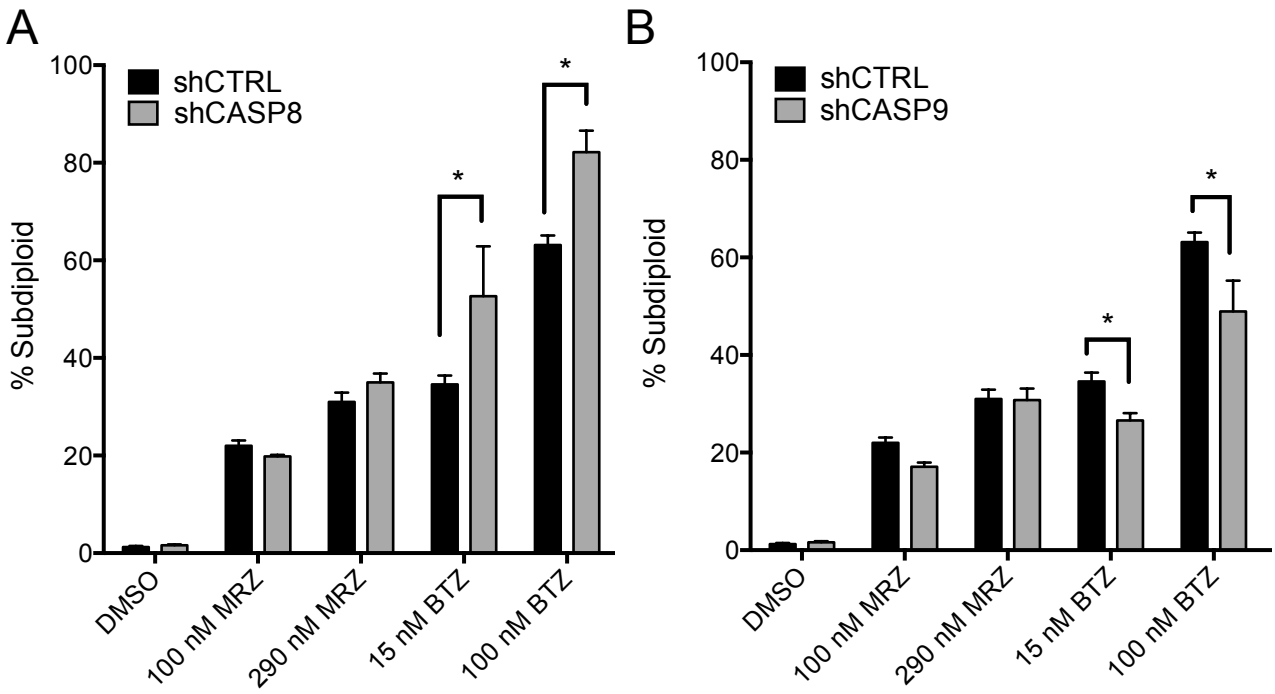

Figure 3.15: Stable knockdown of caspase 8 slightly increases death, while knockdown of caspase 9 slightly decreases death after 48 h. A-B) LN18 cells stably expressing shCTRL, shCASP8 (A), or shCASP9 (B) were treated for 48 h with proteasome inhibitors. Cells were stained with propidium iodide for analysis of DNA fragmentation (*$p < 0.05$).

induce mitochondria permeability and cytochrome C release [145], was used as a control. Both BTZ and MRZ induced release of cytochrome C from the mitochondria into cytoplasmic fractions (Fig. 3.16). Decreases in mitochondrial membrane potential were also measured using tetramethylrhodamine, ethyl ester (TMRE), a dye that is retained in intact mitochondria. Representative histograms are shown for flow cytometric analysis of TMRE staining of LN18 cells treated for 16 h with STS or proteasome inhibitors (Fig. 3.17A). The mean fluorescence was recorded for TMRE-stained cells treated with proteasome inhibitors for 4 to 16 h. Mitochondrial membrane potential significantly increased 12 to 16 h following treatment with both BTZ and MRZ (Fig. 3.17B). This data confirms the occurrence of upstream events necessary for caspase 9 activation by proteasome inhibitors.

To further investigate the role of the mitochondria in proteasome inhibitor-induced death, LN18 cells were generated that expressed either vector (PLRS) or the anti-apoptotic Bcl-2 family member Bcl-XL, which blocks mitochondrial permeability by binding to BH3 domains of pro-apoptotic Bcl-2 family members (Fig. 3.18A) [146]. Cells that overexpressed Bcl-XL were less sensitive to both MRZ- and BTZ-induced DNA fragmentation (Fig. 3.18B). I examined the functional effect of Bcl-XL overexpression on mitochondrial permeability and subsequent cleavage of caspase 9 (Fig. 3.19). Cells overexpressing Bcl-XL still had decreases in mitochondrial membrane potential, and caspase 9 was still cleaved after proteasome inhibitor treatment. Bcl-XL did prevent caspase 9 cleavage in response to staurosporine treatment, indicating that the overexpression did protect against another agent that has been shown to cause mitochondrial permeability. The fact that Bcl-XL conferred partial protection from DNA fragmentation but not caspase 9 cleavage after proteasome

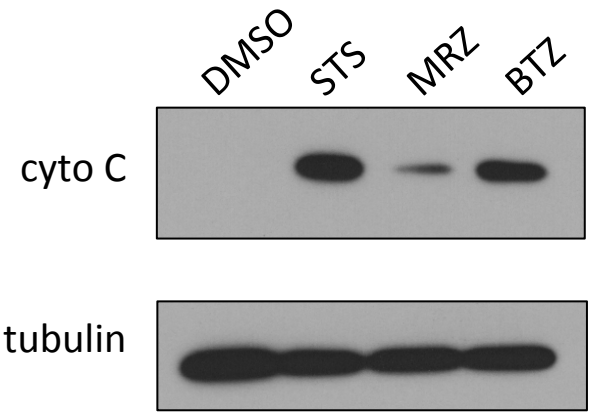

Figure 3.16: Proteasome inhibitors induce release of cytochrome C into the cytoplasm. LN18 cells treated 16 h with 100 nM MRZ or BTZ, or 8 h with 0.5 μM STS. Cells were separated into cytoplasmic and mitochondrial fractions, and the cytoplasmic fractions (shown here) were probed for cytochrome C.

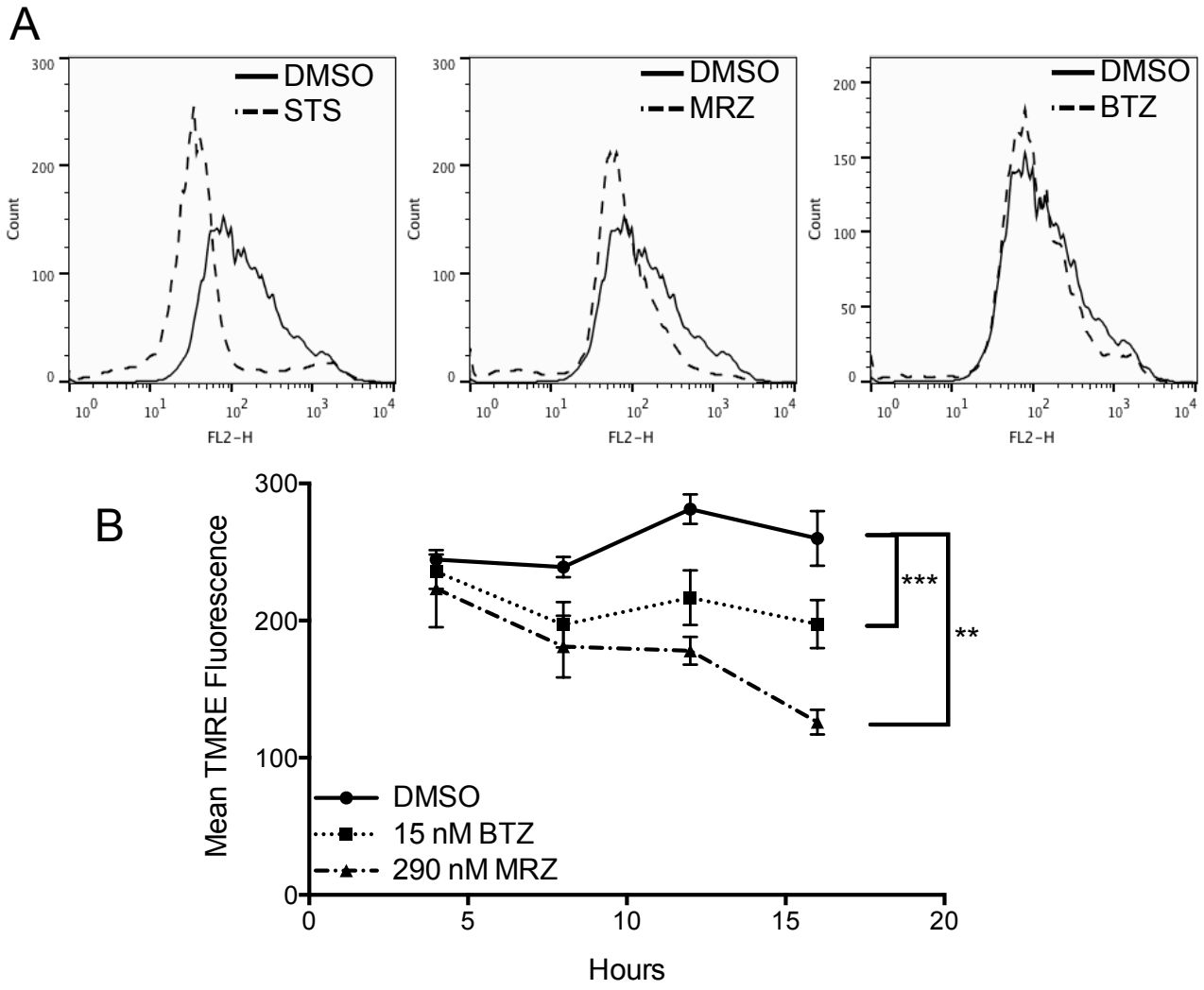

Figure 3.17: Proteasome inhibitors cause decreases in mitochondrial membrane potential. A) LN18 cells were treated 16 h with 1 μM STS, 290 nM MRZ, or 15 nM BTZ. Cells were stained with TMRE, and mitochondrial membrane potential was assessed by flow cytometry. B) LN18 cells were treated for 4, 8, 12, or 16 h with proteasome inhibitors. Mean fluorescence values were obtained by TMRE staining (**$p < 0.05$ for 12 and 16 h; ***$p < 0.05$ for 8, 12, and 16 h).

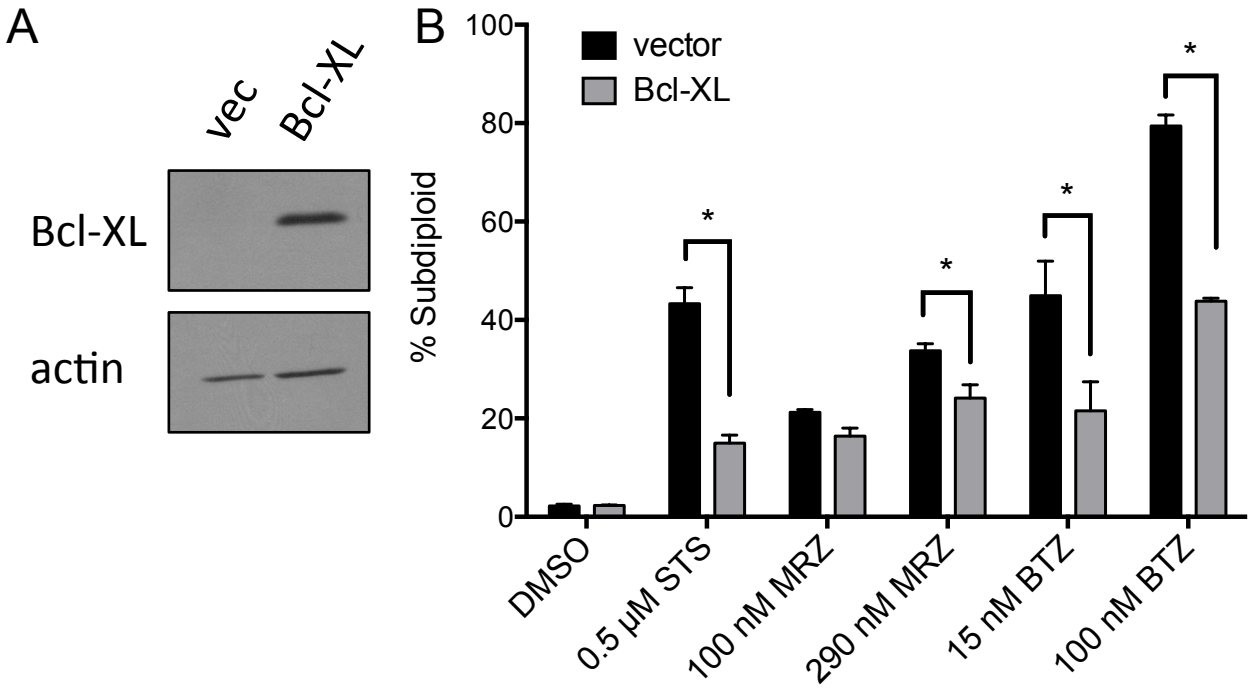

Figure 3.18: Overexpression of Bcl-XL protects against proteasome inhibitor-induced death. A) Bcl-XL was stably overexpressed in LN18 cells. B) LN18 cells expressing vector (PLRS) or Bcl-XL were treated for 48 h with proteasome inhibitors and DNA fragmentation was assessed.

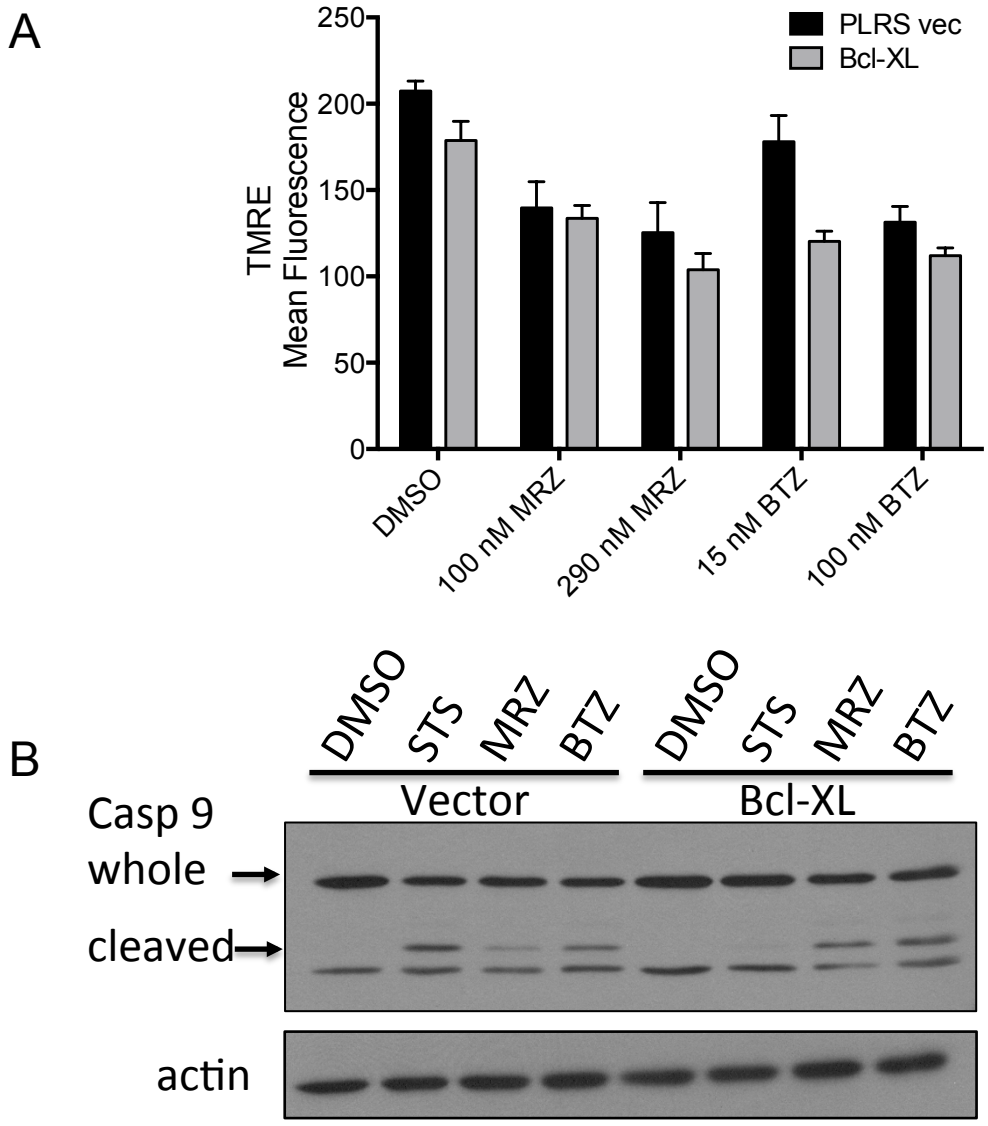

Figure 3.19: Overexpression of Bcl-XL does not prevent proteasome inhibitor-induced mitochondrial permeability. A) LN18 cells expressing vector (PLRS) or Bcl-XL were treated for 16 h with proteasome inhibitors, and mitochondrial membrane potential was assessed by TMRE staining. B) Caspase 9 cleavage was assessed in LN18 cells expressing Bcl-XL after 16 h treatment with 100 nM proteasome inhibitors or 0.5 μM STS.

inhibitor treatment suggests that Bcl-XL overexpression has effects other than protection of mitochondrial membrane permeability.

Caspase 9 activation and death are blocked by reducing agents.

Past studies have indicated that production of ROS is an integral part of proteasome inhibitor-induced death in other types of cancer [47, 68, 82, 84]. To see if this was the case in GBM, LN18 cells were treated with proteasome inhibitors, followed by measurement of hydrogen peroxide by incubation with CM-H_2DCFDA or superoxides by incubation with hydroethidium. Levels of these species in cells were measured by flow cytometric analysis. Both BTZ and MRZ caused only minimal increases in ROS, as is shown by representative histograms for hydrogen peroxide (Fig. 3.20A) and superoxide (Fig. 3.20B) levels, as well as by quantification of the mean fluorescence for these dyes in cells treated with BTZ or MRZ for 4 to 12 h (Fig. 3.20C-D).

Despite minimal ROS increases, it is possible that any perturbation of the oxidative state of cells could be important for proteasome inhibitor induced death. Therefore, I continued to explore the importance of ROS by pre-treating cells with antioxidants to see if this impacted activation of death following proteasome inhibition. NAC is commonly used as an antioxidant due to its ability to flood cells with free cysteine, which is a key step for production of the antioxidant glutathione (GSH) [147].

When LN18 cells were pre-treated with NAC, proteasome inhibitor-induced cleavage of caspase 2 was reduced on Western blot (Fig. 3.21A). Inhibition of caspase 2 activation was confirmed in LN18 cells transfected with caspase 2 Venus BiFC. The percentage of cells that were positive for caspase 2 BiFC signal were quantified either 4 h (Fig. 3.21B) or 24 h (Fig. 3.21C) following treatment with proteasome inhibitors. There were only minor

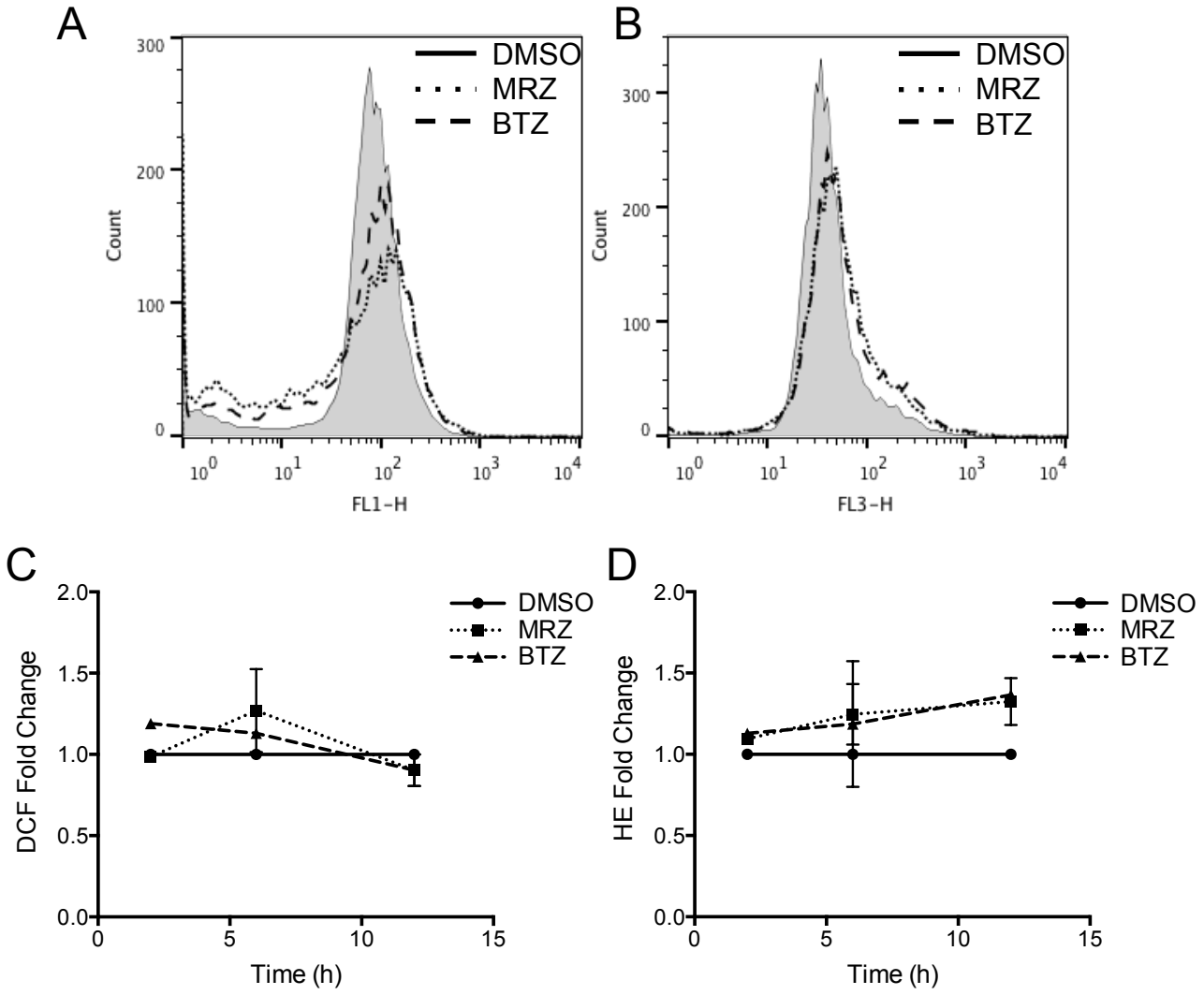

Figure 3.20: Proteasome inhibitors do not greatly increase ROS in LN18 cells. A-B) LN18 cells treated for 6 h with 100 nM proteasome inhibitors were stained with CM-H_2DCFDA for hydrogen peroxide (A) or hydroethidium for superoxides (B). C-D) Mean fluorescence values were obtained for LN18 cells treated with H_2DCFDA for hydrogen peroxide (C) or hydroethidium for superoxides (D).

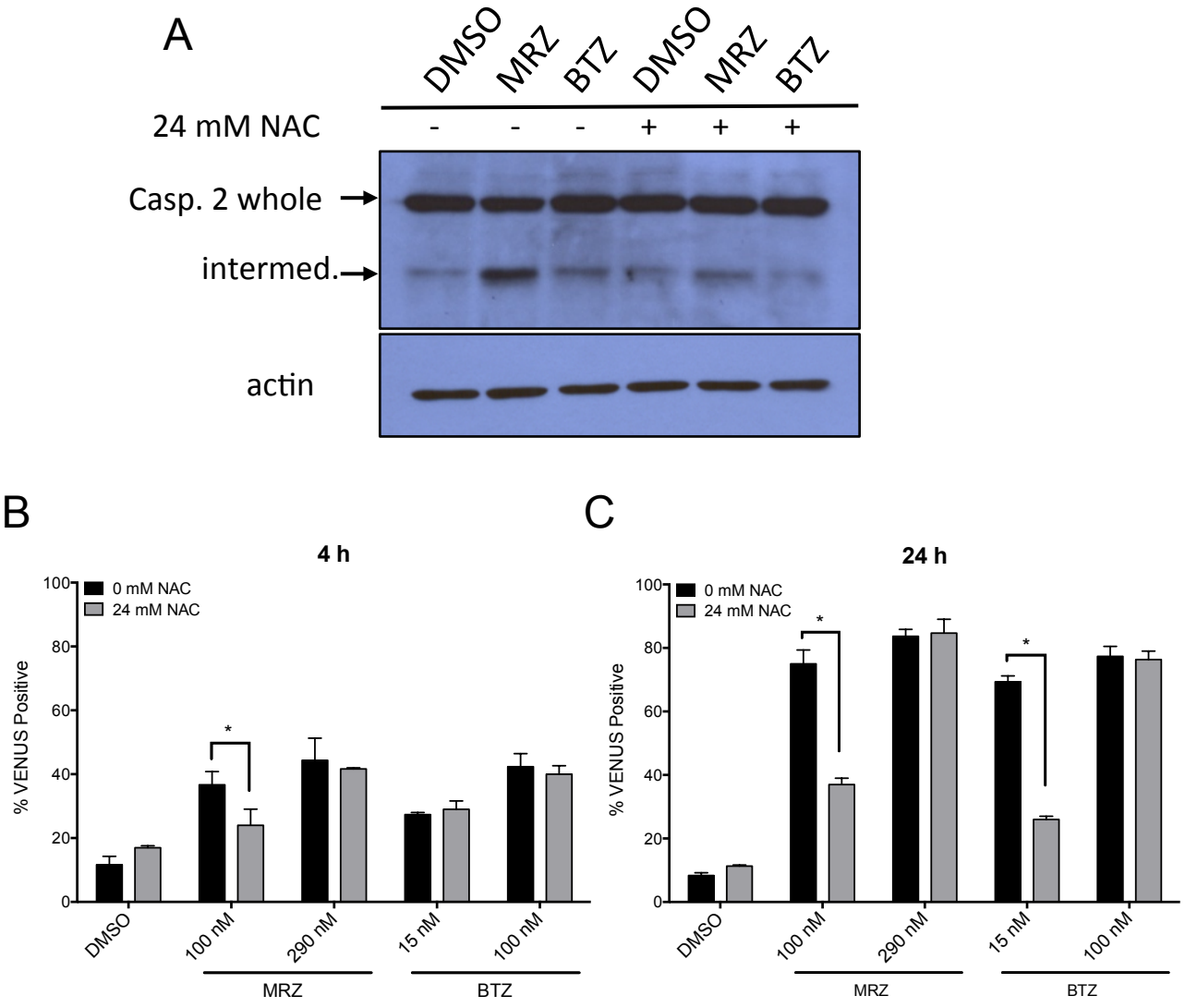

Figure 3.21: NAC prevents caspase 2 activation by proteasome inhibitors. A) Western blot for caspase 2 in LN18 cells pre-treated 30 min with NAC, followed by 16 h treatment with 290 nM MRZ or 15 nM BTZ. B-C) Percentage of cells positive for activation of caspase 2 (VENUS BiFC model) after 30 min pre-treatment with NAC and 4 h (B) or 24 h (C) treatment with MRZ and BTZ (*$p < 0.05$).

increases in the percentage of caspase 2 BiFC positive cells at 4 h. However, at 24 h, pre-treatment with NAC did prevent activation of caspase 2 after treatment with certain lower doses (100 nM MRZ, 15 nM BTZ) of proteasome inhibitors. Given my previous result that caspase 2 is not essential for death induction by proteasome inhibitors (Fig. 3.7-10), it is unclear what effect preventing activation of caspase 2 may have in GBM cells. However, it is clear that its activation is modulated by NAC.

Since I previously determined that caspase 9 was at the top of the hierarchy of caspase activation by proteasome inhibitors in GBM cells (Fig. 3.12-13), I went on to explore the effect of antioxidant treatment on caspase 9. I pre-treated cells with either NAC or dithiothrietol (DTT). Both NAC and DTT can act as general reducing agents that modulate cellular thiol levels [148]. Mitochondrial release of cytochrome C into cytoplasmic fractions and cleavage of caspase 9 were attenuated in cells pre-treated with NAC or, to a slightly lesser extent, DTT (Fig. 3.22A). Caspase 3/7 activity was also decreased in cells treated with NAC before proteasome inhibition (Fig. 3.22B).

Since NAC and DTT blocked caspase activation, I examined whether this corresponded to decreased induction of cell death. Cells pre-treated for 30 min with either NAC or DTT, followed by 48 h treatment with BTZ or MRZ, were examined for DNA fragmentation. Both NAC and DTT caused a strong reduction in DNA fragmentation induced by BTZ and MRZ (Fig. 3.23).

Since the mechanism of NAC as an antioxidant is widely considered to be through increased GSH, I also pre-treated cells with a cell-soluble form of glutathione (glutathione ethyl ester, GSHee). However, GSHee did not prevent proteasome inhibitor-induced DNA fragmentation (Fig. 3.23). To ensure that both NAC and GSHee were causing increases in

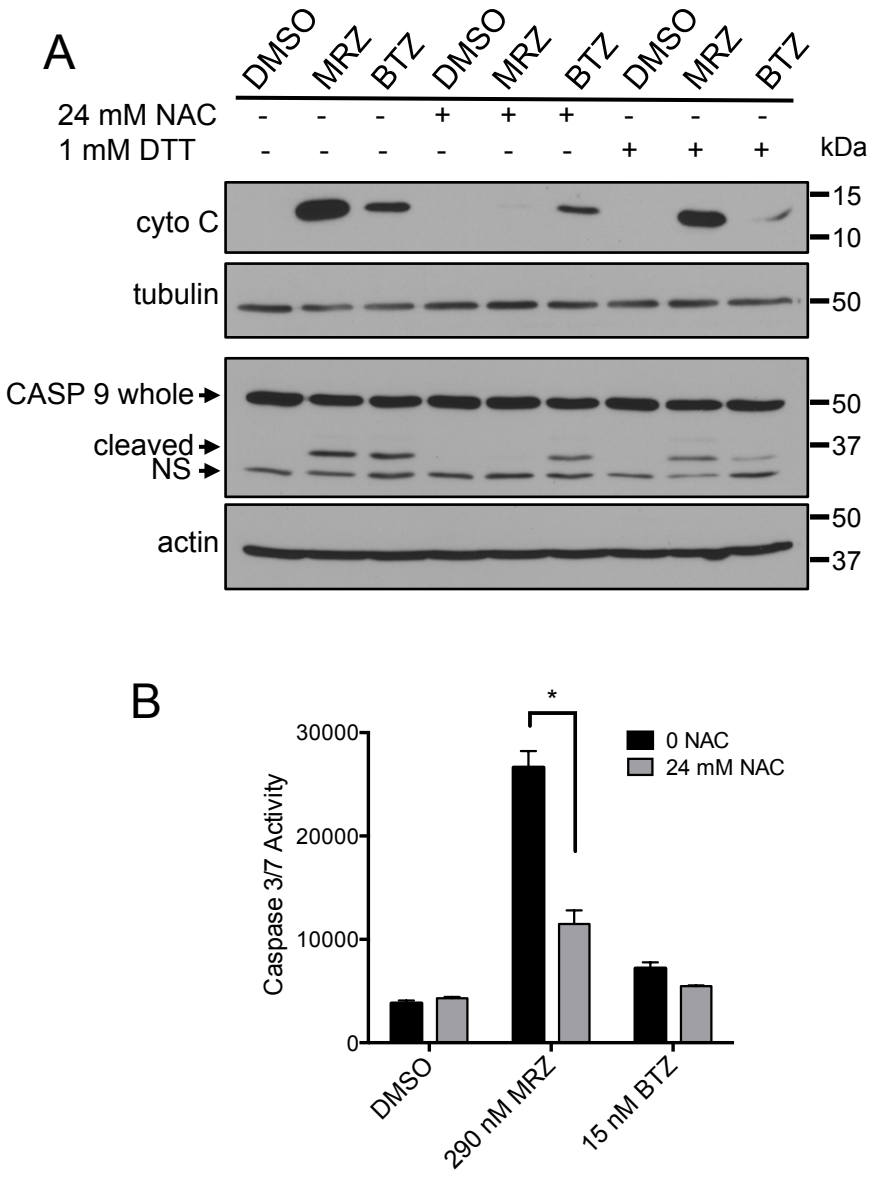

Figure 3.22: Inhibition of proteasome inhibitor-induced apoptosis in cells pre-treated with reducing agents. A) LN18 cells pre-treated for 30 min with NAC or DTT were treated with 100 nM BTZ or MRZ. After 8 h, cytoplasmic fractions were probed for cytochrome C. After 16 h, whole cell lysates were examined for cleaved caspase 9. B) Caspase 3/7 activity in LN18 cells pre-treated 30 min with NAC, followed by 16 h treatment with proteasome inhibitors.

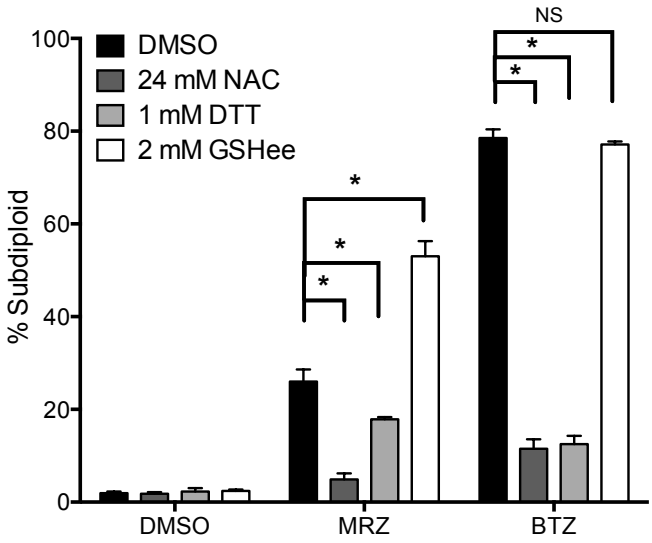

Figure 3.23: NAC and DTT, but not GSHee, attenuate proteasome inhibitor-induced death. DNA fragmentation in LN18 cells pre-treated for 30 min with NAC, DTT, or GSHee, followed by 48 h treatment with BTZ or MRZ.

GSH, cellular GSH levels were measured using monochlorobimane. Once monochlorobimane enters cells, glutathione S-transferases facilitate the formation of GSH-monochlorobimane adducts, which can be measured by fluorescence [149]. Using this method, I was able to see that both NAC and GSHee increased cellular GSH to a similar degree (Fig. 3.24). Since both NAC and GSHee increase GSH, but only NAC protects cells from proteasome inhibitor-induced DNA fragmentation, NAC is functioning independently of its impact on GSH.

To further confirm this, I conducted experiments using buthionine sulfoximine (BSO), an inhibitor of γ-glutamylcysteine synthetase, which is critical for GSH synthesis [150]. Pre-treating LN18 cells with BSO depleted GSH levels, and also prevented NAC-induced increases in GSH (Fig. 3.24). BSO treatment (GSH depletion) had minimal and opposing effects on proteasome inhibitor-induced DNA fragmentation (increased sensitivity to MRZ, slightly decreased sensitivity to BTZ). Most importantly, NAC still protected cells from BTZ and MRZ induced death, even when pre-treatment with BSO prevented NAC from increasing GSH (Fig. 3.24). This confirms that NAC protects cells from proteasome inhibitor-induced death in a manner independent of GSH.

There have been some reports of direct inactivation and prevention of antitumor efficacy of BTZ by certain antioxidants, including Vitamin C and green tea components such as (-)-epigallocatechin gallate (EGCG) [85, 151, 152]. To see whether the effects of NAC and DTT were due to direct prevention of proteasome binding and inhibition by BTZ and MRZ, proteasome activity was measured in LN18 cells pre-treated with NAC and DTT, followed by treatment with BTZ and MRZ.

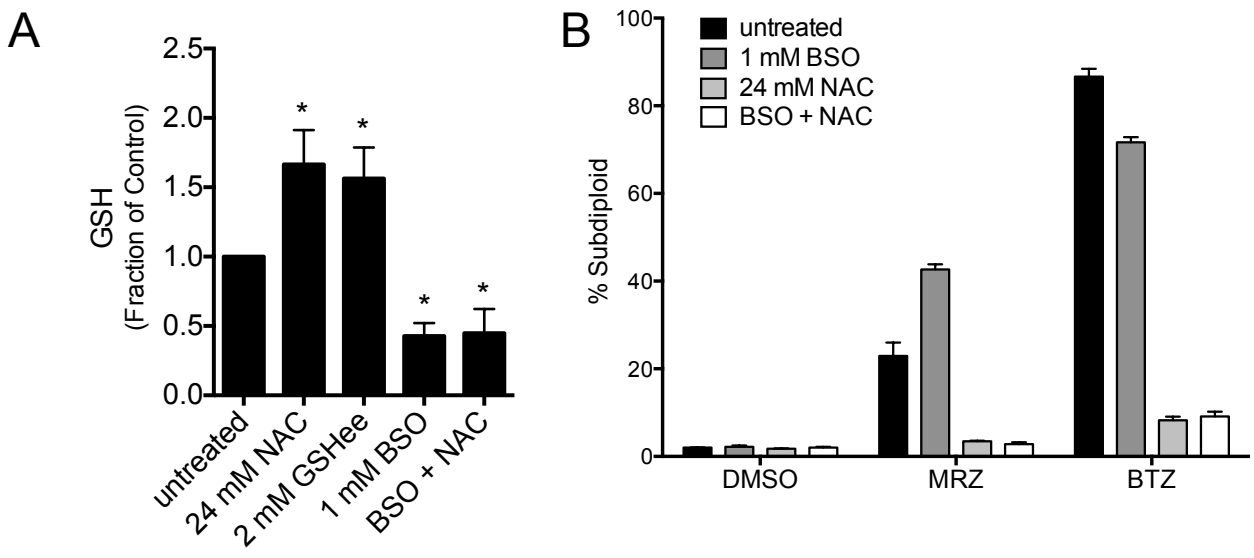

Figure 3.24: Depletion of glutathione levels does not prevent NAC protection against proteasome inhibitors. C) Glutathione levels in LN18 cells treated for 6 h with NAC, GSHee, BSO, or BSO plus NAC. D) DNA fragmentation in LN18 cells pre-treated for 30 min with BSO, NAC, or BSO + NAC, followed by 48 h of treatment with 100 nM proteasome inhibitors.

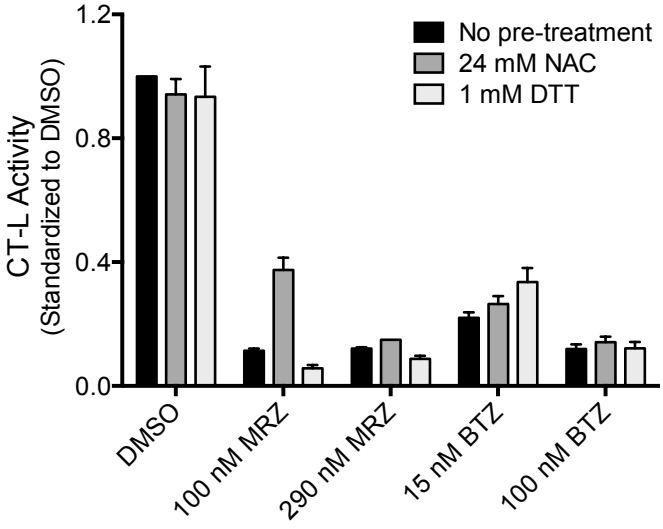

Figure 3.25: NAC and DTT do not suppress the ability of proteasome inhibitors to reduce CT-L proteasome activity. LN18 cells pre-treated 30 min with NAC or DTT were then treated 4 h with proteasome inhibitors. CT-L proteasome activity was assessed using the fluorogenic substrate suc-LLVY-amc (*$p < 0.05$).

Neither NAC nor DTT affected the ability of BTZ or MRZ to inhibit proteasome activity, indicating that they are not directly acting on these agents (Fig. 3.25). There was 1 dose of MRZ that was slightly attenuated by NAC. However, higher doses were not affected, and strong protection from death was observed under conditions where proteasome inhibition capacity was not altered (Fig. 3.23).

Together, these results demonstrate that the reducing agents NAC and DTT protect cells from proteasome inhibitor-induced death in a manner independent of GSH or direct effects on the ability of these drugs to inhibit proteasome activity.

BTZ and MRZ do not deplete cellular amino acid levels.

A report by Suraweera *et al.* [153] suggested an alternative hypothesis for the mechanism of proteasome inhibitor-induced death. They found that MEFs treated with the proteasome inhibitors MG-132 or BTZ had a quick decline in free amino acid levels, particularly of the amino acids cysteine and asparagine. This depletion induced cellular starvation signaling, increasing GCN2 signaling and autophagy. Notably, supplementing cells with the amino acid cysteine greatly protected against cell death, and supplementing with asparagine also slightly protected cells from proteasome inhibitor-induced death.

Since NAC introduces large amounts of cysteine into cells, I wanted to explore whether the amino acid starvation theory of proteasome inhibitor efficacy could apply to GBM cells. First, I pre-treated cells with NAC as well as asparagine to see if another amino acid would have an effect. Asparagine did lend some protection, particularly in cells treated with both asparagine and cysteine, followed by 100 nM BTZ (Fig. 3.26A). Asparagine was not as protective as NAC, which was consistent with the published results in MEFs [153].

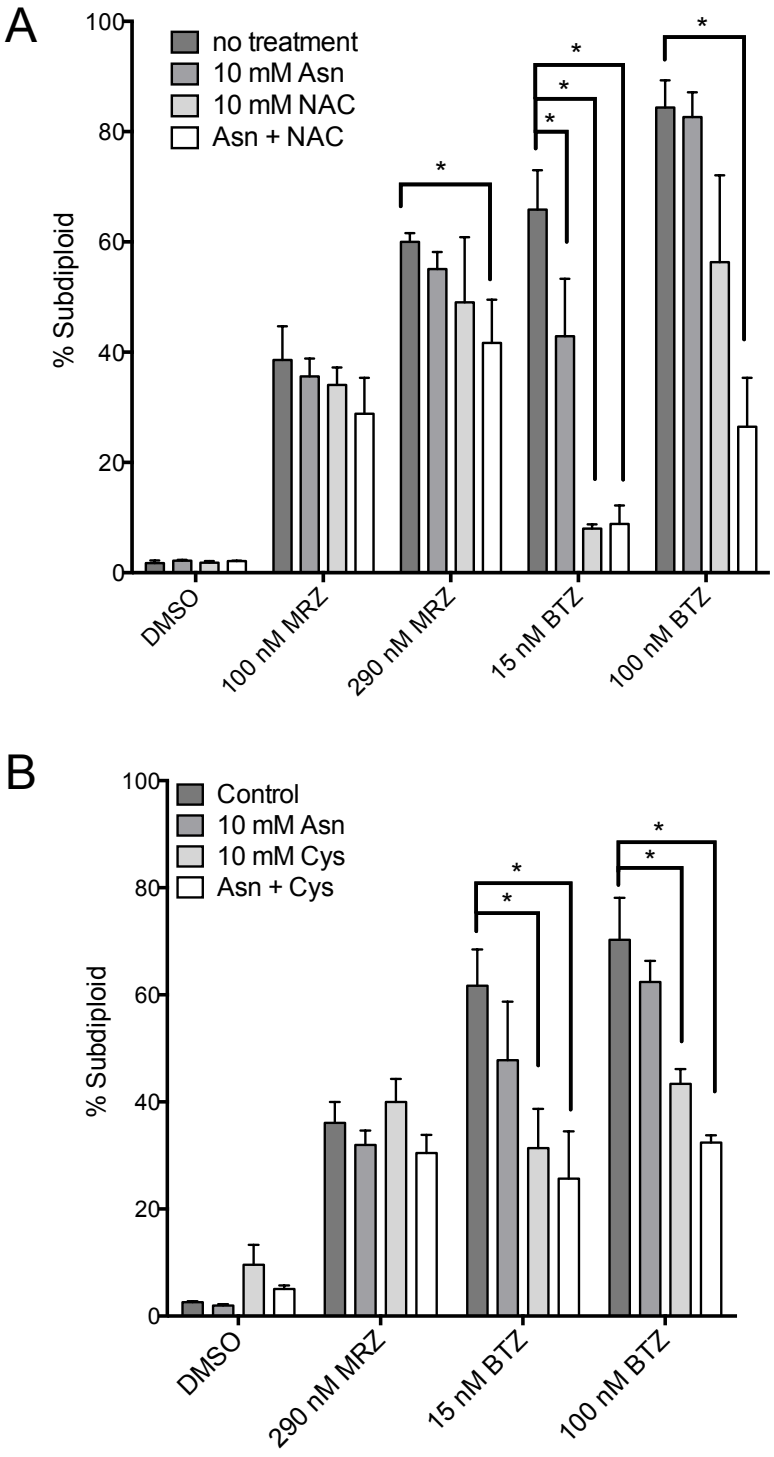

Figure 3.26: Cysteine and asparagine supplementation and proteasome inhibitor induced death. A) DNA fragmentation levels in LN18 cells treated for 48 h with proteasome inhibitors. After 2 hours of proteasome inhibitor treatment, wells were supplemented with 10 mM NAC, asparagine (Asn), or both (*$p < 0.05$). B) DNA fragmentation levels in LN18 cells treated for 48 h with proteasome inhibitors. After 2 hours of proteasome inhibitor treatment, wells were supplemented with 10 mM cysteine, asparagine (Asn), or both (*$p < 0.05$).

When I supplemented cells with cysteine (instead of NAC) as well as asparagine, similar trends were observed; though asparagine had little impact on its own, it slightly augmented the protection conferred by cysteine (Fig. 3.26B).

The selection of cysteine and asparagine was based on the fact that these amino acids were strongly depleted in MEFs treated with proteasome inhibitors [153]. However, these same amino acids may not be the key amino acids depleted by proteasome inhibition in GBM cells. Therefore, I wanted to determine the amino acid profile of cells following treatment with BTZ and MRZ to see if particular amino acids were depleted. To do this, I collaborated with the MD Anderson Cancer Center Proteomics Core. I used a mass spectrometry-based approach for amino acid measurement [154]. Using this method, I was able to determine that there were not widespread decreases in amino acids following proteasome inhibition in LN18 GBM cells (Fig. 3.27). In fact, many amino acids, including cysteine and asparagine, actually increased slightly after proteasome inhibitor treatment. Since most amino acids were increased after proteasome inhibition, not decreased, it is unlikely that amino acid starvation is a main method triggering death in GBM cells following proteasome inhibition. Likewise, cysteine supplementation by NAC is most likely not its mechanism of protection.

A

	4 h			8 h	
	CTRL	MRZ	BTZ	CTRL	MRZ	BTZ
Taurine	14.451	10.241	11.556	23.301	11.155	17.059
Glutamine	24.159	30.313	30.672	38.541	52.212	73.623
Serine	2.637	3.357	3.270	4.477	6.200	8.823
Glycine	2.563	2.925	2.703	4.110	4.718	6.914
Aspartic Acid	3.630	3.620	3.635	4.815	4.223	5.897
Threonine	10.016	12.506	12.431	15.279	22.206	28.158
Glutamic Acid	9.383	9.694	9.054	12.899	11.648	15.878
Alanine	1.479	1.936	1.912	2.381	3.097	4.323
Cysteine	22.117	28.332	31.462	45.336	75.061	108.573
Citrulline	1.086	1.469	1.641	2.330	4.116	5.963
Proline	2.557	3.231	3.419	4.094	5.158	7.375
Valine	2.007	2.607	2.558	3.559	6.259	8.518
Tyrosine	3.788	5.473	5.063	7.756	10.787	16.726
Ornithine	1.143	1.302	1.334	2.019	2.960	4.583
Lysine	6.816	8.954	9.107	13.394	23.207	33.299
Methionine	2.658	4.066	3.745	4.464	7.259	9.804
Histidine	9.539	13.134	12.329	16.780	27.337	35.198
Sarcosine	90.555	127.531	130.164	149.906	200.297	284.306
Isoleucine	1.827	2.447	2.369	3.189	5.315	7.241
Arginine	4.855	6.354	6.088	9.362	16.731	21.813
Leucine	1.147	1.499	1.570	2.015	3.459	4.681
Phenylalanine	1.932	2.529	2.562	3.368	5.516	7.634
Putrescine	1.218	3.002	2.252	1.616	1.568	2.224
Tryptophan	0.248	0.315	0.277	0.368	0.607	0.840
Spermidine	0.866	1.345	1.115	1.381	1.520	1.803
Spermine	1.604	2.848	1.755	2.571	2.221	2.225

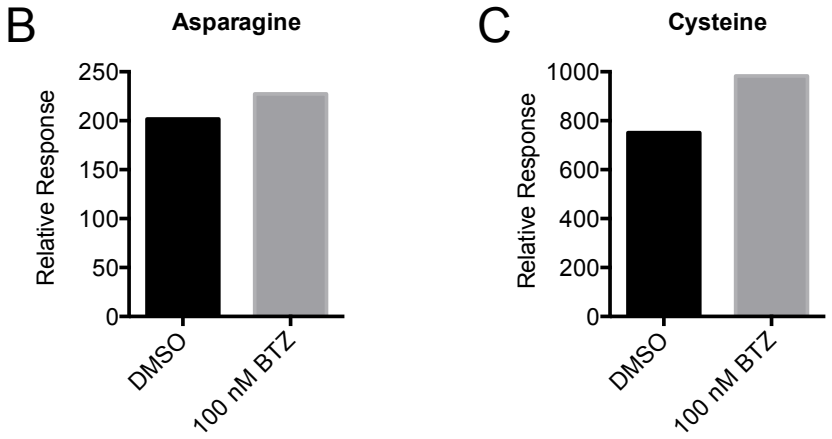

Figure 3.27: Amino acid and metabolite levels after treatment with proteasome inhibitors. A) Levels of amino acids and metabolites 4 and 8 h after treatment with 100 nM proteasome inhibitors. Units are relative response (µg/µL, normalized to DNA content). Cells highlighted in red increased compared to control at same timepoint, cells highlighted in green decreased. B-C) Levels of cysteine (B) and asparagine (C) after 8 h treatment with 100 nM BTZ under analysis conditions optimized for these amino acids.

Summary

The work in this chapter provides a detailed examination of the kinetics and mechanism of death induction by initiator caspases in GBM cells treated with the proteasome inhibitors BTZ and MRZ. Proteasome inhibitor-induced death was apparent by multiple measures; loss of viability, induction of DNA fragmentation, and inhibition of colony growth. GBM cells were sensitive to BTZ at lower doses than MRZ, which corresponds to the more sustained proteasome inhibition after BTZ treatment that was observed in Chapter 2. However, both inhibitors induced death at reasonably low doses in the nanomolar range.

As I hypothesized, both BTZ and MRZ did activate caspases in GBM cells. A key part of this chapter is the examination of the time course of activation as well as the relative dependence of BTZ and MRZ on each initiator caspase. While caspase 2 was activated quickly after treatment with BTZ and MRZ (4 h), knockdown experiments revealed that it is not essential for death induction by these inhibitors. Subsequent experiments determined that caspase 9 is the initiating caspase for both BTZ- and MRZ-induced death in GBM cells.

This chapter also identified that the reducing agents NAC and DTT blocked mitochondrial release of cytochrome C, caspase 9 activation, and cell death induced by proteasome inhibitors. This protection was independent of effects on GSH or the ability of BTZ and MRZ to inhibit the proteasome. I also demonstrated that amino acids are not depleted following BTZ and MRZ treatment in GBM cells, indicating that NAC is likely not acting by rescuing cells from amino acid starvation following proteasome inhibition. Given the similarities between NAC and DTT, which both modulate cellular thiol levels, it is likely that these agents are acting as more general reducing agents. These experiments provide

supporting evidence that a stimulus that prevents caspase activation also prevents final death induction, drawing an additional indirect correlation between these events.

As I hypothesized, delineation of the pathway of caspase activation does give clues to potential biomarkers of drug efficacy and resistance. Since I determined that caspase 9 is the apical caspase in apoptosis induced by BTZ and MRZ in GBM, efficacy could be monitored by examining events such as mitochondrial membrane permeability and cleavage of caspase substrates. Additionally, based on the role of caspase 9 defined here, future studies of proteasome inhibitor resistance in GBM could focus on the role of antagonists of this pathway, such as anti-apoptotic Bcl-2 family members and IAP proteins.

Chapter 4

BTZ and MRZ modulation of proteasome substrates in orthtopic brain tumors, and *in vitro* and *in vivo* synergy between proteasome inhibitors and HDACi in GBM.

Specific Aim 3: Evaluate the ability of BTZ and MRZ to inhibit proteasomes and induce death in combination with HDACi in an orthotopic GBM model.

This chapter examines questions relevant to establishing the clinical potential of the proteasome inhibitors BTZ and MRZ. Past studies have not definitively answered questions about the ability of BTZ and MRZ to exert functional effects on proteasomes in brain tumors in relevant models [97, 99]. Additionally, combination strategies that potentiate the mechanism of death induced by BTZ and MRZ are needed to enhance their clinical potential. Therefore, I hypothesized that examination of the molecular effects of BTZ and MRZ in an orthotopic brain tumor model would establish a framework for their clinical use.

First, an orthotopic intracranial GBM xenograft mouse model was used to examine the ability of BTZ and MRZ to cause accumulation of proteasome substrates in brain tumors. Next, combination therapy strategies that could enhance the efficacy of proteasome inhibitors were examined. Based on my previous data showing that proteasome inhibitors induce caspase-dependent death, I considered combinations that could potentiate the effectiveness of caspase activation. Since IAP family members bind and inhibit caspases, it is possible that they are capable of attenuating the caspase cascade in proteasome inhibitor-treated cells. Therefore, I examined combinations of proteasome inhibitors with the therapeutic agents birinapant and LCL-161, which are mimetics of Smac, a cellular inhibitor of IAPs.

Combinations of proteasome inhibitors and HDACi were also examined for synergistic effects on death induction *in vitro*. Multiple HDACi were tested: the pan-HDACi vorinostat and panobinostat, and the class I HDACi entinostat. Potential interactions between the proteasome system and HDACs were examined by looking at the effects of proteasome inhibitors on acetylation, and the effect of HDACi on proteasome catalytic subunit mRNA.

Potentiation of caspase 9 cleavage by the combination of HDACi and proteasome inhibitors was also examined.

Finally, the potential of the HDACi and proteasome inhibitor combination was tested in an orthotopic mouse model. Brain tumors from mice treated with combinations of vorinostat plus BTZ or MRZ were examined for cleaved caspase 3 and cleavage of lamin A, which is a caspase substrate. Overall, the work in this chapter provides information about the ability of BTZ and MRZ to reach brain tumors and exert effects on proteasome function as well as induction of death in combination with HDACi.

BTZ and MRZ cause accumulation of proteasome substrates in orthotopic brain tumors.

To establish whether BTZ and MRZ are viable drug candidates for GBM, it is important to first examine their ability to reach brain tumors at quantities high enough to exert functional effects on the proteasome. To address this question, I used an orthotopic model of GBM. A total of 500,000 U87 GBM cells were implanted in athymic nude mice through a guidescrew inserted in the cranium. For the first experiment, tumors were allowed to develop for 7 days based on a report by Lal *et al.* showing visible tumor formation at that time [155]. After this time, the mice were injected intraperitoneally (IP) with a single dose of BTZ or MRZ that was based on established maximum tolerated doses for these agents (1.0 mg/kg for BTZ and 0.15 mg/kg for MRZ). Twenty-four hours after treatment, mice were sacrificed, and the tumor-bearing portion of the brain was isolated.

The brain tumor section was then homogenized, and lysate was examined for p27, a cell cycle inhibitor that is also a proteasome substrate. I previously showed that p27 accumulated in LN18 GBM cells following proteasome inhibition with either BTZ or MRZ

(Fig. 2.3). Levels of p27 were significantly elevated in the tumors of mice treated with MRZ, but not those treated with BTZ (Fig. 4.1A). Levels of p27 were quantified using densitometry for multiple mice (Fig. 4.1B).

As a second measure of proteasome inhibition, I examined mice treated for a more extended period. In this case, mice implanted with U87 tumor cells were allowed to develop tumors for 14 days. Mice were then treated for 2 weeks with twice weekly IP injections with BTZ or MRZ. Twenty-four hours following the last treatment, mice were sacrificed and the brains were preserved in formalin for eventual paraffin embedding and immunohistochemistry (IHC) analysis. A hematoxylin & eosin-stained brain from a mouse in the control group is shown in Figure 4.2A.

Sections from these mice were stained for p21, another cell cycle inhibitor that is a proteasome substrate. Brain tumors from mice treated with either BTZ or MRZ had increases in p21 staining as quantified by the average number of p21-positive cells per 40X field (Fig. 4.2B). Representative IHC images also show increases in p21 staining in brain tumors (Fig. 4.2C). Therefore, both BTZ and MRZ have the ability to exert functional effects on proteasome substrates in an orthotopic brain tumor model, with MRZ exerting slightly stronger effects, particularly on p27.

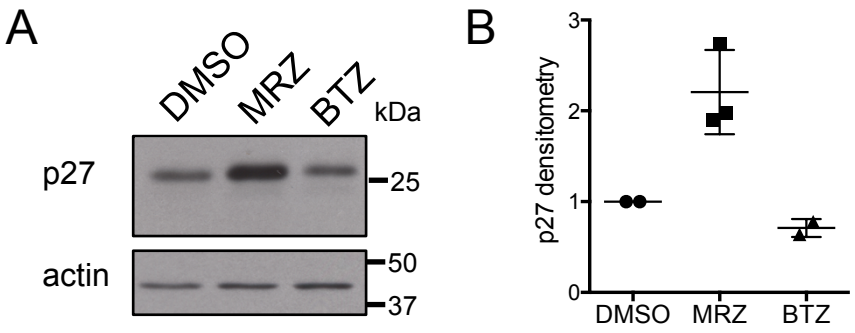

Figure 4.1: Accumulation of p27 in brain tumors of mice treated with MRZ. A) Mice with brain tumors that developed for 7 days were treated with 1 IP injection of proteasome inhibitors (0.15 mg/kg MRZ or 1.0 mg/kg BTZ). After 24 h, mice were sacrificed and the brain tumor-containing half of the brain was lysed and probed for the proteasome substrate p27. B) Densitometry of p27 levels compared to DMSO for individual mice.

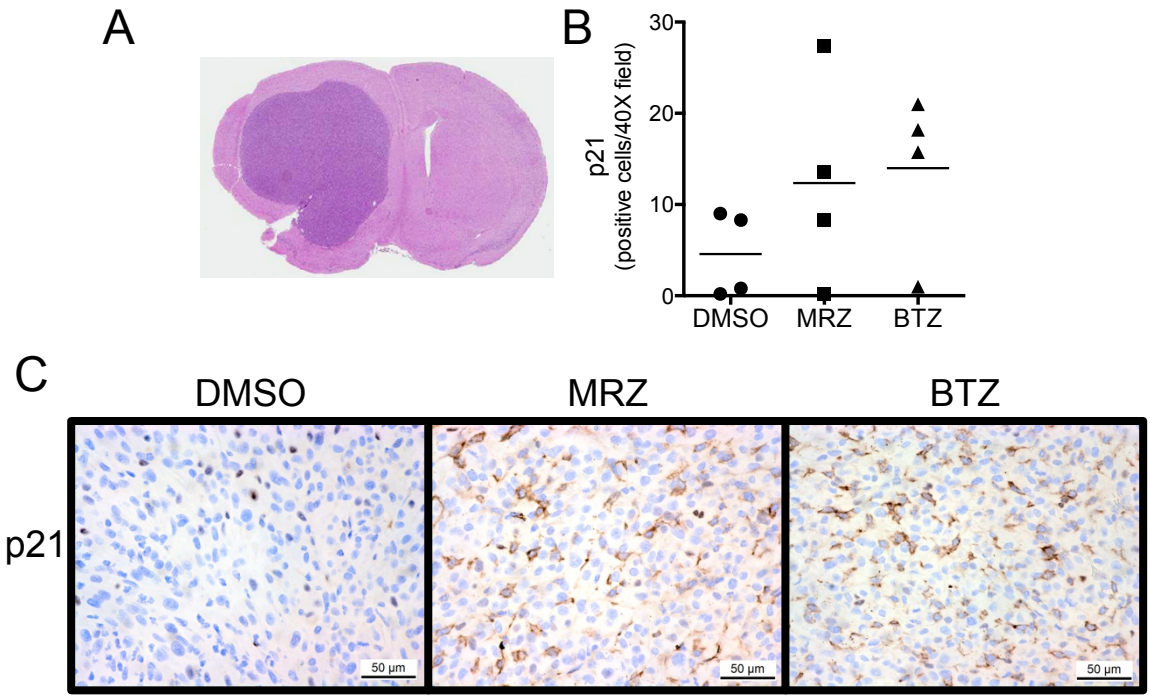

Figure 4.2: Accumulation of p21 in brain tumors of mice treated with proteasome inhibitors. A) Tumors were allowed to develop for 14 days, followed by 2 weeks of twice-weekly treatment with proteasome inhibitors (0.15 mg/kg MRZ or 1.0 mg/kg BTZ). Shown is a representative tumor from a control (DMSO-treated) mouse. B) The average number of p21-positive cells per 40X field from individual mice treated as described in (A). C) Representative images showing p21 in brain tumors of mice treated as described in (A) (40X).

Chemical inhibitors of IAPs potentiate proteasome inhibitor-induced death, but siRNA against IAPs does not.

An interesting trend emerged when I examined activation of initiator caspases 2, 8, and 9 in LN18 cells treated with equipotent doses of proteasome inhibitors. Though the doses used resulted in equal amounts of DNA fragmentation, MRZ induced more cleavage of all 3 initiator caspases compared to BTZ (Fig. 4.3A). There was also more caspase 3/7 activity in GBM cells treated with equipotent MRZ versus BTZ (Fig. 4.3B). I hypothesized that this may be due to a difference in IAP family members, which bind and inhibit caspases. Specifically, XIAP, cIAP-1, and cIAP-2 can bind to caspases 9, 3, and 7 and act as ubiquitin ligases to target caspases for degradation [114]. Based on my previous data, this indicates that IAPs could inhibit the function of both the apical initiating caspase (caspase 9) as well as executioner caspases following proteasome inhibition in GBM. It is possible that MRZ in particular increased levels of an IAP, preventing death even though caspases were being activated. If this is the case, then targeting of IAPs could potentiate death induction by proteasome inhibitors.

Western blot analysis of XIAP protein levels showed that neither BTZ nor MRZ increased levels of XIAP (Fig. 4.4). However, basal XIAP expression was detectable in GBM cells, suggesting that it may be able to suppress apoptosis. I tested this possibility using the Smac mimetics birinapant and LCL-161. Though these agents did not induce DNA fragmentation on their own, they did potentiate the DNA fragmentation caused by both BTZ and MRZ (Fig. 4.5A). Though other reports have indicated that Smac mimetics target IAPs for degradation, decreasing their protein levels [156], I did not see any changes in protein levels of either XIAP or cIAP-1 after treatment with birinapant or LCL-161 (Fig. 4.5B).

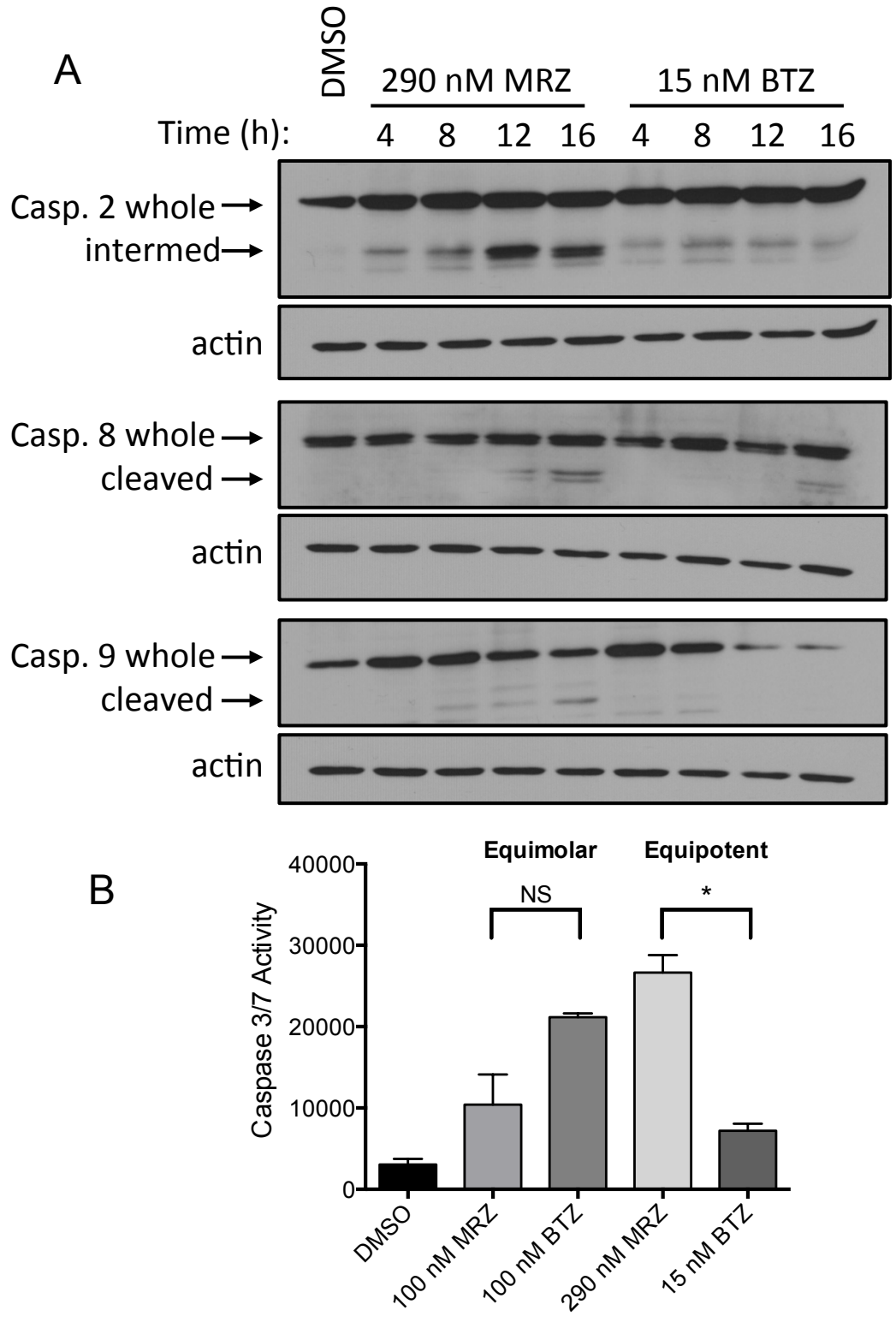

Figure 4.3: Initiator caspase cleavage after treatment with equipotent BTZ and MRZ. A) LN18 cells were treated with equipotent doses (IC50 based on DNA fragmentation) of BTZ or MRZ, and cleavage of initiator caspases was examined. B) Caspase 3/7 activity in LN18 cells treated 16 h with equimolar (100 nM) or equipotent (290 nM MRZ, 15 nM BTZ) doses of proteasome inhibitors (*$p<0.05$, NS=not significant).

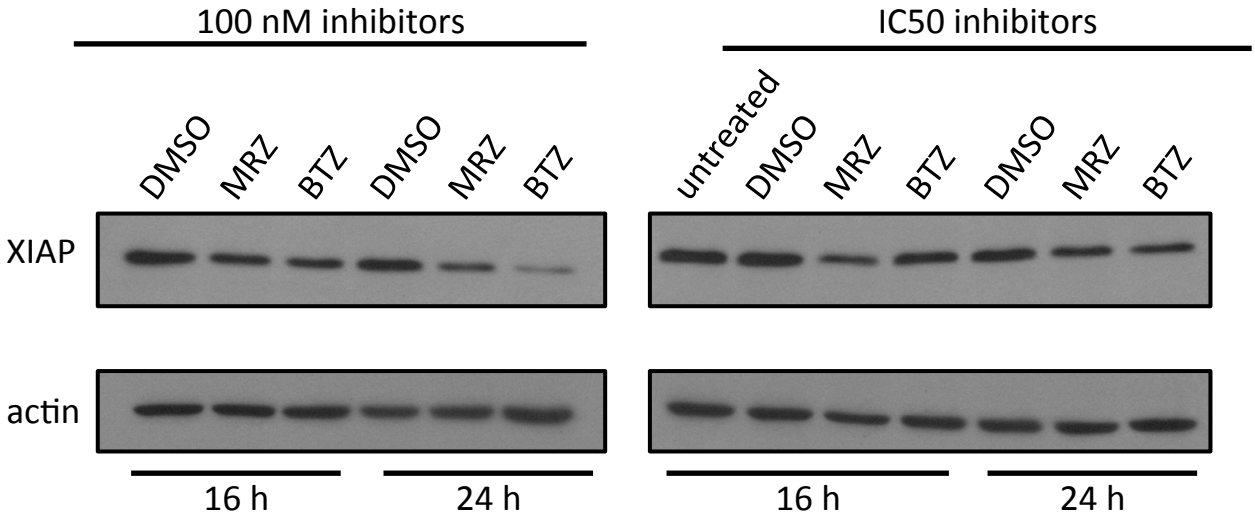

Figure 4.4: Effect of proteasome inhibitor treatment on XIAP levels. LN18 cells were treated for 16 or 24 h with 100 nM or IC50 doses (290 nM MRZ, 15 nM BTZ) of proteasome inhibitors. Cell lysates were probed for XIAP.

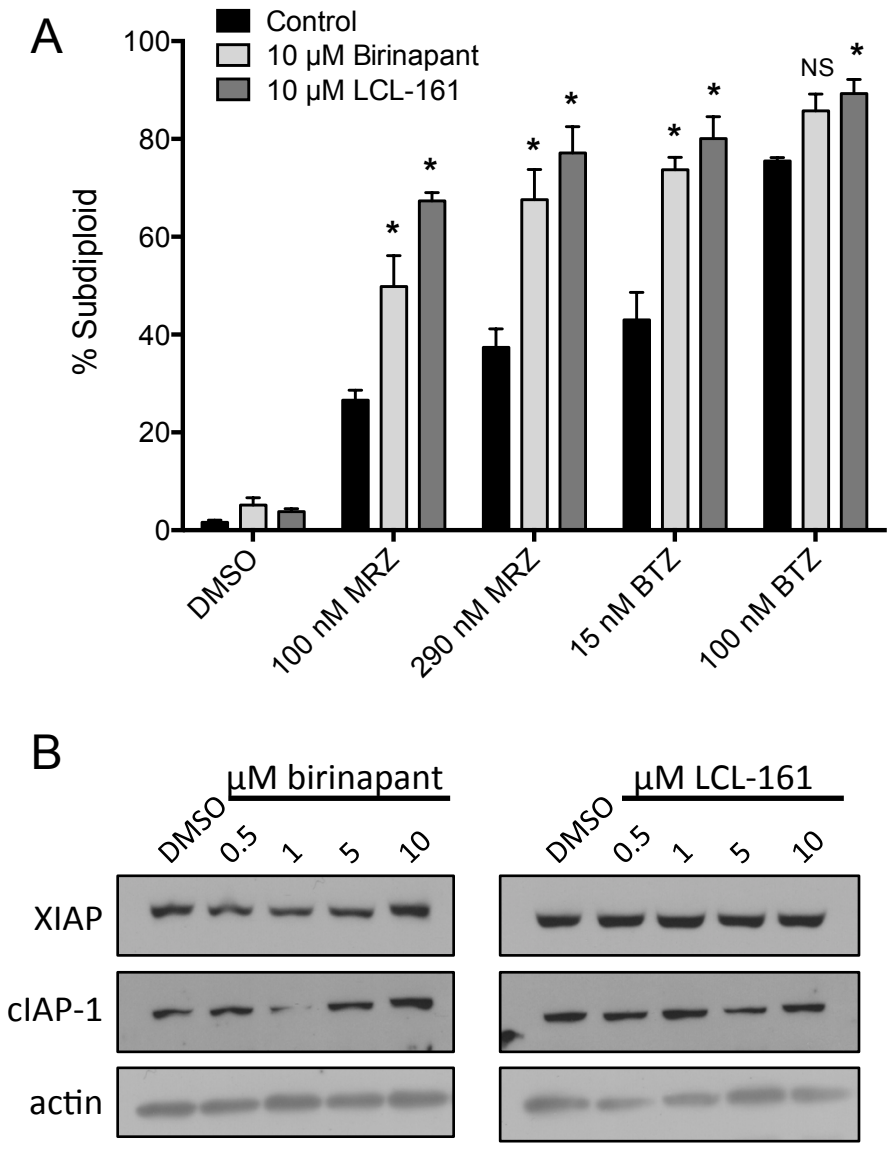

Figure 4.5: Death induction by combinations of proteasome inhibitors and IAP inhibitors. A) LN18 cells were pre-treated 24 h with the IAP inhibitors birinapant and LCL-161, followed by 48 h treatment with BTZ or MRZ and assessment of DNA fragmentation. B) LN18 cells treated 24 h with birinapant or LCL-161 were probed for levels of XIAP and cIAP-1.

Though these proteins were not degraded, the Smac mimetics still may have been disrupting IAP-caspase binding or IAP ligase activity.

To test more specifically whether increases in death with proteasome inhibitors was due to specific IAP targeting or off-target effects of birinapant and LCL-161, I transfected cells with siRNA against cIAP-1, XIAP, or the combination of cIAP-1 plus XIAP, and examined whether this sensitized cells to proteasome inhibitors. Though siRNA achieved knockdown of cIAP-1 and XIAP (Fig. 4.6A), cells transfected with the siRNA, either alone or in combination, were not more sensitive to proteasome inhibitors (Fig. 4.6B). Therefore, the sensitizing effect of the chemical Smac mimetics may be due to off-target effects in these cells. Depleting IAPs does not seem to potentiate the activity of proteasome inhibitors, possibly due to sufficient release of Smac from mitochondria, or because other IAPs besides cIAP-1 and XIAP are important in these cells. The synergy observed with birinapant and LCL-161 may be due to alternative targets.

HDACi potentiate the apoptotic mechanism of BTZ and MRZ *in vitro*.

Studies in other cancer types such as leukemia have found that combining proteasome inhibitors and HDACi induces synergistic cell death [139, 157]. Therefore, I investigated the potential of this combination in GBM. I focused on combinations of BTZ and MRZ with 3 different HDACi: the pan-HDACi vorinostat and panobinostat and the class I HDACi entinostat. LN18 cells treated with combinations of either BTZ or MRZ and vorinostat showed strong increases in DNA fragmentation (Fig. 4.7). Similar trends were seen when BTZ and MRZ were combined with panobinostat (Fig. 4.8).

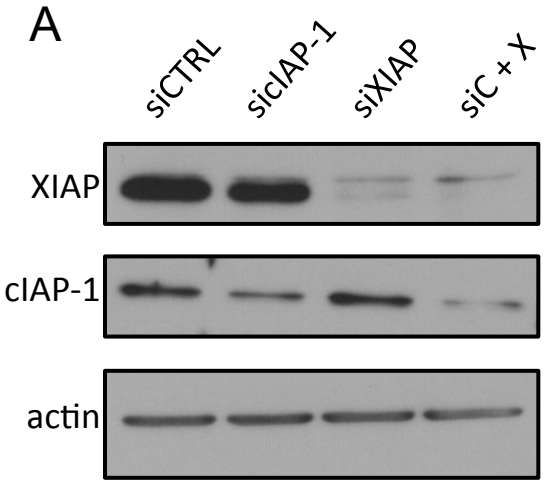

Figure 4.6: Death induction by proteasome inhibitors after knockdown of IAPs. A) LN18 cells transfected with siXIAP, sicIAP-1, or the combination of both siRNAs (siC + X). B) LN18 cells transfected with siRNA were treated for 48 h with proteasome inhibitors, followed by analysis of DNA fragmentation.

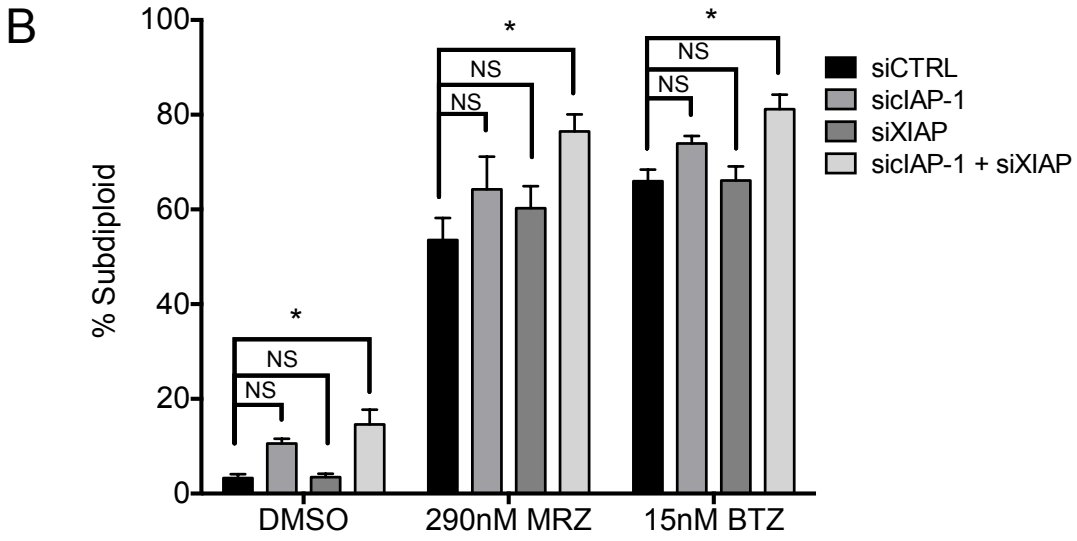

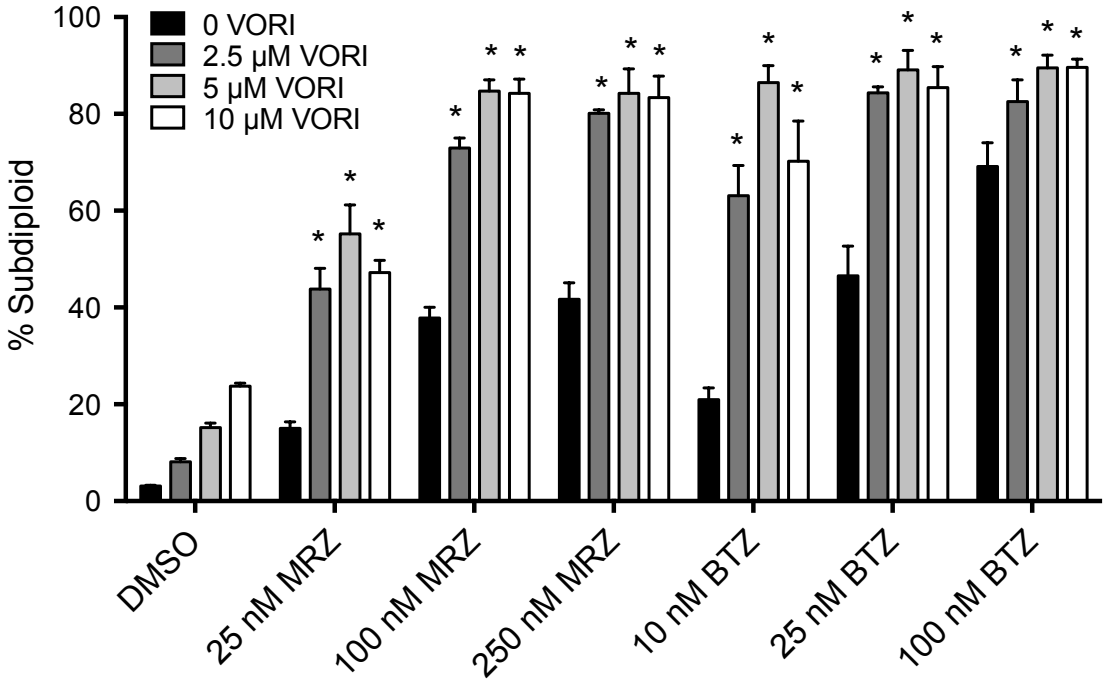

Figure 4.7: Increased death with proteasome inhibitors and vorinostat. LN18 cells were treated 48 h with combinations of proteasome inhibitors (MRZ and BTZ) with vorinostat (*$p < 0.05$ compared to either single agent alone).

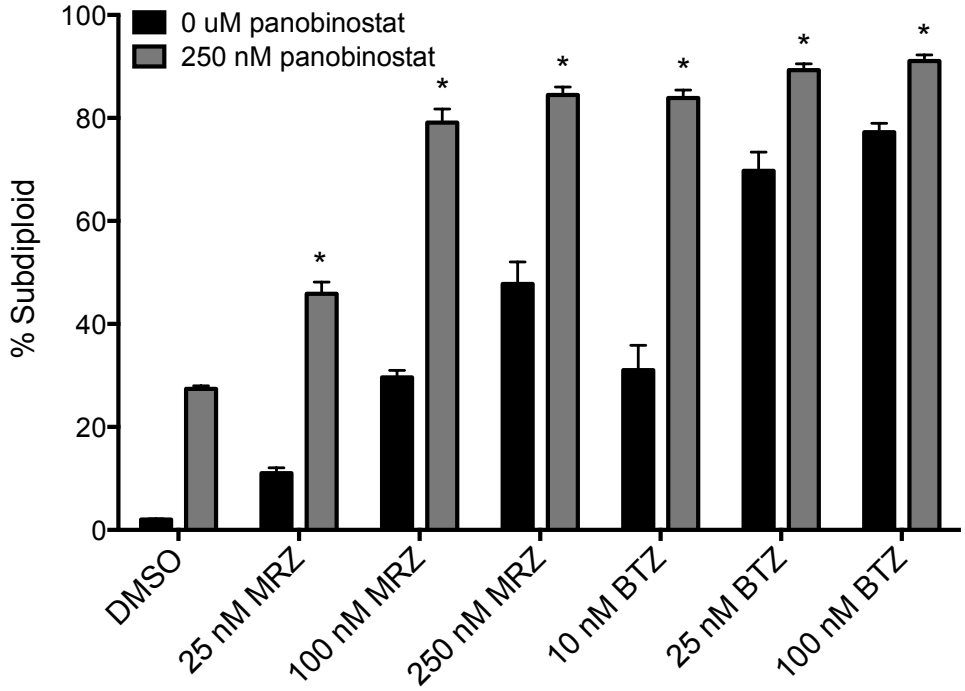

Figure 4.8: Increased death with proteasome inhibitors and panobinostat. LN18 cells were treated 48 h with combinations of proteasome inhibitors (MRZ and BTZ) with panobinostat (*$p < 0.05$ compared to either single agent alone).

The synergistic potential of these combinations was evaluated using CalcuSyn software. This method uses the Chou and Talalay method for evaluating synergy [158]. Values <1 indicate synergistic effects, values = 1 indicate additive effects, and values >1 indicate antagonistic effects. According to this method, synergy occurred in cells treated with multiple doses of BTZ or MRZ with vorinostat or panobinostat. In particular, the most synergistic combinations were 10 nM BTZ or 100 nM MRZ with 5 μM vorinostat or 250 nM panobinostat (Table 4.1).

Though the class I HDACi entinostat was also examined, it did not exert very strong effects on DNA fragmentation when combined with proteasome inhibitors (Fig. 4.9). Therefore, only the pan-HDACi were examined in future experiments.

Vorinostat interacts with the proteasome pathway by reducing PSMB5 mRNA.

To better understand interactions between proteasome inhibitors and HDACi, I examined potential areas where the drug mechanisms could overlap. First, I examined whether proteasome inhibitors could alter histone acetylation in GBM cells, which has been previously reported for MRZ in leukemia [139]. Acid extracted histones were examined by Western blot. Though vorinostat caused a strong accumulation of acetylated histone H3, MRZ and BTZ did not impact these levels, either alone or in combination with vorinostat (Fig. 4.10A). This was confirmed by densitometry analysis (Fig. 4.10B).

Next, I examined whether the HDACi vorinostat impacted levels of proteasome catalytic subunit mRNA, which has also been previously observed in leukemia [139]. Vorinostat significantly reduced levels of PSMB5 (β5 catalytic subunit) mRNA in LN18 cells, both alone and in combination with BTZ and MRZ (Fig. 4.11).

Prot. Inhib.	CI: 2.5 µM VORI	CI: 5 µM VORI	CI: 100 nM pano	CI: 250 nM pano
25 nM MRZ	0.226	0.209	0.279	0.203
100 nM MRZ	0.117	**0.075**	0.304	**0.102**
250 nM MRZ	0.144	0.126	0.448	0.168
10 nM BTZ	0.217	**0.100**	0.376	**0.086**
25 nM BTZ	0.192	0.161	0.248	0.124
100 nM BTZ	0.766	0.527	0.497	0.396

Table 4.1: Combination index (CI) values for synergy of proteasome inhibitors plus HDACi. CalcuSyn software was used to determine CI values for combinations of MRZ and BTZ with vorinostat and panobinostat. Values <1 are synergistic, values = 1 are additive, and values >1 are antagonistic.

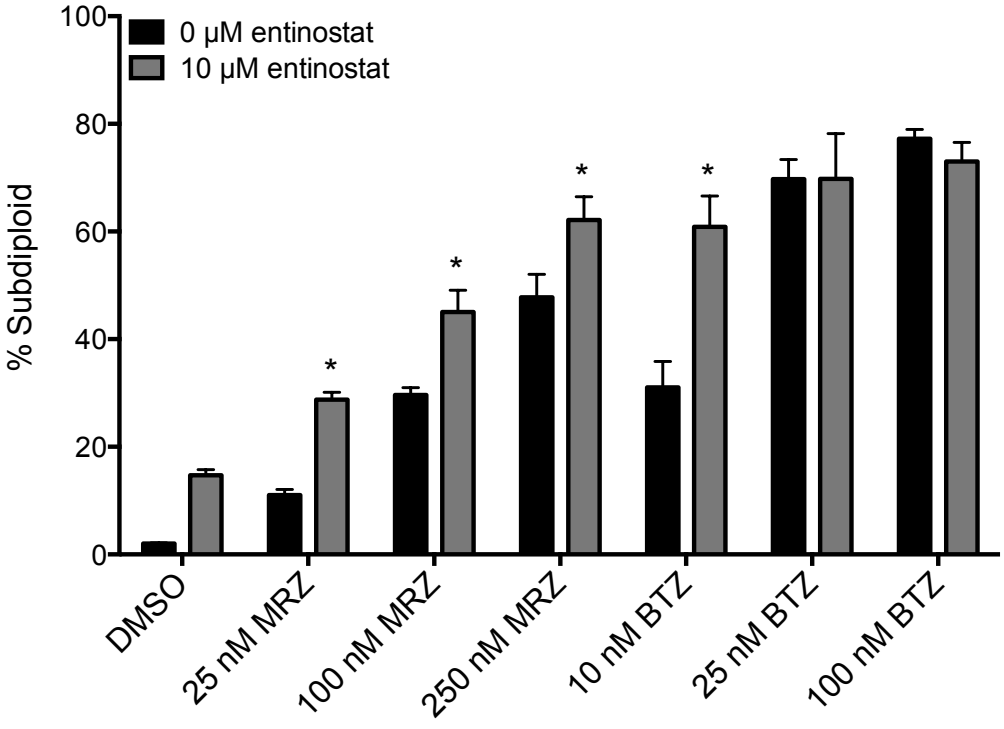

Figure 4.9: Death induction by proteasome inhibitors and entinostat. LN18 cells were treated 48 h with combinations of proteasome inhibitors (MRZ and BTZ) with entinostat (*$p < 0.05$ compared to either single agent alone).

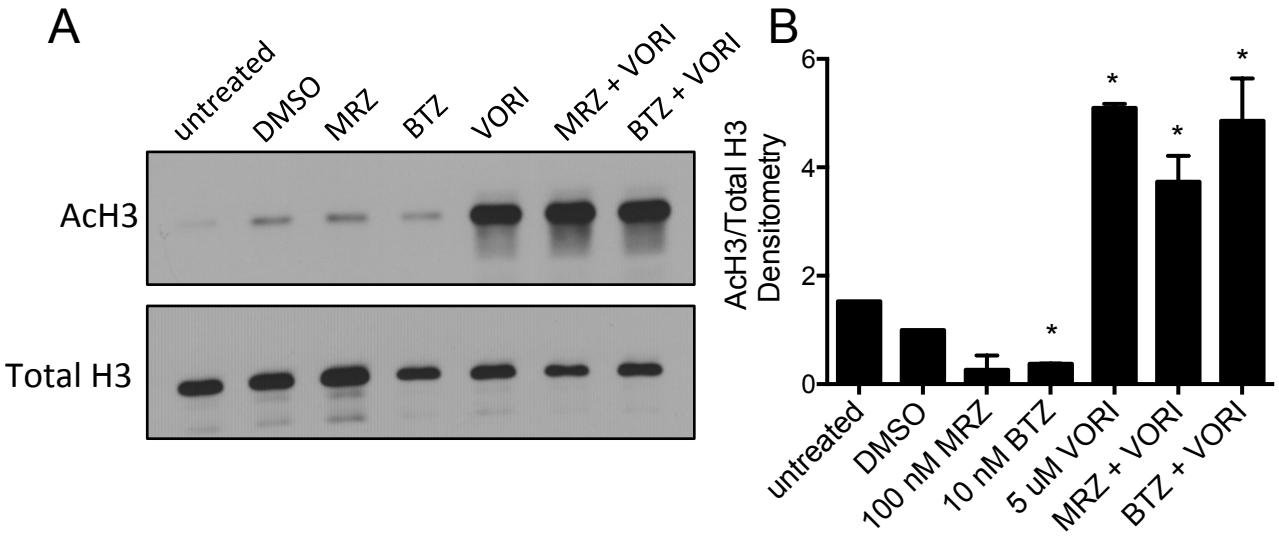

Figure 4.10: Vorinostat, but not proteasome inhibitors, alters histone acetylation. A) Acetylated H3 and total H3 in acid extracted histones from LN18 cells treated for 6 h with 100 nM MRZ, 10 nM BTZ, and 5 μM vorinostat. B) Densitometry showing the ratio of acetylated to total H3 in Western blots from (A) (*$p < 0.05$ compared to DMSO).

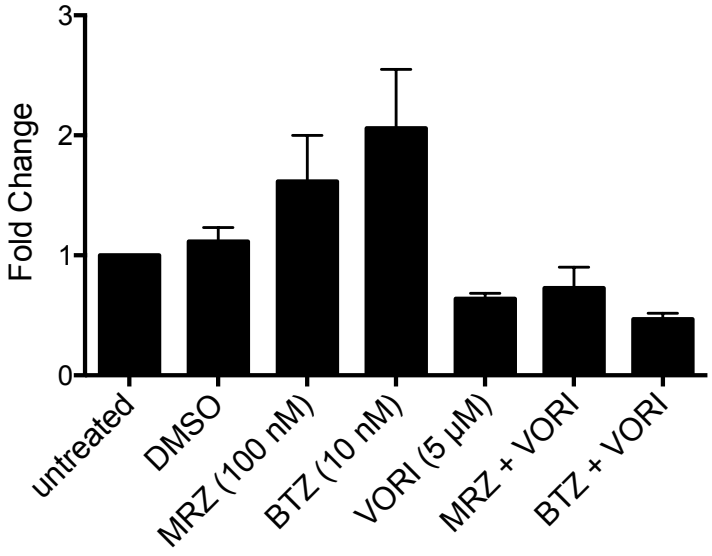

Figure 4.11: Vorinostat suppresses transcription of the proteasome subunit PSMB5. Levels of PSMB5 mRNA were assessed in LN18 cells treated for 8 h with proteasome inhibitors (MRZ and BTZ) and vorinostat.

While proteasome inhibitors caused trends toward slightly increased PSMB5 mRNA, likely as a "bounce back" response to inhibition, this was ameliorated in cells that were also treated with vorinostat.

To examine whether the decrease in PSMB5 mRNA had functional consequences, I examined proteasome activity in LN18 cells treated with either vorinostat or panobinostat in combination with proteasome inhibitors. Both vorinostat (Fig. 4.12A) and panobinostat (Fig. 4.12B) slightly decreased the CT-L proteasome activity that is associated with the β5 proteasome subunit by around 20%. Both vorinostat and panobinostat also significantly augmented proteasome inhibition in cells treated with either BTZ or MRZ for 24 h.

Though these differences were significant, they were difficult to discern due to the strong suppression of proteasome activity that already occurs with single agent BTZ and MRZ treatment. Therefore, I examined whether vorinostat augmented proteasome inhibition in cells treated with low doses of BTZ and MRZ. At the doses used (10 nM MRZ, 1 nM BTZ, and 5 μM vorinostat), all 3 therapeutic agents reduced proteasome activity by roughly 20% to 30% as single agents (Fig. 4.13). Proteasome activity was further reduced, to roughly 50% to 60%, in cells treated with the combinations of low dose BTZ and MRZ with vorinostat. Therefore, HDACi such as vorinostat are able to augment proteasome inhibition caused by BTZ and MRZ, potentially increasing their therapeutic efficacy.

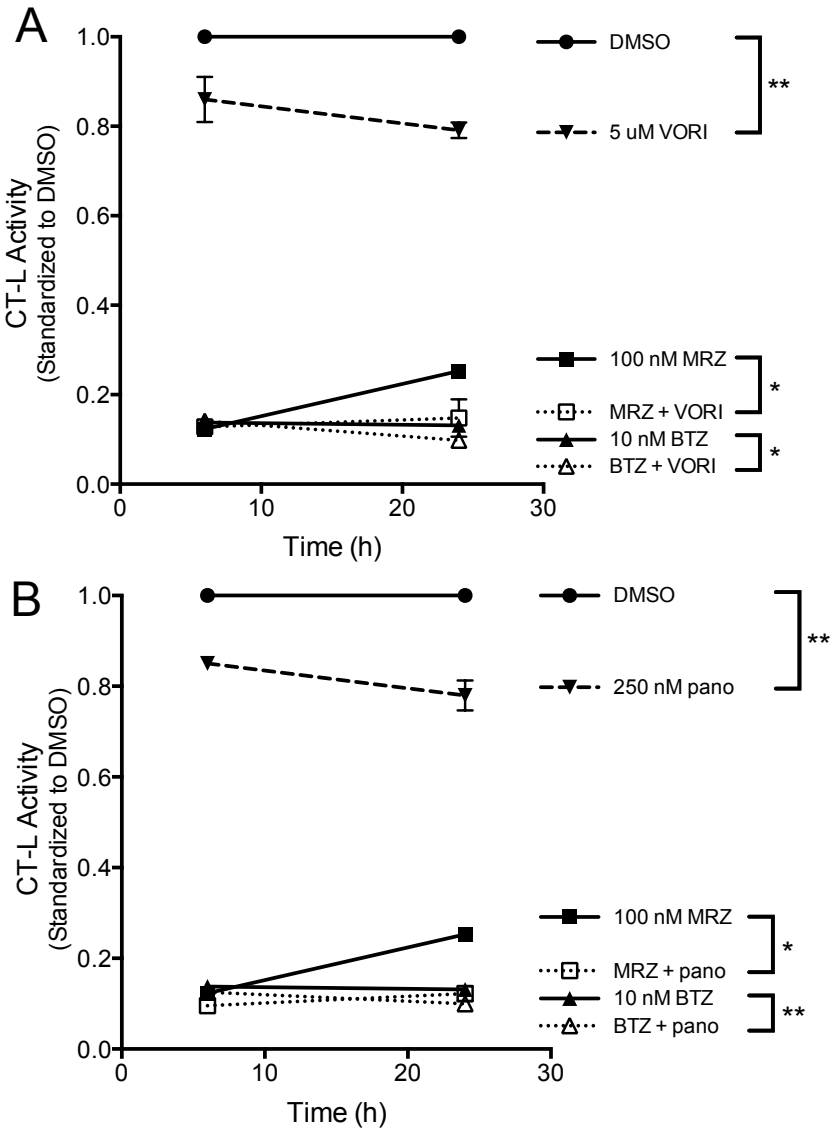

Figure 4.12: Vorinostat and panobinostat suppress CT-L proteasome activity, alone and in combination with proteasome inhibitors. A-B) LN18 cells treated for 6 or 24 h with proteasome inhibitors (MRZ and BTZ) and HDACi (A, vorinostat; B, panobinostat). CT-L activity was measured using the fluorogenic substrate suc-LLVY-amc (*$p < 0.05$ at 24 h only; **$p < 0.05$ at both 6 and 24 h).

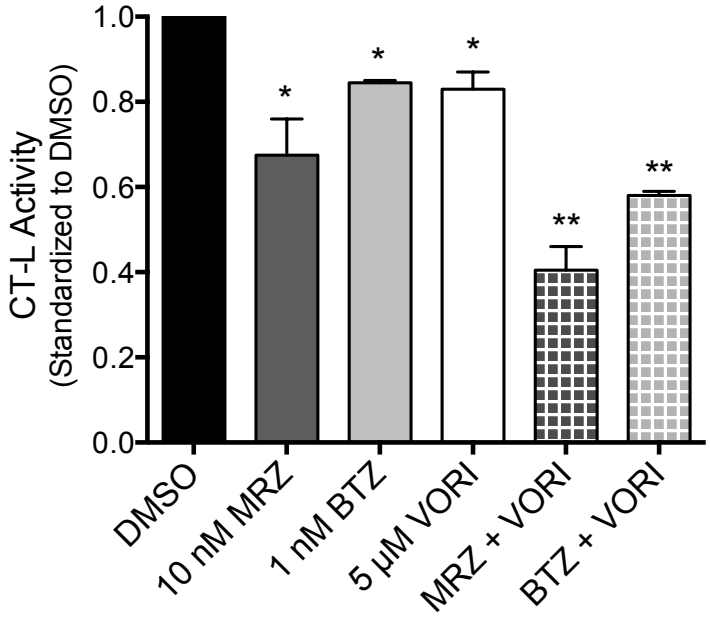

Figure 4.13: Vorinostat enhances proteasome suppression in combination with low doses of MRZ and BTZ. LN18 cells treated for 24 h with low doses of proteasome inhibitors (MRZ and BTZ) and vorinostat. CT-L activity was measured using the fluorogenic substrate suc-LLVY-amc (*$p < 0.05$ compared to DMSO; **$p < 0.05$ compared to either single agent alone).

Vorinostat augments caspase cleavage in combination with proteasome inhibitors *in vitro* and *in vivo*.

A report in GBM cell lines found that the combination of BTZ and vorinostat induced a strong reduction in mitochondrial membrane potential [96]. Together with my results that the intrinsic apoptosis pathway (involving mitochondria permeability, cytochrome C release, and activation of caspase 9) activates apoptosis after proteasome inhibition in GBM, it seems possible that the combination of proteasome inhibitors with vorinostat causes augmented activation of caspase 9. Indeed, when I examined caspase 9 in LN18 cells treated with the most highly synergistic combinations of BTZ or MRZ with vorinostat, I found strong enhancement of caspase 9 cleavage in the combination-treated cells (Fig. 4.14). Potentiation of this mechanism by the combination indicates that markers of caspase activation, such as cleavage of executioner caspases and their substrates, might act as markers of death induction in brain tumors *in vivo*.

To examine this possibility, I once again utilized an orthotopic xenograft model, as described at the beginning of this chapter. For these experiments, tumors were allowed to develop for 14 days. Following this time, mice were treated for 2 weeks with a schedule of twice weekly proteasome inhibitors (1.0 mg/kg BTZ or 0.15 mg/kg MRZ) with 5 times per week vorinostat (50 mg/kg), all injected IP. Mice were treated both with single agents, or with combinations of BTZ or MRZ with vorinostat. The schedule of treatment is shown in Figure 4.15. Mice were sacrificed 24 h following the final proteasome inhibitor treatment. Brains were preserved in formalin for later paraffin embedding and IHC analysis.

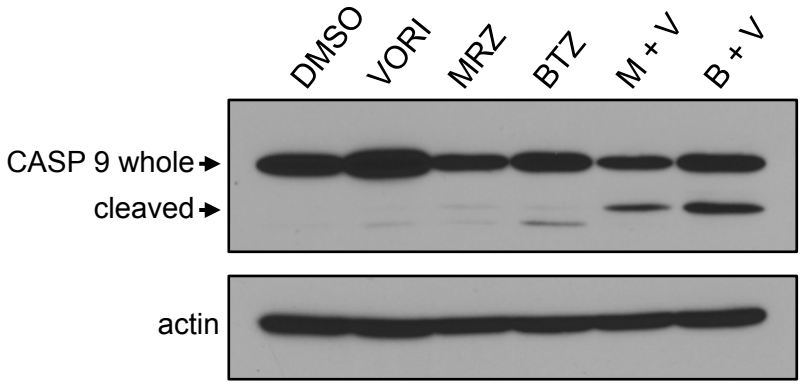

Figure 4.14: Synergistic induction of caspase 9 cleavage by combinations of vorinostat and proteasome inhibitors. Caspase 9 cleavage in LN18 cells treated for 16 h with 5 μM vorinostat with 100 nM MRZ or 10 nM BTZ for 16 h.

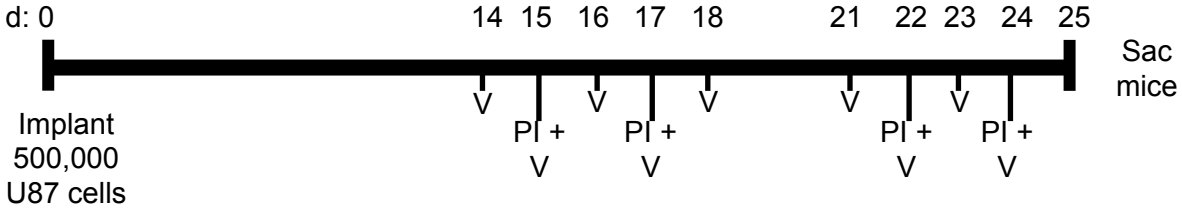

Figure 4.15: Treatment schedule for mice with orthotopic brain tumors treated with proteasome inhibitors and vorinostat. Mice were implanted with 500,000 U87 cells through intracranial guidescrews, and tumors were allowed to develop for 2 weeks. Mice were then treated for 2 weeks with vorinostat (5 days/ week, 50 mg/kg) or twice weekly proteasome inhibitors (0.15 mg/kg MRZ or 1.0 mg/kg BTZ) injected IP. Mice were sacrificed 24 h following the last proteasome inhibitor treatment.

First, brain tumors were examined by IHC for cleaved caspase 3. Cleaved caspase 3 staining was faint, and only 2 brain tumors-both in the group that received MRZ plus vorinostat-showed any positivity for cleaved caspase 3. This is clear in representative images (Fig. 4.16A), as well as in quantification of the average number of positive cells per 40X field for individual mice (Fig. 4.16B). Though there were only a few positive cells, it is notable that both samples that had minor signs of positivity were in the same group (MRZ plus vorinostat).

Next, levels of cleaved lamin A were examined in brain tumors from these mice. Lamin A is a substrate of executioner caspases [159]. There was a marked lack of single agent effects on lamin A cleavage. However, there were signs of lamin A cleavage in tumors from both the BTZ plus vorinostat and MRZ plus vorinostat groups (Fig. 4.17A). The increases in lamin A cleavage in the combination treatment groups were significant (Fig. 4.17B). There was a slight trend towards increased cleavage of lamin A in the MRZ plus vorinostat treated brain tumors compared to the BTZ plus vorinostat treated brain tumors.

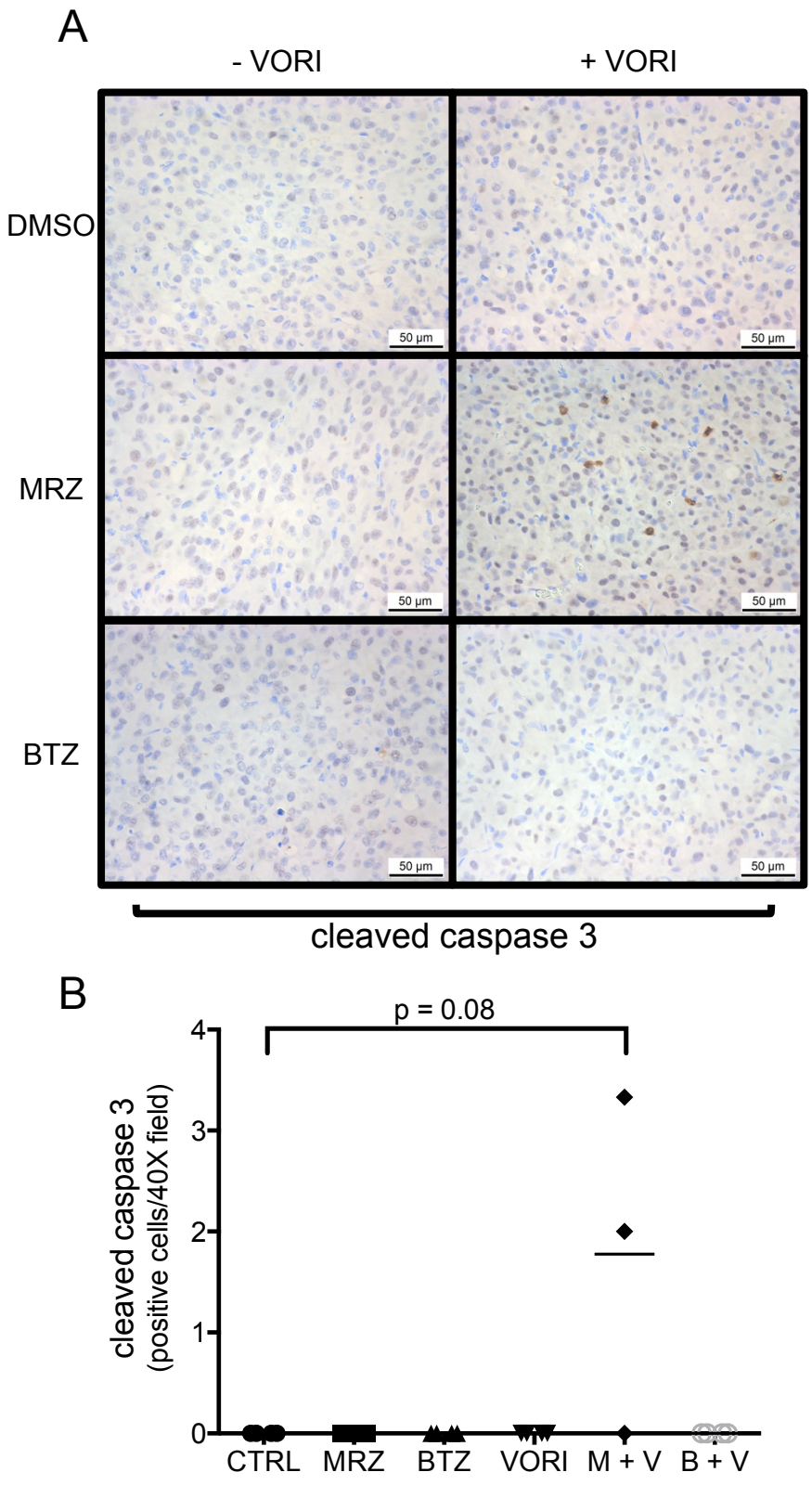

Figure 4.16: Cleaved caspase 3 in brain tumors of mice treated with vorinostat plus proteasome inhibitors. A) Representative images from IHC of cleaved caspase 3 in the brain tumors of mice treated for 2 weeks with combinations of vorinostat with BTZ or MRZ (40X). B) Quantification of the average number of positively stained cells per 40X field.

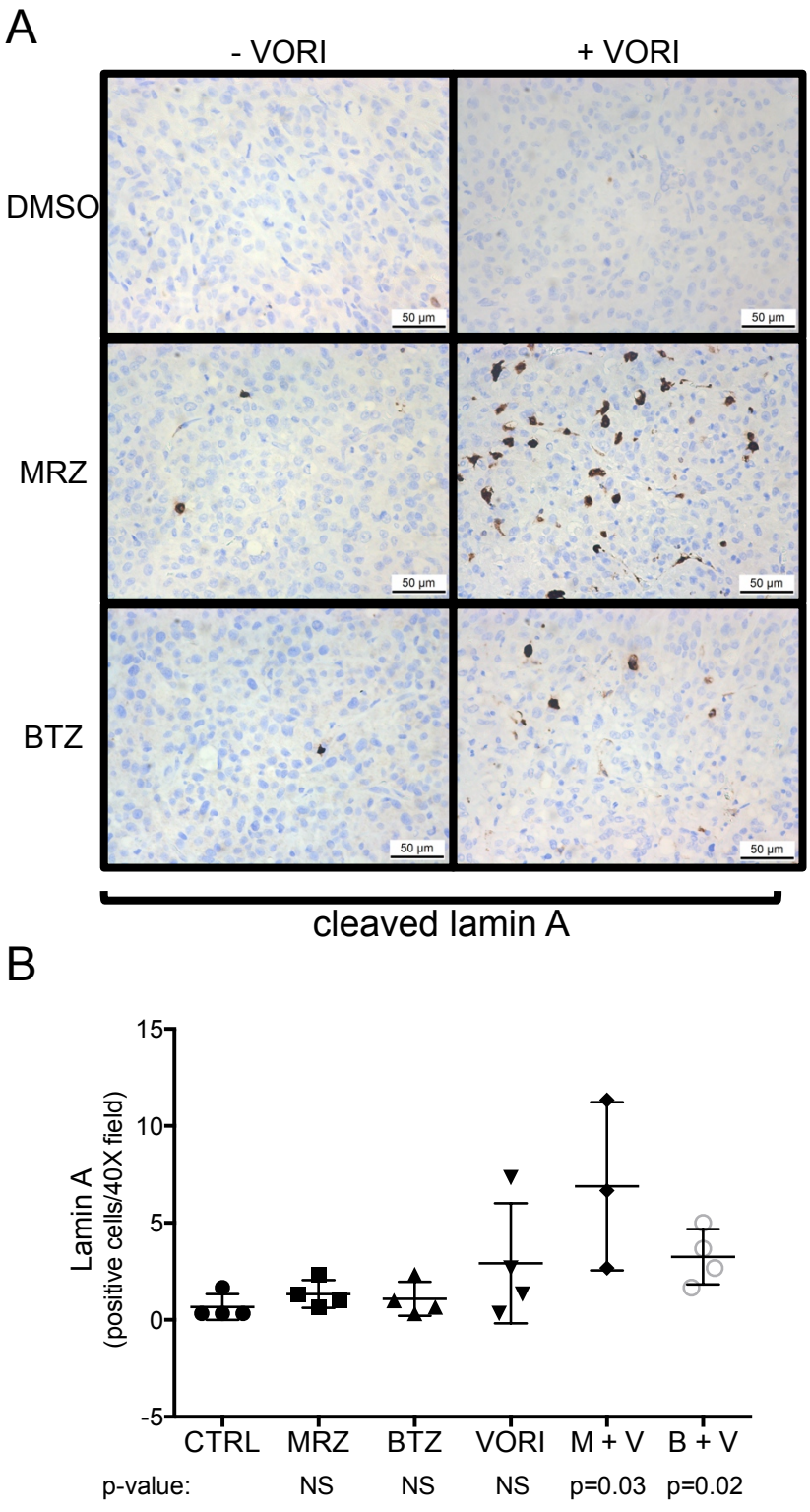

Figure 4.17: Lamin A cleavage in brain tumors of mice treated with vorinostat plus proteasome inhibitors. A) Representative images from IHC of cleaved lamin A in the brain tumors of mice treated for 2 weeks with combinations of vorinostat with BTZ or MRZ (40X). B) Average number of cells per 40X field positive for cleaved lamin A in mice from (A).

Summary

In this chapter, I examined questions of key clinical importance for proteasome inhibitors in GBM: the ability of the drugs to inhibit the proteasome in orthotopic brain tumors, and the combination effect of proteasome inhibitors with HDACi. Two separate proteasome substrates were examined, p21 and p27, in brain tumors of mice treated either with a single injection of proteasome inhibitors (p27) or with twice-weekly treatment for 2 weeks (p21). Together, these results indicate that BTZ and MRZ do exert functional effects on proteasome substrates. Notably, MRZ seems to exert slightly stronger effects, particularly on p27, which was not elevated by BTZ treatment.

Combinations of proteasome inhibitors and HDACi revealed strong combination effects between both BTZ and MRZ and 2 pan-HDACi, vorinostat and panobinostat. Notably, a class I HDACi did not exert strong effects in combination with BTZ and MRZ. Examination of potential areas of crosstalk between the mechanisms of these drugs revealed that vorinostat reduces mRNA of the proteasome catalytic subunit PSMB5. This change in mRNA was indicative of functional effects, as both vorinostat and panobinostat decreased CT-L proteasome activity, both alone and in combination with proteasome inhibitors.

I also determined that the combination of proteasome inhibitors with vorinostat augmented caspase 9 cleavage, which was shown to be important for proteasome inhibitor-induced death in Chapter 3. Following up on this result, I examined markers of caspase activation in orthotopic brain tumors from mice treated with BTZ, MRZ, and vorinostat for 2 weeks. This experiment revealed minor increases in cleaved caspase 3 in brain tumors of mice only in the MRZ plus vorinostat group. Additional examination of the caspase substrate lamin A revealed that though there was a lack of single agent effects, increases in cleaved

lamin A were noted in mice treated either with MRZ plus vorinostat or BTZ plus vorinostat, with a slight trend toward greater lamin A cleavage in some of the brain tumors treated with MRZ plus vorinostat.

The results of this chapter indicate that BTZ and MRZ exert functional effects on proteasome substrates and induce activation of caspases and cleavage of the caspase substrate lamin A in orthotopic brain tumors. Trends such as increased p27 accumulation in brain tumors and increased lamin A cleavage in combination with vorinostat indicate that MRZ may have slightly more potent properties than BTZ *in vivo*. As I hypothesized, the work in this chapter provided insight into the clinical utility of BTZ and MRZ by demonstrating their ability to affect proteasome substrates as single agents and to induce death in combination with HDACi.

Chapter 5

Discussion and Future Directions

The goal of this work was to characterize the proteasome inhibitory and death inducing properties of the proteasome inhibitors BTZ and MRZ in order to establish factors that contribute to their efficacy and their potential as therapeutic agents in GBM. This study also sought to provide *in vivo* evidence of the clinical feasibility of proteasome inhibition therapy in GBM by examining brain tumor permeance and combination therapy strategies to enhance the efficacy of BTZ and MRZ.

Chapter 2 Discussion

Targeting standard proteasome subunits with BTZ and MRZ

The first goal of this study was to investigate the kinetics of proteasome inhibition by BTZ and MRZ. Past studies have indicated that MRZ causes longer-lasting proteasome inhibition in other cancer types such as leukemia, and this property is thought to be why MRZ induces greater cell death than BTZ in some model systems [160]. The potency of irreversible inhibitors was further established by studies of MRZ analogs. Different MRZ analogs were developed that were either irreversible due to the presence of a leaving group (LG analogs) in the chemical structure, or reversible due to the lack of a leaving group (non-LG analogs) [60]. The irreversible LG analogs were found to induce more sustained proteasome inhibition and greater death than the non-LG analogs in myeloma and leukemia [60, 61, 161]. Therefore, the question of whether proteasome inhibitors cause sustained inhibition of proteasome activity is important for establishing their potential therapeutic efficacy.

In a panel of GBM cell lines, I found that BTZ actually caused more sustained inhibition of the chymotryptic-like proteasome activity than MRZ (Fig. 2.1). This was unexpected, as it was the opposite of what was seen in the previously mentioned studies in

hematologic malignancies. BTZ also exerted stronger effects on the caspase-like and trypsin-like activities compared to MRZ (Fig. 2.2), which is counter to past studies that have indicated that MRZ is a stronger inhibitor of trypsin-like proteasome activity [62].

To determine possible reasons why BTZ was causing more sustained inhibition of proteasome activity, I examined 2 possibilities: efflux of MRZ through P-glycoprotein and differential proteasome binding ability in GBM cells. When I used verapamil to inhibit P-glycoprotein, I found that this did not enhance the activity of either BTZ or MRZ, indicating that it is not a major mechanism of efflux for either agent (Fig. 2.5). To examine binding to the proteasome, I examined inhibition of proteasomes by these agents in cell lysates (Fig. 2.6). Interestingly, under these conditions, both BTZ and MRZ had similar effects on the chymotryptic-like proteasome activity at both early (1 h) and late (24 h) timepoints. Since BTZ and MRZ demonstrate similar inhibitory abilities in lysed cells, it is likely that some factor in the cellular milieu is attenuating MRZ, such as a compensatory increase in proteasome subunits, inactivating modifications such as oxidation, or drug metabolism.

A study of MRZ in mice characterized proteasome activity using fluorogenic substrates in a wide variety of tissues from 10 min to 24 h following intravenous injection with 0.15 mg/kg MRZ [99]. In this study, MRZ initially inhibited proteasome activity in several normal tissues including lung, liver, and kidney; however, proteasome activity in these cells recovered within 24 h. More sustained inhibition was only observed in the blood and in plasmacytoma tumors. This suggests that normal cells have a mechanism for recovering proteasome activity, even after treatment with an irreversible inhibitor. It is possible that GBM cells have a similar mechanism. One possible way this could occur is through increased production of new proteasome subunits. My data suggests that levels of the

catalytic subunit β5 remain steady after proteasome inhibitor treatment (Fig. 2.4) Recovery of proteasome activity could also occur through increased proteasome assembly, which can be facilitated by factors such as proteasome maturation protein (POMP), which facilitates formation of proteasome core particles [162]. Future experiments analyzing proteasome assembly, such as by analysis of POMP or by examination of assembled proteasome levels using native gel electrophoresis would be informative about whether MRZ-treated LN18 cells recover proteasome activity through changes in assembled proteasomes.

Another explanation is that MRZ could be metabolized or subject to inactivating modifications in GBM cells. Past studies of BTZ have revealed that Vitamin C can directly bind to BTZ and inhibit its function [85]; similar mechanisms could exist for MRZ. Experiments that determine whether MRZ is sensitive to oxidation or other inactivating modifications would be informative on this issue. Pharmacodynamic studies of MRZ have indicated that it is relatively stable *in vivo*, indicating that drug inactivation does not seem to be a major issue [99]. In addition, the data presented in this study indicates that MRZ affects proteasome substrates in brain tumors 24 h after injection of mice (Fig. 4.1-2); therefore, the effects of MRZ are reasonably sustained *in vivo*.

As an additional measure of proteasome inhibition, I examined proteasome activity and DNA fragmentation after shorter pulse treatments (2–24 h) with BTZ and MRZ (Fig. 2.7). This is an important indicator of clinical potential, as it likely mirrors *in vivo* conditions better than continuous treatment. Past experiments with radiolabeled MRZ indicated that the levels of MRZ in mouse blood and kidneys spiked within 30 min of treatment before quickly diminishing [163]. Under these conditions, it is important that the inhibitors can cause strong proteasome inhibition with only a short exposure time.

In GBM cells, short (2 h) and long (24 h) exposure to MRZ had very similar effects in terms of reduction in proteasome activity and induction of cell death. However, BTZ required longer exposure times to cause significant effects, and effects on proteasome activity and death induction were amplified as exposure time increased. Therefore, while BTZ can cause stronger effects overall with continuous exposure, MRZ is more potent after brief exposure. This could have important implications for clinical efficacy.

Lastly, to further explore the kinetics of MRZ in GBM, I examined the effects of a variety of irreversible (LG) versus reversible (non-LG) analogs of MRZ (Fig. 2.8). Since MRZ-treated GBM cells recovered proteasome activity, I was curious to see if there was still a clearly defined difference between MRZ and its reversible analogs. I hypothesized that the irreversible nature of MRZ may be compromised in GBM, leading to a lack of distinction between these analogs. However, there were still clear differences between the two classes of agents; irreversible analogs caused longer lasting proteasome inhibition and greater decreases in viability compared to reversible analogs. Therefore, the presence of the LG still enhances the potency of MRZ. Interestingly, BTZ behaved more like one of the irreversible analogs in terms of degree of proteasome inhibition and decreases in viability at a dose that was 1/10 the dose of the MRZ analogs (10 nM BTZ versus 100 nM analogs). This indicates that BTZ is simply more potent in these cells. Future experiments focused on the effect of the proteasome inhibitors on various proteasome subunits and assembly as well as examination of drug metabolism in these cells could help explain the enhanced potency of BTZ compared to MRZ *in vitro*.

Though BTZ treatment was more advantageous *in vitro*, my data in an orthotopic brain tumor model indicated that MRZ more potently caused accumulation of proteasome

substrates, and also caused slightly stronger effects on death activation in combination with vorinostat. Therefore, MRZ may have increased clinical utility despite differences in the dynamics of proteasome inhibition *in vitro*.

Targeting the immunoproteasome in GBM

Immunoproteasome subunits were found to be overexpressed in a subset of GBM tumors by immunohistochemistry [40], and my analysis of the REMBRANDT database showed that they are also more highly expressed in GBM tumors versus normal brain (Fig. 2.9B). Further analysis of the REMBRANDT database showed that lower LMP7 (β5i) expression was associated with better overall survival of glioma patients (Fig. 2.10). Therefore, I hypothesized that targeting the immunoproteasome may be effective for GBM therapy. However, inhibiting the immunoproteasome with ONX-0914, a specific inhibitor of β5i, did not cause much cell death (Fig. 15). This is likely because the immunoproteasome constitutes only a fraction of the proteasome pool in GBM cells. Therefore, dual targeting of the standard and immunoproteasome may be a more effective therapeutic strategy.

For combination with standard proteasome inhibitors, I wanted to ensure the doses of ONX-0914 I was using were specifically targeting only the immunoproteasome. At high doses, ONX-0914 loses specificity and also inhibits β5. To ensure that the doses I was using were specifically inhibiting only the immunoproteasome, I used the ELISA-based ProCISE assay, which can measure binding of agents to each standard and immunoproteasome subunit (Fig. 2.12). Having established which doses were specific, I tested combinations of ONX-0914 with BTZ and MRZ. The combinations did not show increases in DNA fragmentation, indicating that addition of a specific immunoproteasome inhibitor did not enhance the potency of either BTZ or MRZ.

One main reason for this may be the fact that BTZ and MRZ can already affect immunoproteasome subunits on their own. Though the main target of these drugs is the standard proteasome, the active sites of the proteasome are so similar that the drugs often react with other subunits. It can be difficult to determine whether immunoproteasome activity is inhibited, as the fluorogenic substrates commonly used to measure proteasome activity do not distinguish between proteasome and immunoproteasome activity. Berkers *et al.* used a probe for proteasome active sites to demonstrate that BTZ can bind to multiple proteasome catalytic subunits, including β1i and β5i [43]. To really determine whether targeting the immunoproteasome enhances ubiquitin-proteasome system targeting in GBM, it would be necessary to use an agent that specifically targets only the standard proteasome; its lack of immunoproteasome-targeting would need to be confirmed with a specific assay such as ProCISE. Then, combinations of standard and immunoproteasome targeting could be more accurately studied. However, from a therapeutics perspective, this data indicates that additional targeting of the immunoproteasome does not enhance the efficacy of BTZ or MRZ.

It is unknown whether upregulation of immunoproteasomes could be a mechanism of resistance to standard proteasome inhibitors in GBM. A past study demonstrated that a specific inhibitor of β1i, IPSI-001, was able to induce death in myeloma cells resistant to BTZ [63]. Though ONX-0914 was not effective in the current study, it would be interesting to study whether it can induce death in GBM cells that are resistant to BTZ, such as those that have been continuously exposed to increasing doses of BTZ or MRZ to select for resistant cells.

Targeting of regulatory cap elements: PA28γ

Though the proteasome has several alternative regulatory cap subunits, PA28γ is relevant to this work because it has been found to be expressed at high levels in the brain [35], and reports indicate that it may regulate important cellular functions such as ubiquitin-independent degradation of select proteins including the cell cycle regulator p21 [36]. For these reasons, I hypothesized that PA28γ might play a role in GBM.

Though PA28γ was expressed in GBM cell lines, knocking it down with siRNA did not enhance sensitivity to BTZ or MRZ (Fig. 2.14). This is likely because BTZ and MRZ cause strong inhibition of the catalytic activity of the proteasome, making targeting of a cap subunit redundant. Overall, additional targeting of PA28γ did not enhance the therapeutic efficacy of BTZ or MRZ.

Chapter 2 Future Directions: The future of proteasome targeting in GBM

Experiments with proteasome inhibitors such as BTZ and MRZ have provided evidence that manipulation of the proteasome can be a useful strategy in cancer therapy. Looking forward, several other methods of targeting the ubiquitin-proteasome system are being developed that offer potential in two key areas: improved tolerability and increased specificity of targeting (Fig. 5.1).

Studies have frequently suggested that green tea has cancer preventative properties [164]. An interesting line of investigation has revealed that the polyphenol epigallocatechin-3-gallate (EGCG) is an inhibitor of the proteasome. Specifically, EGCG inhibited chymotrypsin-like proteasome activity in purified proteasomes and Jurkat leukemia cells at doses that were suggested to be achievable in the serum of people who consumed green tea [165]. As a consequence, EGCG caused accumulation of p27 and cell cycle arrest in Jurkat cells. Since then, synthetic EGCG analogs have also been investigated for their proteasome

inhibitory abilities [166]. This line of work is an interesting example of a proteasome inhibitor from a natural product that appears to be non-toxic. Due to its tolerability, EGCG is frequently considered to have potential as a cancer preventive agent. Future experiments will reveal whether EGCG can augment other types of therapy specifically by inhibiting the proteasome. Notably, EGCG has been shown to antagonize BTZ, preventing it from inhibiting the proteasome [152]. Therefore, consumption of green tea polyphenols is contraindicated for patients receiving BTZ. The potential of EGCG lies in augmentation of other therapeutic strategies in a highly tolerable manner.

Another strategy for inhibition of the ubiquitin-proteasome pathway involves targeting of the ubiquitin conjugating system. This process can be targeted at numerous steps. Inhibitors of E1 activating enzymes have developed, including PYR-41, an agent that inhibits formation of the thioester bond between ubiquitin and the active site cysteine of E1 ubiquitin activating enzymes [167]. This agent blocks ubiquitination in cells, which is a fairly broad mechanism, as the E1 enzyme is responsible for all ubiquitin activation and is not specific for certain substrates.

More finely targeted inhibitors target E3 ubiquitin ligases. Cullins, which are components of cullin-RING E3 ubiquitin ligases, are modified by the addition of NEDD8, a small ubiquitin family member that is activated in a process similar to that of ubiquitin. The addition of NEDD8 to cullins is necessary for their activation. Inhibitors have been designed to target the NEDD8 activating enzyme, which therefore prevents activation of cullin-RING E3 ligases [168]. MLN4924, an inhibitor of NEDD8 activation, was shown to radiosensitize breast cancer cells in a manner dependent on p21 accumulation after cullin-RING ligase inhibition [169].

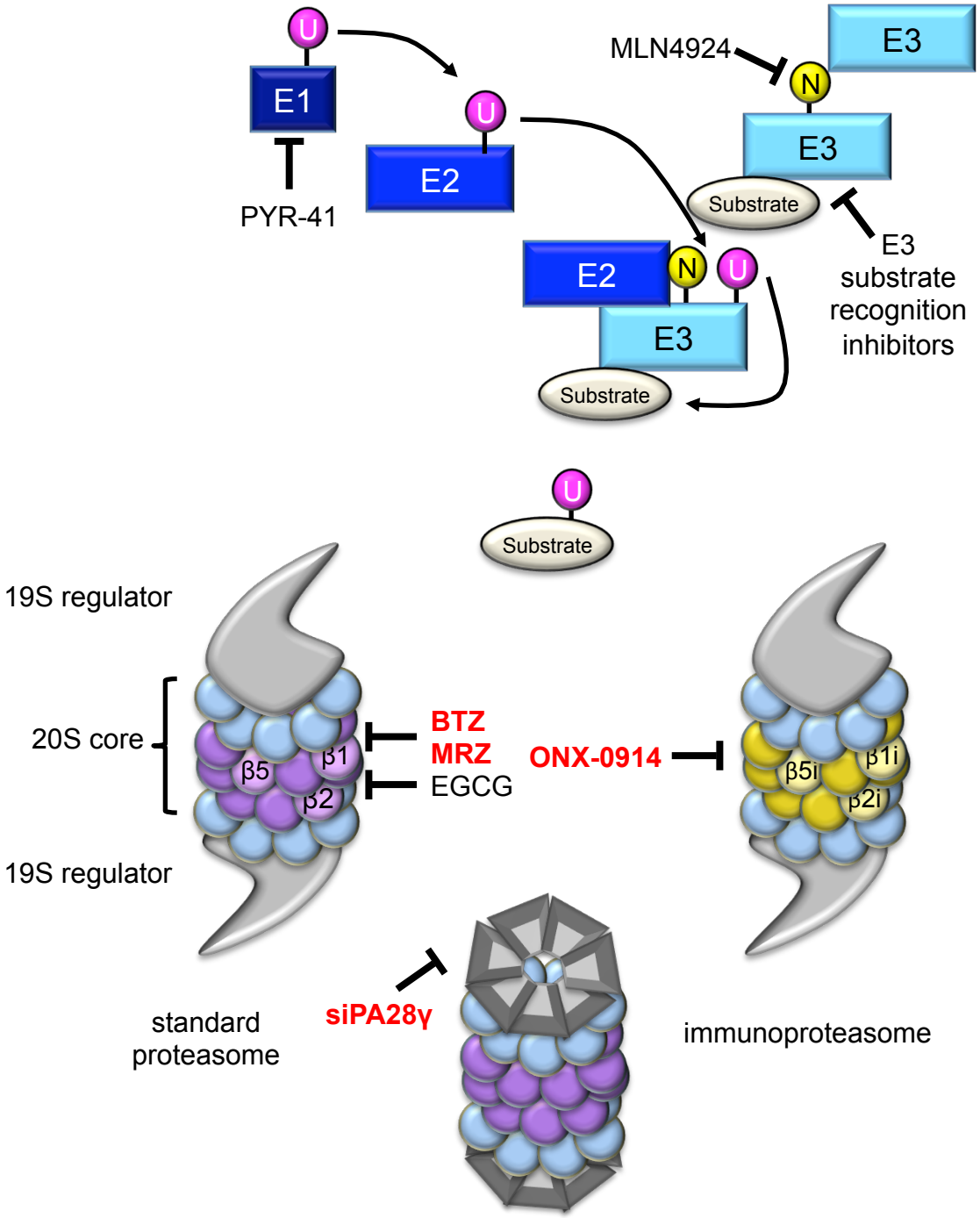

Figure 5.1: Targeting the ubiquitin-proteasome pathway. Inhibitors of the proteasome used in this study (highlighted in red, bold text) included inhibitors of the standard proteasome (BTZ and MRZ), immunoproteasome (ONX-0914) and PA28γ (siPA28γ). Other strategies for inhibiting protein degradation include inhibition of ubiquitin activating enzymes (PYR-41), inhibitors of E3 ligase substrate recognition, inhibitors of neddylation (MLN4924), and natural inhibitors of the proteasome (EGCG, epigallocatechin gallate) Abbreviations: N, NEDD8; U, ubiquitin.

Attempts have been made to develop more direct inhibitors of E3 ligases that interfere with their ability to recognize and bind substrates [170, 171]. Since E3 ligases are responsible for specific substrate recognition and ubiquitylation, it is possible that targeting them could be honed for more specific inhibition of protein degradation. For example, S phase kinase-associated protein 2 (Skp2) has been shown to recognize both p21 and p27 and target them for proteasomal degradation as part of E3 ligase SCF (Skp1-Cullin1-F-box protein) complexes [172, 173]. Therefore, inhibition of this E3 ligase complex could prevent degradation of these important cell cycle regulators.

Notably, targeting the ubiquitin conjugating pathway would only inhibit ubiquitin-dependent proteasome degradation; the proteasome is also capable of degrading some proteins independently of ubiquitin conjugation [174]. It will be interesting to determine whether more refined targeting of protein degradation can reduce toxicity while maintaining potent anticancer activity.

Perhaps most intriguing in the future of proteasome targeting is the possibility of specifically targeting the proteasomes that are assembled in response to the increased proteotoxic stress frequently present in cancer cells. A recent study in yeast reported a heat shock-induced protein, Adc17, that was specifically involved in assembly of proteasome regulatory caps under stress conditions [175]. Though no human homolog for Adc17 was identified by sequence analysis, it is possible that a functional homolog exists. Screens in mammalian cells that identify factors necessary for assembly of proteasomes specifically under stress conditions could provide intriguing targets for specific targeting of stress-induced proteasomes in cancer cells.

My work in this report has demonstrated that BTZ and MRZ strongly suppress proteasome activity, leading to accumulation of ubiquitinated substrates. Concordant avenues of investigation have presented new tools for inhibiting the ubiquitin-proteasome system, such as natural extracts and specific inhibitors of the ubiquitin conjugating system. Since strength and duration of proteasome inhibition have been linked to the anticancer efficacy of proteasome inhibitors such as BTZ and MRZ [61], new inhibitors must be tested to ensure they are capable of achieving desired effects on the function of this pathway. I have investigated some alternative targeting strategies, including an immunoproteasome inhibitor and knockdown of PA28γ, and have concluded that these strategies do not induce GBM cell death as single agents, nor do they enhance the activity of BTZ or MRZ. New agents should be tested in a similar manner in GBM.

Chapter 3 Discussion

Death induction by proteasome inhibitors in GBM

Having studied the dynamics with which BTZ and MRZ inhibited proteasome activity in GBM cells, I went on to investigate how that inhibition translated into effects on cell death. I examined multiple readouts of death and growth inhibition in GBM cells treated with proteasome inhibitors: viability by trypan blue exclusion, DNA fragmentation by propidium iodide staining, and colony growth in soft agarose (Fig. 3.1-3).

Proteasome inhibitors decreased viability and increased DNA fragmentation in GBM cells. BTZ caused these effects at lower doses than MRZ, which is consistent with my previous observations that BTZ caused longer-lasting proteasome inhibition than MRZ. Overall, however, GBM cells were sensitive to both BTZ and MRZ at reasonably low doses in the nanomolar range. These experiments establish that proteasome inhibition potently

induces death in GBM cells. Examination of the growth of colonies in soft agarose also showed inhibition of colony growth by BTZ and MRZ.

Proteasome inhibitors have been shown to induce caspase-dependent death in a variety of cancer cell types [66-68]; however, the dependence of proteasome inhibitors on caspases in GBM has not yet been established. This information is important for determining biomarkers of drug efficacy and for anticipation of mechanisms of drug resistance. Therefore, I set about examining the three initiator caspases: caspases 2, 8, and 9. I observed cleaved caspase bands, representing the initial steps of caspase activation, for all three initiator caspases after proteasome inhibition (Fig. 3.4). Activity of the executioner caspases 3/7 was detected 16 and 24 h following proteasome inhibitor treatment. To test the hypothesis that caspase activation was an essential part of proteasome inhibitor-mediated cell death, I pre-treated cells with a pan-caspase inhibitor, z-VAD-fmk. This agent blocked nearly all the DNA fragmentation induced by both BTZ and MRZ (Fig. 3.5). Together, this data indicates that death induction by proteasome inhibitors is caspase-dependent in GBM, and all three initiating caspases may play a role in this death.

Activation of caspase 2 by proteasome inhibitors in GBM

I observed that caspase 2 was cleaved earlier than the other initiator caspases after proteasome inhibitors. Therefore, I became interested in the role caspase 2 may be playing in proteasome inhibitor-induced apoptosis in GBM. Caspase 2 can be activated following heat shock and DNA damage [73, 76, 176, 177], but activation of this caspase has not been extensively studied in GBM. The signals initiate recruitment of caspase 2 to the PIDDosome, a complex including PIDD and RAIDD, where caspase 2 CARD domains interact and catalytic processing occurs to activate caspase 2 [73, 178, 179]. Caspase 2 goes on to cleave

Bid, which leads to mitochondrial permeabilization and downstream activation of caspase 9 [75, 76]. Caspase 2 has been described as a tumor suppressor, as cells deficient in caspase 2 are resistant to DNA damaging agents and do not properly initiate apoptosis after cell cycle inhibition [77]. These background studies indicate that activation of caspase 2 by proteasome inhibitors would be a logical mechanism of death.

I wanted to be sure that the cleavage of caspase 2 that I observed was truly indicative of activation, as cleavage can sometimes occur in a manner not associated with activation. Therefore, I studied another step in caspase 2 activation; induced proximity that occurs as caspase 2 is recruited to the PIDDosome. This step is a definitive step in the activation process, and can be measured using the Venus bimolecular fluorescence protein attached to caspase 2 CARD domains [178]. I used this system as a second readout, in addition to cleavage on Western blot, to show that caspase 2 is activated quickly after proteasome inhibitor treatment, especially with MRZ (Fig. 3.6).

Though caspase 2 was definitely activated, experiments with caspase 2 knockdown revealed that it was not essential for death induction by BTZ or MRZ. In fact, cells stably expressing caspase 2 shRNA actually had slightly increased cleavage of caspase 9, caspase 3/7 activity, and DNA fragmentation (Fig. 3.8). This was very interesting given that it was the opposite of what was expected. One piece of evidence that caspase 2 serves a different purpose than the other initiator caspases is the kinetics of caspase activation. The Venus BiFC model indicates that caspase 2 is recruited to the PIDDosome as early as 1 h to 2 h. However, activation of other caspases does not occur until 12 h to 24 h, and DNA fragmentation is seen at even later times (24 h to 48 h). This could have interesting implications for alternative roles of caspase 2, perhaps even in cell cycle checkpoints in a

manner that is more ameliorative than death inducing. Data from caspase 2-deficient mice indicates that caspase 2 has opposing roles in death induction in different cell lineages. Oocytes and lymphoblasts from caspase-2 deficient mice were more resistant to death, while sympathetic neurons from these same mice were more susceptible to death following withdrawal of nerve growth factor [180]. The conflicting roles of caspase 2, particularly evidence that it can protect neurons from death, lends support to the idea that caspase 2 could also be protective in GBM cells. In the case of GBM cells, caspase 2 is not required for death induction by proteasome inhibitors.

Induction of death by caspase 9 after proteasome inhibition in GBM

I then examined the importance of caspases 8 and 9, which were both activated around 12 h following proteasome inhibition. I used 2 methods to examine the importance of caspases 8 and 9: chemical inhibitors that use substrate specificity to block caspase protease activity and shRNA specifically targeting either caspase 8 or 9. These experiments revealed that inhibition of caspase 9 blocked activation of caspase 8, and also blocked some DNA fragmentation in both models. This indicates that caspase 9 is at the top of the caspase hierarchy after treatment with BTZ and MRZ in GBM (Fig. 5.2).

There were some differences between the chemical inhibitors and shRNA that should be noted. Mainly, chemical inhibitors of both caspase 8 and caspase 9 blocked a significant portion of the DNA fragmentation induced by BTZ and MRZ. However, when I repeated these experiments with shRNA, only a small portion of DNA fragmentation was blocked, and only by shCASP9 and not by shCASP8. One reason for this difference is the lack of specificity of the chemical inhibitors. Caspases have overlapping cleavage specificities, so the inhibitors recognize different caspases to varying degrees [144]. For instance, the peptide

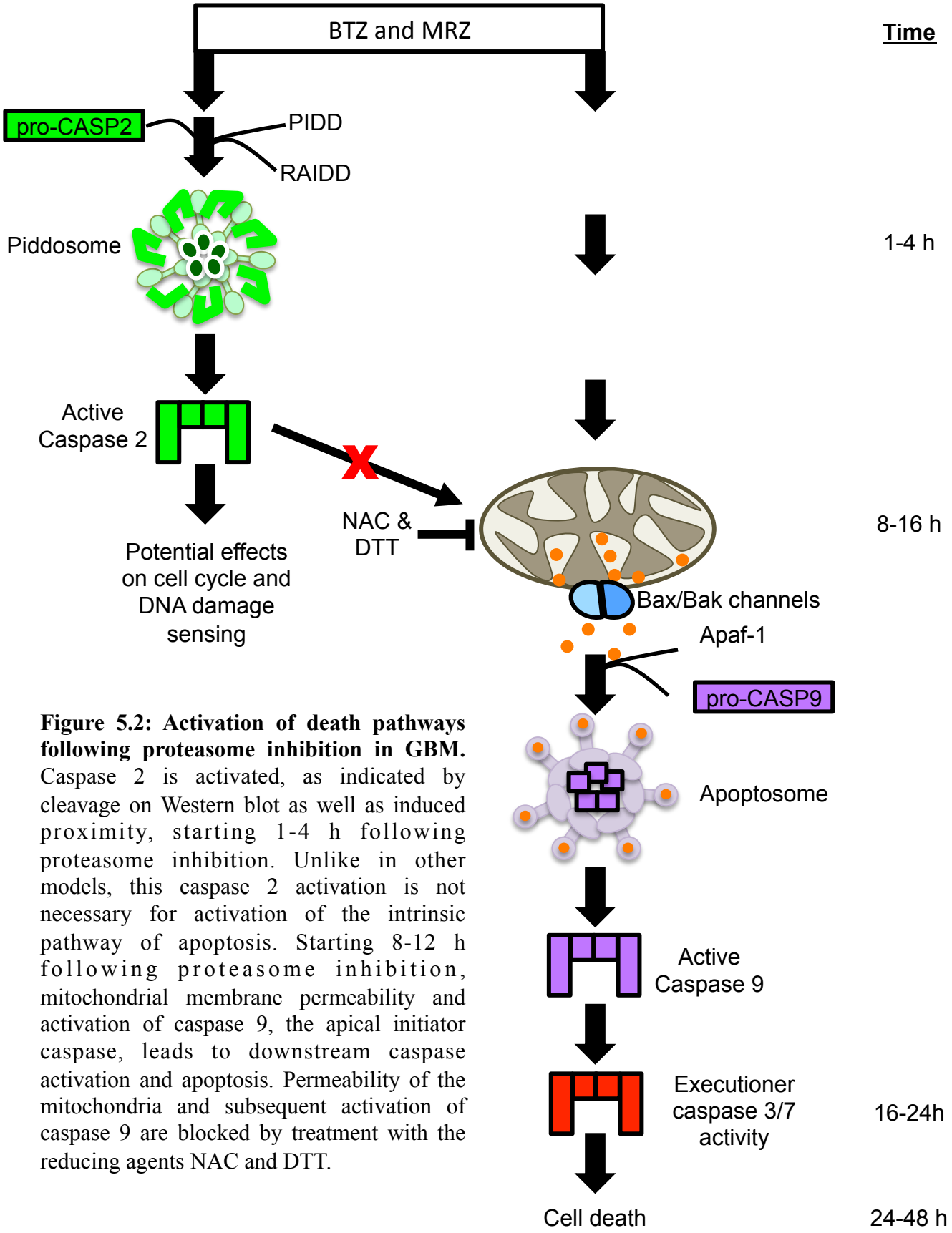

Figure 5.2: Activation of death pathways following proteasome inhibition in GBM. Caspase 2 is activated, as indicated by cleavage on Western blot as well as induced proximity, starting 1-4 h following proteasome inhibition. Unlike in other models, this caspase 2 activation is not necessary for activation of the intrinsic pathway of apoptosis. Starting 8-12 h following proteasome inhibition, mitochondrial membrane permeability and activation of caspase 9, the apical initiator caspase, leads to downstream caspase activation and apoptosis. Permeability of the mitochondria and subsequent activation of caspase 9 are blocked by treatment with the reducing agents NAC and DTT.

used for caspase 8 (IETD) is also recognized by the executioner caspases 3 and 6. Therefore, it is logical that this inhibitor would have a strong protective effect on DNA fragmentation. Notably, the caspase 8 inhibitor has a very low affinity for the other initiator caspases, which is why it is still useful for experiments that seek to determine the apical initiating caspase in GBM. Similarly, the caspase 9 inhibitor (LEHD) has some affinity for the executioner caspases, but much lower affinities for the other initiators [144]. This explains the strong effects of these inhibitors on DNA fragmentation suppression, but also indicates that they are still valid tools due to their relative specificity as far as the initiator caspases are concerned. In fact, blockade of the executioner caspases by these inhibitors will prevent downstream cleavage of initiator caspases by activated executioner caspases, which adds reassurance that the effects I observed with these inhibitors on initiator caspase cleavage are really due to initiating and not late events.

With the shRNA, there were differences between early (24 h) and later (48 h) death in cells expressing shCASP8 or shCASP9 (Fig. 3.14-15). At 24 h, shCASP9 suppressed death by both BTZ and MRZ. Interestingly, shCASP8 also suppressed death, but only in cells treated with MRZ, not BTZ. This is consistent with previous studies in leukemia that have found an increased dependence on caspase 8 for MRZ [68]. However, only caspase 9 prevented death by both inhibitors. This could have interesting implications for the intrinsic sensitivity of brain-derived cells to death induction by specific caspases.

Caspase 9 has a notable connection to brain development and apoptosis after brain injury. Caspase 9 homozygous knockout mice usually die before birth and are marked by enlarged cerebrums, indicating defective apoptosis during brain development [181]. Though genes involved in caspase 9 activation, such as Apaf-1, have been found to be repressed in

the brain as development progresses, insults such as traumatic brain injury have been shown to cause re-expression of this pathway and subsequent caspase 9-dependent cell death [182]. This evidence, particularly the marked effects on brain development in caspase 9-deficient mice, supports the hypothesis that brain-derived cells, such as GBM cells, may be more susceptible to caspase 9-dependent apoptosis versus death induced by other caspases.

A final point that needs to be addressed concerning the experiments with caspase 8 and 9 shRNA has to do with the fact that after 48 h, there were only minor effects on death in the shCASP9 cells (Fig. 3.15). This would seem to indicate that the effects of caspase 9 are not particularly strong. However, there is precedent for the idea that reduction in the main death-inducing caspase can be compensated for by other caspases. For example, a study by Zheng *et al*. of a Fas agonistic antibody, Jo2, showed that mitochondrial permeability and activation of caspases 9 and 3 were necessary events for death induction in hepatocytes after treatment with Jo2 [183]. However, hepatocytes from mice deficient in caspases 9 or 3 were not protected from Jo2-induced apoptosis. In fact, apoptosis still occurred, and it was due to activation of caspases 2, 6, and 7, which were not detected in wild-type mice. Interestingly, the activation of compensatory caspases was still downstream of mitochondrial membrane permeability in caspase 3 and 9 deficient mice, indicating that the requirement for this event remained the same.

This study illustrates that the caspase pathways exhibit flexibility, and activation of compensatory caspase pathways is possible in cases of caspase deficiency. While this could explain the blunted effects on death that I observed after 48 h in shCASP8 and 9 cells, it is notable that early events (24 h) were still dependent on caspase 9. Therefore, failure of activate caspase 9 at the very least will delay apoptosis, and will prohibit death completely in

some cells. Together, my data indicates that compensatory pathways are possible, but the strongest death induction occurs through cleavage of caspase 9.

Bcl-XL protection from proteasome inhibitor-induced death, but not caspase 9 cleavage

As a method for further probing the role of caspase 9 in proteasome inhibitor-induced death, I overexpressed the anti-apoptotic Bcl-2 family member Bcl-XL in LN18 GBM cells. I expected Bcl-XL to maintain mitochondrial integrity, preventing activation of caspase 9 and subsequent apoptosis. While Bcl-XL did reduce DNA fragmentation in response to proteasome inhibitors (Fig. 3.18), it did not prevent decreases in mitochondrial membrane potential or cleavage of caspase 9 after proteasome inhibition (Fig. 3.19). Notably, both caspase 9 cleavage and DNA fragmentation were prevented in Bcl-XL overexpressing cells treated with staurosporine, which activates the mitochondrial pathway of apoptosis.

The lack of protection against caspase 9 cleavage in Bcl-XL overexpressing cells could simply mean that the degree of Bcl-XL overexpression is inadequate for preventing these events. However, it is possible that overexpression of this protein has other unintended effects on cells besides protection of the mitochondrial membrane. Bcl-2 family members have also been shown to localize to the endoplasmic reticulum (ER), and Bcl-XL has been shown to cause release of calcium from the ER [184, 185]. As a regulator of intracellular calcium flux, Bcl-XL could have numerous effects such as stimulating mitochondrial energy production or potentially activation of calpains [185]. Calpains are a family of proteases that have been shown to activate caspases in response to ER stress [186]. These studies demonstrate the Bcl-XL has complex functions that go beyond its regulation of mitochondrial membrane permeability. Overexpressing Bcl-XL can affect all of these aspects, and future investigation of alternative roles of Bcl-XL may lend insight into why

cells overexpressing this protein are protected from proteasome inhibitor-induced apoptosis independently of mitochondrial membrane protection and cleavage of caspase 9.

The protective effect of thiol reducing agents against proteasome inhibitor-induced death in GBM.

Given previous reports that generation of ROS is important for proteasome inhibitor-mediated death [47, 68, 82, 84], I investigated ROS induction as well as the effect of antioxidants in GBM cells treated with BTZ or MRZ. Treatment with NAC or DTT blocked caspase activation and cell death in a manner independent of GSH (Fig. 3.23-24). Also, despite previous reports that NAC directly inactivates BTZ [187], I found that both BTZ and MRZ were still able to proteasome activity in cells pre-treated with NAC (Fig. 3.25). Therefore, NAC and DTT block proteasome-inhibitor induced death in a manner independent of GSH or direct inactivation of proteasome inhibitors.

It has also been reported that proteasome inhibitors cause amino acid starvation, particularly through depletion of the amino acids cysteine and asparagine in MEFs [153]. In that study, supplementing with cysteine and asparagine was protective against the proteasome inhibitor MG132. I hypothesized that NAC may be protecting cells from proteasome inhibitors by flooding cells with cysteine, rescuing them from starvation. However, amino acid levels were not reduced following proteasome inhibition in LN18 cells, and additional supplementation with asparagine had minimal effects on proteasome inhibitor-induced death (Fig. 3.26-27). Therefore, I concluded that amino acid starvation was not a likely mechanism of proteasome inhibitor efficacy in GBM.

Alternatively, NAC and DTT impact thiol levels to create a reduced cellular environment. Given their broad effects on cellular reduction potential, NAC and DTT may

affect many proteins in stress response and cell death pathways, such as caspases and components of caspase activating complexes. Thiol modulation can also impact cellular stress responses, as DTT and NAC have been shown to attenuate heat shock death in endothelial cells, whereas GSH did not prevent death [148]. DTT has also been found to inhibit the heat shock response and decrease translation by increasing phosphorylation of eukaryotic initiation factor 2α [188, 189]. The way NAC and DTT modulate the cellular reducing environment and influence stress pathways may provide insight into the mechanism by which they protect cells from proteasome inhibitor-induced death.

Chapter 3 Future Directions: Looking at indicators of sensitivity to caspase 9-depentent apoptosis following proteasome inhibition in GBM.

Since caspase 9 is the initiating caspase in GBM cells treated with proteasome inhibitors, examination of factors related to caspase 9 activation could serve as biomarkers of drug efficacy as well as help anticipate drug resistance. For example, mitochondrial membrane permeability or cleavage of caspase substrates could be examined in tumors to evaluate whether BTZ and MRZ are exerting effects at the molecular level in GBM patients.

As for mechanisms of resistance, factors that mediate mitochondrial permeability could impact caspase 9 activation, and therefore efficacy of proteasome inhibitors. Bcl-2 and Bcl-XL, which are anti-apoptotic regulators of mitochondrial membrane integrity, have been found to be expressed in GBM and other cancer types, which could be an important mechanism of resistance to proteasome inhibitors [112]. Drugs have been developed to inhibit these anti-apoptotic proteins, such as ABT-737, a therapeutic agent that mimics the BH3 proteins that are natural antagonists of pro-apoptotic Bcl-2 family members [190]. Targeting Bcl-2 and Bcl-XL induces apoptosis in GBM cell lines, suggesting these proteins

are important mediators of apoptosis in GBM [113]. High levels of these proteins in a GBM patient would suggest possible resistance to MRZ and BTZ, and would encourage the use of therapeutics like ABT-737 that would ameliorate the effects of high levels of these anti-apoptotic proteins.

As I mentioned earlier, my data concerning the protective effects of NAC and DTT also suggests the potential for future studies into how modulation of cellular stress by these agents could be involved in protection from proteasome inhibitor-induced death. This data also has clinical implications. Vitamin C and other antioxidants have already been shown to prevent BTZ efficacy in myeloma [151], and thiol-rich agents such as NAC and DTT that alter the reducing environment in cells should also be evaluated for contraindications. Additionally, this work suggests that GSH, but not NAC, may be an appropriate treatment for the peripheral neuropathy associated with BTZ treatment [102], as it does not attenuate proteasome inhibitor efficacy.

Chapter 4 Discussion

Accumulation of proteasome substrates in orthotopic brain tumors after BTZ and MRZ treatment.

A main goal of this work was to establish the ability of BTZ and MRZ to have functional effects on proteasomes in orthotopic brain tumors. These experiments answered important questions about BBB permeance that have not been adequately addressed by studies that used subcutaneous models [80, 98] or by trials where biomarkers of drug efficacy were not reported [97]. Both BTZ and MRZ caused accumulation of the proteasome substrate p21 in orthotopic brain tumors, while only MRZ increased p27 (Fig. 4.1-2). This indicates that MRZ may have a stronger effect *in vivo,* particularly on specific substrates like p27.

Interestingly, MRZ did not cause longer lasting proteasome inhibition than BTZ *in vitro*, but data from *in vivo* experiments suggests a different dynamic in an orthotopic animal model, perhaps due to better BBB penetration of MRZ in tumor bearing mice. Importantly, these experiments demonstrate that BTZ and MRZ do have the ability to be delivered to brain tumors, which was uncertain as past studies of mice without brain tumors, and therefore with intact BBB, have indicated that these drugs may not reach brains [99]. This work emphasizes the importance of using relevant *in vivo* models that represent the actual clinical condition as closely as possible. Also, given the negative clinical trial results with BTZ in GBM, it is especially important to monitor biomarkers of drug function.

Proteasome inhibition combination therapy: targeting IAPs

Another step toward establishing the clinical potential of BTZ and MRZ is designing rational combination strategies to enhance therapeutic efficacy. The decision to target IAPs was based on the observation that MRZ induced greater cleavage of initiator caspases, but not stronger death, compared to BTZ (Fig. 4.3). IAPs can bind to active caspases, particularly caspases 9, 3, and 7, and inhibit apoptosis [114]. Therefore, I hypothesized that MRZ may increase IAPs, inhibiting cell death even in the presence of caspase activation.

I found that neither MRZ or BTZ increased protein levels of XIAP (Fig. 4.4). However, even though protein levels were not altered, there is still a possibility that IAP-caspase interactions were somehow enhanced in MRZ-treated cells. To discover if targeting IAPs was a useful strategy for enhancing efficacy of MRZ, I utilized mimetics of Smac, a cellular inhibitor of IAPs. The Smac mimetics birinapant and LCL-161 increased death in combination with both BTZ and MRZ (Fig. 4.5), suggesting an overall role of IAPs in

preventing the efficacy of proteasome inhibitors, though it demonstrated that this effect was not unique to MRZ.

Though birinapant and LCL-161 have been shown to cause ubiquitination and degradation of IAPs [156], I did not observe changes in IAP levels following treatment. This raised concerns that the drugs were not acting as previously described. Therefore, I silenced XIAP and cIAP-1 with siRNA to see if specific targeting of these proteins enhanced combination efficacy. Knockdown of cIAP-1 and XIAP did not enhance the efficacy of BTZ and MRZ (Fig 4.6). This suggests that either other IAPs besides XIAP and cIAP-1 are targeted by birinapant and LCL-161, or off-target effects of these agents are responsible for their combination effects. Since birinapant and LCL-161 do enhance death induction by proteasome inhibitors, future studies are needed to understand how these drugs are functioning to yield this effect.

Proteasome inhibition combination therapy: targeting HDACi

I also examined targeting of HDACi in combination with proteasome inhibitors. The combination of BTZ with vorinostat in GBM has shown promise in preliminary *in vitro* studies [95], but a clinical trial of this combination that did not report molecular markers of efficacy for either agent failed to prevent disease progression [97].

In this study, I found that MRZ and BTZ synergized in GBM cells with the pan-HDACi vorinostat and panobinostat, but not with the class I HDACi entinostat (Fig. 4.7-9, Table 1.1). Therefore, targeting of class I HDACs is not sufficient for combination effects. I also investigated areas where the mechanisms of proteasome inhibitors and HDACi might intersect, and I found that vorinostat decreased mRNA of the proteasome catalytic subunit β5 (Fig. 4.11). This decrease in mRNA was accompanied by functional changes, as both

vorinostat and panobinostat decreased proteasome activity, alone and in combination with proteasome inhibitors (Fig. 4.12-13). The decrease in mRNA is consistent with past experiments in leukemia [139]. Upregulation of β5 expression has been shown to cause resistance to proteasome inhibitors [106], so the fact that HDACi suppress expression could have interesting implications for preventing resistance to BTZ and MRZ.

I also investigated the combination of BTZ and MRZ with vorinostat in an orthotopic model of GBM. Given strong *in vitro* data from past studies and the data from this current study, further examination of the reason for the disappointing clinical result is warranted [95, 96]. Also, MRZ has not been tested with vorinostat *in vivo* in GBM. Based on my result that proteasome inhibitors induce caspase 9-dependent death in GBM, and also the fact that the combination of BTZ or MRZ with vorinostat enhances cleavage of caspase 9, I chose to examine cleavage of the executioner caspase 3, as well as cleavage of the caspase substrate lamin A in tumors of mice treated with proteasome inhibitor and HDACi combinations. Though there was a lack of single-agent efficacy for any of the drugs *in vivo*, cleaved lamin A was notably increased in tumors from mice treated with the combinations of BTZ or MRZ with vorinostat (Fig. 4.17). There was a trend toward increased lamin A cleavage in mice treated with vorinostat plus MRZ versus the combination with BTZ, indicating once again that MRZ may be exerting a stronger effect than BTZ *in vivo*. Though cleaved caspase 3 staining was weak, it is notable that the only samples that showed any positivity were tumors treated with MRZ and vorinostat (Fig. 4.16). It is possible that MRZ shows increased efficacy in this combination due to stronger effects on proteasomes, as indicated by its effects on proteasome substrates in brain tumors.

Chapter 4 Future Directions: Confirming effects of proteasome inhibitors on survival of orthotopic GBM models.

My initial experiments demonstrate that BTZ and MRZ are capable of causing accumulation of proteasome substrates in orthotopic brain tumors. More definitive experiments are necessary to confirm this, as well as to determine whether there is truly a difference between BTZ and MRZ *in vivo*. One way to measure this would be to use radiolabeled drug to confirm delivery to brain tumors. Previous studies have used similar systems, but they have generally focused on delivery to other organs [99]. Another possibility for monitoring proteasome activity uses a technique in which a degradation-targeting is fused to a green fluorescence protein. Vlashi *et al.* demonstrated that a protein constructed in this manner accumulated in the absence of proteasome activity, allowing for fluorescence monitoring of proteasome activity in live cells [191]. GBM cells could be modified to express this protein, allowing for analysis of proteasome activity in brain tumors that have been treated with proteasome inhibitors.

My *in vitro* data also supports further investigation of newer HDACi *in vivo*. Panobinostat was effective at lower doses than vorinostat *in vitro* (nanomolar doses versus micromolar). This increased potency should be examined *in vivo*. Panobinostat is already being studied in the clinic for high grade glioma in combination with the angiogenesis inhibitor bevacizumab [192], further indicating its relevance for treatment of brain tumors.

This study focused on molecular markers of death in brain tumors. However, to further establish the clinical relevance of these agents and combinations, future experiments are needed to examine whether these agents reduce tumor size and enhance survival of mice. To examine tumor size, U87 cells expressing luciferase can be injected into mice, which

allows for imaging of tumor size as treatment progresses. This non-invasive imaging allows for monitoring of direct tumor effects while also looking at overall survival of the mice.

As a final piece of evidence supporting these agents clinically, it is possible to use different tumor models that are considered to be more representative of clinical GBM. Though U87 cells are commonly used to generate xenograft tumors, there is concern over the fact that these cells were isolated over 40 years ago, and long-term culture may make them less similar to the clinical disease state [193]. More recent studies have focused on isolation of glioma stem cells from patient specimens; that is, cells that display multipotency and the ability to recapitulate brain tumors from single cells [194]. Using glioma stem cells to establish orthotopic tumors allows for testing of therapeutic agents on a putative stem cell population, which is thought to be more resistant to therapy, and which has also been described as a main cause of tumor recurrence [195]. The evidence for the clinical relevance of BTZ and MRZ would be bolstered by experiments with combination agents with increased potency in relevant animal models that utilize cancer stem cells and measure effects on tumor size and survival.

Concluding remarks

The goal of this study was to establish the clinical relevance of proteasome inhibitors in GBM by first determining the optimal subunits for targeted therapy, then by defining the mechanism of apoptosis induction for optimal monitoring of drug efficacy and prediction of resistance, and finally by establishing the properties of these agents in a relevant orthotopic brain tumor model. By answering these questions, I have established a framework for future clinical experiments.

Targeting alternative proteasome components, such as the immunoproteasome and PA28γ, did not enhance the effects of BTZ and MRZ. Treatment with BTZ or MRZ was sufficient to induce death in GBM cells without combined targeting of other pathway components.

Having determined that targeting the standard proteasome with BTZ and MRZ was an optimal strategy, I then performed experiments that allowed me to ascertain that these agents induce caspase 9-dependent apoptosis in GBM cells. This information can be used to monitor treatment efficacy in future studies, such as by examination of mitochondrial permeability and cleavage of caspase substrates. Additionally, this information opens the door for future studies into whether factors that limit caspase 9 activation, such as overexpression of anti-apoptotic Bcl-2 family members, can serve as biomarkers for predicting resistance to proteasome inhibitors in GBM.

I also determined that proteasome inhibitor efficacy was blocked by the cellular reducing agents NAC and DTT, but not by GSH. Notably, NAC and DTT blocked early steps in apoptosis, including release of cytochrome C from the mitochondria and caspase cleavage. NAC and DTT potentially perform this function through as-yet undefined changes in the cellular reducing environment or stress responses. This information also has important implications for the clinical use of proteasome inhibitors, as antioxidants are being examined as supplements that may reduce side effects, particularly peripheral neuropathy induced by BTZ. My work suggests that GSH could be safe for co-administration with proteasome inhibitors, as it does not interfere with drug efficacy. However, other agents with reducing properties, such as NAC, should not be used.

Finally, I presented results that establish the potential of BTZ and MRZ in a relevant orthotopic model. I showed that both agents cause accumulation of proteasome substrates in brain tumors, with MRZ having slightly stronger effects. I also demonstrated that the combination of vorinostat with proteasome inhibitors effects molecular markers of death in brain tumors, especially in tumors from mice treated with MRZ and vorinostat. Together, these results suggest a need for future examination of these agents in clinical trials that carefully monitor the molecular biomarkers of drug efficacy.

This study demonstrates that targeting the proteasome is a potent strategy in GBM. Future studies of alternative methods of proteasome targeting, such as inhibitors of E3 ligases or stress-induced proteasome induction, could provide more tolerable and specific options for targeting protein degradation. Additionally, this study provided ideas for development of biomarkers of drug efficacy and resistance that are based on the mechanism of death induction by caspase 9 that I have defined here. Finally, the *in vivo* experiments I presented here represent a basis for more exhaustive investigation of proteasome inhibition and survival enhancement achieved by proteasome inhibition therapy in various models of GBM. The work presented here, along with the future experiments, provides a detailed examination of the kinetics and mechanism of death induced by proteasome inhibitors in GBM cell lines and orthotopic tumors.

Chapter 6

Materials & Methods

Cell Culture and Reagents

All cells were maintained in an incubator at 37 °C with 5% CO_2. GBM cell lines (LN18, SNB19, U87, and U251) were obtained from ATCC and were maintained in DMEM/F12 media with 10% FBS, 1% penicillin and streptomycin, and 1% L-glutamine. Cells were authenticated by the Characterized Cell Line Core Facility at MD Anderson Cancer Center using the short tandem repeat method. Normal human astrocytes (NHA, E6/E7/TERT immortalized) were obtained from Kenneth Aldape (MD Anderson Cancer Center, Houston, TX) and were maintained in DMEM/F12 media with 10% FBS, 1% penicillin and streptomycin, 1% L-glutamine, 0.2 μg/mL puromycin, and 10 μg/mL blasticidin. PA28$\gamma^{-/-}$ MEFs were provided by Lance Barton (Austin College, Sherman, TX). PA28$\gamma^{-/-}$ MEFs were cultured in DMEM media supplemented with 10% FBS, 1 mM sodium pyruvate, 50 μM β-mercaptoethanol, 2 mM L-glutamine, 1X non-essential amino acids, and 1% penicillin and streptomycin. Caspase $2^{-/-}$ MEFs (E1A/Ras immortalized) were provided by Lisa Bouchier-Hayes (Baylor College of Medicine). Caspase $2^{-/-}$ MEFs were cultured in DMEM media with 10% FBS, 2 mM L-glutamine, 1% penicillin and streptomycin, 1X sodium pyruvate, 1X non-essential amino acids, and 55 μM β-mercaptoethanol.

BTZ was obtained from LC Labs (Woburn, MA) and MRZ was provided by Nereus Pharmaceuticals (San Diego, CA).

Proteasome Activity Assay

Cells incubated with indicated treatments were harvested by brief incubation with 0.05% trypsin. Cells were pelleted by centrifugation (1,700 rpm for 3 min) and pellets were washed 1X in ice cold PBS. Cells were resuspended in 20S proteasome lysis buffer (20 mM

Tris, pH 7.5, 0.1 mM ethylenediaminetetraacetic acid, 20% glycerol, and 0.05% NP-40 supplemented each time with fresh 1 mM β-mercaptoethanol and 1 mM adenosine triphosphate). Cells were lysed by freezing and thawing 3X on dry ice. Samples were then spun for 1 min at 12,000 rpm. Samples were aliquoted to duplicate wells (100 µL/well) of a black 96-well plate. Next, 98 µL substrate buffer (50 mM HEPES, pH 7.5, and 50 mM EGTA, pH 7-8) were added to each well along with 2 µL fluorogenic substrate: suc-LLVY-amc for chymotrypsin-like activity or z-LLE-amc for caspase-like activity (AG Scientific, San Diego, CA, USA), and boc-LRR-amc for trypsin-like activity (Enzo Life Sciences, Inc., Farmingdale, NY, USA). After 1 h incubation with fluorogenic substrates, fluorescence was read on a Gemini EM Microplate Reader (Molecular Devices, Sunnyvale, CA, USA) at an excitation of 380 nM and an emission of 460 nM. For experiments that indicate they were standardized to DMSO, all samples were divided by the fluorescence value for control (DMSO treated) cells.

Western Blotting

Cells were lysed for 1 h at 4 °C in Triton X-100 lysis buffer (PBS containing 1% Triton X-100, 25 mM Tris, pH 7.5, and 157 mM NaCl) supplemented with a cOmplete Mini protease inhibitor cocktail tablet (Roche, Basel, Switzerland) and 1 mM glycerol phosphate, 1 mM NaF, and 1 mM NaOrthoV, with the exception of lysates for analysis of histones (please see "Analysis of acetylated and total histone levels" section). Debris was pelleted by spinning samples for 20 min at 12,000 rpm at 4 °C, and protein concentrations were determined by Bradford Assay (Bio-Rad, Hercules, CA, USA).

Proteins were separated by sodium dodecyl sulfate polyacrylamide gel electrophoresis and transferred onto polyvinylidene fluoride membranes. After blocking for 1 h at room temperature in 5% milk or bovine serum albumin in TBS-T, membranes were incubated with 1:1,000 dilutions of the following primary antibodies: LMP7 (Abcam, Cambridge, England), actin (Sigma, St. Louis, MO, USA), β5 (Enzo, Farmingdale, NY, USA), caspase 8, caspase 9, LC3B, tubulin (Cell Signaling, Beverly, MA, USA), acetylated histone H3, caspase 2, total histone H3 (EMD Millipore, Billerica, MA, USA), cytochrome C, p27 Kip1, XIAP (BD, San Jose, CA, USA), Bcl-XL, cIAP-1, ubiquitin (Santa Cruz, Dallas, TX, USA) and PA28γ (provided by Lance Barton, Austin College). Membranes were then washed 3X with TBS-T before being incubated with appropriate horseradish peroxidase conjugated secondary antibodies (mouse and rabbit: GE Healthcare, Buckinghamshire, England; rat: Cell Signaling, Beverly, MA, USA). Chemiluminescent visualization of bands was performed using a Kodak film developer (Rochester, NY, USA). Densitometry was evaluated using Image J software (National Institutes of Health, Bethesda, MD).

DNA Fragmentation

Cells were harvested by brief incubation with 0.05% trypsin. Cells were pelleted by centrifugation (1,700 rpm for 3 min) and washed 1X in PBS. Cells were fixed in 70% ethanol by resuspending cell pellets in 300 µL ice cold PBS, then adding 700 µL ice cold ethanol dropwise with gentle vortexing. After fixation for at least 24 h, samples were centrifuged (1,700 rpm for 3 min), washed 1X in PBS, and resuspended in a PBS solution containing 50 µg/mL propidium iodide and 100 µg/mL ribonuclease A. After incubation for 30 min to 1 h

with propidium iodide, the cell cycle was analyzed on the FL-3 channel of a flow cytometer (FACSCalibur™, BD Biosciences, San Jose, CA, USA).

Proteasome Activity in Cell Lysates

LN18 cells were resuspended in 20S proteasome lysis buffer (20 mM Tris, pH 7.5, 0.1 mM ethylenediaminetetraacetic acid, 20% glycerol, and 0.05% NP-40 supplemented each time with fresh 1 mM β-mercaptoethanol and 1 mM adenosine triphosphate) and lysed by freezing and thawing 3X on dry ice. Samples were centrifuged at 12,000 rpm for 1 min, and 100 μL supernatant was aliquoted into duplicate wells in a 96-well plate. Proteasome inhibitors were added to wells at indicated concentrations and incubated for varying lengths of time. Proteasome activity was measured by adding substrate buffer containing fluorogenic substrates and reading fluorescence on a plate reader, as described under "Proteasome Activity Assay."

Viability Assessment

Cells were harvested by brief incubation with 0.05% trypsin. Cells were pelleted by centrifugation (1,700 rpm for 3 min) and resuspended in 500 μL PBS. Viability was measured by the ability of cells to exclude trypan blue using a Vi-CELL® (Beckman Coulter, Inc., Pasadena, CA, USA).

Profiling of Specific Subunit Targeting by ONX-0914

The ProCISE (proteasome constitutive/immunoproteasome subunit enzyme-linked immunosorbent) assay was performed in collaboration with Onyx Pharmaceuticals as

previously described [142]. LN18 cells plated in 10 cm^2 dishes were treated with indicated doses of drugs in sufficient numbers to obtain $10X10^6$ cells at the end of treatment. Cells were then analyzed by Onyx using an active site probe to isolate active proteasome subunits, followed by analysis with primary antibodies specific for each subunit to determine the amount of each subunit unbound by the i-proteasome inhibitor in each sample.

Knockdown of PA28γ

Cells ($1X10^6$) were electroporated with 1 or 2 μM ON TARGET plus SMART pool siRNA for PSME3 or the control SMART pool (Thermo Scientific Dharmacon) using an Amaxa™ Nucleofector™ (Lonza, Basel, Switzerland). Efficiency of knockdown was checked by Western blot. To test sensitivity to proteasome inhibitors, cells electroporated with 2 μM siRNA were re-plated 24 h after transfection. Then, 24 h after plating, cells were treated for 48 h with proteasome inhibitors.

Colony Assay

A base agarose layer was formed by mixing 10 mL sterile water containing 4% low-melt agarose with 85 mL DMEM/F12 media containing 10% FBS and 15 mL additional FBS. The base agarose (0.5 mL) was added to each well in a 24-well plate. Then, a top agarose layer was formed by mixing 10 mL sterile water containing 3% low-melt agarose with 42.5 mL DMEM/F12 media containing 10% FBS and 7.5 mL additional FBS. LN18 cells were added to the top agarose (1,300 cells/mL), and 0.5 mL top agarose containing cells was added to each well of the 24-well plate on top of the base layer of agarose. After the top matrix solidified, 300 μL warm media was added to the top of each well. Cells were grown in

these plates for 5 days. After 5 days, proteasome inhibitors were added to the top media of each well, and cells were incubated with the drug for 3 additional days. Wells were analyzed using a GelCount™ machine (Oxford Optronix, Oxfordshire, England). Biomass was calculated as the number of colonies multiplied by the average volume.

Caspase 3/7 Activity

Harvested cells were re-suspended in PBS and aliquoted to duplicate wells (50 µL per well) of a 96-well plate on dry ice. After freezing, samples were thawed and incubated for 3 h with 150 µL DEVD buffer, pH 7.25 (100 mM HEPES, 10% sucrose, 5 mM DTT, 0.0001% IGEPAL, 0.1% CHAPS) containing 50 µM Ac-DEVD-amc fluorogenic substrate (Enzo Life Sciences, Farmingdale, NY, USA). Fluorescence was read on a Gemini EM Microplate Reader (Molecular Devices, Sunnyvale, CA, USA) at an excitation of 355 nM and an emission of 460 nM.

Caspase 2 Venus bimolecular fluorescence complementation

Measurement of induced proximity of caspase 2 using the caspase-2 BiFC was performed as previously described [178]. LN18 cells were plated in a 4-chamber dish containing coverslips (Nunc, Roskilde, Denmark) 24 h prior to transfection. Cells were transfected with caspase 2-CARD-VC (100 ng/well), caspase 2-CARD-VN (100 ng/well), and dsRed mito (20 ng/well) using lipofectamine 2000 (Life Technologies, Carlsbad, CA, USA). The following day, cells were treated with 290 nM MRZ or 15 nM BTZ. Cells were imaged using a spinning disk confocal microscope (Zeiss, Jena, Germany). Temperature was maintained at 37°C and 5% CO_2 using an environmental control chamber. Zen 2012 software

(Zeiss, Jena, Germany) was used to acquire images using a Zeiss Plan-Neofluar 40x 1.3 NA objective on an Orca R2 CCD camera and to analyze average Venus intensity.

Transient knockdown (siRNA) of caspase 2, caspase 9, cIAP-1, and XIAP

Cells were plated at 100,000 cells per well in 6-well dishes. After 24 h, cells were transected with siRNA against caspase 2 (L-003465-00, Thermo Scientific, both siRNA pool and individual siRNAs were used), caspase 9 (sc-29931, Santa Cruz), cIAP-1 (sc-29848, Santa Cruz), XIAP (sc-37508, Santa Cruz), or corresponding control siRNA pools using Lipofectamine® RNAiMAX (Life Technologies, Carlsbad, CA, USA). Twenty-four h post-transfection, fresh media was added to each well, and cells were then treated as indicated.

Generation of cells with stable knockdown (shRNA) of caspases 2, 8, and 9

GIPZ lentiviral shRNA was obtained from GE Healthcare (Buckinghamshire, England) with sequences targeting caspase 2 (V3LHS_338913, sequence: CAGACATCTCCTTGCACCG), caspase 8 (V2LHS_12733, sequence: TTCTTAGTGTGAAAGTAGG), and caspase 9 (V3LHS_412093, sequence: TGTCGTCAATCTGGAAGCT). Lentiviral infection of LN18 cells was performed using a Trans-Lentiviral Packaging Kit from Thermo Fisher Scientific (Waltham, MA, USA). Cells stably expressing the shRNA were selected using puromycin.

Cytochrome C Western blots in cytoplasmic fractions

LN18 cells grown in 10 cm^2 dishes were harvested by brief incubation with 0.05% trypsin. Cells were pelleted, then washed 1X in PBS. Cells were then lysed on ice in 50–75

μL cold STE buffer (250 mM sucrose, 1 mM EDTA, 25 mM Tris, pH 6.8) for 2–4 min, until cells were trypan blue positive. Samples were then centrifuged at 14,000 rpm for 5 min at 4 °C. Supernatants were transferred to a new tube; pellets contained mitochondria. Supernatants were then analyzed by Western blot for cytochrome C.

Mitochondrial membrane potential measurement

At the end of treatment, cells were harvested by brief incubation with 0.05% trypsin and pelleted by centrifugation (1,700 rpm for 3 min). Cells were then washed 1X in PBS. Cells were then resuspended in 1 mL PBS containing 25 nM TMRE and incubated for 30 min at 37 °C. Samples were then centrifuged (1,700 rpm for 3 min) and pellet was resuspended in 300 μL PBS for analysis on the FL-2 channel of a flow cytometer (FACSCalibur™, BD Biosciences, San Jose, CA, USA).

Generation of Bcl-XL overexpressing cells

Bcl-XL overexpression and pLZRS control retroviral vectors were obtained from Lisa Bouchier-Hayes (Baylor College of Medicine). A 3-plasmid system was used to produce retrovirus. First, $3X10^6$ 293T cells were plated in 10 cm^2 plates in 10 mL DMEM containing 10% FBS, 1% penicillin and streptomycin, and 1% glutamine. The following day, the media was changed 2–4 h before transfection. Plasmids were mixed together in tubes (12 μg pLZRS or Bcl-XL retroviral vector, 6 μg pMD "old" Gag-pol, and 2 μg VSVG). Sterile water was added up to 500 μL. Next, 500 μL 2X HBS buffer was added, and tubes were mixed well. Finally, 50 μL $CaCl_2$ solution, pH 5.5, was added, and plasmids were incubated 20–30 min at room temperature, gently mixing and shaking periodically. The plasmid mix was then added

to the 293T cells, and cells were incubated overnight at 37 °C. After harvesting virus and changing media 3 times, pooled virus was filtered through a 0.45 micron filter. Filtered virus (1.5–2 mL) was added to target cells (LN18) with 8 μg/mL polybrene for 1–2 h. Fresh media was added to wells for overnight incubation. Cells were selected for stable expression using zeocin.

Reactive oxygen species detection

Hydroethidium staining for superoxides

Treated samples were centrifuged for 3 min at 1,700 rpm to pellet cells. Cells were resuspended in 1 mL PBS containing 10 μM hydroethidium dye. After 30 min incubation at 37 °C, samples were pelleted (3 min at 1,700 rpm) and resuspended in 300 μL PBS for analysis on the FL-3 channel of a flow cytometer (FACSCalibur™, BD Biosciences, San Jose, CA, USA).

CM-H_2DCFDA staining for hydrogen peroxide

Treated samples were centrifuged for 3 min at 1,700 rpm to pellet cells. Cells were resuspended in 1 mL DMEM/F12 media containing 10 μM CM-H_2DCFDA and incubated for 30 min at 37 °C. Then, samples were washed 1X in PBS and resuspended in 300 μL PBS for analysis on the FL-1 channel of a flow cytometer (FACSCalibur™, BD Biosciences, San Jose, CA, USA).

Measurement of glutathione levels

Cells were harvested by brief incubation with 0.05% trypsin, followed by centrifugation (1,700 rpm for 3 min) and 1X wash in PBS. Cells were resuspended in 1 mL PBS and 2 μL monochlorobimane solution (2.2 mg monochlorobimane in 194.12 μL acetonitrile) was added to each sample. Samples were vortexed and incubated at 37 °C for 15 min. The reaction was halted by adding 50 μL trichloroacetic acid and vortexing. Samples were spun for 5 min at 10,000 rpm, and 1 mL supernatant was added to a glass tube containing 1 mL dichloromethane. Glass tubes were vortexed and centrifuged for 2 min at 3,500 rpm. For each sample, 200 μL of the top aqueous layer was plated in duplicate wells in a white 96-well plate. Fluorescence was read on a Gemini EM Microplate Reader (Molecular Devices, Sunnyvale, CA, USA) at an excitation of 360 nM and an emission of 460 nM. Glutathione concentrations were determined by comparing samples to a standard curve composed of varying concentrations of glutathione ethyl ester dissolved in PBS.

Amino acid and metabolite measurement

Analysis of amino acid and metabolite levels was performed as previously described [154] in collaboration with Preeti Purwaha, Philip Lorenzi, and David Hawke in the Proteomics Core at MD Anderson Cancer Center. LN18 cells were treated for indicated time periods in 10 cm^2 dishes. Media was suctioned off plate, and plate was placed on dry ice. Next, plates were washed 2X with 5 mL methanol ambic. A solution of methanol, chloroform, and water (7:2:1) was then added to each plate (500 μL) directly to the center of the plate. Cells were scraped using a cell scraper, and mixture was transferred to a simport tube. Samples were shaken using a Disruptor Genie for 30 sec in a cold room, then debris

was pelleted by spinning at 20,000 xg for 2 min. Samples were then analyzed by mass spectrometry as described [154].

Intracranial mouse xenograft model

An intracranial guidescrew model of GBM was used, as previously described [155]. We implanted 500,000 U87 GBM cells though a guidescrew in 5-week-old female athymic nude mice (Experimental Radiation Oncology, MD Anderson, Houston, TX) and let tumors develop for 1–2 weeks (as noted in Results). Mice were then injected intraperitoneally with 1 mg/kg BTZ, 0.15 mg/kg MRZ, and/or 50 mg/kg vorinostat in dosing schedules outlined in the Results. For lysates, the tumor sections were frozen in liquid nitrogen, then homogenized by vortexing with zirconia/silica beads (Biospec, Bartlesville, OK, USA) in lysis buffer (20 mM Tris, pH 7.5, 0.1 mM EDTA, 20% glycerol, and 0.05% NP-40). For IHC analysis, samples were preserved in formalin, then paraffin-embedded.

Immunohistochemistry

Slides were deparaffinized and hydrated in xylene and graded ethanol solutions. Endogenous peroxidase activity was blocked with 3% H_2O_2 in water for 10 min. Slides were washed, then antigen retrieval was performed using 1.0 mM EDTA buffer, pH 8.0 (for p21) or 10 mM citrate buffer, pH 6.0 (for cleaved caspase 3 and lamin A) in a microwave (3 min at 100% power, 10–15 min at 50% power). After cooling and washing in water, slides were incubated with blocking reagent (Biocare, Concord, CA) for 10 min. Slides were then incubated with antibodies for p21 (sc-6246, 1:50 dilution: Santa Cruz, Dallas, TX), cleaved caspase 3 (AF835, 1:500 dilution: R&D Systems, Minneapolis, MN), or cleaved lamin A

(2035, 1:100 dilution: Cell Signaling, Beverly, MA) overnight at 4 °C. Slides were then washed and incubated with secondary antibody (for p21: biotinylated rabbit-anti mouse for 15 min, [Accurate Chem, Westbury, NY]; for cleaved caspase 3: biotinylated goat-anti-rabbit for 30 min [Vector Laboratories, Burlingame, CA]; for lamin A: anti-rabbit horseradish peroxidase for 30 min [Dako, Glostrup, Denmark]). Slides were then incubated with Tablet DAB (for p21 and cleaved caspase 3; Sigma, St. Louis, MO) or Dako (Glostrup, Denmark) DAB. Slides were washed, counterstained with hematoxylin, dehydrated, and coverslipped. Slides were visualized and the number of positive cells per 40X was counted and averaged for 5 fields.

Analysis of acetylated and total histone levels

Cells were pelleted by centrifugation (1,700 rpm for 3 min) and washed 1X with PBS. Pellets were resuspended in 100 µL Triton Extraction Buffer (TEB: PBS containing 0.5% Triton X-100 and 0.02% NaN_3, with freshly added 2 mM PMSF and 5 mM sodium butyrate) and lysed on ice for 10 min with gentle stirring. Samples were centrifuged at 6,500 xg for 10 min at 4 °C to pellet nuclei. Supernatant was discarded, and nuclei were washed with 50 µL TEB and pelleted as before. Pellets were then resuspended in 40 µL 0.2 N HCl, and histones were acid extracted overnight at 4 °C. Samples were centrifuged at 6,500 xg for 10 min at 4 °C to pellet debris, and supernatants containing histones were analyzed by Western blot.

Measurement of PSMB5 mRNA

RNA was isolated using an RNeasy Mini Kit (Qiagen, Limburg, Netherlands). The concentration of RNA was determined using a Nanodrop (Thermo Scientific, Waltham, MA),

and equal amounts of RNA were used for reverse transcription to cDNA using an Omniscript RT Kit (Qiagen). PSMB5 and actin levels were then assessed by mixing cDNA with SYBR green (Bio Rad, Hercules, CA) and primers (PSMB5 primers: forward, 5'-TAAGGAACGCATCTCTGTAGCA; reverse, 5'-TCCACTTCCAGGTCATAGGAAT-3'; actin primers: forward, 5'-CTGTGGCATCCACGAAACTA-3'; reverse, 5'-CGCTCAGGAGGAGCAATG-3') and measuring amplification on an iCycler qPCR machine (Bio Rad). Amplification was performed using the following qPCR protocol: initial temperature of 95 °C for 10 min, followed by 40 cycles of 95 °C for 15 seconds and 63 °C for 1 min, followed by 95 °C for 1 min, then a hold at 55 °C.

Statistical analysis

Values are given as the mean ± standard error of the mean, with all experiments performed at least in triplicate. Comparisons were made using Student's *t* tests performed using GraphPad Prism software, version 6 (GraphPad software, La Jolla, CA, USA). P-values < 0.05 were considered significant. Synergy was determined with the method described by Chou and Talalay [158] using CalcuSyn software (Biosoft, Cambridge, United Kingdom), with combination index (CI) values < 1 being considered synergistic.

Chapter 7

References

1. Deorah S, Lynch CF, Sibenaller ZA, Ryken TC (2006) Trends in brain cancer incidence and survival in the United States: Surveillance, Epidemiology, and End Results Program, 1973 to 2001. Neurosurg Focus 20:E1. doi: 10.3171/foc.2006.20.4.E1

2. Hess KR, Broglio KR, Bondy ML (2004) Adult glioma incidence trends in the United States, 1977-2000. Cancer 101:2293–2299. doi: 10.1002/cncr.20621

3. Johnson DR, O'Neill BP (2011) Glioblastoma survival in the United States before and during the temozolomide era. J Neurooncol 107:359–364. doi: 10.1007/s11060-011-0749-4

4. Stupp R, Mason WP, van den Bent MJ, Weller M, Fisher B, Taphoorn MJB, Belanger K, Brandes AA, Marosi C, Bogdahn U, Curschmann J, Janzer RC, Ludwin SK, Gorlia T, Allgeier A, Lacombe D, Cairncross JG, Eisenhauer E, Mirimanoff RO, European Organisation for Research and Treatment of Cancer Brain Tumor and Radiotherapy Groups, National Cancer Institute of Canada Clinical Trials Group (2005) Radiotherapy plus concomitant and adjuvant temozolomide for glioblastoma. N Engl J Med 352:987–996. doi: 10.1056/NEJMoa043330

5. McLendon R, Friedman A, Bigner D, Van Meir EG, Brat DJ, M Mastrogianakis G, Olson JJ, Mikkelsen T, Lehman N, Aldape K, Alfred Yung WK, Bogler O, VandenBerg S, Berger M, Prados M, Muzny D, Morgan M, Scherer S, Sabo A, Nazareth L, Lewis L, Hall O, Zhu Y, Ren Y, Alvi O, Yao J, Hawes A, Jhangiani S, Fowler G, San Lucas A, Kovar C, Cree A, Dinh H, Santibanez J, Joshi V, Gonzalez-Garay ML, Miller CA, Milosavljevic A, Donehower L, Wheeler DA, Gibbs RA, Cibulskis K, Sougnez C, Fennell T, Mahan S, Wilkinson J, Ziaugra L, Onofrio R, Bloom T, Nicol R, Ardlie K,

Baldwin J, Gabriel S, Lander ES, Ding L, Fulton RS, McLellan MD, Wallis J, Larson DE, Shi X, Abbott R, Fulton L, Chen K, Koboldt DC, Wendl MC, Meyer R, Tang Y, Lin L, Osborne JR, Dunford-Shore BH, Miner TL, Delehaunty K, Markovic C, Swift G, Courtney W, Pohl C, Abbott S, Hawkins A, Leong S, Haipek C, Schmidt H, Wiechert M, Vickery T, Scott S, Dooling DJ, Chinwalla A, Weinstock GM, Mardis ER, Wilson RK, Getz G, Winckler W, Verhaak RGW, Lawrence MS, O'Kelly M, Robinson J, Alexe G, Beroukhim R, Carter S, Chiang D, Gould J, Gupta S, Korn J, Mermel C, Mesirov J, Monti S, Nguyen H, Parkin M, Reich M, Stransky N, Weir BA, Garraway L, Golub T, Meyerson M, Chin L, Protopopov A, Zhang J, Perna I, Aronson S, Sathiamoorthy N, Ren G, Yao J, Wiedemeyer WR, Kim H, Won Kong S, Xiao Y, Kohane IS, Seidman J, Park PJ, Kucherlapati R, Laird PW, Cope L, Herman JG, Weisenberger DJ, Pan F, Van Den Berg D, Van Neste L, Mi Yi J, Schuebel KE, Baylin SB, Absher DM, Li JZ, Southwick A, Brady S, Aggarwal A, Chung T, Sherlock G, Brooks JD, Myers RM, Spellman PT, Purdom E, Jakkula LR, Lapuk AV, Marr H, Dorton S, Gi Choi Y, Han J, Ray A, Wang V, Durinck S, Robinson M, Wang NJ, Vranizan K, Peng V, Van Name E, Fontenay GV, Ngai J, Conboy JG, Parvin B, Feiler HS, Speed TP, Gray JW, Brennan C, Socci ND, Olshen A, Taylor BS, Lash A, Schultz N, Reva B, Antipin Y, Stukalov A, Gross B, Cerami E, Qing Wang W, Qin L-X, Seshan VE, Villafania L, Cavatore M, Borsu L, Viale A, Gerald W, Sander C, Ladanyi M, Perou CM, Neil Hayes D, Topal MD, Hoadley KA, Qi Y, Balu S, Shi Y, Wu J, Penny R, Bittner M, Shelton T, Lenkiewicz E, Morris S, Beasley D, Sanders S, Kahn A, Sfeir R, Chen J, Nassau D, Feng L, Hickey E, Zhang J, Weinstein JN, Barker A, Gerhard DS, Vockley J, Compton C, Vaught J, Fielding P, Ferguson ML, Schaefer C, Madhavan S, Buetow KH, Collins F, Good P,

Guyer M, Ozenberger B, Peterson J, Thomson E (2008) Comprehensive genomic characterization defines human glioblastoma genes and core pathways. Nature 455:1061–1068. doi: 10.1038/nature07385

6. Brennan CW, Verhaak RGW, McKenna A, Campos B, Noushmehr H, Salama SR, Zheng S, Chakravarty D, Sanborn JZ, Berman SH, Beroukhim R, Bernard B, Wu C-J, Genovese G, Shmulevich I, Barnholtz-Sloan J, Zou L, Vegesna R, Shukla SA, Ciriello G, Yung WK, Zhang W, Sougnez C, Mikkelsen T, Aldape K, Bigner DD, Van Meir EG, Prados M, Sloan A, Black KL, Eschbacher J, Finocchiaro G, Friedman W, Andrews DW, Guha A, Iacocca M, O'Neill BP, Foltz G, Myers J, Weisenberger DJ, Penny R, Kucherlapati R, Perou CM, Hayes DN, Gibbs R, Marra M, Mills GB, Lander E, Spellman P, Wilson R, Sander C, Weinstein J, Meyerson M, Gabriel S, Laird PW, Haussler D, Getz G, Chin L, Network TR, Benz C, Barnholtz-Sloan J, Barrett W, Ostrom Q, Wolinsky Y, Black KL, Bose B, Boulos PT, Boulos M, Brown J, Czerinski C, Eppley M, Iacocca M, Kempista T, Kitko T, Koyfman Y, Rabeno B, Rastogi P, Sugarman M, Swanson P, Yalamanchii K, Otey IP, Liu YS, Xiao Y, Auman JT, Chen P-C, Hadjipanayis A, Lee E, Lee S, Park PJ, Seidman J, Yang L, Kucherlapati R, Kalkanis S, Mikkelsen T, Poisson LM, Raghunathan A, Scarpace L, Bernard B, Bressler R, Eakin A, Iype L, Kreisberg RB, Leinonen K, Reynolds S, Rovira H, Thorsson V, Shmulevich I, Annala MJ, Penny R, Paulauskis J, Curley E, Hatfield M, Mallery D, Morris S, Shelton T, Shelton C, Sherman M, Yena P, Cuppini L, Dimeco F, Eoli M, Finocchiaro G, Maderna E, Pollo B, Saini M, Balu S, Hoadley KA, Li L, Miller CR, Shi Y, Topal MD, Wu J, Dunn G, Giannini C, O'Neill BP, Aksoy BA, Antipin Y, Borsu L, Berman SH, Brennan CW, Cerami E, Chakravarty D, Ciriello G, Gao J, Gross B, Jacobsen A, Ladanyi M, Lash A, Liang Y, Reva B, Sander C,

Schultz N, Shen R, Socci ND, Viale A, Ferguson ML, Chen Q-R, Demchok JA, Dillon LAL, Shaw KRM, Sheth M, Tarnuzzer R, Wang Z, Yang L, Davidsen T, Guyer MS, Ozenberger BA, Sofia HJ, Bergsten J, Eckman J, Harr J, Myers J, Smith C, Tucker K, Winemiller C, Zach LA, Ljubimova JY, Eley G, Ayala B, Jensen MA, Kahn A, Pihl TD, Pot DA, Wan Y, Eschbacher J, Foltz G, Hansen N, Hothi P, Lin B, Shah N, Yoon J-G, Lau C, Berens M, Ardlie K, Beroukhim R, Carter SL, Cherniack AD, Noble M, Cho J, Cibulskis K, DiCara D, Frazer S, Gabriel SB, Gehlenborg N, Gentry J, Heiman D, Kim J, Jing R, Lander ES, Lawrence M, Lin P, Mallard W, Meyerson M, Onofrio RC, Saksena G, Schumacher S, Sougnez C, Stojanov P, Tabak B, Voet D, Zhang H, Zou L, Getz G, Dees NN, Ding L, Fulton LL, Fulton RS, Kanchi K-L, Mardis ER, Wilson RK, Baylin SB, Andrews DW, Harshyne L, Cohen ML, Devine K, Sloan AE, VandenBerg SR, Berger MS, Prados M, Carlin D, Craft B, Ellrott K, Goldman M, Goldstein T, Grifford M, Haussler D, Ma S, Ng S, Salama SR, Sanborn JZ, Stuart J, Swatloski T, Waltman P, Zhu J, Foss R, Frentzen B, Friedman W, McTiernan R, Yachnis A, Hayes DN, Perou CM, Zheng S, Vegesna R, Mao Y, Akbani R, Aldape K, Bogler O, Fuller GN, Liu W, Liu Y, Lu Y, Mills G, Protopopov A, Ren X, Sun Y, Wu C-J, Yung WKA, Zhang W, Zhang J, Chen K, Weinstein JN, Chin L, Verhaak RGW, Noushmehr H, Weisenberger DJ, Bootwalla MS, Lai PH, Triche TJ Jr, Van Den Berg DJ, Laird PW, Gutmann DH, Lehman NL, VanMeir EG, Brat D, Olson JJ, Mastrogianakis GM, Devi NS, Zhang Z, Bigner D, Lipp E, McLendon R (2013) The Somatic Genomic Landscape of Glioblastoma. Cell 155:462–477. doi: 10.1016/j.cell.2013.09.034

7. Verhaak RGW, Hoadley KA, Purdom E, Wang V, Qi Y, Wilkerson MD, Miller CR, Ding L, Golub T, Mesirov JP, Alexe G, Lawrence M, O'Kelly M, Tamayo P, Weir BA,

Gabriel S, Winckler W, Gupta S, Jakkula L, Feiler HS, Hodgson JG, James CD, Sarkaria JN, Brennan C, Kahn A, Spellman PT, Wilson RK, Speed TP, Gray JW, Meyerson M, Getz G, Perou CM, Hayes DN, Cancer Genome Atlas Research Network (2010) Integrated genomic analysis identifies clinically relevant subtypes of glioblastoma characterized by abnormalities in PDGFRA, IDH1, EGFR, and NF1. Cancer Cell 17:98–110. doi: 10.1016/j.ccr.2009.12.020

8. Madhavan S, Zenklusen J-C, Kotliarov Y, Sahni H, Fine HA, Buetow K (2009) Rembrandt: helping personalized medicine become a reality through integrative translational research. Mol Cancer Res 7:157–167. doi: 10.1158/1541-7786.MCR-08-0435

9. Snuderl M, Fazlollahi L, Le LP, Nitta M, Zhelyazkova BH, Davidson CJ, Akhavanfard S, Cahill DP, Aldape KD, Betensky RA, Louis DN, Iafrate AJ (2011) Mosaic Amplification of Multiple Receptor Tyrosine Kinase Genes in Glioblastoma. Cancer Cell 20:810–817. doi: 10.1016/j.ccr.2011.11.005

10. Szerlip NJ, Pedraza A, Chakravarty D, Azim M, McGuire J, Fang Y, Ozawa T, Holland EC, Huse JT, Jhanwar S, Leversha MA, Mikkelsen T, Brennan CW (2012) Intratumoral heterogeneity of receptor tyrosine kinases EGFR and PDGFRA amplification in glioblastoma defines subpopulations with distinct growth factor response. Proc Natl Acad Sci USA 109:3041–3046. doi: 10.1073/pnas.1114033109

11. Patel AP, Tirosh I, Trombetta JJ, Shalek AK, Gillespie SM, Wakimoto H, Cahill DP, Nahed BV, Curry WT, Martuza RL, Louis DN, Rozenblatt-Rosen O, Suva ML, Regev A, Bernstein BE (2014) Single-cell RNA-seq highlights intratumoral heterogeneity in

primary glioblastoma. Science 344:1396–1401. doi: 10.1126/science.1254257

12. Brown PD, Krishnan S, Sarkaria JN, Wu W, Jaeckle KA, Uhm JH, Geoffroy FJ, Arusell R, Kitange G, Jenkins RB, Kugler JW, Morton RF, Rowland KM, Mischel P, Yong WH, Scheithauer BW, Schiff D, Giannini C, Buckner JC, North Central Cancer Treatment Group Study N0177 (2008) Phase I/II trial of erlotinib and temozolomide with radiation therapy in the treatment of newly diagnosed glioblastoma multiforme: North Central Cancer Treatment Group Study N0177. J Clin Oncol 26:5603–5609. doi: 10.1200/JCO.2008.18.0612

13. Rock KL, Gramm C, Rothstein L, Clark K, Stein R, Dick L, Hwang D, Goldberg AL (1994) Inhibitors of the proteasome block the degradation of most cell proteins and the generation of peptides presented on MHC class I molecules. Cell 78:761–771.

14. Goldberg AL (2003) Protein degradation and protection against misfolded or damaged proteins. Nature 426:895–899.

15. Hershko A (1997) Roles of ubiquitin-mediated proteolysis in cell cycle control. Curr Opin Cell Biol 9:788–799.

16. Haupt Y, Maya R, Kazaz A, Oren M (1997) Mdm2 promotes the rapid degradation of p53. Nature 387:296–299. doi: 10.1038/387296a0

17. Ciechanover A, Heller H, Katz-Etzion R, Hershko A (1981) Activation of the heat-stable polypeptide of the ATP-dependent proteolytic system. Proc Natl Acad Sci USA 78:761–765.

18. Pickart CM, Rose IA (1985) Functional heterogeneity of ubiquitin carrier proteins. J Biol Chem 260:1573–1581.

19. Hershko A, Heller H, Elias S, Ciechanover A (1983) Components of ubiquitin-protein ligase system. Resolution, affinity purification, and role in protein breakdown. J Biol Chem 258:8206–8214.

20. Hershko A, Ciechanover A (1998) The ubiquitin system. Annu Rev Biochem 67:425–479. doi: 10.1146/annurev.biochem.67.1.425

21. van Nocker S, Vierstra RD (1993) Multiubiquitin chains linked through lysine 48 are abundant in vivo and are competent intermediates in the ubiquitin proteolytic pathway. J Biol Chem 268:24766–24773.

22. Ye Y, Rape M (2009) Building ubiquitin chains: E2 enzymes at work. Nat Rev Mol Cell Biol 10:755–764. doi: 10.1038/nrm2780

23. Hough R, Pratt G, Rechsteiner M (1987) Purification of two high molecular weight proteases from rabbit reticulocyte lysate. J Biol Chem 262:8303–8313.

24. Waxman L, Fagan JM, Tanaka K, Goldberg AL (1985) A soluble ATP-dependent system for protein degradation from murine erythroleukemia cells. Evidence for a protease which requires ATP hydrolysis but not ubiquitin. J Biol Chem 260:11994–12000.

25. Eytan E, Ganoth D, Armon T, Hershko A (1989) ATP-dependent incorporation of 20S protease into the 26S complex that degrades proteins conjugated to ubiquitin. Proc Natl Acad Sci USA 86:7751–7755.

26. Driscoll J, Goldberg AL (1990) The proteasome (multicatalytic protease) is a component of the 1500-kDa proteolytic complex which degrades ubiquitin-conjugated proteins. J Biol Chem 265:4789–4792.

27. Glickman MH, Rubin DM, Coux O, Wefes I, Pfeifer G, Cjeka Z, Baumeister W, Fried VA, Finley D (1998) A subcomplex of the proteasome regulatory particle required for ubiquitin-conjugate degradation and related to the COP9-signalosome and eIF3. Cell 94:615–623.

28. Glickman MH, Ciechanover A (2002) The ubiquitin-proteasome proteolytic pathway: destruction for the sake of construction. Physiol Rev 82:373–428. doi: 10.1152/physrev.00027.2001

29. Groll M, Heinemeyer W, Jäger S, Ullrich T, Bochtler M, Wolf DH, Huber R (1999) The catalytic sites of 20S proteasomes and their role in subunit maturation: a mutational and crystallographic study. Proc Natl Acad Sci USA 96:10976–10983.

30. Orlowski M, Wilk S (2000) Catalytic activities of the 20 S proteasome, a multicatalytic proteinase complex. Arch Biochem Biophys 383:1–16. doi: 10.1006/abbi.2000.2036

31. Kisselev AF, Goldberg AL (2001) Proteasome inhibitors: from research tools to drug candidates. Chem Biol 8:739–758.

32. Rechsteiner M, Realini C, Ustrell V (2000) The proteasome activator 11 S REG (PA28) and class I antigen presentation. Biochem J 345 Pt 1:1–15.

33. Whitby FG, Masters EI, Kramer L, Knowlton JR, Yao Y, Wang CC, Hill CP (2000)

Structural basis for the activation of 20S proteasomes by 11S regulators. Nature 408:115–120. doi: 10.1038/35040607

34. Rechsteiner M, Hill CP (2005) Mobilizing the proteolytic machine: cell biological roles of proteasome activators and inhibitors. Trends Cell Biol 15:27–33. doi: 10.1016/j.tcb.2004.11.003

35. Noda C, Tanahashi N, Shimbara N, Hendil KB, Tanaka K (2000) Tissue Distribution of Constitutive Proteasomes, Immunoproteasomes, and PA28 in Rats. Biochem Biophys Res Commun 277:348–354. doi: 10.1006/bbrc.2000.3676

36. Chen X, Barton LF, Chi A, Clurman BE, Roberts JM (2007) Ubiquitin-independent degradation of cell-cycle inhibitors by the REGgamma proteasome. Mol Cell 26:843–852. doi: 10.1016/j.molcel.2007.05.022

37. Groettrup M, Ruppert T, Kuehn L, Seeger M, Standera S, Koszinowski U, Kloetzel PM (1995) The interferon-gamma-inducible 11 S regulator (PA28) and the LMP2/LMP7 subunits govern the peptide production by the 20 S proteasome in vitro. J Biol Chem 270:23808–23815. doi: 10.1074/jbc.270.40.23808

38. Cascio P, Hilton C, Kisselev AF, Rock KL, Goldberg AL (2001) 26S proteasomes and immunoproteasomes produce mainly N-extended versions of an antigenic peptide. EMBO J 20:2357–2366. doi: 10.1093/emboj/20.10.2357

39. Toes R, Nussbaum AK, Degermann S, Schirle M, Emmerich N, Kraft M, Laplace C, Zwinderman A, Dick TP, Müller J (2001) Discrete cleavage motifs of constitutive and immunoproteasomes revealed by quantitative analysis of cleavage products. J Exp Med

194:1–12.

40. Piccinini M, Rinaudo MT, Anselmino A, Ramondetti C, Buccinnà B, Fiano V, Ghimenti C, Schiffer D (2005) Characterization of the 20S proteasome in human glioblastomas. Anticancer Res 25:3203–3210.

41. Epstein FH, Mitch WE, Goldberg AL (1996) Mechanisms of muscle wasting—the role of the ubiquitin–proteasome pathway. N Engl J Med 335:1897–1905.

42. Groll M, Berkers CR, Ploegh HL, Ovaa H (2006) Crystal Structure of the Boronic Acid-Based Proteasome Inhibitor Bortezomib in Complex with the Yeast 20S Proteasome. Structure 14:451–456. doi: 10.1016/j.str.2005.11.019

43. Berkers CR, Verdoes M, Lichtman E, Fiebiger E, Kessler BM, Anderson KC, Ploegh HL, Ovaa H, Galardy PJ (2005) Activity probe for in vivo profiling of the specificity of proteasome inhibitor bortezomib. Nat Methods 2:357–362. doi: 10.1038/nmeth759

44. Cusack JC, Liu R, Houston M, Abendroth K, Elliott PJ, Adams J, Baldwin AS (2001) Enhanced chemosensitivity to CPT-11 with proteasome inhibitor PS-341: implications for systemic nuclear factor-kappaB inhibition. Cancer Res 61:3535–3540.

45. Nawrocki ST, Bruns CJ, Harbison MT, Bold RJ, Gotsch BS, Abbruzzese JL, Elliott P, Adams J, McConkey DJ (2002) Effects of the proteasome inhibitor PS-341 on apoptosis and angiogenesis in orthotopic human pancreatic tumor xenografts. Mol Cancer Ther 1:1243–1253.

46. Nawrocki ST, Sweeney-Gotsch B, Takamori R, McConkey DJ (2004) The proteasome

inhibitor bortezomib enhances the activity of docetaxel in orthotopic human pancreatic tumor xenografts. Mol Cancer Ther 3:59–70.

47. Ling Y-H, Liebes L, Zou Y, Perez-Soler R (2003) Reactive oxygen species generation and mitochondrial dysfunction in the apoptotic response to Bortezomib, a novel proteasome inhibitor, in human H460 non-small cell lung cancer cells. J Biol Chem 278:33714–33723. doi: 10.1074/jbc.M302559200

48. Hideshima T, Richardson P, Chauhan D, Palombella VJ, Elliott PJ, Adams J, Anderson KC (2001) The proteasome inhibitor PS-341 inhibits growth, induces apoptosis, and overcomes drug resistance in human multiple myeloma cells. Cancer Res 61:3071–3076.

49. Jagannath S, Barlogie B, Berenson J, Siegel D, Irwin D, Richardson PG, Niesvizky R, Alexanian R, Limentani SA, Alsina M, Adams J, Kauffman M, Esseltine DL, Schenkein DP, Anderson KC (2004) A phase 2 study of two doses of bortezomib in relapsed or refractory myeloma. Br J Haematol 127:165–172. doi: 10.1111/j.1365-2141.2004.05188.x

50. Richardson PG, Sonneveld P, Schuster M, Irwin D, Stadtmauer E, Facon T, Harousseau JL, Ben-Yehuda D, Lonial S, Goldschmidt H, Reece D, Miguel JS, Blade J, Boccadoro M, Cavenagh J, Alsina M, Rajkumar SV, Lacy M, Jakubowiak A, Dalton W, Boral A, Esseltine DL, Schenkein D, Anderson KC (2007) Extended follow-up of a phase 3 trial in relapsed multiple myeloma: final time-to-event results of the APEX trial. Blood 110:3557–3560. doi: 10.1182/blood-2006-08-036947

51. Kane RC, Bross PF, Farrell AT, Pazdur R (2003) Velcade: U.S. FDA approval for the

treatment of multiple myeloma progressing on prior therapy. Oncologist 8:508–513.

52. Kane RC, Farrell AT, Sridhara R, Pazdur R (2006) United States Food and Drug Administration approval summary: bortezomib for the treatment of progressive multiple myeloma after one prior therapy. Clin Cancer Res 12:2955–2960. doi: 10.1158/1078-0432.CCR-06-0170

53. Kane RC, Dagher R, Farrell A, Ko CW, Sridhara R, Justice R, Pazdur R (2007) Bortezomib for the Treatment of Mantle Cell Lymphoma. Clin Cancer Res 13:5291–5294. doi: 10.1158/1078-0432.CCR-07-0871

54. Potts BC, Albitar MX, Anderson KC, Baritaki S, Berkers C, Bonavida B, Chandra J, Chauhan D, Cusack JC, Fenical W, Ghobrial IM, Groll M, Jensen PR, Lam KS, Lloyd GK, McBride W, McConkey DJ, Miller CP, Neuteboom STC, Oki Y, Ovaa H, Pajonk F, Richardson PG, Roccaro AM, Sloss CM, Spear MA, Valashi E, Younes A, Palladino MA (2011) Marizomib, a proteasome inhibitor for all seasons: preclinical profile and a framework for clinical trials. Curr Cancer Drug Targets 11:254–284.

55. Millward M, Price T, Townsend A, Sweeney C, Spencer A, Sukumaran S, Longenecker A, Lee L, Lay A, Sharma G, Gemmill RM, Drabkin HA, Lloyd GK, Neuteboom STC, McConkey DJ, Palladino MA, Spear MA (2011) Phase 1 clinical trial of the novel proteasome inhibitor marizomib with the histone deacetylase inhibitor vorinostat in patients with melanoma, pancreatic and lung cancer based on in vitro assessments of the combination. Invest New Drugs 30:2303–2317. doi: 10.1007/s10637-011-9766-6

56. Williams PG, Buchanan GO, Feling RH, Kauffman CA, Jensen PR, Fenical W (2005)

New cytotoxic salinosporamides from the marine Actinomycete Salinispora tropica. J Org Chem 70:6196–6203. doi: 10.1021/jo050511

57. Corey EJ, Li WD (1999) Total synthesis and biological activity of lactacystin, omuralide and analogs. Chem Pharm Bull 47:1–10.

58. Feling RH, Buchanan GO, Mincer TJ, Kauffman CA, Jensen PR, Fenical W (2003) Salinosporamide A: a highly cytotoxic proteasome inhibitor from a novel microbial source, a marine bacterium of the new genus salinospora. Angew Chem Int Ed Engl 42:355–357. doi: 10.1002/anie.200390115

59. Groll M, Huber R, Potts BCM (2006) Crystal structures of Salinosporamide A (NPI-0052) and B (NPI-0047) in complex with the 20S proteasome reveal important consequences of beta-lactone ring opening and a mechanism for irreversible binding. J Am Chem Soc 128:5136–5141. doi: 10.1021/ja058320b

60. Manam RR, McArthur KA, Chao T-H, Weiss J, Ali JA, Palombella VJ, Groll M, Lloyd GK, Palladino MA, Neuteboom STC, Macherla VR, Potts BCM (2008) Leaving groups prolong the duration of 20S proteasome inhibition and enhance the potency of salinosporamides. J Med Chem 51:6711–6724. doi: 10.1021/jm800548b

61. Miller CP, Manton CA, Hale R, DeBose L, Macherla VR, Potts BC, Palladino MA, Chandra J (2011) Specific and prolonged proteasome inhibition dictates apoptosis induction by marizomib and its analogs. Chem Biol Interact 194:58–68. doi: 10.1016/j.cbi.2011.08.005

62. Chauhan D, Catley L, Li G, Podar K, Hideshima T, Velankar M, Mitsiades C, Mitsiades

N, Yasui H, Letai A, Ovaa H, Berkers C, Nicholson B, Chao T-H, Neuteboom STC, Richardson P, Palladino MA, Anderson KC (2005) A novel orally active proteasome inhibitor induces apoptosis in multiple myeloma cells with mechanisms distinct from Bortezomib. Cancer Cell 8:407–419. doi: 10.1016/j.ccr.2005.10.013

63. Kuhn DJ, Hunsucker SA, Chen Q, Voorhees PM, Orlowski M, Orlowski RZ (2009) Targeted inhibition of the immunoproteasome is a potent strategy against models of multiple myeloma that overcomes resistance to conventional drugs and nonspecific proteasome inhibitors. Blood 113:4667–4676. doi: 10.1182/blood-2008-07-171637

64. Muchamuel T, Basler M, Aujay MA, Suzuki E, Kalim KW, Lauer C, Sylvain C, Ring ER, Shields J, Jiang J, Shwonek P, Parlati F, Demo SD, Bennett MK, Kirk CJ, Groettrup M (2009) A selective inhibitor of the immunoproteasome subunit LMP7 blocks cytokine production and attenuates progression of experimental arthritis. Nat Med 15:781–787. doi: 10.1038/nm.1978

65. Basler M, Dajee M, Moll C, Groettrup M, Kirk CJ (2010) Prevention of experimental colitis by a selective inhibitor of the immunoproteasome. J Immunol 185:634–641. doi: 10.4049/jimmunol.0903182

66. Almond JB, Snowden RT, Hunter A, Dinsdale D, Cain K, Cohen GM (2001) Proteasome inhibitor-induced apoptosis of B-chronic lymphocytic leukaemia cells involves cytochrome c release and caspase activation, accompanied by formation of an approximately 700 kDa Apaf-1 containing apoptosome complex. Leukemia 15:1388–1397.

67. Naujokat C, Sezer O, Zinke H, Leclere A, Hauptmann S, Possinger K (2000) Proteasome inhibitors induced caspase-dependent apoptosis and accumulation of p21WAF1/Cip1 in human immature leukemic cells. Eur J Haematol 65:221–236.

68. Miller CP, Ban K, Dujka ME, McConkey DJ, Munsell M, Palladino M, Chandra J (2007) NPI-0052, a novel proteasome inhibitor, induces caspase-8 and ROS-dependent apoptosis alone and in combination with HDAC inhibitors in leukemia cells. Blood 110:267–277. doi: 10.1182/blood-2006-03-013128

69. Boatright KM, Salvesen GS (2003) Mechanisms of caspase activation. Curr Opin Cell Biol 15:725–731. doi: 10.1016/j.ceb.2003.10.009

70. Tait SW, Green DR (2010) Mitochondria and cell death: outer membrane permeabilization and beyond. Nat Rev Mol Cell Biol 11:621–632.

71. Shimizu S, Narita M, Tsujimoto Y (1999) Bcl-2 family proteins regulate the release of apoptogenic cytochrome c by the mitochondrial channel VDAC. Nature 399:483–487. doi: 10.1038/20959

72. Pop C, Timmer J, Sperandio S, Salvesen GS (2006) The Apoptosome Activates Caspase-9 by Dimerization. Mol Cell 22:269–275. doi: 10.1016/j.molcel.2006.03.009

73. Tinel A, Tschopp J (2004) The PIDDosome, a protein complex implicated in activation of caspase-2 in response to genotoxic stress. Science 304:843–846. doi: 10.1126/science.1095432

74. Lassus P, Opitz-Araya X, Lazebnik Y (2002) Requirement for caspase-2 in stress-

induced apoptosis before mitochondrial permeabilization. Science 297:1352–1354. doi: 10.1126/science.1074721

75. Guo Y, Srinivasula SM, Druilhe A, Fernandes-Alnemri T, Alnemri ES (2002) Caspase-2 induces apoptosis by releasing proapoptotic proteins from mitochondria. J Biol Chem 277:13430–13437. doi: 10.1074/jbc.M108029200

76. Bonzon C, Bouchier-Hayes L, Pagliari LJ, Green DR, Newmeyer DD (2006) Caspase-2-induced apoptosis requires bid cleavage: a physiological role for bid in heat shock-induced death. Mol Biol Cell 17:2150–2157. doi: 10.1091/mbc.E05-12-1107

77. Ho LH, Taylor R, Dorstyn L, Cakouros D, Bouillet P, Kumar S (2009) A tumor suppressor function for caspase-2. Proc Natl Acad Sci USA 106:5336–5341. doi: 10.1073/pnas.0811928106

78. Styczynski J, Olszewska-Slonina D, Kolodziej B, Napieraj M, Wysocki M (2006) Activity of bortezomib in glioblastoma. Anticancer Res 26:4499–4503.

79. Yin D, Zhou H, Kumagai T, Liu G, Ong JM, Black KL, Koeffler HP (2005) Proteasome inhibitor PS-341 causes cell growth arrest and apoptosis in human glioblastoma multiforme (GBM). Oncogene 24:344–354. doi: 10.1038/sj.onc.1208225

80. Vlashi E, Mattes M, Lagadec C, Donna LD, Phillips TM, Nikolay P, McBride WH, Pajonk F (2010) Differential Effects of the Proteasome Inhibitor NPI-0052 against Glioma Cells. Transl Oncol 3:50–55.

81. Pei X-Y, Dai Y, Grant S (2004) Synergistic induction of oxidative injury and apoptosis in

human multiple myeloma cells by the proteasome inhibitor bortezomib and histone deacetylase inhibitors. Clin Cancer Res 10:3839–3852.

82. Perez-Galan P (2006) The proteasome inhibitor bortezomib induces apoptosis in mantle-cell lymphoma through generation of ROS and Noxa activation independent of p53 status. Blood 107:257–264. doi: 10.1182/blood-2005-05-2091

83. Minami T, Adachi M, Kawamura R, Zhang Y, Shinomura Y, Imai K (2005) Sulindac enhances the proteasome inhibitor bortezomib-mediated oxidative stress and anticancer activity. Clin Cancer Res 11:5248–5256.

84. Fribley A, Zeng Q, Wang C-Y (2004) Proteasome inhibitor PS-341 induces apoptosis through induction of endoplasmic reticulum stress-reactive oxygen species in head and neck squamous cell carcinoma cells. Mol Cell 24:9695–9704. doi: 10.1128/MCB.24.22.9695-9704.2004

85. Zou W, Yue P, Lin N, He M, Zhou Z, Lonial S, Khuri FR, Wang B, Sun S-Y (2006) Vitamin C inactivates the proteasome inhibitor PS-341 in human cancer cells. Clin Cancer Res 12:273–280. doi: 10.1158/1078-0432.CCR-05-0503

86. Baehrecke EH (2005) Autophagy: dual roles in life and death? Nat Rev Mol Cell Biol 6:505–510. doi: 10.1038/nrm1666

87. Zhu K, Dunner K, McConkey DJ (2009) Proteasome inhibitors activate autophagy as a cytoprotective response in human prostate cancer cells. Oncogene 29:451–462.

88. Selimovic D, Porzig BBOW, El-Khattouti A, Badura HE, Ahmad M, Ghanjati F,

Santourlidis S, Haikel Y, Hassan M (2013) Bortezomib/proteasome inhibitor triggers both apoptosis and autophagy-dependent pathways in melanoma cells. Cell Signal 25:308–318. doi: 10.1016/j.cellsig.2012.10.004

89. Yao F, Wang G, Wei W, Tu Y, Tong H, Sun S (2012) An autophagy inhibitor enhances the inhibition of cell proliferation induced by a proteasome inhibitor in MCF-7 cells. Mol Med Rep 5:84–88. doi: 10.3892/mmr.2011.590

90. Ding WX, Ni HM, Gao W, Chen X, Kang JH, Stolz DB, Liu J, Yin XM (2009) Oncogenic transformation confers a selective susceptibility to the combined suppression of the proteasome and autophagy. Mol Cancer Ther 8:2036–2045. doi: 10.1158/1535-7163.MCT-08-1169

91. Belloni D, Veschini L, Foglieni C, Dell'Antonio G, Caligaris-Cappio F, Ferrarini M, Ferrero E (2010) Bortezomib induces autophagic death in proliferating human endothelial cells. Exp Cell Res 316:1010–1018. doi: 10.1016/j.yexcr.2009.11.005

92. Abbott NJ, Patabendige AAK, Dolman DEM, Yusof SR, Begley DJ (2010) Structure and function of the blood-brain barrier. Neurobiol Dis 37:13–25. doi: 10.1016/j.nbd.2009.07.030

93. Zünkeler B, Carson RE, Olson J, Blasberg RG, Devroom H, Lutz RJ, Saris SC, Wright DC, Kammerer W, Patronas NJ (1996) Quantification and pharmacokinetics of blood-brain barrier disruption in humans. J Neurosurg 85:1056–1065.

94. Balyasnikova IV, Ferguson SD, Han Y, Liu F, Lesniak MS (2011) Therapeutic effect of neural stem cells expressing TRAIL and bortezomib in mice with glioma xenografts.

Cancer Lett 310:148–159. doi: 10.1016/j.canlet.2011.06.029

95. Asklund T, Kvarnbrink S, Holmlund C, Wibom C, Bergenheim T, Henriksson R, Hedman H (2012) Synergistic killing of glioblastoma stem-like cells by bortezomib and HDAC inhibitors. Anticancer Res 32:2407–2413.

96. Premkumar DR, Jane EP, Agostino NR, DiDomenico JD, Pollack IF (2011) Bortezomib-induced sensitization of malignant human glioma cells to vorinostat-induced apoptosis depends on reactive oxygen species production, mitochondrial dysfunction, Noxa upregulation, Mcl-1 cleavage, and DNA damage. Mol Carcinog 52:118–133. doi: 10.1002/mc.21835

97. Friday BB, Anderson SK, Buckner J, Yu C, Giannini C, Geoffroy F, Schwerkoske J, Mazurczak M, Gross H, Pajon E, Jaeckle K, Galanis E (2012) Phase II trial of vorinostat in combination with bortezomib in recurrent glioblastoma: a north central cancer treatment group study. Neuro-Oncology 14:215–221. doi: 10.1093/neuonc/nor198

98. Labussiere M, Pinel S, Delfortrie S, Plenat F, Chastagner P (2008) Proteasome inhibition by bortezomib does not translate into efficacy on two malignant glioma xenografts. Oncol Rep 20:1283–1287. doi: 10.3892/or_00000142

99. Singh AV, Palladino MA, Lloyd GK, Potts BC, Chauhan D, Anderson KC (2010) Pharmacodynamic and efficacy studies of the novel proteasome inhibitor NPI-0052 (marizomib) in a human plasmacytoma xenograft murine model. Br J Haematol 149:550–559. doi: 10.1111/j.1365-2141.2010.08144.x

100. Berkowitz A, Walker S (2012) Bortezomib-induced peripheral neuropathy in patients

with multiple myeloma. Clin J Oncol Nurs 16:86–89. doi: 10.1188/12.CJON.86-89

101. Argyriou AA, Iconomou G, Kalofonos HP (2008) Bortezomib-induced peripheral neuropathy in multiple myeloma: a comprehensive review of the literature. Blood 112:1593–1599. doi: 10.1182/blood-2008-04-149385

102. Wolf S, Barton D, Kottschade L, Grothey A, Loprinzi C (2008) Chemotherapy-induced peripheral neuropathy: prevention and treatment strategies. Eur J Cancer 44:1507–1515. doi: 10.1016/j.ejca.2008.04.018

103. Delforge M, Bladé J, Dimopoulos MA, Facon T, Kropff M, Ludwig H, Palumbo A, Van Damme P, San Miguel JF, Sonneveld P (2010) Treatment-related peripheral neuropathy in multiple myeloma: the challenge continues. Lancet Oncol 11:1086–1095. doi: 10.1016/S1470-2045(10)70068-1

104. Richardson PG, Spencer A, Cannell P, Harrison SJ, Catley L, Underhill C, Zimmerman TM, Hofmeister CC, Jakubowiak AJ, Laubach J, Palladino M, Longenecker AM, Lay A, Wear S, Lloyd GK, Hannah AL, Reich S, Spear MA, Anderson KC (2011) Phase I clinical evaluation of twice-weekly marizomib (NPI-0052), a novel proteasome inhibitor, in patients with relapsed/refractory multiple myeloma (MM). American Society of Hematology Meeting Abstract

105. Fuchs D, Berges C, Opelz G, Daniel V, Naujokat C (2008) Increased expression and altered subunit composition of proteasomes induced by continuous proteasome inhibition establish apoptosis resistance and hyperproliferation of Burkitt lymphoma cells. J Cell Biochem 103:270–283. doi: 10.1002/jcb.21405

106. Oerlemans R, Franke NE, Assaraf YG, Cloos J, van Zantwijk I, Berkers CR, Scheffer GL, Debipersad K, Vojtekova K, Lemos C, van der Heijden JW, Ylstra B, Peters GJ, Kaspers GL, Dijkmans BAC, Scheper RJ, Jansen G (2008) Molecular basis of bortezomib resistance: proteasome subunit beta5 (PSMB5) gene mutation and overexpression of PSMB5 protein. Blood 112:2489–2499. doi: 10.1182/blood-2007-08-104950

107. Ruschak AM, Slassi M, Kay LE, Schimmer AD (2011) Novel proteasome inhibitors to overcome bortezomib resistance. J Natl Cancer Inst 103:1007–1017. doi: 10.1093/jnci/djr160

108. Chauhan D, Hideshima T, Anderson KC (2006) A novel proteasome inhibitor NPI-0052 as an anticancer therapy. Br J Cancer 95:961–965. doi: 10.1038/sj.bjc.6603406

109. Rushworth SA, Bowles KM, MacEwan DJ (2011) High basal nuclear levels of Nrf2 in acute myeloid leukemia reduces sensitivity to proteasome inhibitors. Cancer Res 71:1999–2009. doi: 10.1158/0008-5472.CAN-10-3018

110. Weniger MA, Rizzatti EG, Pérez-Galán P, Liu D, Wang Q, Munson PJ, Raghavachari N, White T, Tweito MM, Dunleavy K, Ye Y, Wilson WH, Wiestner A (2011) Treatment-induced oxidative stress and cellular antioxidant capacity determine response to bortezomib in mantle cell lymphoma. Clin Cancer Res 17:5101–5112. doi: 10.1158/1078-0432.CCR-10-3367

111. Zhu K, Dunner K, McConkey DJ (2010) Proteasome inhibitors activate autophagy as a cytoprotective response in human prostate cancer cells. Oncogene 29:451–462. doi:

10.1038/onc.2009.343

112. Liu G, Yuan X, Zeng Z, Tunici P, Ng H, Abdulkadir IR, Lu L, Irvin D, Black KL, Yu JS (2006) Analysis of gene expression and chemoresistance of CD133+ cancer stem cells in glioblastoma. Mol Cancer 5:67. doi: 10.1186/1476-4598-5-67

113. Jiang Z, Zheng X, Rich KM (2003) Down-regulation of Bcl-2 and Bcl-xL expression with bispecific antisense treatment in glioblastoma cell lines induce cell death. J Neurochem 84:273–281.

114. Nachmias B, Ashhab Y, Ben-Yehuda D (2004) The inhibitor of apoptosis protein family (IAPs): an emerging therapeutic target in cancer. Semin Cancer Biol 14:231–243. doi: 10.1016/j.semcancer.2004.04.002

115. Suzuki Y, Nakabayashi Y, Takahashi R (2001) Ubiquitin-protein ligase activity of X-linked inhibitor of apoptosis protein promotes proteasomal degradation of caspase-3 and enhances its anti-apoptotic effect in Fas-induced cell death. Proc Natl Acad Sci USA 98:8662–8667. doi: 10.1073/pnas.161506698

116. Tamm I, Kornblau SM, Segall H, Krajewski S, Welsh K, Kitada S, Scudiero DA, Tudor G, Qui YH, Monks A, Andreeff M, Reed JC (2000) Expression and prognostic significance of IAP-family genes in human cancers and myeloid leukemias. Clin Cancer Res 6:1796–1803.

117. Ferreira CG, Van Der Valk P, Span SW, Jonker JM, Postmus PE, Kruyt FA, Giaccone G (2001) Assessment of IAP (inhibitor of apoptosis) proteins as predictors of response to chemotherapy in advanced non-small-cell lung cancer patients. Ann Oncol 12:799–805.

118. McEleny KR, Watson RWG, Coffey RNT, O'Neill AJ, Fitzpatrick JM (2002) Inhibitors of apoptosis proteins in prostate cancer cell lines. Prostate 51:133–140. doi: 10.1002/pros.10061

119. Sasaki T, Lopes BM, Hankins GR, Helm GA (2002) Expression of survivin, an inhibitor of apoptosis protein, in tumors of the nervous system. Acta Neuropathol 104:105–109. doi: 10.1007/s00401-002-0532-x

120. Das A, Tan W-L, Teo J, Smith DR (2002) Expression of survivin in primary glioblastomas. J Cancer Res Clin Oncol 128:302–306. doi: 10.1007/s00432-002-0343-4

121. Wu G, Chai J, Suber TL, Wu JW, Du C, Wang X, Shi Y (2000) Structural basis of IAP recognition by Smac/DIABLO. Nature 408:1008–1012. doi: 10.1038/35050012

122. Creagh EM, Murphy BM, Duriez PJ, Duckett CS, Martin SJ (2004) Smac/Diablo Antagonizes Ubiquitin Ligase Activity of Inhibitor of Apoptosis Proteins. J Biol Chem 279:26906–26914. doi: 10.1074/jbc.M313859200

123. Benetatos CA, Mitsuuchi Y, Burns JM, Neiman EM, Condon SM, Yu G, Seipel ME, Kapoor GS, Laporte MG, Rippin SR, Deng Y, Hendi MS, Tirunahari PK, Lee Y-H, Haimowitz T, Alexander MD, Graham MA, Weng D, Shi Y, McKinlay MA, Chunduru SK (2014) Birinapant (TL32711), a bivalent SMAC mimetic, targets TRAF2-associated cIAPs, abrogates TNF-induced NF-κB activation, and is active in patient-derived xenograft models. Mol Cancer Ther 13:867–879. doi: 10.1158/1535-7163.MCT-13-0798

124. Weisberg E, Ray A, Barrett R, Nelson E, Christie AL, Porter D, Straub C, Zawel L, Daley JF, Lazo-Kallanian S, Stone R, Galinsky I, Frank D, Kung AL, Griffin JD (2010)

Smac mimetics: implications for enhancement of targeted therapies in leukemia. Leukemia 24:2100–2109. doi: 10.1038/leu.2010.212

125. Ziegler DS, Wright RD, Kesari S, Lemieux ME, Tran MA, Jain M, Zawel L, Kung AL (2008) Resistance of human glioblastoma multiforme cells to growth factor inhibitors is overcome by blockade of inhibitor of apoptosis proteins. J Clin Invest 118:3109–3122. doi: 10.1172/JCI34120DS1

126. Fulda S, Wick W, Weller M, Debatin K-M (2002) Smac agonists sensitize for Apo2L/TRAIL- or anticancer drug-induced apoptosis and induce regression of malignant glioma in vivo. Nat Med. doi: 10.1038/nm735

127. Vellanki SHK, Grabrucker A, Liebau S, Proepper C, Eramo A, Braun V, Boeckers T, Debatin K-M, Fulda S (2009) Small-Molecule XIAP Inhibitors Enhance γ-Irradiation–Induced Apoptosis in Glioblastoma. Neoplasia 11:743–W9. doi: 10.1593/neo.09436

128. Lehrmann H, Pritchard LL, Harel-Bellan A (2002) Histone acetyltransferases and deacetylases in the control of cell proliferation and differentiation. Adv Cancer Res 86:41–65.

129. Weichert W (2009) HDAC expression and clinical prognosis in human malignancies. Cancer Lett 280:168–176. doi: 10.1016/j.canlet.2008.10.047

130. Lucio-Eterovic AK, Cortez MA, Valera ET, Motta FJ, Queiroz RG, Machado HR, Carlotti CG, Neder L, Scrideli CA, Tone LG (2008) Differential expression of 12 histone deacetylase (HDAC) genes in astrocytomas and normal brain tissue: class II and IV are hypoexpressed in glioblastomas. BMC Cancer 8:243. doi: 10.1186/1471-2407-8-243

131. Richon VM, Webb Y, Merger R, Sheppard T, Jursic B, Ngo L, Civoli F, Breslow R, Rifkind RA, Marks PA (1996) Second generation hybrid polar compounds are potent inducers of transformed cell differentiation. Proc Natl Acad Sci USA 93:5705–5708.

132. Marks PA, Breslow R (2007) Dimethyl sulfoxide to vorinostat: development of this histone deacetylase inhibitor as an anticancer drug. Nat Biotechnol 25:84–90. doi: 10.1038/nbt1272

133. Bolden JE, Peart MJ, Johnstone RW (2006) Anticancer activities of histone deacetylase inhibitors. Nat Rev Drug Discov 5:769–784. doi: 10.1038/nrd2133

134. Marks PA, Rifkind RA, Richon VM, Breslow R (2001) Inhibitors of histone deacetylase are potentially effective anticancer agents. Clin Cancer Res 7:759–760.

135. Mann BS, Johnson JR, Cohen MH, Justice R, Pazdur R (2007) FDA Approval Summary: Vorinostat for Treatment of Advanced Primary Cutaneous T-Cell Lymphoma. Oncologist 12:1247–1252. doi: 10.1634/theoncologist.12-10-1247

136. Saito A, Yamashita T, Mariko Y, Nosaka Y, Tsuchiya K, Ando T, Suzuki T, Tsuruo T, Nakanishi O (1999) A synthetic inhibitor of histone deacetylase, MS-27-275, with marked in vivo antitumor activity against human tumors. Proc Natl Acad Sci USA 96:4592–4597.

137. Khan N, Jeffers M, Kumar S, Hackett C, Boldog F, Khramtsov N, Qian X, Mills E, Berghs SC, Carey N, Finn PW, Collins LS, Tumber A, Ritchie JW, Jensen PB, Lichenstein HS, Sehested M (2008) Determination of the class and isoform selectivity of small-molecule histone deacetylase inhibitors. Biochem J 409:581. doi:

10.1042/BJ20070779

138. Lee E, Reardon D, Schiff D, Drappatz J, Hammond S, Grimm S, Norden A, Beroukhim R, McCluskey C, Chi A, Batchelor T, Doherty L, Lafrankie D, Ruland S, Rifenburg J, Jacobs J, Smith K, Gaffey S, Gerard M, Snodgrass S, Raizer J, Wen P (2013) Interim analysis of a phase I/II study of panobinostat in combination with bevacizumab for recurrent glioblastoma. Neuro-Oncology

139. Miller CP, Rudra S, Keating MJ, Wierda WG, Palladino M, Chandra J (2009) Caspase-8 dependent histone acetylation by a novel proteasome inhibitor, NPI-0052: a mechanism for synergy in leukemia cells. Blood 113:4289–4299. doi: 10.1182/blood-2008-08-174797

140. Miller TP, Grogan TM, Dalton WS, Spier CM, Scheper RJ, Salmon SE (1991) P-glycoprotein expression in malignant lymphoma and reversal of clinical drug resistance with chemotherapy plus high-dose verapamil. J Clin Oncol 9:17–24.

141. Seifert U, Bialy LP, Ebstein F, Bech-Otschir D, Voigt A, Schröter F, Prozorovski T, Lange N, Steffen J, Rieger M, Kuckelkorn U, Aktas O, Kloetzel P-M, Krüger E (2010) Immunoproteasomes preserve protein homeostasis upon interferon-induced oxidative stress. Cell 142:613–624. doi: 10.1016/j.cell.2010.07.036

142. Parlati F, Lee SJ, Aujay M, Suzuki E, Levitsky K, Lorens JB, Micklem DR, Ruurs P, Sylvain C, Lu Y, Shenk KD, Bennett MK (2009) Carfilzomib can induce tumor cell death through selective inhibition of the chymotrypsin-like activity of the proteasome. Blood 114:3439–3447. doi: 10.1182/blood-2009-05-223677

143. Mitsiades N, Mitsiades CS, Poulaki V, Chauhan D, Fanourakis G, Gu X, Bailey C, Joseph M, Libermann TA, Treon SP, Munshi NC, Richardson PG, Hideshima T, Anderson KC (2002) Molecular sequelae of proteasome inhibition in human multiple myeloma cells. Proc Natl Acad Sci USA 99:14374–14379. doi: 10.1073/pnas.202445099

144. McStay GP, Salvesen GS, Green DR (2007) Overlapping cleavage motif selectivity of caspases: implications for analysis of apoptotic pathways. Cell Death Differ 15:322–331. doi: 10.1038/sj.cdd.4402260

145. Scarlett JL, Sheard PW, Hughes G, Ledgerwood EC, Ku HH, Murphy MP (2000) Changes in mitochondrial membrane potential during staurosporine-induced apoptosis in Jurkat cells. FEBS Letters 475:267–272.

146. Maiuri MC, Le Toumelin G, Criollo A, Rain JC, Gautier F, Juin P, Tasdemir E, Pierron G, Troulinaki K, Tavernarakis N (2007) Functional and physical interaction between Bcl-XL and a BH3-like domain in Beclin-1. EMBO J 26:2527–2539.

147. Deneke SM, Fanburg BL (1989) Regulation of cellular glutathione. Am J Physiol 257:L163–73.

148. Abello PA, Fidler SA, Buchman TG (1994) Thiol reducing agents modulate induced apoptosis in porcine endothelial cells. Shock 2:79–83.

149. Kamencic H, Lyon A, Paterson PG, Juurlink BHJ (2000) Monochlorobimane Fluorometric Method to Measure Tissue Glutathione. Anal Biochem 286:35–37. doi: 10.1006/abio.2000.4765

150. Hibi T, Nii H, Nakatsu T, Kimura A, Kato H, Hiratake J, Oda J (2004) Crystal structure of γ-glutamylcysteine synthetase: insights into the mechanism of catalysis by a key enzyme for glutathione homeostasis. Proc Natl Acad Sci USA 101:15052–15057.

151. Perrone G, Hideshima T, Ikeda H, Okawa Y, Calabrese E, Gorgun G, Santo L, Cirstea D, Raje N, Chauhan D, Baccarani M, Cavo M, Anderson KC (2009) Ascorbic acid inhibits antitumor activity of bortezomib in vivo. Leukemia 23:1679–1686. doi: 10.1038/leu.2009.83

152. Golden EB, Lam PY, Kardosh A, Gaffney KJ, Cadenas E, Louie SG, Petasis NA, Chen TC, Schonthal AH (2009) Green tea polyphenols block the anticancer effects of bortezomib and other boronic acid-based proteasome inhibitors. Blood 113:5927–5937. doi: 10.1182/blood-2008-07-171389

153. Suraweera A, Münch C, Hanssum A, Bertolotti A (2012) Failure of Amino Acid Homeostasis Causes Cell Death following Proteasome Inhibition. Mol Cell 48:242–253. doi: 10.1016/j.molcel.2012.08.003

154. Purwaha P, Lorenzi PL, Silva LP, Hawke DH, Weinstein JN (2014) Targeted metabolomic analysis of amino acid response to L-asparaginase in adherent cells. Metabolomics 10:909–919. doi: 10.1007/s11306-014-0634-1

155. Lal S, Lacroix M, Tofilon P, Fuller GN, Sawaya R, Lang FF (2000) An implantable guide-screw system for brain tumor studies in small animals. J Neurosurg 92:326–333. doi: 10.3171/jns.2000.92.2.0326

156. Varfolomeev E, Blankenship JW, Wayson SM, Fedorova AV, Kayagaki N, Garg P,

Zobel K, Dynek JN, Elliott LO, Wallweber HJA, Flygare JA, Fairbrother WJ, Deshayes K, Dixit VM, Vucic D (2007) IAP Antagonists Induce Autoubiquitination of c-IAPs, NF-κB Activation, and TNFα-Dependent Apoptosis. Cell 131:669–681. doi: 10.1016/j.cell.2007.10.030

157. Pitts TM, Morrow M, Kaufman SA, Tentler JJ, Eckhardt SG (2009) Vorinostat and bortezomib exert synergistic antiproliferative and proapoptotic effects in colon cancer cell models. Mol Cancer Ther 8:342–349. doi: 10.1158/1535-7163.MCT-08-0534

158. Chou T-C, Talalay P (1983) Analysis of combined drug effects: a new look at a very old problem. Trends Pharmacol Sci 4:450–454.

159. Ruchaud S, Korfali N, Villa P, Kottke TJ, Dingwall C, Kaufmann SH, Earnshaw WC (2002) Caspase-6 gene disruption reveals a requirement for lamin A cleavage in apoptotic chromatin condensation. EMBO J 21:1967–1977. doi: 10.1093/emboj/21.8.1967

160. Ruiz S, Krupnik Y, Keating M, Chandra J, Palladino M, McConkey D (2006) The proteasome inhibitor NPI-0052 is a more effective inducer of apoptosis than bortezomib in lymphocytes from patients with chronic lymphocytic leukemia. Mol Cancer Ther 5:1836–1843. doi: 10.1158/1535-7163.MCT-06-0066

161. Obaidat A, Weiss J, Wahlgren B, Manam RR, Macherla VR, Mcarthur K, Chao T-H, Palladino MA, Lloyd GK, Potts BC, Enna SJ, Neuteboom STC, Hagenbuch B (2011) Proteasome regulator marizomib (NPI-0052) exhibits prolonged inhibition, attenuated efflux, and greater cytotoxicity than its reversible analogs. J Pharmacol Exp Ther 1–35.

doi: 10.1124/jpet.110.177824

162. Fricke B, Heink S, Steffen J, Kloetzel P-M, Krüger E (2007) The proteasome maturation protein POMP facilitates major steps of 20S proteasome formation at the endoplasmic reticulum. EMBO Rep 8:1170–1175. doi: 10.1038/sj.embor.7401091

163. Singh MM, Manton CA, Bhat KP, Tsai WW, Aldape K, Barton MC, Chandra J (2011) Inhibition of LSD1 sensitizes glioblastoma cells to histone deacetylase inhibitors. Neuro-Oncology 13:894–903. doi: 10.1093/neuonc/nor049

164. Jankun J, Selman SH, Swiercz R, Skrzypczak-Jankun E (1997) Why drinking green tea could prevent cancer. Nature 387:561. doi: 10.1038/42381

165. Nam S, Smith DM, Dou QP (2001) Ester bond-containing tea polyphenols potently inhibit proteasome activity in vitro and in vivo. J Biol Chem 276:13322–13330. doi: 10.1074/jbc.M004209200

166. Smith DM, Wang Z, Kazi A, Li L-H, Chan TH, Dou QP (2002) Synthetic analogs of green tea polyphenols as proteasome inhibitors. Mol Med 8:382–392.

167. Yang Y, Kitagaki J, Dai R-M, Tsai YC, Lorick KL, Ludwig RL, Pierre SA, Jensen JP, Davydov IV, Oberoi P, Li C-CH, Kenten JH, Beutler JA, Vousden KH, Weissman AM (2007) Inhibitors of ubiquitin-activating enzyme (E1), a new class of potential cancer therapeutics. Cancer Res 67:9472–9481. doi: 10.1158/0008-5472.CAN-07-0568

168. Nawrocki ST, Griffin P, Kelly KR, Carew JS (2012) MLN4924: a novel first-in-class inhibitor of NEDD8-activating enzyme for cancer therapy. Expert Opin Investig Drugs

21:1563–1573. doi: 10.1517/13543784.2012.707192

169. Yang D, Tan M, Wang G, Sun Y (2012) The p21-dependent radiosensitization of human breast cancer cells by MLN4924, an investigational inhibitor of NEDD8 activating enzyme. PloS One 7:e34079. doi: 10.1371/journal.pone.0034079.g006

170. Orlicky S, Tang X, Neduva V, Elowe N, Brown ED, Sicheri F, Tyers M (2010) An allosteric inhibitor of substrate recognition by the SCF(Cdc4) ubiquitin ligase. Nat Biotechnol 28:733–737. doi: 10.1038/nbt.1646

171. Aghajan M, Jonai N, Flick K, Fu F, Luo M, Cai X, Ouni I, Pierce N, Tang X, Lomenick B (2010) Chemical genetics screen for enhancers of rapamycin identifies a specific inhibitor of an SCF family E3 ubiquitin ligase. Nat Biotechnol 28:738–742.

172. Carrano AC, Eytan E, Hershko A, Pagano M (1999) SKP2 is required for ubiquitin-mediated degradation of the CDK inhibitor p27. Nat Cell Biol 1:193–199.

173. Bornstein G, Bloom J, Sitry-Shevah D, Nakayama K, Pagano M, Hershko A (2003) Role of the SCFSkp2 Ubiquitin Ligase in the Degradation of p21Cip1 in S Phase. J Biol Chem 278:25752–25757. doi: 10.1074/jbc.M301774200

174. Orlowski M, Wilk S (2003) Ubiquitin-independent proteolytic functions of the proteasome. Arch Biochem Biophys 415:1–5. doi: 10.1016/S0003-9861(03)00197-8

175. Hanssum A, Zhong Z, Rousseau A, Krzyzosiak A, Sigurdardottir A, Bertolotti A (2014) An inducible chaperone adapts proteasome assembly to stress. Mol Cell 55:566–577. doi: 10.1016/j.molcel.2014.06.017

176. Tu S, McStay GP, Boucher L-M, Mak T, Beere HM, Green DR (2005) In situ trapping of activated initiator caspases reveals a role for caspase-2 in heat shock-induced apoptosis. Nat Cell Biol 8:72–77. doi: 10.1038/ncb1340

177. Olsson M, Vakifahmetoglu H, Abruzzo PM, Högstrand K, Grandien A, Zhivotovsky B (2009) DISC-mediated activation of caspase-2 in DNA damage-induced apoptosis. Oncogene 28:1949–1959. doi: 10.1038/onc.2009.36

178. Bouchier-Hayes L, Oberst A, McStay GP, Connell S, Tait SWG, Dillon CP, Flanagan JM, Beere HM, Green DR (2009) Characterization of Cytoplasmic Caspase-2 Activation by Induced Proximity. Mol Cell 35:830–840. doi: 10.1016/j.molcel.2009.07.023

179. Baliga BC, Read SH, Kumar S (2004) The biochemical mechanism of caspase-2 activation. Cell Death Differ 11:1234–1241. doi: 10.1038/sj.cdd.4401492

180. Bergeron L, Perez GI, Macdonald G, Shi L, Sun Y, Jurisicova A, Varmuza S, Latham KE, Flaws JA, Salter JC, Hara H, Moskowitz MA, Li E, Greenberg A, Tilly JL, Yuan J (1998) Defects in regulation of apoptosis in caspase-2-deficient mice. Genes Dev 12:1304–1314.

181. Kuida K, Haydar TF, Kuan CY, Gu Y, Taya C, Karasuyama H, Su MS, Rakic P, Flavell RA (1998) Reduced apoptosis and cytochrome c-mediated caspase activation in mice lacking caspase 9. Cell 94:325–337.

182. Yakovlev AG, Ota K, Wang G, Movsesyan V, Bao WL, Yoshihara K, Faden AI (2001) Differential expression of apoptotic protease-activating factor-1 and caspase-3 genes and susceptibility to apoptosis during brain development and after traumatic brain injury. J

Neurosci 21:7439–7446.

183. Zheng TS, Hunot S, Kuida K, Momoi T, Srinivasan A, Nicholson DW, Lazebnik Y, Flavell RA (2000) Deficiency in caspase-9 or caspase-3 induces compensatory caspase activation. Nat Med 6:1241–1247.

184. Krajewski S, Tanaka S, Takayama S, Schibler MJ, Fenton W, Reed JC (1993) Investigation of the subcellular distribution of the bcl-2 oncoprotein: residence in the nuclear envelope, endoplasmic reticulum, and outer mitochondrial membranes. Cancer Res 53:4701–4714.

185. White C, Li C, Yang J, Petrenko NB, Madesh M, Thompson CB, Foskett JK (2005) The endoplasmic reticulum gateway to apoptosis by Bcl-XL modulation of the InsP3R. Nat Cell Biol 7:1021–1028. doi: 10.1038/ncb1302

186. Nakagawa T, Yuan J (2000) Cross-talk between two cysteine protease families activation of caspase-12 by calpain in apoptosis. J Cell Biol 150:887–894.

187. Halasi M, Wang M, Chavan TS, Gaponenko V, Hay N, Gartel AL (2013) ROS inhibitor N-acetyl-L-cysteine antagonizes the activity of proteasome inhibitors. Biochem J 454:201–208. doi: 10.1042/BJ20130282

188. Huang LE, Zhang H, Bae SW, Liu AY (1994) Thiol reducing reagents inhibit the heat shock response. Involvement of a redox mechanism in the heat shock signal transduction pathway. J Biol Chem 269:30718–30725.

189. Prostko CR, Brostrom MA, Malara EM, Brostrom CO (1992) Phosphorylation of

eukaryotic initiation factor (eIF) 2 alpha and inhibition of eIF-2B in GH3 pituitary cells by perturbants of early protein processing that induce GRP78. J Biol Chem 267:16751–16754.

190. van Delft MF, Wei AH, Mason KD, Vandenberg CJ, Chen L, Czabotar PE, Willis SN, Scott CL, Day CL, Cory S, Adams JM, Roberts AW, Huang DCS (2006) The BH3 mimetic ABT-737 targets selective Bcl-2 proteins and efficiently induces apoptosis via Bak/Bax if Mcl-1 is neutralized. Cancer Cell 10:389–399. doi: 10.1016/j.ccr.2006.08.027

191. Vlashi E, Kim K, Lagadec C, Donna LD, McDonald JT, Eghbali M, Sayre JW, Stefani E, McBride W, Pajonk F (2009) In vivo imaging, tracking, and targeting of cancer stem cells. J Natl Cancer Inst 101:350–359. doi: 10.1093/jnci/djn509

192. Drappatz J, Lee EQ, Hammond S, Grimm SA, Norden AD, Beroukhim R, Gerard M, Schiff D, Chi AS, Batchelor TT, Doherty LM, Ciampa AS, LaFrankie DC, Ruland S, Snodgrass SM, Raizer JJ, Wen PY (2011) Phase I study of panobinostat in combination with bevacizumab for recurrent high-grade glioma. J Neurooncol 107:133–138. doi: 10.1007/s11060-011-0717-z

193. Pontén J, Macintyre EH (1968) Long term culture of normal and neoplastic human glia. Acta Pathol Microbiol Scand 74:465–486.

194. Galli R, Binda E, Orfanelli U, Cipelletti B, Gritti A, De Vitis S, Fiocco R, Foroni C, Dimeco F, Vescovi A (2004) Isolation and characterization of tumorigenic, stem-like neural precursors from human glioblastoma. Cancer Res 64:7011–7021. doi: 10.1158/0008-5472.CAN-04-1364

195. Tabatabai G, Weller M (2011) Glioblastoma stem cells. Cell Tissue Res 343:459–465. doi: 10.1007/s00441-010-1123-0

VITA

Christa Ann Manton was born in Springfield, Missouri on January 13, 1987, the daughter of Susan Ruth Manton and Robert Howard Manton. After graduating from Camdenton High School in Camdenton, Missouri in 2005, she entered Truman State University in Kirksville, MO. She received the degree of Bachelor of Science with a major in biology and a minor in English from Truman in May 2009. She also began her graduate studies at the University of Texas Graduate School of Biomedical Sciences at Houston in May 2009. As a graduate student, Christa was named an American Legion Auxiliary Fellow and was also the recipient of an Andrew Sowell-Wade Huggins Endowed Scholarship. Christa was also supported by a Research Training Award from the Cancer Prevention and Research Institute of Texas (CPRIT RP140106) and a Julia Jones Matthews Cancer Research Scholar training award.

Permanent Address:

15087 State Road A

Richland, MO 65556